

Arborescent Polymers from “Click” Chemistry and Other Methods

by

Toufic Nabil Aridi

A thesis
presented to the University of Waterloo
in fulfillment of the
thesis requirement for the degree of
Doctor of Philosophy
in
Chemistry

Waterloo, Ontario, Canada, 2013

© Toufic Nabil Aridi 2013

Author's Declaration

I hereby declare that I am the sole author of this thesis. This is a true copy of the thesis, including any required final revisions, as accepted by my examiners.

I understand that my thesis may be made electronically available to the public.

Abstract

Graft polymers with a dendritic architecture (arborescent polymers) were synthesized by “click”, anionic, and cationic grafting. Arborescent polystyrene and polybutadiene systems were synthesized by “click” coupling using alkyne and azide functional groups, one of which was introduced randomly on the polymer substrate, while the other functionality was located at one end of the polymer serving as side chains. The two possible combinations of randomly and end-functionalized components were investigated for both polymer systems, but the best method for polystyrene involved side chains with an azide end group and randomly acetylenated substrates; for polybutadiene, acetylene-terminated side chains and randomly azidated substrates were preferred. The end-functionalized polymers were derived from a bifunctional initiator to introduce a protected hydroxyl group, which was converted into either an azide or an acetylene functionality. Coupling of the end-functionalized side chains with the substrate polymer serving as backbone yielded a comb-branched (or G0 arborescent) polymer. Further cycles of substrate functionalization and grafting led to the subsequent (G1 and G2) generations of arborescent polymers. Linear and branched (G0 and G1) hydroxylated polystyrene derivatives, some of which served as intermediates in the synthesis of the randomly functionalized “click” grafting substrates, were also explored as macroinitiators for the cationic polymerization of ethyl vinyl ether. The substrates functionalized with either secondary or tertiary alcohol groups yielded the desired arborescent polystyrene-*graft*-poly(ethyl vinyl ether) copolymers, without formation of linear contaminant. Arborescent polybutadiene of generations G1 and G2, with different side chain molecular weights, were also synthesized by anionic coupling of living polybutadienyllithium side chains with substrates functionalized with chlorosilane groups for comparison with the “click” methodology.

Acknowledgements

I would like to thank my supervisor Prof. Mario Gauthier for giving me this chance, and for all the help, support, guidance, knowledge, and expertise that was vital for the success of this research.

I would like to thank my supervisory committee members Prof. Jean Duhamel, Prof. Eric Fillion, and Prof. Neil McManus for their help and support.

I would also like to thank the following colleagues and friends for their friendship and help throughout my research: Daisuke Aoki, Mosa Alsehli, Ala Alturk, Yahya Alzahrany, Ryan Amos, Jennipher Aumis, Matthew Benoit, Dr. Jason Dockendorff, Joanne Fernandez, Doug Grandy, Dr. Eda Güngör, Dr. Jonathan Juger, Dr. Hemali Lad, Dan Larocque, Dr. Ilias Mahmud, Dr. Firmin Moingeon, Olivier Nguon, An Nguyen, Shannon Scriver, Dr. Howard Siu, Dr. Deepak Vishnu, Coline Voirin, Dr. Greg Whitton, and Aklilu Worku.

I wish to thank the following agencies and organizations for financial support: The Natural Sciences and Engineering Research Council of Canada (NSERC), the University of Waterloo, and LANXESS Canada.

Last but not least I would like to thank my loving parents, brothers and their families, and beloved wife for their encouragement, love, and support throughout my journey; I love you all.

Dedication

I dedicate this work to my loving mom and dad, brothers, and to my beloved wife for their love, support, and prayers.

“I do not know what I may appear to the world; but to myself I seem to have been only like a boy playing on the seashore, and diverting myself in now and then finding a smoother pebble or a prettier shell than ordinary, whilst the great ocean of truth lay all undiscovered before me”

Sir Isaac Newton

Table of Contents

Author's Declaration	ii
Abstract	iii
Acknowledgements.....	iv
Dedication	v
List of Figures.....	xiii
List of Schemes.....	xviii
List of Tables	xx
List of Abbreviations and Symbols.....	xxi
Chapter 1 Foreword	1
1.1 Opening Remarks	2
1.2 Research Objectives and Thesis Outline	2
Chapter 2 Arborescent Polymers and “Click” Chemistry.....	4
2.1 Introduction	5
2.2 Arborescent Polystyrene.....	8
2.2.1 Arborescent Polystyrene from Chloromethyl Coupling Sites	8
2.2.2 Arborescent Polystyrene from Acetyl Coupling Sites.....	10
2.2.3 Arborescent Polystyrene from Epoxide Coupling Sites	14
2.2.4 One-pot Synthesis of Arborescent Polystyrene	16
2.2.5 Physical Characterization of Arborescent Polystyrene.....	19
2.2.5.1 Neutron Scattering.....	19
2.2.5.2 Solution Thermodynamics	21
2.3 Arborescent Polystyrene- <i>graft</i> -Poly(2-vinylpyridine) Copolymers.....	23
2.3.1 Physical Characterization of Arborescent Polystyrene- <i>graft</i> -Poly(2-vinylpyridine)	
.....	25
2.3.1.1 Neutron and Light Scattering.....	25

2.3.1.2	Micellar Properties	27
2.3.1.3	Self-assembly in Solution.....	30
2.4	Arborescent Polystyrene- <i>graft</i> -Polystyrene- <i>block</i> -Poly(2-vinylpyridine)	32
2.5	Arborescent Polystyrene- <i>graft</i> -Polyisoprene	34
2.5.1	Rheological Properties	37
2.6	Arborescent Polystyrene- <i>graft</i> -Poly(<i>tert</i> -butyl methacrylate)	37
2.6.1	Solution Properties.....	38
2.7	Arborescent Polystyrene- <i>graft</i> -Poly(ethylene oxide).....	39
2.7.1	Self-assembly at the Air-water Interface	40
2.8	Arborescent Polyisoprene.....	43
2.9	Arborescent Polybutadiene.....	45
2.10	“Click” Chemistry	47
2.10.1	Block Copolymers from “Click” Chemistry.....	48
2.10.2	Star Copolymers from “Click” Chemistry.....	49
2.11	Conclusions	52
Chapter 3	Synthesis of Arborescent Polystyrene by “Click” Grafting.....	53
3.1	Abstract	54
3.2	Introduction	55
3.3	Experimental Section	57
3.3.1	Solvent and Reagent Purification.....	58
3.3.2	Backbone Synthesis and Functionalization (Strategy A).....	59
3.3.2.1	Styrene Polymerization	59
3.3.2.2	Acetylation of Polystyrene	60
3.3.2.3	Acetylenation of Polystyrene	60
3.3.3	Side Chain Synthesis and Functionalization (Strategy A).....	61
3.3.3.1	Synthesis of 6- <i>tert</i> -Butyldimethylsiloxyhexyllithium.....	61
3.3.3.2	Styrene Polymerization with 6- <i>tert</i> -Butyldimethylsiloxyhexyllithium.....	62
3.3.3.3	Deprotection of the Hydroxyl Chain Ends.....	63
3.3.3.4	End Group Tosylation	63
3.3.3.5	End Group Azidation	64
3.3.3.6	Polystyrene Side Chains with $M_n \approx 50,000$	64

3.3.4	Coupling of Azide-terminated Polystyrene with Acetylenated Polystyrene	65
3.3.5	Backbone Synthesis and Functionalization (Strategy B).....	66
3.3.5.1	Linear Polystyrene and Acetylation	66
3.3.5.2	Reduction of Acetylated Polystyrene.....	66
3.3.5.3	Chlorination of Hydroxylated Polystyrene	67
3.3.5.4	Transformation from Chloride to Azide.....	68
3.3.6	Side Chain Functionalization with Alkyne End Groups (Strategy B).....	68
3.3.7	Coupling of Acetylene End-functionalized Side Chains with the Azidated Substrate	69
3.3.8	Polymer Characterization.....	69
3.4	Results and Discussion.....	70
3.4.1	Grafting Onto Acetylenated Substrates (Strategy A).....	72
3.4.1.1	Linear Polystyrene and Acetylation	72
3.4.1.2	Alkynylation of Acetylated Polystyrene	74
3.4.1.3	Synthesis of 6- <i>tert</i> -Butyldimethylsiloxyhexyl Chloride	74
3.4.1.4	Linear Polystyrene from 6- <i>tert</i> -Butyldimethylsiloxyhexyllithium (Target $M_n = 5000$)	75
3.4.1.5	Deprotection of the <i>tert</i> -Butyldimethylsiloxy End Group and Conversion to an Azide.....	77
3.4.1.6	Linear Polystyrene from 6- <i>tert</i> -Butyldimethylsiloxyhexyllithium (Target $M_n = 50,000$)	79
3.4.1.7	Deprotection of the <i>tert</i> -Butyldimethylsiloxy Group and Conversion to an Azide	81
3.4.1.8	Coupling of Azide-terminated Polystyrene ($M_n = 5200$) with Linear Acetylenated Polystyrene.....	82
3.4.1.9	Coupling of Azide-terminated Polystyrene ($M_n = 5200$) with G0 Acetylenated Polystyrene.....	86
3.4.1.10	Coupling of Azide-terminated Polystyrene ($M_n = 5200$) with G1 Acetylenated Polystyrene.....	87
3.4.1.11	Coupling of Azide-terminated Polystyrene ($M_n = 45,000$) with Linear Acetylenated Polystyrene.....	89
3.4.1.12	Coupling of Azide-terminated Polystyrene ($M_n = 45,000$) with G0 Acetylenated Polystyrene.....	90

3.4.1.13	Characterization of the Purified Arborescent Polymers	91
3.4.2	Grafting Onto Azidated Substrates (Strategy B)	93
3.4.2.1	Linear Polystyrene Acetylation, and Reduction.....	93
3.4.2.2	Chlorination of Hydroxylated Polystyrene and Conversion to the Azide.....	94
3.4.2.3	Side Chain Functionalization with Alkyne End Groups	95
3.4.2.4	Coupling of Acetylene-terminated Polystyrene with Azidated Polystyrene	97
3.5	Conclusions	98
Chapter 4	Arborescent Polystyrene- <i>graft</i> -Poly(ethyl vinyl ether) Copolymers	100
4.1	Abstract	101
4.2	Introduction	101
4.3	Experimental Section	103
4.3.1	Solvent and Reagent Purification.....	103
4.3.2	Synthesis of Hydroxylated Substrates	105
4.3.2.1	Styrene Polymerization	105
4.3.2.2	Acetylation of Polystyrene.....	105
4.3.2.3	Secondary Alcohol Groups from Acetylated Polystyrene	106
4.3.2.4	Tertiary Alcohol Groups from Acetylated Polystyrene	107
4.3.2.5	Functionalization of G0 Polystyrene.....	107
4.3.2.6	Functionalization of G1 Polystyrene.....	108
4.3.3	Grafting of Poly(ethyl vinyl ether) from Hydroxylated Substrates	109
4.3.3.1	Grafting from Linear Polystyrene	109
4.3.3.2	Grafting from G0 Polystyrene.....	110
4.3.3.3	Grafting from G1 Polystyrene.....	111
4.3.4	Polymer Characterization.....	111
4.4	Results and Discussion.....	112
4.4.1	Synthesis of Hydroxylated Substrates	113
4.4.1.1	Linear Polystyrene and Acetylation	113
4.4.1.2	Secondary Alcohol-functionalized Linear Polystyrene.....	114
4.4.1.3	Tertiary Alcohol-functionalized Linear Polystyrene.....	115
4.4.1.4	Functionalization of G0 and G1 Polystyrene	117
4.4.2	Grafting of Poly(ethyl vinyl ether) from Hydroxylated Substrates	117

4.4.2.1	Grafting of Poly(ethyl vinyl ether) from Linear Polystyrene.....	117
4.4.2.2	Grafting of Poly(ethyl vinyl ether) from G0 Polystyrene	121
4.4.2.3	Grafting of Poly(ethyl vinyl ether) from G1 Polystyrene	122
4.5	Conclusions	125
Chapter 5 Synthesis of Arborescent Polybutadiene by “Click” Grafting		127
5.1	Abstract	128
5.2	Introduction	128
5.3	Experimental Section	130
5.3.1	Solvent and Reagent Purification.....	131
5.3.2	Backbone Synthesis and Functionalization (Strategy A).....	132
5.3.2.1	Butadiene Polymerization	132
5.3.2.2	Epoxidation of Polybutadiene	132
5.3.2.3	Reduction of Epoxidized Polybutadiene	133
5.3.2.4	Tosylation of Hydroxylated Polybutadiene.....	134
5.3.2.5	Transformation from Tosyl to Azide	134
5.3.3	Side Chain Synthesis and Functionalization (Strategy A).....	135
5.3.3.1	Butadiene Polymerization Using 6- <i>tert</i> -Butyldimethylsiloxyhexyllithium.....	135
5.3.3.2	Deprotection of Hydroxyl Chain End	135
5.3.3.3	Transformation from Hydroxyl to Acetylene.....	136
5.3.4	Grafting of Acetylene-terminated Polybutadiene onto Azidated Polybutadiene..	136
5.3.5	Backbone Synthesis and Functionalization with Acetylene Groups (Strategy B)	137
5.3.6	Side Chain Functionalization with Azide End Groups (Strategy B)	138
5.3.7	Grafting of Azide-terminated Polybutadiene on Acetylenated Polybutadiene.....	138
5.3.8	Polymer Characterization.....	139
5.4	Results and Discussion.....	139
5.4.1	Grafting onto Azidated Substrates (Strategy A).....	141
5.4.1.1	Random Hydroxylation of Linear Polybutadiene	141
5.4.1.2	Tosylation of Hydroxylated Polybutadiene and Conversion to Azide.....	143
5.4.1.3	Linear Polybutadiene from 6- <i>tert</i> -Butyldimethylsiloxyhexyllithium	145
5.4.1.4	Deprotection of the <i>tert</i> -Butyldimethylsiloxy Group and Conversion to an Acetylene	147

5.4.1.5	Coupling of Acetylene-terminated Polybutadiene with Randomly Azidated Polybutadiene.....	148
5.4.1.6	Coupling of Acetylene-terminated Polybutadiene with G0 and G1 Azidated Polybutadiene.....	152
5.4.1.7	Characterization of the Purified Arborescent Polymers.....	154
5.4.2	Grafting onto Acetylenated Substrates (Strategy B).....	156
5.4.2.1	Random Acetylenation of Polybutadiene.....	156
5.4.2.2	Conversion of the Hydroxyl Chain End to an Azide	157
5.4.2.3	Coupling of Azide-terminated Polybutadiene ($M_n = 5200$) with Linear Acetylene Polybutadiene.....	158
5.5	Conclusions	160
Chapter 6 Synthesis of Arborescent Polybutadiene by Anionic Grafting		162
6.1	Abstract	163
6.2	Introduction	163
6.3	Experimental Section	166
6.3.1	Solvent and Reagent Purification.....	166
6.3.2	Synthesis of High 1,2-Microstructure Content G0 polybutadiene.....	167
6.3.2.1	Butadiene Polymerization	167
6.3.2.2	Hydrosilylation of Linear Polybutadiene	168
6.3.2.3	Grafting of High 1,2-Microstructure Content Polybutadienyllithium onto Linear Hydrosilylated Polybutadiene.....	168
6.3.3	Synthesis of High 1,4-Microstructure Content G1 Polybutadiene	169
6.3.3.1	Hydrosilylation of High 1,2-Microstructure Content G0 Polybutadiene.....	169
6.3.3.2	Grafting of $M_n \approx 5, 30, 50,$ and $80,000$ High 1,4-Microstructure Content Polybutadienyllithium onto Hydrosilylated G0 Polybutadiene	169
6.3.4	Synthesis of High 1,2-Microstructure Content G1 Polybutadiene	171
6.3.5	Synthesis of High 1,4-Microstructure Content G2 Polybutadiene	171
6.3.5.1	Hydrosilylation of High 1,2-Microstructure Content G1 Polybutadiene.....	171
6.3.5.2	Grafting of $M_n \approx 5, 30, 50,$ and $80,000$ High 1,4-Microstructure Content Polybutadienyllithium onto Hydrosilylated G1 Polybutadiene	172
6.3.6	Polymer Characterization.....	172
6.4	Results and Discussion.....	173

6.4.1	Synthesis of High 1,2-Microstructure Content G0 polybutadiene.....	175
6.4.1.1	Butadiene Polymerization and Hydrosilylation	175
6.4.1.2	Grafting of High 1,2-Microstructure Content $M_n \approx 5000$ Polybutadienyllithium onto Linear Hydrosilylated Polybutadiene	176
6.4.2	Synthesis of High 1,4-Microstructure Content G1 Polybutadiene with $M_n \approx 5, 30,$ 50, and 80,000 Side Chains	179
6.4.3	Synthesis of High 1,2-Microstructure Content G1 Polybutadiene	183
6.4.4	Synthesis of High 1,4-Microstructure Content G2 Polybutadiene with $M_n \approx 5, 30,$ 50, and 80,000 Side Chains	185
6.5	Conclusions	188
Chapter 7 Concluding Remarks and Suggestions for Future Work.....		190
7.1	Original Contributions to Knowledge	191
7.2	Suggestions for Future Work	193
7.2.1	Synthesis of G3 and G4 Polystyrene by “Click” Coupling	193
7.2.2	Synthesis of G3 and G4 Arborescent Polybutadiene by “Click” Coupling and Optimization of the Alternate “Click” Coupling Method	194
7.2.3	Synthesis of Arborescent Polystyrene and Polybutadiene Copolymers by “Click” Coupling	195
7.2.4	Application of the Cationic Macroinitiators to Other Monomers and to Sequential Monomer Addition.....	195
References		197
Chapter 1		197
Chapter 2		198
Chapter 4		205
Chapter 5		207
Chapter 6		209
Chapter 7		211

List of Figures

Figure 2.1. Schematic representation of (a) dendrimers, (b) hyperbranched, and (c) dendrigraft polymers.	6
Figure 2.2. Molecular weight dependence of hydrodynamic volume expansion for linear and arborescent P2VP and PMMA graft copolymers	27
Figure 2.3. Release profiles for (a) indomethacin and (b) lidocaine	30
Figure 2.4. Schematic representation of (a) core-shell morphology and (b) temperature-responsive supramolecular self-assembly.....	31
Figure 2.5. Schematic representation of an arborescent G2 copolymer template synthesis	34
Figure 2.6. AFM images for samples prepared by spin-casting from solutions	36
Figure 2.7. Self-assembly of arborescent G1 polystyrene- <i>graft</i> -poly(ethylene oxide) copolymers at the air-water interface	42
Figure 2.8. Synthetic scheme for dendrigraft star-comb polybutadiene.....	47
Figure 2.9. Preparation of PS-PCL-PMMA-PEG and PS-PCL- <i>Pt</i> BA-PEG 4-miktoarm star quarterpolymers	51
Figure 3.1. ¹ H NMR spectra for (a) acetylated polystyrene and (b) acetylenated polystyrene.....	73
Figure 3.2. SEC trace for acetylated polystyrene.....	73
Figure 3.3. ¹ H NMR spectra for (a) 6-chloro-1-hexanol and (b) 6- <i>tert</i> -butyldimethylsiloxyhexyl chloride.	75
Figure 3.4. SEC trace for linear polystyrene with target $M_n = 5000$ synthesized using 6- <i>tert</i> -butyldimethylsiloxyhexyllithium.....	76
Figure 3.5. ¹ H NMR spectrum for polystyrene with a silyl ether-protected chain-end	77

Figure 3.6. ¹ H NMR spectra for (a) hydroxyl-, (b) tosyl-, and (c) azide-terminated polystyrene .	78
Figure 3.7. SEC trace for azide-terminated polystyrene	79
Figure 3.8. SEC trace for linear polystyrene with target $M_n = 50,000$ synthesized using 6- <i>tert</i> -butyldimethylsiloxyhexyllithium.....	80
Figure 3.9. ¹ H NMR spectrum for polystyrene ($M_n = 45,000$) with a silyl ether-protected chain-end.	80
Figure 3.10. ¹ H NMR spectra for (a) hydroxyl-, (b) tosyl-, and (c) azide-terminated polystyrene	82
Figure 3.11. SEC trace for azide-terminated polystyrene	82
Figure 3.12. SEC traces for the reactions in (a) DMF/PMDETA, (b) THF/PMDETA, and (c) DMF/bipyridyl at room temperature.	85
Figure 3.13. SEC trace for the grafting reaction of azide-terminated ($M_n = 5200$) side chains onto an acetylenated G0 substrate.	87
Figure 3.14. SEC trace for the grafting of azide-terminated ($M_n = 5200$) side chains onto an acetylenated G1 substrate	88
Figure 3.15. SEC trace for grafting azide-terminated ($M_n = 45,000$) side chains onto an acetylenated linear polystyrene substrate	89
Figure 3.16. SEC trace for the reaction in DMF after 4 days at room temperature using PMDETA as ligand.....	90
Figure 3.17. SEC trace of arborescent polystyrene of different generations	93
Figure 3.18. ¹ H NMR spectra for (a) reduced, (b) chlorinated, and (c) azide-functionalized polystyrene.....	94
Figure 3.19. ¹ H NMR spectra for (a) hydroxyl-, and (b) acetylene-terminated polystyrene.	96
Figure 3.20. SEC trace for acetylene-terminated polystyrene	96

Figure 3.21. SEC trace for grafting acetylene-terminated $M_n = 5200$ side chains onto azide-functionalized linear polystyrene.....	98
Figure 4.1. ^1H NMR spectra for (a) acetylated polystyrene and (b) secondary alcohol-functionalized linear polystyrene.....	114
Figure 4.2. SEC trace for linear secondary alcohol-functionalized polystyrene	115
Figure 4.3. ^1H NMR spectra for tertiary alcohol-functionalized polystyrene.....	116
Figure 4.4. SEC trace for tertiary alcohol-functionalized polystyrene	116
Figure 4.5. SEC traces for grafting of poly(ethyl vinyl ether) chains from linear polystyrene with secondary alcohol sites.	120
Figure 4.6. SEC traces for grafting of poly(ethyl vinyl ether) chains from linear polystyrene with tertiary alcohol sites.....	120
Figure 4.7. SEC traces for grafting of poly(ethyl vinyl ether) chains from secondary alcohol-functionalized G0 polystyrene.....	122
Figure 4.8. SEC traces for grafting of poly(ethyl vinyl ether) chains from tertiary alcohol-functionalized G0 polystyrene.....	122
Figure 4.9. SEC traces for grafting of poly(ethyl vinyl ether) chains from secondary alcohol-functionalized G1 polystyrene.....	123
Figure 4.10. SEC traces for grafting of poly(ethyl vinyl ether) chains from tertiary alcohol-functionalized G1 polystyrene	124
Figure 5.1. SEC trace for linear polybutadiene	143
Figure 5.2. ^1H NMR spectra for (a) polybutadiene, (b) epoxidized polybutadiene, and (c) hydroxylated polybutadiene.....	143

Figure 5.3. ¹ H NMR spectra for (a) tosylated polybutadiene, and (b) azide-functionalized polybutadiene.....	144
Figure 5.4. SEC trace for azidated polybutadiene	145
Figure 5.5. SEC trace for linear polybutadiene synthesized with 6- <i>tert</i> -butyldimethylsiloxyhexyllithium	146
Figure 5.6. ¹ H NMR spectra for polybutadiene with (a) a silyl ether end group, and (b) a hydroxyl end group.....	147
Figure 5.7. ¹ H NMR spectrum for acetylene-terminated polybutadiene	148
Figure 5.8. SEC traces for the reactions in (a) toluene, (b) THF/DMF, and (c) toluene/DMF at 23 °C, using PMDETA as ligand.....	150
Figure 5.9. SEC trace for the reactions in toluene/DMF using PMDETA as ligand at (a) room temperature and (b) 50 °C.....	151
Figure 5.10. SEC trace for grafting in toluene/DMF with PMDETA at 50 °C for 48 h.....	152
Figure 5.11. SEC trace for grafting acetylene-terminated side chains ($M_n = 5200$) onto an azidated G0 substrate.....	153
Figure 5.12. SEC trace for grafting acetylene-terminated side chains ($M_n = 5200$) onto an azidated G1 substrate.....	154
Figure 5.13. ¹ H NMR spectrum for linear acetylenated polybutadiene	157
Figure 5.14. SEC trace for randomly acetylene-functionalized polybutadiene	157
Figure 5.15. ¹ H NMR spectra for (a) hydroxyl-, (b) tosyl-, and (c) azide-terminated polybutadiene	158
Figure 5.16. SEC trace for grafting azide-terminated ($M_n = 5200$) side chains onto a linear acetylenated substrate	160

Figure 6.1. SEC trace for linear polybutadiene.....	176
Figure 6.2. ¹ H NMR spectra for (a) linear and (b) hydrosilylated polybutadiene	176
Figure 6.3. SEC trace for grafting $M_n = 5800$ high 1,2-microstructure content polybutadienyllithium onto linear hydrosilylated polybutadiene.....	178
Figure 6.4. SEC trace for pure G0 graft polybutadiene.....	178
Figure 6.5. SEC trace for grafting high 1,4-microstructure content ($M_n = 5600$) polybutadienyllithium onto hydrosilylated G0 substrate.....	180
Figure 6.6. SEC trace for grafting high 1,4-microstructure content ($M_n = 31,000$) polybutadienyllithium onto a hydrosilylated G0 substrate.....	181
Figure 6.7. SEC trace for grafting high 1,4-microstructure content $M_n = 51,000$ polybutadienyllithium onto a hydrosilylated G0 substrate.....	181
Figure 6.8. SEC trace for grafting high 1,4-microstructure content $M_n = 78,000$ polybutadienyllithium onto a hydrosilylated G0 substrate.....	182
Figure 6.9. SEC trace for grafting $M_n = 5700$ high 1,2-unit content polybutadienyllithium onto hydrosilylated G0 polybutadiene.....	184
Figure 6.10. SEC trace for purified G1 graft polybutadiene with a high 1,2-microstructure content.....	185
Figure 6.11. SEC traces for grafting (a) $M_n = 51,000$ (b) $M_n = 29,000$ and (c) $M_n = 5400$ 1,4- microstructure polybutadienyllithium onto the G1 hydrosilylated substrate.	187

List of Schemes

Scheme 2.1. General scheme for the synthesis of arborescent polymers..	7
Scheme 2.2. Arborescent polystyrene synthesis by grafting onto chloromethylated polystyrene.	10
Scheme 2.3. Arborescent polystyrene synthesis by grafting onto acetylated polystyrene	12
Scheme 2.4. One-pot synthesis of a G1 arborescent polystyrene.	18
Scheme 2.5. Reaction steps used to synthesize an arborescent copolymer incorporating a G1 polystyrene core and a poly(ethylene oxide) shell.	40
Scheme 2.6. Synthesis of arborescent polyisoprene by grafting onto epoxidized polyisoprene.	45
Scheme 3.1. “Click” coupling between a terminal azide and an alkyne to yield a 1,2,3-triazole.	56
Scheme 3.2. Proposed strategies for the synthesis of arborescent polystyrene.	57
Scheme 3.3. Synthesis and acetylation of polystyrene substrate.	70
Scheme 3.4. Synthesis and azide-end functionalization of polystyrene side chains.	71
Scheme 3.5. Synthesis and azidation of polystyrene substrate.	71
Scheme 4.1. Synthesis of polystyrene substrates with secondary or tertiary alcohol functionalities.	112
Scheme 4.2. Grafting of poly(ethyl vinyl ether) chains from hydroxylated polystyrene.	113
Scheme 5.1. Proposed strategies for the synthesis of arborescent polybutadiene.	130
Scheme 5.2. Synthesis of azidated polybutadiene substrate.	140
Scheme 5.3. Synthesis of alkyne-terminated polybutadiene side chains.	140
Scheme 5.4. Synthesis of alkynylated polybutadiene substrate.	141
Scheme 5.5. Synthesis of azide-terminated polybutadiene side chains	141

Scheme 6.1. Synthesis of G1 polybutadiene by grafting onto hydrosilylated substrates. 174

List of Tables

Table 2.1 Characteristics of successive generations of two series of arborescent polystyrene....	14
Table 3.1. Grafting yield in DMF and THF at 50 °C using PMDETA as ligand.	83
Table 3.2. Grafting yield in DMF and THF at room temperature using PMDETA and bipyridyl as ligands.	84
Table 3. 3 Characteristics of arborescent polystyrene of different generations.....	91
Table 4.1. Characteristics of arborescent graft PEVE copolymers.....	125
Table 5.1 Grafting yield in DMF, THF, and toluene using PMDETA and bipyridyl as ligands.	146
Table 5.2 Characteristics of arborescent polybutadiene of successive generations.....	155
Table 6.1 Characteristics of G1 arborescent polybutadiene	175
Table 6.2. Characteristics of G2 arborescent polybutadiene.	187

List of Abbreviations and Symbols

DTBP	2,6-Di- <i>tert</i> -butylpyridine
2VP	2-Vinylpyridine
ATRP	Atom transfer radical polymerization
b	Block
BHT	2,6-Di- <i>tert</i> -butyl-4-methylphenol
bipy	2,2'-Bipyridyl
CuAAC	Copper (I)-catalyzed azide-alkyne Huisgen cycloaddition
<i>d</i>	Deuterated
DCM	Dichloromethane
D_h	Hydrodynamic diameter
DIB	1,3-Diisopropenylbenzene
DLS	Dynamic light scattering
DMF	N,N-Dimethylformamide
dn/dc	Refractive index increment
DPE	1,1-Diphenylethylene
DRI	Differential refractive index
EO	Ethylene oxide
equiv	Equivalent(s)
EVE	Ethyl vinyl ether
f_n	Number-average branching functionality
G	Generation

<i>g</i>	Graft
G_y	Grafting yield
h	Hour(s)
$^1\text{H NMR}$	Proton nuclear magnetic resonance
LHAA	(6-Lithiohexyl)acetaldehyde acetal
<i>m</i> -CPBA	3-Chloroperoxybenzoic acid
meq	Milliequivalent(s)
MeOH	Methanol
M_n	Number-average molecular weight
MW	Molecular weight
M_w	Weight-average molecular weight
MWD	Molecular weight distribution
n	Refractive index
<i>n</i> -BuLi	<i>n</i> -Butyllithium
P2VP	Poly(2-vinylpyridine)
PBD	Polybutadiene
PCL	Poly(ϵ -caprolactone)
PDI	Polydispersity index
PEG	Poly(ethylene glycol)
PEO	Poly(ethylene oxide)
PEVE	Poly(ethyl vinyl ether)
PIP	Polyisoprene
PMDETA	<i>N,N,N',N'',N''</i> -Pentamethyldiethylenetriamine

PMMA	Poly(methacrylic acid)
PS	Polystyrene
PS- <i>d</i>	Deuterated polystyrene
P <i>t</i> BA	Poly(<i>tert</i> -butyl acrylate)
P <i>t</i> BMA	Poly(<i>tert</i> -butyl methacrylate)
PTFE	Polytetrafluoroethylene
PVME	Poly(vinyl methyl ether)
R _g	Radius of gyration
ROP	Ring-opening polymerization
SANS	Small-angle neutron scattering
SEC	Size exclusion chromatography
<i>sec</i> -BuLi	<i>sec</i> -Butyllithium
SEC-MALLS	Size exclusion chromatography multi angle laser light scattering
TBAF	Tetrabutylammonium fluoride
TBDMS-O-Hexyl-Li	6- <i>tert</i> -Butyldimethylsiloxyhexyllithium
<i>t</i> Bu	<i>tert</i> -Butyl
TESPLi	5-Triethylsilyl-4-pentynyllithium
THF	Tetrahydrofuran
TMEDA	<i>N,N,N',N'</i> -Tetramethylethylenediamine
TsCl	<i>p</i> -Toluenesulfonyl chloride
UV	Ultraviolet
VLE	Vapor-liquid equilibrium

Chapter 1

Foreword

1.1 Opening Remarks

Arborescent polymers are characterized by a dendritic (multi-level) branched architecture derived from a generation-based growth scheme, typically involving cycles of substrate functionalization and (mainly anionic) grafting reactions.¹ These polymers are of interest, among others, because of their distinctive physical properties and well-defined architectures.² The main distinguishing features of arborescent polymers are their assembly from polymeric building blocks of uniform size, and the very high molecular weights attained in few synthetic steps.

Different monomers can be polymerized by anionic techniques, and the incorporation of more than one monomer type in the synthetic scheme has allowed the preparation of a variety of arborescent homopolymers^{3,4} and copolymers.^{5,6} Unfortunately the synthesis of arborescent polymers by anionic coupling is tedious, and the grafting yield attained decreases rapidly as the size of the coupling substrate (generation number) and the side chains increase. Alternate coupling techniques, for example using “click” chemistry,^{7,8} are of considerable interest as they could alleviate some of the problems encountered in anionic coupling.

1.2 Research Objectives and Thesis Outline

The synthesis of arborescent polymers by “click” chemistry is the main focus of the research described herein. Some of the intermediates serving in the “click” grafting schemes developed were also explored as cationic macroinitiators for the preparation of novel types of arborescent copolymers. Finally, anionic coupling was utilized for comparison to “click” grafting in the synthesis of arborescent polymers.

This dissertation comprises seven chapters. Following this Foreword, a literature review is presented (Chapter 2) which provides background information divided into two sections: The first part discusses the synthesis of arborescent polymers, by summarizing the results obtained in our laboratory up to date; the second part discusses work by other research groups on the synthesis of arborescent polybutadiene, as well as the synthesis of star and block copolymer structures by “click” coupling. Chapter 3 reports on the synthesis and the characterization of arborescent polystyrene obtained by a novel “click” grafting technique. Comb-branched, first-generation (G1), and second-generation (G2) arborescent polystyrenes were synthesized from $M_n \approx 5000$ side chains, as well as G0 and G1 systems with $M_n \approx 45,000$ side chains. Chapter 4 discusses the utilization of the polystyrene systems synthesized by “click” chemistry, functionalized with secondary or tertiary hydroxyl groups, as macroinitiators for the cationic polymerization of ethyl vinyl ether. The synthesis of arborescent polybutadiene by “click” grafting, which also represents a novel synthetic route for the preparation of these materials, is discussed in Chapter 5. The synthesis of G0, G1, and G2 arborescent polybutadiene structures from $M_n \approx 5000$ side chains is reported. The synthesis of arborescent polybutadiene by anionic coupling was also completed (Chapter 6), for comparison with the “click” grafting path, using chlorosilane-functionalized substrates.

In agreement with the University of Waterloo Thesis guidelines, Chapters 2-6 are written in the format of individual papers to be submitted for publication in scientific journals. Included within each chapter is an introductory section providing background related to the specific topic considered, experimental methods, results, discussion, and conclusions.

Chapter 2

Arborescent Polymers and “Click”

Chemistry

2.1 Introduction

Branched macromolecules fall into three main classes: star-branched polymers, characterized by multiple chains linked at one central point,¹ comb-branched polymers, having one linear backbone and side chains randomly distributed along it,² and dendritic polymers, with a multi-level branched architecture.³ The cascade-branched structure of dendritic polymers is typically derived from polyfunctional monomers under more or less strictly controlled polymerization conditions. This class of macromolecules has a unique combination of features and, as a result, a broad spectrum of applications is being developed for these materials in areas including microencapsulation, drug delivery, nanotechnology, polymer processing additives, and catalysis.

Dendritic polymers may be further subdivided into three categories on the basis of their architecture, namely dendrimers, hyperbranched polymers, and dendrigraft polymers³ (Figure 2.1). Dendrimers, the first dendritic polymers reported in the literature, are obtained from a generation-based scheme using small molecule monomers as building blocks. Their synthesis is performed either in a core-first (divergent) or core-last (convergent) manner, using cycles of protection, condensation, and deprotection of AB_n -type monomers. Since strict control is attained over molecular architecture in this approach, dendrimers can have extremely narrow molecular weight distributions (MWD), with polydispersity indices $M_w/M_n < 1.01$, and exactly predictable molecular weights. However, since small molecule building blocks are used, many reaction cycles are necessary to synthesize high molecular weight dendrimers. These complex reaction sequences are avoided in the synthesis of hyperbranched polymers, the second family of dendritic polymers. Hyperbranched polymers with a high molecular weight can be obtained in one-pot self-condensation reactions of AB_n monomers without protecting groups, with the tradeoff that control over the molecular weight and branching is much more limited. The random

nature of the condensation reaction leads to polymers with many structural flaws and a broad MWD ($M_w/M_n > 2$) in most cases.

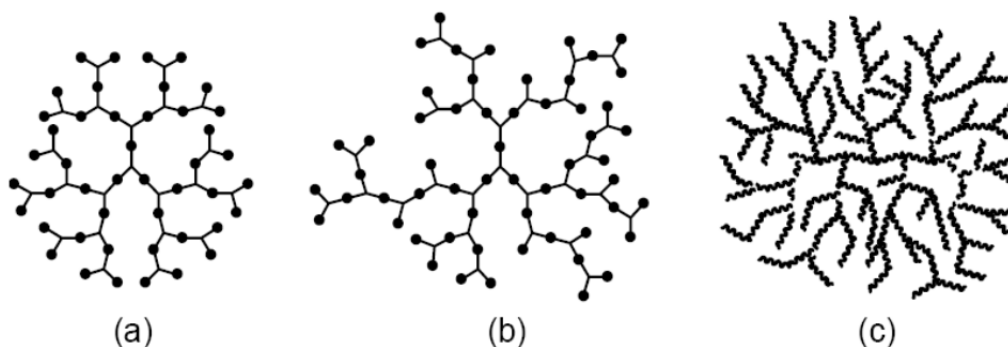
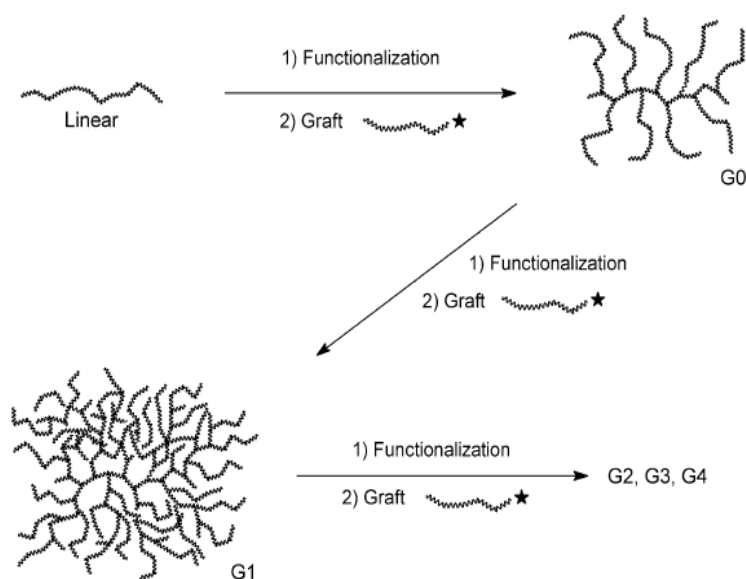


Figure 2.1. Schematic representation of (a) dendrimers, (b) hyperbranched, and (c) dendrigraft polymers. Reprinted with permission from Reference 8. Copyright 2004 Elsevier.

The third family of dendritic polymers, the dendrigraft systems, was introduced simultaneously in 1991 as the Comb-burst polymers by Tomalia et al.,⁴ and as the arborescent polymers by Gauthier and Möller.⁵ Dendrigraft (or arborescent) polymers are synthesized in a generation-based scheme analogous to dendrimers, but using cycles of ionic polymerization and grafting reactions, and polymeric chains as building blocks rather than small molecules (Scheme 2.1). A linear polymer substrate functionalized with coupling sites is first reacted with ‘living’ polymer chains to yield a comb-branched structure, also called a generation zero (G0) arborescent polymer. A further cycle of functionalization to introduce coupling sites on the G0 substrate and grafting with side chains leads to the first-generation (G1) arborescent polymer, and subsequently to higher generations (G2, G3, etc.). It should be noted that the G1 (twice-grafted) macromolecules represent the first polymer generation with a true dendritic (multi-level) branched architecture. Because the building blocks in arborescent polymer syntheses are

polymeric chain segments and a large number of coupling sites are introduced in each cycle (branching multiplicity $f = 10-15$ coupling sites per side chain), rapid molecular growth is observed over successive generations. Since the functionalization reaction used to introduce coupling sites on the substrates takes place randomly, the branched structure obtained also bears similarities to hyperbranched polymers. While this architecture is not as strictly controlled as for dendrimers, the MWD achieved for these materials still remains narrow ($M_w/M_n \approx 1.1$ typically).



Scheme 2.1. General scheme for the synthesis of arborescent polymers. Reprinted with permission from Reference 8. Copyright 2004 Elsevier.

This Chapter focuses on the efforts aimed at the synthesis and physical characterization of arborescent polymers, and the synthesis of star and block copolymers by “click” chemistry coupling. The synthesis of arborescent styrene, isoprene and butadiene homopolymers is discussed, together with copolymers incorporating a polystyrene substrate grafted with side chains of different compositions such as poly(2-vinylpyridine), polyisoprene, poly(*tert*-butyl

methacrylate), and poly(ethylene oxide). The synthesis of arborescent polybutadiene and various star and block copolymer systems by “click” chemistry is also discussed. Earlier developments in the field of arborescent polymers have been the topic of other reviews.⁶⁻⁸

2.2 Arborescent Polystyrene

Arborescent homopolymers are interesting, among others, as model compounds to study the properties of branched macromolecules beyond other systems such as star-branched polymers and microgels, due to the high branching functionalities and the extensive control achieved over the architecture (branching density, side chain molecular weight) of the molecules. The synthesis of arborescent styrene homopolymers and some of their physical properties will be discussed first.

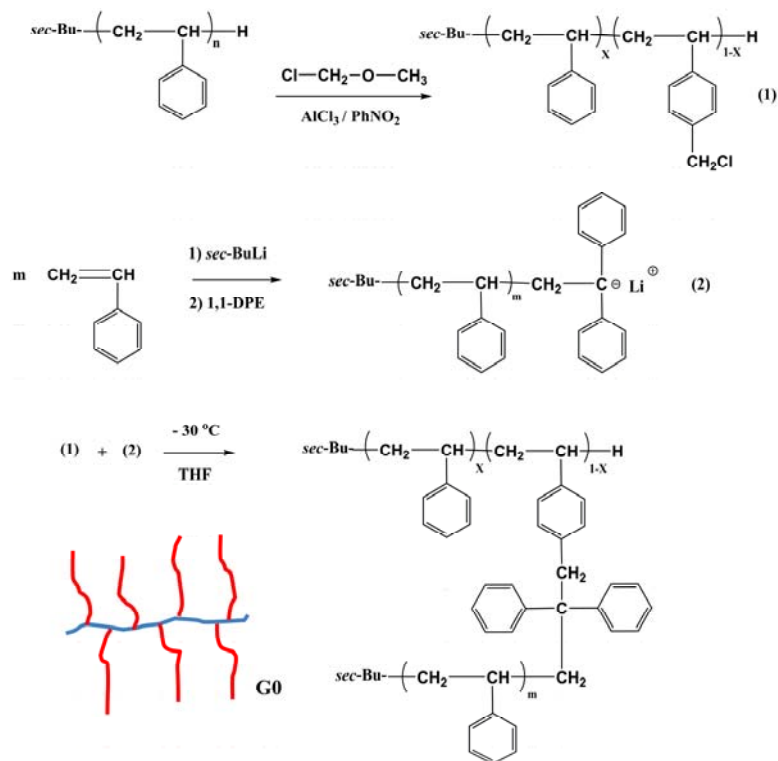
Polystyrene is a convenient starting material for the synthesis of arborescent polymers, since its aromatic pendent groups allow the facile introduction of coupling sites suitable for the synthesis of successive generations. The preparation of arborescent polystyrene has been achieved by three different methods. The first two are based on the “grafting onto” procedure described in Scheme 2.1 using chloromethyl or acetyl coupling sites; the third approach uses a one-pot “grafting from” technique.

2.2.1 Arborescent Polystyrene from Chloromethyl Coupling Sites

The first synthetic path, relying on the partial chloromethylation of linear polystyrene⁵ (Scheme 2.2), was introduced in 1991 and reviewed on a few occasions. Consequently, only the main features of these reactions will be considered here for comparison with the methods

developed more recently for copolymers. Chloromethylation poses two major obstacles to the synthesis of arborescent polymers. It is sensitive to cross-linking, since further reaction of the chloromethylated ring with another styrene unit leads to the formation of a methylene bridge either intra- or intermolecularly. These side reactions were minimized by working in dilute solution with a large excess of chloromethyl methyl ether, using Lewis acids such as SnCl_4 ⁵ or AlCl_3 /1-nitropropane.⁹ Another important issue is the occurrence of metal-halogen exchange competing with the coupling reaction and lowering the *grafting yield* (defined as the fraction of living chains generated in the reaction becoming attached to the substrate). This problem was overcome by capping the polystyryllithium chains with a single 1,1-diphenylethylene (DPE) unit. Another interesting feature of DPE capping is that the resulting deep red coloration of the DPE macroanions is convenient for visual monitoring of the coupling step, as a solution of chloromethylated polystyrene substrate is slowly added to the living chains until the color fades. Repetition of cycles of chloromethylation and grafting reactions according to these procedures led to arborescent polystyrene of generations G0-G3 in up to 96% yield.

Anionic polymerization produces side chains with a controllable molecular weight and a narrow MWD. The number of coupling sites on the grafting substrate can also be varied, providing a handle over the branching density for each generation. The side chain molecular weight and branching density may thus be controlled independently for each generation.



Scheme 2.2. Arborescent polystyrene synthesis by grafting onto chloromethylated polystyrene.

2.2.2 Arborescent Polystyrene from Acetyl Coupling Sites

The introduction of coupling sites on polystyrene via chloromethylation, besides being complicated by side reactions, also relies upon hazardous and expensive reagents including chloromethyl methyl ether and carbon tetrachloride. An alternate grafting method was developed to eliminate these problems with acetyl coupling sites¹⁰ as depicted in Scheme 2.3. Acetyl chloride, apart from being less harmful than chloromethyl methyl ether, reacts quantitatively in the reaction and is not susceptible to cross-linking. The synthesis begins with the random acetylation of polystyrene with acetyl chloride and AlCl_3 in nitrobenzene, followed by coupling with polystyryllithium. In this approach capping of the polystyryllithium chains with a few units of 2-vinylpyridine (2VP), and the addition of LiCl were necessary to avoid deactivation of the

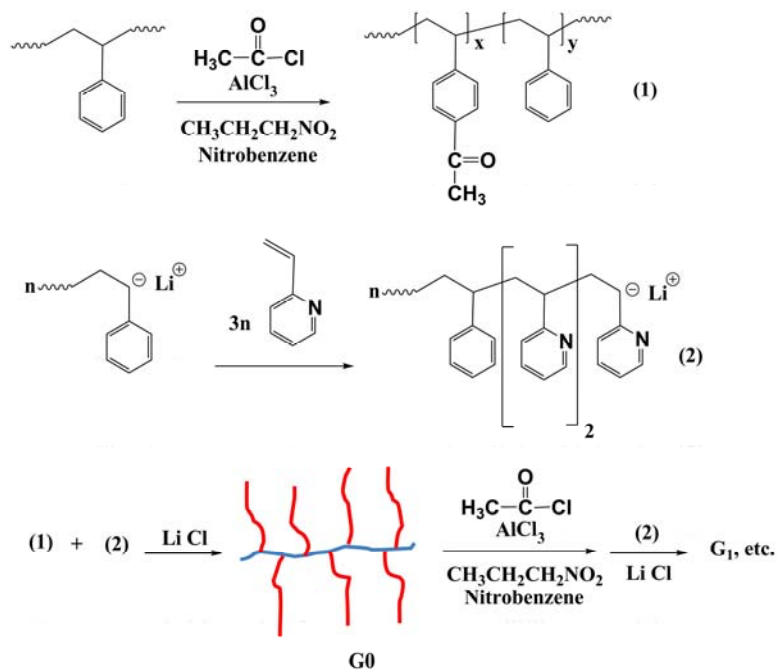
polystyryllithium species by proton abstraction from the acetyl groups. This side reaction was indeed found to limit the grafting yield to ca. 65% for direct coupling of polystyryllithium with acetylated polystyrene in the absence of reactivity modifiers, independently of the solvent type and temperature used. After capping the chains with 2VP, repetition of the acetylation and grafting reaction cycle yielded arborescent polystyrene of generations G0-G3 in 43-95% yield.

Characterization data for two series of arborescent polystyrene samples based on the acetylation path are provided in Table 2.1 as an example.¹⁰ The polymers were synthesized from either $M_w \approx 5000$ (PS5) or $M_w \approx 30,000$ (PS30) polystyrene side chains. The sample nomenclature used identifies the generation number of the substrate as well as the molecular weight of the side chains grafted in the last reaction. For example, G1PS-PS5 refers to a G1 polystyrene substrate grafted with $M_w \approx 5000$ side chains, while G1PS-PS30 refers to the same substrate grafted with $M_w \approx 30,000$ side chains. It should be noticed that sample PS-PS5 became substrate G0PS after acetylation, and so on. The weight-average branching functionality of the polymers, defined as the number of chains added in the last grafting reaction, was calculated according to the equation

$$f_w = \frac{M_w(G) - M_w(G - 1)}{M_w^{br}}$$

where $M_w(G)$, $M_w(G - 1)$, and M_w^{br} are the absolute weight-average molecular weight of graft polymers of generation G, of the preceding generation and of the side chains, respectively. A wide range of molecular weights and branching functionalities were attained by the procedure described in Scheme 2.3 while maintaining a narrow MWD ($M_w/M_n \leq 1.1$). The absolute molecular weight (from light scattering measurements) and branching functionality increase in an approximately geometric fashion over successive generations, however the grafting yield

decreases due to steric hindrance within the highly branched substrates limiting the accessibility of the coupling sites. Other factors lowering the grafting yield are residual protic impurities and side reactions with the solvent (THF) deactivating the living chains. Comparison of the apparent molecular weights (M_w , column 7 of Table 2.1), from size exclusion chromatography (SEC) analysis using a linear polystyrene standards calibration curve, with the absolute M_w determined from light scattering measurements (column 5) shows that the linear standards calibration method strongly underestimates the molecular weight of arborescent polymers, due to their very compact structure.



Scheme 2.3. Arborescent polystyrene synthesis by grafting onto acetylated polystyrene substrates.

Table 2.1. Characteristics of successive generations of two series of arborescent polystyrene. Adapted with permission from Reference 10. Copyright 2001 American Chemical Society.

Sample	side chains				graft polymers		
	M_w^a	M_w/M_n^a	Yield (%) ^b	M_w^a	M_w/M_n^a	M_w^c	f_w
PS-PS5	4400	1.09	95	5.3×10^4	1.08	3.3×10^4	11
G0PS-PS5	4500	1.07	89	4.3×10^5	1.08	1.3×10^5	84
G1PS-PS5	5000	1.08	84	3.9×10^6	1.09	4.5×10^5	690
G2PS-PS5	5500	1.09	75	2.5×10^7			3800
PS-PS30	28500	1.09	87	3.2×10^5	1.08	1.9×10^5	11
G0PS-PS30	28700	1.07	75	2.1×10^6	1.07	4.7×10^5	71
G1PS-PS30	27800	1.06	55	1.1×10^7	1.09	7.1×10^5	380
G2PS-PS30	28500	1.08	43	6.1×10^7			2000

^a Absolute values determined from SEC-MALLS or laser light scattering measurements.

^b Fraction of side chains generated attached to the substrate.

^c Apparent values determined by SEC analysis with linear polystyrene standards calibration.

The availability of arborescent polymers on a large scale (100 g and over) is important for their detailed physical characterization and in the development of applications. Munam and Gauthier¹¹ demonstrated the large (100-g) scale synthesis of arborescent polystyrene according to the acetylation path described in Scheme 2.3. When the large scale reactions were carried out by the procedure developed for the small (10-15 g) scale synthesis, lower grafting yields were observed due in part to dimerization of the side chains prior to grafting. The origin of the problem was traced to decreased stirring efficiency in the large scale reactions: The very quick consumption of 2VP as it was added to the reactor left a portion of the macroanions non-capped,

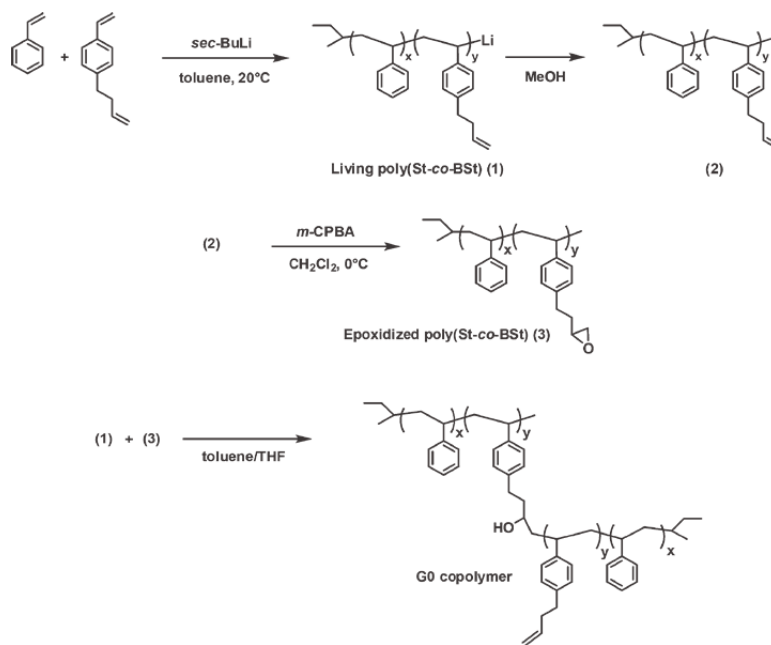
simply as a result of mixing inhomogeneities. Under these conditions, the highly reactive residual polystyryl anions can attack the 2VP ring of another chain already capped and cause dimerization of the side chains, which greatly hinders the coupling reaction. This problem was solved by adding DPE as a capping agent before 2VP. Since DPE does not homopolymerize, using 1.2 equiv of DPE per living end ensures that all the chains are capped with one DPE unit. The rate of the cross-over reaction from DPE to 2VP being lower than from styrene to 2VP, the 2VP capping reaction becomes less sensitive to mixing inhomogeneities and dimer formation is suppressed under these conditions. It should be noted that DPE alone is not suitable as a capping agent for the polystyryllithium chains, because the congested DPE macroanions favor proton abstraction from the acetyl coupling sites at the expense of nucleophilic addition. Grafting yields reaching 95% were achieved after capping with DPE and 3 equiv of 2VP for short ($M_w \approx 5000$) polystyrene side chains, while longer side chains ($M_w \approx 30,000$) made it necessary to increase the amount of 2VP in the capping step to 6 equiv per living end to maintain a high grafting yield.

2.2.3 Arborescent Polystyrene from Epoxide Coupling Sites

The introduction of coupling sites on polystyrene via acetylation definitely represents an improvement over chloromethylation, however acetylation still relies upon somewhat hazardous chemicals. The use of epoxide functionalities¹² can offer interesting advantages over chloromethyl or acetyl groups, as epoxidation can be achieved with common oxidants. Furthermore, attenuation of the reactivity of the polystyryl anions before the coupling reaction is unnecessary. The synthesis of arborescent polystyrene by that method (Scheme 2.4) began with the copolymerization of styrene and *p*-(3-butenyl)styrene initiated with *sec*-butyllithium in toluene, to produce a linear copolymer with a weight-average molecular weight $M_w = 4000$ and

$M_w/M_n = 1.05$. The pendant double bonds of the copolymer were then epoxidized with *m*-chloroperbenzoic acid. Coupling of the epoxidized substrate with living styrene-*p*-(3-butenyl)styrene copolymer chains having $M_w = 5000$ in a toluene/tetrahydrofuran mixture provided the G0 copolymer in 76% yield. The repetition of cycles of epoxidation and coupling with ‘living’ copolymer chains led to arborescent copolymer molecules of generations G1-G3 in 25-62% yield. The somewhat lower grafting yields achieved for the copolymers in the epoxidation path (in comparison to the acetylation method) was explained in part through chain end deactivation by the hydroxyl functionalities present at the branching points of the substrates (Scheme 2.4), in addition to living end deactivation by the solvent (THF) at room temperature.

A series of arborescent styrene homopolymers was also obtained by grafting $M_w = 5000$ polystyrene side chains onto the linear and G0-G2 copolymer substrates. SEC measurements showed that the graft polymers obtained had low polydispersity indices and molecular weights increasing geometrically over successive generations, albeit the grafting yields obtained were lower than for the copolymer side chains. This was attributed to the living polystyryl anions being less reactive than the styrene-*p*-(3-butenyl)styrene copolymer chains.



Scheme 2.4. Synthesis of a G0 arborescent styrene copolymer from epoxidized substrates.

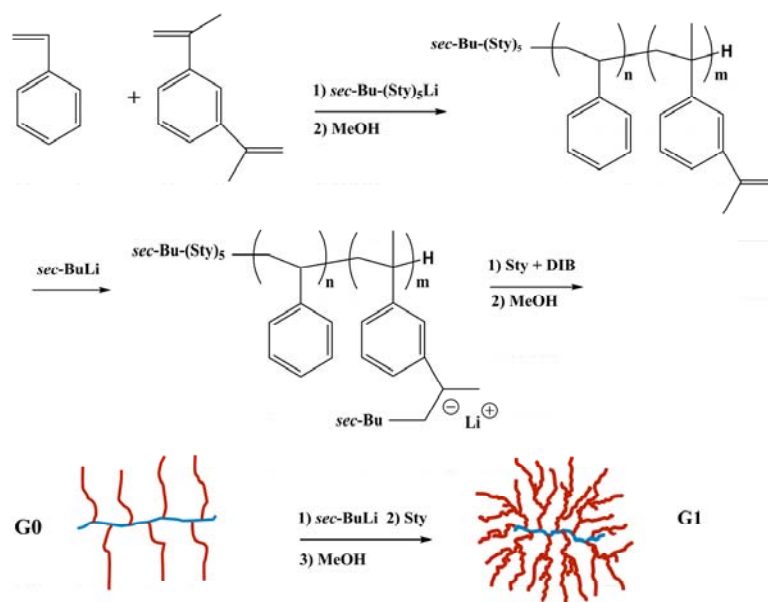
Reprinted with permission from Reference 12. Copyright 2012 John Wiley and Sons.

2.2.4 One-pot Synthesis of Arborescent Polystyrene

The step-wise synthesis of arborescent polymers, while able to generate large amounts of materials in good yield, requires isolation and purification of the crude product prior to substrate functionalization. For less demanding applications not requiring stringent removal of the linear polymer contaminant, a one-pot method was developed by Yuan and Gauthier¹³ for the synthesis of arborescent polystyrene without isolation of the reaction intermediates.

The synthesis, represented in Scheme 2.5, starts with the preparation of a linear copolymer of styrene and 1,3-diisopropenylbenzene (DIB) in a semi-batch copolymerization process. To this end it was necessary to optimize the reaction conditions in terms of the initiation method, the reaction temperature, and the monomer addition protocol used. The copolymerization reaction

was initiated with oligostyryllithium rather than *sec*-butyllithium (*sec*-BuLi), because of its greater selectivity toward monoaddition on DIB. A temperature of -78 °C was selected for the copolymerization with stepwise addition of the monomer, to ensure a uniform distribution of DIB units within the copolymer chains. The semi-batch addition protocol developed corresponds to successive additions of a monomer mixture containing 3 equiv of styrene and 1 equiv of DIB per living end, followed by a delay of 80-120 s to allow incorporation of the DIB unit at the chain end. This protocol, apart from achieving a more uniform distribution of branching points along the substrate, also yielded superior results in terms of polydispersity index and reproducibility in comparison with the drop-wise continuous addition of a styrene-DIB monomer mixture. The average spacing between branching points (DIB units) is thus expected to be 3 styrene units under these conditions (for a 3:1 styrene:DIB ratio). After terminating the linear copolymer chains by titration with methanol, the pendent isopropenyl moieties of the DIB units were activated *in situ* with 0.95 equiv of *sec*-BuLi for 4 h at -20 °C to generate a polyfunctional anionic macroinitiator. Further additions of styrene-DIB monomer mixture to the activated linear substrate yielded a comb-branched (generation G0) copolymer, also suitable as a polyfunctional anionic initiator after activation with *sec*-BuLi. The addition of styrene to the linear and G0 macroinitiators yielded G0 and G1 arborescent polystyrene structures, respectively.



Scheme 2.5. One-pot synthesis of a G1 arborescent polystyrene.

The synthesis of the G1 polymers with sub-stoichiometric activation of the DIB units was sensitive to cross-linking or gelation in the side chain growth step, due to the attack of residual (non-activated) isopropenyl moieties on the substrate by the polystyryllithium propagating centers. This problem was minimized by the addition of 6 equiv of LiCl per living end as a common ion salt to shift the dissociation equilibrium to the ion pair form. While the addition of styrene monomer to the activated G0 substrate in the absence of LiCl led to gelation in less than 1-2 min, no gelation was observed in the presence of LiCl over a few minutes; the reaction was nonetheless terminated 2 min after monomer addition as a precaution. Another strategy to avoid cross-linking was the addition of excess *sec*-BuLi in the activation step, to ensure the full consumption of the pendent isopropenyl moieties on the substrate, with the drawback of increased linear polymer contaminant formation.

The molecular weight of the side chains in the G1 polymers was conveniently controlled by varying the amount of monomer added to the G0 macroinitiator. Polymers with relatively low polydispersity indices ($M_w/M_n = 1.1-1.3$) and absolute M_w reaching 7×10^6 were thus obtained.

2.2.5 Physical Characterization of Arborescent Polystyrene

The influence of branching functionality and side chain molecular weight on the physical properties of arborescent polystyrene has been the topic of a number of investigations already reviewed.⁶⁻⁸ The main conclusion of these studies is that arborescent polymers behave increasingly like rigid spheres as their branching functionality is increased and/or the molecular weight of the side chains is decreased. Many of these investigations hinted at a *dual phase* morphology for arborescent polystyrene: Even the upper generation molecules retained residual interpenetrability, while their central (core) portion was much more hindered and less accessible. The validity of the hard core-soft shell – or perturbed hard sphere – model for arborescent polystyrene was verified in a number of investigations including the small-angle neutron scattering (SANS) experiments outlined below.

2.2.5.1 Neutron Scattering

The radius of gyration (R_g) of two series of arborescent polystyrene with different side chain molecular weights ($M_w \approx 5000$, PS5; $M_w \approx 30,000$, PS30) was determined in SANS experiments as a function of molecular weight over successive generations.¹⁴ The scaling relation $R_g \propto M_w^\nu$ was determined with scaling exponents $\nu = 0.26$ and 0.32 for the PS5 and PS30 series, respectively. These scaling factors correspond to an increase in average density over successive

generations for molecules with short side chains (PS5), while the average segmental density of the polymers with long side chains (PS30) remains approximately constant. The SANS data collected in cyclohexane-*d* displayed a pronounced maximum for the G1-G3 polymers in Kratky plots (scattering intensity $I(q)$ vs. q^2 , where $q = \sin(\theta)4\pi/\lambda$ is the scattering vector for a scattering angle θ and a wavelength λ), also observed for star and hyperbranched polymers, and predicted for spherical objects. Interestingly, no maximum was detected for the G0 polymer, corresponding to a comb-branched structure with twelve PS5 side chains grafted onto a PS5 backbone and expected to have a more ellipsoidal shape. The scattering peak became more pronounced for upper generations, the G3 polymer having multiple peaks characteristic for hard spheres of uniform size.

The morphology of the arborescent polystyrene molecules was also investigated by the SANS contrast matching method.¹⁴ To this end, G3 and G4 “copolymers” were synthesized by grafting deuterated polystyrene (PS-*d*) side chains onto G2 and G3 protonated arborescent polystyrene substrates in the last reaction cycle. The SANS measurements were carried out in both PS core-matching and PS-*d* shell-matching solvents. The R_g of the core should be obtained in a shell-matching solvent, since the polymer chains in the shell are invisible. When the scattering length density of the solvent matches the core, the R_g determined from the SANS data corresponds to a hollow sphere. The R_g for the G3 (G2PS-*graft*-PS-*d*) and G4 (G3PS-*graft*-PS-*d*) polymers was larger in THF-*d* than in cyclohexane-*d*, indicating excluded volume effects (core swelling) in the good solvent. SANS contrast matching also allowed detailed profiling of the radial segment density within the core and shell phases of arborescent graft polymers. It was thus shown that the higher generation G3PS-*graft*-PS-*d* polymer had better defined core-shell morphology (sharper core-shell interface) than the lower generation G2PS-*graft*-PS-*d* sample.

Enhanced phase separation between the core and the shell is an expected consequence of the preferential reaction of coupling sites located at the periphery of the grafting substrates, favored by the inaccessibility of coupling sites buried deeper within their structure.

SANS also served to probe interpenetration in blends of arborescent polystyrene with linear deuterated poly(vinyl methyl ether) (*d*-PVME) and polystyrene (*d*-PS).¹⁵ The interactions between the blend components were monitored as a function of the molar mass of the two components and temperature. The radius of gyration of the arborescent polymers decreased in all polymer blends in comparison to the values measured in solution. For G0, G1, and G2 polymers the R_g was comparable in blends with *d*-PVME and *d*-PS while for the G3 sample, the R_g in *d*-PS was smaller than in *d*-PVME and close to the value calculated for a collapsed sphere having the bulk density of PS. This indicates that the G3 molecules behave mainly like non-interpenetrating spheres, the linear *d*-PS matrix chains being largely excluded from the interior of the arborescent molecules. Fitting the single particle form factor for the arborescent polymers in the blends with a power law model for the density profile, corresponding to a diffuse arborescent polymer-matrix interface in the blends, was found to be more appropriate than fitting with a hard sphere model representing a sharp interface.

2.2.5.2 Solution Thermodynamics

The influence of polymer architecture on intermolecular interactions in dilute solutions was investigated by membrane osmometry in toluene (good solvent for polystyrene), cyclohexane (theta or θ solvent), and methylcyclohexane (poor solvent).¹⁶ The osmotic second virial coefficient (B_{22}) measured for arborescent polystyrene in toluene was lower than for homologous linear polymers, as expected due to their smaller R_g . In a θ solvent (cyclohexane), branching

lowered the θ temperature from 34.5 °C (linear homologue) to 32.2 °C (G0 polymer). The θ temperature for the G0 polystyrene sample in methylcyclohexane was likewise lowered to 36 °C, as compared to values estimated between 60 and 70 °C for linear polystyrene samples. The experimental osmotic pressure data were successfully fitted with a molecular-thermodynamic equation suitable for colloids, indicating that the behavior of arborescent polystyrene molecules in dilute solution corresponds to a perturbed (weakly interacting or interpenetrable) hard sphere.

Vapor-liquid equilibrium (VLE) measurements for binary solutions of arborescent and linear polystyrene samples in chloroform, toluene, and cyclohexane were performed by a classic gravimetric sorption method.¹⁷ In cyclohexane, the VLE data indicated that solvent absorption depends on the generation number (branching functionality) of the polymers. No dependence on generation number was observed in the VLE data for toluene or chloroform, however. The solvent-polymer interaction parameter (Flory parameter χ_{12}) calculated from the VLE data was compared with that calculated from the second virial coefficient derived from light scattering measurements.¹⁸ While the interaction parameter increased with the generation number for all solvents based on the second virial coefficients method, the trend was not as clear for the VLE results. The poor agreement between the two methods was attributed to the concentrated solution regime used for the VLE measurements, causing the solvent-polymer interactions to become primarily a function of enthalpic contributions. For example, chloroform and toluene are good solvents for arborescent polystyrene and favorable polymer-solvent interactions may result from favorable enthalpic contributions with relatively small entropic contributions. In contrast, cyclohexane is a poor solvent for arborescent polystyrene, perhaps because the enthalpic contribution to the solvation process is low. As the entropic contribution to solvation may be

significant in cyclohexane, the VLE results for polymers in cyclohexane may become dependent on the generation number.

The systematic manner in which the characteristics of dendrigraft homopolymers can be varied is useful to establish structure-property relationships for branched polymers. When considering potential applications, however, materials with a wider range of physical and chemical properties are of interest. An easy way to broaden the range of properties observed for arborescent macromolecules is by extending the scope of the synthetic techniques developed for arborescent polystyrene to allow the preparation of copolymers. The generation-based grafting scheme developed for arborescent polystyrene indeed relies on the presence of aromatic units enabling further functionalization with coupling sites, but this does not preclude the introduction of side chains with a different chemical composition in the last grafting reaction. The synthesis and properties of copolymers incorporating polymer segments of different compositions grafted on arborescent polystyrene substrates will be reviewed in the following sections.

2.3 Arborescent Polystyrene-*graft*-Poly(2-vinylpyridine)

Copolymers

The synthesis of arborescent copolymers from polystyrene substrates and poly(2-vinylpyridine) side chains (PS-*graft*-P2VP), useful as precursors for highly branched cationic polyelectrolytes, was achieved using both chloromethyl¹⁹ and acetyl²⁰ coupling sites. The synthesis of the copolymers follows the paths illustrated in Schemes 2.2 and 2.3 with minor changes, by substituting polystyryllithium with poly(2-vinylpyridinyl)lithium in the final grafting step. Two series of arborescent PS-*graft*-P2VP copolymers were synthesized by grafting either

short ($M_w \approx 5000$, P2VP5) or long ($M_w \approx 30,000$, P2VP30) side chains on the polystyrene substrates. Similar copolymer architectures and compositions were obtained using both chloromethyl and acetyl coupling sites.²⁰ Due to the relatively low reactivity of the P2VP anions, no capping was necessary prior to grafting on chloromethylated polystyrene to suppress metal-halogen exchange reactions, but the addition of LiCl was still beneficial to avoid proton abstraction from the acetylated substrates. Since the synthesis of P2VP copolymers from chloromethylated substrates was already reviewed, it will not be discussed in details here. The general characteristics of the arborescent P2VP copolymers obtained (molecular weight, branching functionality, polydispersity index) are comparable with those quoted for the styrene homopolymers (Table 2.1), the P2VP content varying from ca. 90-98% depending on the molecular weight of the side chains and the characteristics of the substrate.

A one-pot synthesis of arborescent PS-*graft*-P2VP copolymers incorporating P2VP chains was described according to the method illustrated in Scheme 2.5, by substituting styrene with 2-vinylpyridine in the final side chain growth step.²¹ Monomer addition to the linear and G0 styrene-diisopropenylbenzene copolymers activated with *sec*-BuLi led to the formation of the G0 and G1 copolymers, respectively, the side chain length being controlled by the amount of monomer added in the reaction. Interestingly, the MWD of the copolymers became narrower as the length of the side chains was increased. This effect was attributed to averaging of the propagating site reactivity in the larger molecules. The chemical compositions estimated by NMR analysis and calculated from the absolute molecular weight determined from light scattering measurements were in good agreement. This divergent “grafting from” strategy is clearly a powerful method to synthesize arborescent copolymers, providing control over both copolymer composition and structure.

2.3.1 Physical Characterization of Arborescent Polystyrene-*graft*-Poly(2-vinylpyridine)

2.3.1.1 Neutron and Light Scattering

The morphology of G0-G3 arborescent PS-*graft*-P2VP copolymers was characterized by SANS measurements in deuterated methanol (CD₃OD).²² Both polydispersed core-shell and (monodispersed) power law radial density models worked reasonably well to fit the SANS data but the power law model, corresponding to a somewhat diffuse P2VP shell surrounding a dense polystyrene core, provided the best fit. The density profiles obtained for all generations of arborescent PS-*graft*-P2VP copolymers in deuterated methanol otherwise provided no clear indication for the presence of a collapsed polystyrene core in the copolymers. This was explained by the low weight fraction (10-20%) of the polystyrene component in the copolymers, and a relatively diffuse core-shell interface due to the random distribution of grafting sites on the substrate. The scaling exponent for $R_g \propto M^\nu$ was determined as $\nu = 0.24$, hinting that the overall density of the molecules increased over successive generations.

The aggregation of weakly charged PS-*graft*-P2VP copolymers in methanol-*d*₄ and in D₂O was investigated by a combination of the SANS and dynamic light scattering (DLS) techniques in dilute solutions (mass fraction $\phi = 0.005$ - 0.05).²³ The most notable effect upon addition of a sub-stoichiometric amount of acid (< 1 equiv HCl/2VP unit) was the appearance of a scattering peak characteristic for polyelectrolyte solutions, and in agreement with previous observations for dendritic polyelectrolytes.²⁴ In analogy to the latter, the peak was interpreted as a correlation peak defined by the inter-particle distance in arborescent polymer aggregates resulting from

long-range Coulombic interactions. The interparticle distance calculated from the scattering peak for a uniform particle size distribution was consistent with liquid-like ordering of the charged arborescent graft copolymer molecules within the aggregates. The lower dielectric constant of methanol- d_4 led to long-range electrostatic interactions persisting to lower polymer concentrations than in D_2O . The DLS data displayed two diffusive relaxation processes upon addition of HCl to a G0PS-*graft*-P2VP copolymer solution. The slow mode dynamics were attributed to local structural inhomogeneities (aggregation) in the arborescent polyelectrolyte solutions: Both the SANS scattering peak and the slow diffusion mode disappeared upon addition of excess HCl to the solutions, which screened the electrostatic interactions and induced breakup of the aggregates. Molecular expansion was more significant for copolymers with long (P2VP30K) vs. short polyelectrolyte side chains (P2VP5K), which led to the P2VP30K molecules forming a gel upon addition of a sub-stoichiometric amount of HCl at low concentrations.

The extensive association of PS-*graft*-P2VP copolymers observed at low HCl/2VP ratios is in stark contrast with the situation encountered when excess HCl is present in solution: Dynamic light scattering measurements have shown that P2VP copolymers derived from polystyrene substrates of generations G0 and above exist as isolated (unimolecular) species under these conditions.²⁰ DLS measurements served to monitor changes in molecular dimensions upon ionization of the P2VP side chains,¹⁹ by comparing the hydrodynamic radius of the arborescent copolymer molecules measured in methanol and in methanol with 0.1 N HCl. The structure dependence of hydrodynamic volume expansion, expressed as the ratio of the hydrodynamic volume in acidic methanol (ionized) to that in pure methanol (neutral), is compared for linear and arborescent PS-*graft*-P2VP samples in Figure 2.2a. The DLS results show that the arborescent

P2VP copolymers expand much more in solution than the linear homologous polymers when protonated with HCl. This effect is attributed to the higher charge density attained in the branched, compact molecules. Copolymers with long, flexible P2VP30 side chains displayed the largest volume increases due to their enhanced flexibility relative to short side chain materials (P2VP5). Interestingly, volume expansion decreased within each copolymer series as the generation number increased, most likely as a result of structural stiffening.

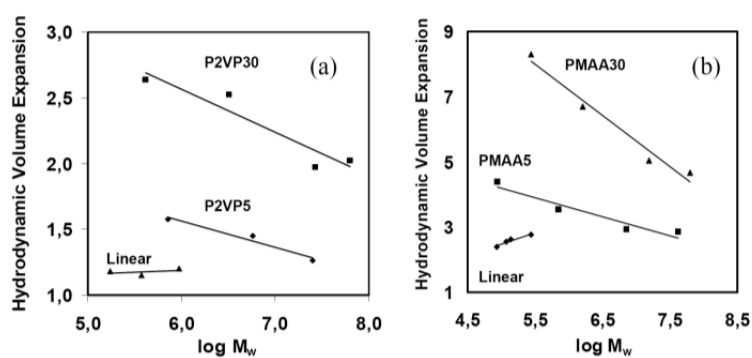


Figure 2.2. (a) Molecular weight dependence of hydrodynamic volume expansion for linear and arborescent P2VP graft copolymers dissolved in MeOH/H₂O 95/5 with HCl. (b) Molecular weight dependence of hydrodynamic volume expansion for linear and arborescent PMAA graft copolymers dissolved in MeOH/H₂O 95/5 with 0.05 N NaCl and NaOH. Volume expansion is expressed as the ratio of hydrodynamic volumes in the ionized and neutral forms. Reprinted with permission from Reference 19. Copyright 2002 American Chemical Society.

2.3.1.2 Micellar Properties

The amphiphilic character and the covalently bonded, stable structure of the PS-*graft*-P2VP copolymers is particularly interesting for applications as unimolecular micelles in the

solubilization of hydrophobic compounds in aqueous environments, and the sustained release of bioactive compounds.

The solubilization of various model hydrophobic probes (polycyclic aromatic hydrocarbons, PAH) by arborescent PS-*graft*-P2VP micelles of different generations and compositions in aqueous solutions was monitored by UV and fluorescence spectroscopy analysis.²⁵ The partitioning behavior of hydrophobic probes including naphthalene and pyrene derivatives between the arborescent micelles and water was found to depend on both the characteristics of the copolymers and the nature of the probes. Not surprisingly, arborescent copolymers with a higher polystyrene content had a greater solubilization capacity, but the solubilization rate and capacity also decreased for the upper generation copolymers, presumably due to their stiffer structure. Partition coefficients reaching around 10^6 were observed for very hydrophobic probes (e.g. pyrene), but the less hydrophobic PAH (e.g. naphthalene derivatives) gave higher micelle loadings due to non-specific sorption in the polystyrene core and the P2VP shell of the micelles.

The release kinetics of two drugs (indomethacin and lidocaine) from the dendritic PS-*graft*-P2VP micelles in dilute HCl solutions were also investigated by fluorescence and UV spectroscopy.²⁶ The copolymers were loaded with the drugs by dissolution in a common solvent (CH_2Cl_2 or CH_3Cl) before precipitation and washing with hexanes. Release from the micelles was monitored by dialysis in 0.05 M HCl. The release profiles obtained for indomethacin- and lidocaine-loaded G1 arborescent PS-*graft*-P2VP copolymers are compared in Figure 2.3. In contrast to the rapid equilibration observed for the free probes from dialysis tubing (100% release in less than 5 h) the release from the dendritic micelles was slow, corresponding to sustained characteristics. For both indomethacin and lidocaine, an initial burst in release over the first 5 h was followed by more gradual release until equilibration was attained over 1-2 days.

Furthermore, while roughly 80% of the loaded lidocaine was released from the micelles over the duration of the experiment, only about 40% of the indomethacin was released under the same conditions. Lidocaine being less hydrophobic than indomethacin, a large fraction of it was presumably located within the P2VP shell after encapsulation. This represents the fraction completely released within the time scale of the experiment. Incomplete release of the drugs from the micelles is more likely related to physical entrapment within the hydrophobic core and/or the palisade (interfacial) regions of the micelles. Another possibility, in the case of indomethacin, could be hydrogen bonding interactions between the pyridine ring of the P2VP chains and the carboxylate group of the drug. There are no such interactions between lidocaine and the arborescent micelles, which could also explain why a larger fraction of the encapsulated drug was released.

The results discussed above show that arborescent PS-*graft*-P2VP copolymers can be designed to solubilize or release hydrophobic compounds of different polarities at controllable rates.

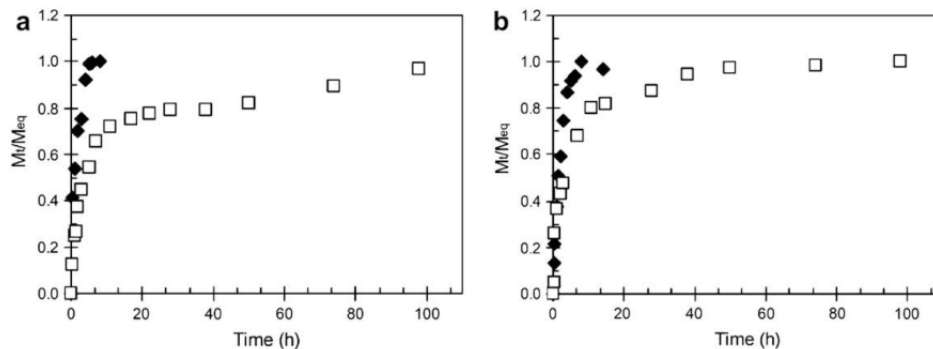


Figure 2.3. Release profiles for (a) indomethacin and (b) lidocaine in 0.05 M HCl in the free state (■) and from G1PS-*graft*-P2VP copolymer (□). M_t is the cumulative mass released at time t , and M_{eq} is the mass released at equilibrium. Reprinted with permission from Reference 26. Copyright 2008 Elsevier.

2.3.1.3 Self-assembly in Solution

In contrast to micelles formed by the self-assembly of linear block copolymer chains, rigid arborescent PS-*graft*-P2VP copolymer molecules are unable to reverse their core and shell components when exposed to a solvent selective for the polystyrene core, thus forcing the P2VP shell to directly contact the poor solvent. This unusual micellar morphology with a solvophilic core and a solvophobic shell is interesting with respect to the core-shell structure of unimolecular micelles and their self-assembly. The self-assembly of arborescent PS-*graft*-P2VP copolymers derived from a G1PS substrate was investigated as a function of temperature in toluene,²⁷ a solvent selective for the polystyrene core (Figure 2.4a). DLS measurements were used to monitor the hydrodynamic diameter (D_h) of G1PS-*graft*-P2VP5 in methanol and in toluene as a function of temperature. The D_h of the copolymer in methanol, a solvent selective for the P2VP shell, was essentially independent of temperature and no aggregation was observed, in agreement with

previous results.²² The copolymer also did not dissolve in toluene at low temperatures, as expected for this copolymer having a composition with 87% of insoluble P2VP branches within its shell. However the solution became transparent and the copolymer was molecularly dissolved above 26 °C, defined as the critical self-assembly temperature (cst). The size of the molecularly dissolved G1PS-*graft*-P2VP5 copolymer in toluene at these temperatures was about 10% lower than in methanol, indicating shrinkage of the P2VP shell in toluene as a consequence of the poor solvent quality.

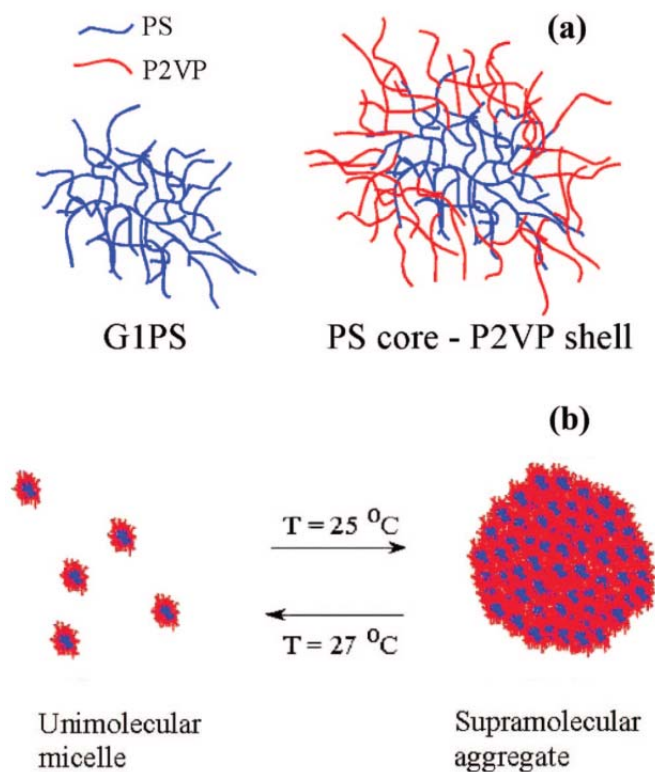


Figure 2.4. Schematic representation of (a) core-shell morphology and (b) temperature-responsive supramolecular self-assembly of arborescent PS-*graft*-P2VP5 copolymers in toluene.

Reprinted with permission from Reference 27. Copyright 2008 American Chemical Society.

Upon decreasing the temperature to 25 °C the D_h increased abruptly to a few micrometers, due to the formation of large aggregates having a somewhat broad size distribution but nonetheless a spherical topology. The DLS measurements confirmed that the supramolecular structures (Figure 2.4b) persisted at low temperatures, albeit some very large aggregates precipitated at temperatures below 20 °C. The influence of the P2VP chain length on the temperature-sensitive self-assembly process was analyzed by comparing copolymers with P2VP side chains having a number-average molecular weight (M_n) of either 5000 (P2VP5) or 30,000 (P2VP30). Similar thermoreversible self-assembly was observed for the copolymer with the P2VP30 side chains, but the c_{st} shifted to a higher temperature (41 °C). This shows that the critical temperature for the thermal responsiveness is tunable by varying the length of the P2VP segments within the shell. For comparison, the copolymer grafted with shorter (P2VP5) side chains at the same concentration displayed no aggregation whatsoever down to 27 °C. Clearly, aggregation becomes more favorable as the size of the insoluble branches increases. The self-assembly of arborescent copolymers in solution provides a new path for the creation of well-defined supramolecular structures of large dimensions. Most interestingly, the temperature-responsive self-assembly of the arborescent copolymers offers the possibility to produce new types of “smart” supramolecular structures.

2.4 Arborescent Polystyrene-*graft*-Polystyrene-*block*-Poly(2-vinylpyridine)

Beyond the core-shell morphologies already described, the grafting onto technique may also be applied to the generation of more complex molecular architectures such as layered

morphologies. This was recently demonstrated with the synthesis of arborescent polystyrene-*graft*-[poly(2-vinylpyridine)-*block*-polystyrene] copolymers and their application as templates for the preparation of gold nanoparticles.²⁸ The synthesis of these templates, represented schematically in Figure 2.5, was performed by grafting living polystyrene-*block*-poly(2-vinylpyridine) macroanions onto acetylated linear and branched (G1) polystyrene. The resulting dendritic species have a covalently bonded, layered structure with an inner P2VP shell that can be loaded with metallic compounds such as tetrachloroauric acid (HAuCl₄). The copolymer templates loaded at various levels were subsequently reduced in solution with hydrazine to produce gold nanoparticles. The characteristics of the arborescent copolymer templates governed the distribution of gold salt within the molecules: Templates containing the large G1PS hydrophobic core displayed lower salt loading in the center of the molecules, while smaller templates such as PS-*graft*-(P2VP-*block*-PS) (derived from linear polystyrene) had a uniform distribution of gold throughout. The solution reduction studies revealed that the size and uniformity of the gold nanoparticles obtained were independent of the template generation and rather reliant on the amount of reducing agent used. Excess hydrazine minimized the coalescence and led to a more uniform size distribution of gold nanoparticles within each template molecule.

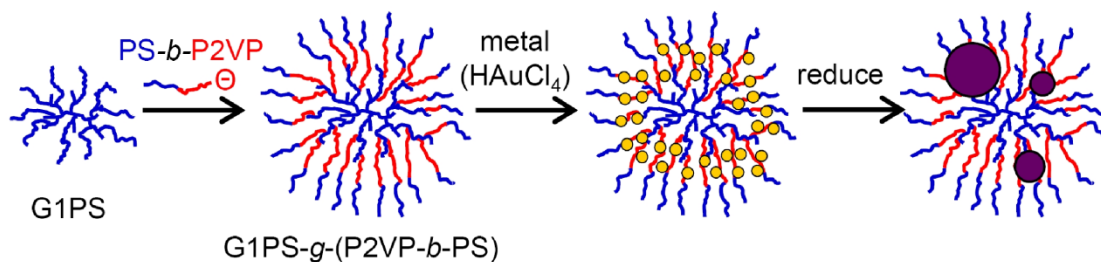


Figure 2.5. Schematic representation of an arborescent G2 copolymer template synthesis, metallic salt loading, and reduction. Reprinted with permission from Reference 28. Copyright 2008 American Chemical Society.

2.5 Arborescent Polystyrene-*graft*-Polyisoprene

The synthesis of polystyrene-*graft*-polyisoprene (PS-*graft*-PIP) copolymers was achieved from both chloromethylated and acetylated polystyrene substrates as illustrated in Schemes 2.2 and 2.3, respectively, using polyisoprenyllithium rather than polystyryllithium in the final grafting step.

The reaction with the acetylated substrates involved the polymerization of isoprene with *sec*-BuLi either in THF to yield polyisoprenyllithium with a mixed microstructure (approximately 1:1:1 ratio of 1,2-, 3,4-, and 1,4-units),²⁹ or in cyclohexane to obtain a high ($\geq 70\%$) *cis*-1,4-microstructure content.³⁰ The living polymer was then titrated with an acetylated substrate to generate the copolymer. The grafting yield was maximized at 25 °C in the presence of 5 equiv of LiCl per living end, to attenuate the reactivity of polyisoprenyllithium. Capping with a few 2VP units was not critical as in the synthesis of arborescent styrene homopolymers, but still

convenient to take advantage of the darker coloration of the polyvinylpyridinyl anions in the colorimetric titration process used to monitor the stoichiometry of the coupling reaction.

Arborescent copolymers were synthesized by grafting PIP side chains with a M_w of either 5000 (PIP5) or 30,000 (PIP30) onto linear, comb-branched (G0), G1, and G2 acetylated polystyrene. The polyisoprene content attained varied from 84-91% by weight for copolymers with short (PIP5) side chains, and from 92 to over 97% by weight for long (PIP30) side chains. The graft copolymers also exhibited the expected geometric increases in branching functionality and molecular weight over successive generations, as well as decreased grafting yields for longer polyisoprene side chains and higher generation substrates, due to steric congestion and increased sensitivity of the living ends to impurities.

A core-shell (heterogeneous) morphology was clearly observed by atomic force microscopy imaging in the phase contrast mode, even for copolymers with PIP30 side chains (Figure 2.6), due to differences in viscoelastic response for the glassy polystyrene-rich core and the rubbery polyisoprene-rich shell. The type of solvent serving to prepare the monolayer films by spin-casting also influenced the extent of phase separation between the core and the shell: Phase contrast was enhanced when using heptane, a solvent selective for the polyisoprene component, but decreased for non-selective solvents such as toluene and chloroform.

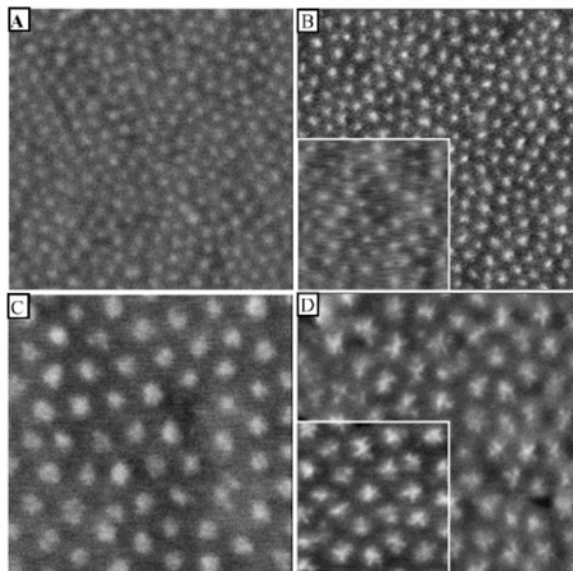


Figure 2.6. AFM images for samples prepared by spin-casting from solutions (concentration 1 mg/mL): (A) G0PS-PIP30 in toluene, (B) G0PS-PIP30 in heptane, (C) G1PS-PIP30 in toluene, (D) G1PS-PIP30 in heptane. The width of each picture is 500 nm. All images are shown in the phase mode to allow visualization of the molecular morphology due to the differences in viscoelastic behaviors of the polystyrene-rich and polyisoprene-rich phases. The insets of (B) and (D) are the height images, showing the topology of the monolayers. Adapted with permission from Reference 29. Copyright 2004 American Chemical Society.

Arborescent polystyrene-*graft*-polyisoprene copolymers, synthesized by grafting polyisoprenyl anions onto acetylated linear and branched polystyrene substrates, were investigated as processing additives for commercial polymers. The polyisoprene segments were modified by hydrosilylation with (tridecafluoro-1,1,2,2-tetrahydrooctyl)dimethylsilane on 17-52% of the isoprene units, and the polymers were blended with linear low density polyethylene

at 0.1 and 0.5% w/w to evaluate their performance as processing additives by extrusion at different shear rates.³¹ The branched copolymers and mainly the G0 copolymer led to significant improvements in the extrusion of linear low-density polyethylene, however the results were still somewhat inferior to a commercial polymer processing additive used for comparison.

2.5.1 Rheological Properties

The viscoelastic properties of arborescent PS-*graft*-PIP copolymers of generations G0-G3 having *cis*-1,4-polyisoprene side chains of different lengths were investigated³⁰ with dynamic mechanical measurements. The zero-shear viscosity (η_0) of the copolymers was 1-3 orders of magnitude lower than for linear polyisoprene samples of comparable molecular weight, but its scaling ($\eta_0 \propto M_w^\nu$, $\nu = 3.5-4$) was nonetheless consistent with entanglement formation. The zero-shear recoverable compliance J_e^0 increased linearly with the molecular weight of the copolymers to reach values up to 10 times larger than the limiting value observed for the linear PIP analogues. The modulus-frequency master curves obtained for the G0 and G1 copolymers were comparable to other branched polymers such as star and comb-branched systems. The G2 and G3 copolymers, in contrast, displayed features analogous to microgels and filled polymer systems. The change in behavior was attributed to a transition from a flexible branched structure (for generations G0 and G1) to a spherical rigid structure for generations G2 and above.

2.6 Arborescent Polystyrene-*graft*-Poly(*tert*-butyl methacrylate)

The synthesis of arborescent copolymers incorporating poly(*tert*-butyl methacrylate) (PtBMA) side chains, useful as precursors for highly branched anionic polyelectrolytes, was

achieved from bromomethylated polystyrene substrates.³² Two series of arborescent copolymers with either short ($M_w \approx 5000$) or long ($M_w \approx 30,000$) PtBMA side chains grafted onto linear, G0, G1, and G2 substrates were obtained by chloromethylation of the corresponding arborescent polystyrene and conversion to its bromomethylated analogue with NaBr in DMF/dibromomethane. The side chains were generated in THF from *tert*-butyl methacrylate and 1,1-diphenyl-2-methylpentyllithium in the presence of LiCl, and the graft copolymers by addition of a solution of the bromomethylated polystyrene substrate at 0 °C. Branching functionalities f_w ranging from 9-4500 and molecular weights ranging from 8.8×10^4 - 6.3×10^7 with narrow MWD ($M_w/M_n \approx 1.05$ -1.10) were thus obtained.

A one-pot method for the synthesis of arborescent polystyrene-*graft*-poly(*tert*-butyl methacrylate) copolymers was also reported²¹ following the reaction path illustrated in Scheme 2.5, the purified *tert*-butyl methacrylate monomer being added to the anionic macroinitiator in the last side chain growth step. The synthesis of G0 and G1 arborescent copolymers was thus achieved by initiating the polymerization of the methacrylate monomer with the linear and G0 styrene-diisopropenylbenzene copolymer substrates activated with *sec*-BuLi, respectively. Copolymers with PtBMA side chains having a target $M_n \approx 2500$, 5000, 10,000, and 20,000 were obtained through successive monomer additions to the polymerization reactor.

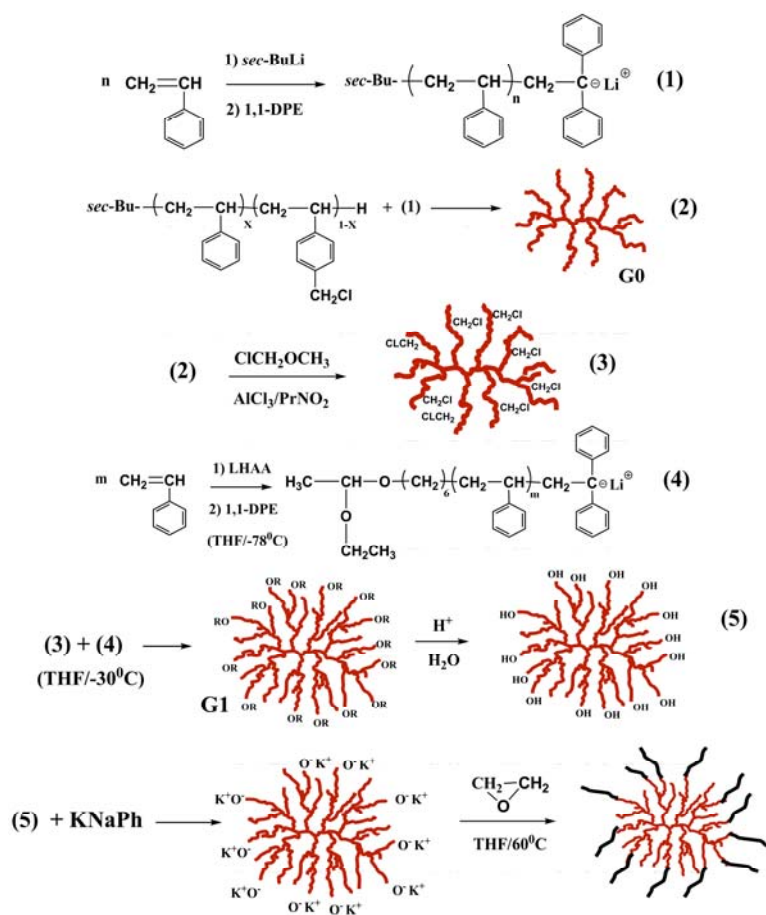
2.6.1 Solution Properties

The highly branched structure of the arborescent polystyrene-*graft*-poly(methacrylic acid) polyelectrolytes (PS-*graft*-PMAA), generated by hydrolysis of the *tert*-butyl methacrylate copolymer precursors, should lead to unusual properties in solution. Indeed, it was shown using dynamic light scattering measurements that the arborescent PMAA copolymers expand more

than linear PMAA upon neutralization with NaOH (Figure 2.2b).³² Interestingly, volume expansion was also more pronounced in this case than for arborescent polyelectrolytes derived from the analogous P2VP copolymers (Figure 2.2a), possibly due to the closer proximity of the charge to the polymer backbone in the PMAA system.

2.7 Arborescent Polystyrene-*graft*-Poly(ethylene oxide)

The synthesis of an amphiphilic arborescent polystyrene-*graft*-poly(ethylene oxide) (PS-*graft*-PEO) copolymer starting from a G1PS core is represented in Scheme 2.6 as an example.⁹ A comb-branched (G0) styrene homopolymer was first synthesized by grafting polystyrene side chains with $M_w \approx 5000$ or 30,000 onto chloromethylated linear polystyrene ($M_w \approx 5000$). The G1 substrate was synthesized by chloromethylation and grafting of the G0 substrate with polystyrene side chains having a molecular weight similar to the G0 substrate but carrying a terminal acetal functionality, obtained by using (6-lithiohexyl)acetaldehyde acetal (LHAA) as the polymerization initiator. The PEO copolymers were obtained by acid-catalyzed hydrolysis of the terminal acetal functionalities, deprotonation of the hydroxyl chain termini with a base (potassium naphthalide), and addition of ethylene oxide to the polyfunctional anionic macroinitiator thus obtained. Before adding the base, a metal-halogen exchange reaction (not shown in Scheme 2.6) served to deactivate residual chloromethyl groups on the substrates and avoid cross-linking in the deprotonation step.



Scheme 2.6. Reaction steps used to synthesize an arborescent copolymer incorporating a G1 polystyrene core and a poly(ethylene oxide) shell.

2.7.1 Self-assembly at the Air-water Interface

The self-assembly of arborescent PS-*graft*-PEO copolymers spread as monolayers at the air/water interface was recently investigated.³³ AFM imaging was used to examine the influence of molecular structure and composition on the characteristics of the monolayers formed by the amphiphilic copolymers under these conditions. The copolymer solutions were initially spread

on the water subphase without compression. Variations in the amount of solution spread had no influence on the film topologies observed, apart from increasing the number of molecules present on the subphase. The amphiphilic molecules assembled spontaneously at the air/water interface to form stable monolayers that were easily transferred onto solid substrates as Langmuir-Blodgett films. Molecules with PEO weight fractions in the 19-31% range formed ribbon-like structures irrespective of architecture, whereas island-like clusters were obtained for low PEO contents, and non-associated species dominated for high PEO contents (Figure 2.7). The predominance of van der Waals attractive interactions between the hydrophobic polystyrene cores for low PEO content samples explains the observed coalescence of the molecules into large clusters (Figure 2.7a). For higher PEO contents, the degree of deformation of the chains in the corona should become an important factor controlling the association process. While repulsive forces arising from the elastic deformation of the PEO chains disfavor coalescence, deformation of the PEO corona as the molecules move closer on the water subphase may give rise to significant van der Waals attraction forces between adjacent cores, inducing the formation of the ribbon-like superstructures shown below (Figure 2.7b). According to the proposed model, molecular assembly is limited to side-by-side aggregation due to the PEO chains within the corona being pushed aside and building a thicker stabilizing layer alongside the ribbon superstructures. Along the same line, the predominance of isolated molecules for copolymers with a high PEO content (Figure 2.7c) can be explained by weakened van der Waals core-core interactions *vs.* strong repulsive forces associated with the deformation of their dense PEO corona. Another factor influencing the assembly process is the structure of the arborescent polystyrene cores: Copolymer micelles incorporating a very rigid core had a more pronounced tendency to form island-like clusters, even for high PEO contents.

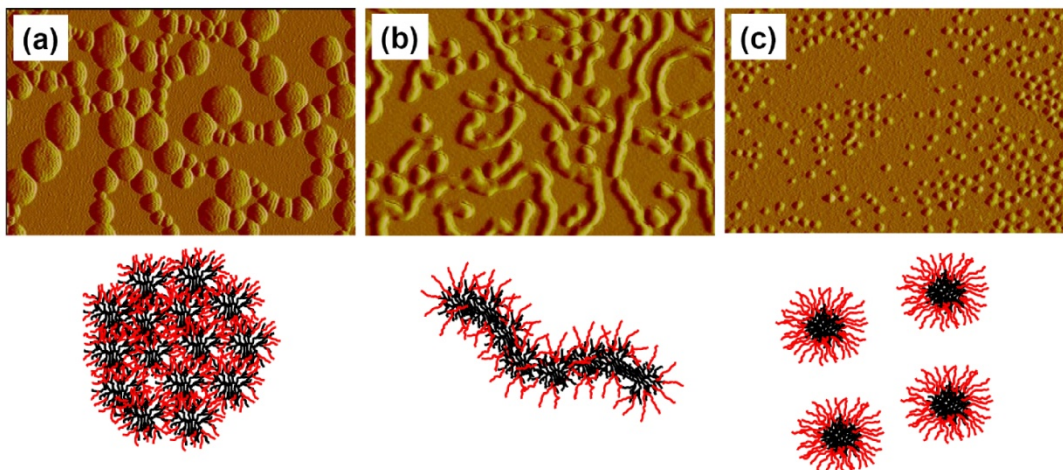


Figure 2.7. Self-assembly of arborescent G1 polystyrene-*graft*-poly(ethylene oxide) copolymers at the air-water interface: Copolymers with PEO contents of (a) 15%, (b) 31%, and (c) 74% by weight. The width of each picture is 1.5 μm . Adapted with permission from Reference 33. Copyright 2008 John Wiley and Sons.

Changes in monolayer topology resulting from surface pressure and subphase temperature variations were also reported for selected arborescent PS-*graft*-PEO copolymers.³⁴ Samples with different branching densities were selected to study the influence of conformational constraints on the assembly process in the presence of these external stimuli. The study was limited to samples with long polystyrene side chains ($M_w \approx 30,000$) because of their interesting association behavior noticed earlier.³³ The formation of superstructures by the dendritic micelles was enhanced by compression and, to a lesser extent, at higher temperatures. The influence of temperature on film topology was examined for copolymers with high PEO contents transferred at a low surface pressure (4 mN/m), to ensure a uniform distribution of molecules on the water.

Molecules with minimal aggregation were observed at 12 °C, whereas a significant number of short ribbon-like features could be identified at 37 °C due to decreased solvation of the PEO chains in the corona. AFM micrographs obtained from monolayers transferred at surface pressures of 0-8 mN/m for low branching functionality ($f_w = 62$) samples with PEO contents $\geq 22\%$ by weight showed that some of the molecules associated to form short ribbon structures even before compression, albeit low-level aggregates and isolated molecules were also present. Under the influence of compression, however, the number of isolated molecules clearly decreased while the average length of the ribbons and their packing density both increased. Enhanced ribbon formation upon compression was also noticed for samples with a high branching density ($f_w = 270$), but the ribbon-like structures were significantly shorter. The height and width measured for the ribbons roughly corresponded to the diameter and thickness of the individual molecules for both the low and high branching density samples, indicating that ribbon formation was taking place mainly through side-by-side assembly of the molecules as indicated in Figure 2.7b. AFM images obtained for some of the samples before and after a compression-decompression cycle did not show a significant increase in the extent of association, demonstrating that the compression-induced formation of ribbon-like superstructures was reversible at least in some cases.

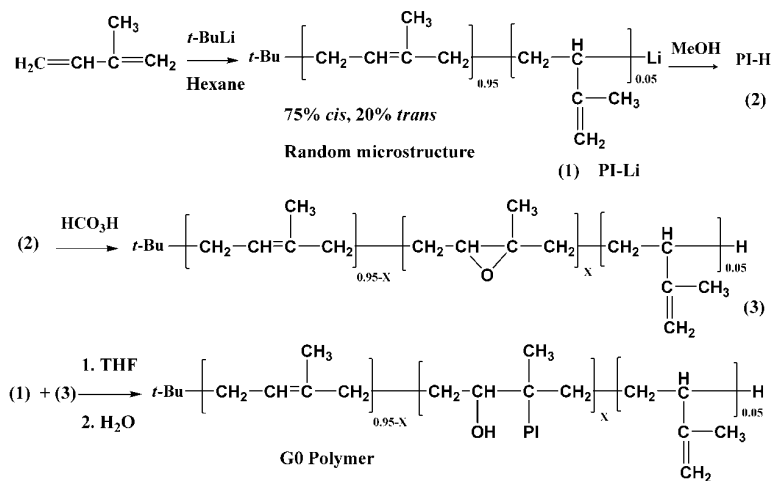
2.8 Arborescent Polyisoprene

The synthesis of arborescent isoprene homopolymers by coupling polyisoprenyllithium with epoxidized polyisoprene substrates as outlined in Scheme 2.7 was demonstrated.³⁵ The reaction path was developed, in analogy to arborescent styrene homopolymers, on the basis of successive functionalization and grafting reaction cycles. Linear polyisoprene was synthesized in hexane

with *tert*-butyllithium to afford a large proportion of *cis*-1,4-isoprene units, and modified by epoxidation with performic acid, generated *in situ* from formic acid and hydrogen peroxide. The epoxidized polyisoprene substrate was then reacted with living *cis*-1,4-polyisoprenyllithium in the presence of THF to yield a comb-branched (G0) polymer. In the absence of coupling promoters, the grafting yield attained ranged from 31-78%. The low grafting yield was linked to the slow polymerization of isoprene in hexane, leading to a small amount of residual monomer reacting in the presence of THF to produce 1,2- and 3,4-isoprene units at the chain ends and modifying the reactivity of the macroanions. The 1,2-units are expected to be less reactive than 3,4- and 1,4-units because they are more sterically hindered, which may explain the limiting grafting yields observed in the absence of promoters.

Three different types of promoters were examined to overcome this hurdle: 1) A Lewis base (*N,N,N',N'*-tetramethylethylenediamine, TMEDA) to complex the lithium counterion and increase the nucleophilicity of the polyisoprenyl anions; 2) Lewis acids to increase the reactivity of the epoxide ring via coordination; and 3) lithium salts to stabilize (decrease the reactivity of) the polyisoprenyl anions by the common ion effect, while also increasing the reactivity of the epoxide ring, since they are weak Lewis acids. The additives TMEDA, BF₃, and AlMe₃ all improved the grafting yield, but LiCl and LiBr were most efficient as promoters. This is presumably due to their ability to minimize the termination of polyisoprenyllithium as well as to promote the coupling reaction with the epoxide functionalities. Using a 25% excess of epoxide functionalities versus living ends and lithium salt promoters, grafting yields reaching 92% were attained in the G0 polymer synthesis. Repetition of the epoxidation and grafting reactions also produced G1 and G2 arborescent polyisoprene with $M_w \approx 5000$ side chains in 83 and 75% yields, respectively, and polydispersity indices $M_w/M_n \leq 1.05$. The attempted synthesis of a G3

polymer failed, possibly due to the inaccessibility of coupling sites within the highly branched substrates and/or limited solubility of the G2 epoxidized substrate.



Scheme 2.7. Synthesis of arborescent polyisoprene by grafting onto epoxidized polyisoprene.

2.9 Arborescent Polybutadiene

The synthesis of arborescent polybutadiene by the “grafting onto” approach was first achieved by Hempenius et al.,³⁶ starting from linear polybutadiene ($M_n \approx 10^4$) obtained by anionic polymerization in hexane to have a microstructure with around 6% of 1,2-units. Hydrosilylation of the linear polybutadiene sample with chlorodimethylsilane was performed to introduce chlorosilane coupling sites. Grafting of the functionalized linear polybutadiene substrate with polybutadienyllithium side chains ($M_n \approx 10^4$) produced a comb-branched polymer with about 10 side chains. Further functionalization and grafting cycles were repeated to

synthesize higher generations of arborescent polybutadiene. A 20% excess of side chains was used in the grafting reactions with respect to chlorosilane functional groups on the backbone.

The synthesis of analogous star-comb polybutadiene on a generation-based approach was reported by Zhang et al.,³⁷ but relied upon epoxidation reactions for the introduction of coupling sites, similarly to the arborescent polyisoprene systems described in Section 2.8. The synthesis started with the living anionic polymerization of butadiene initiated by *n*-butyllithium in cyclohexane, to produce a high content of 1,4-butadiene units. A 4-arm star-like (G0) polymer was obtained by adding SiCl₄ as a coupling agent for the polybutadienyllithium chains. The 1,4-units of the polybutadiene side chains were then partially epoxidized to serve as coupling sites in the subsequent grafting reaction. A dendrigraft star-comb polymer (G1) was obtained by further coupling of polybutadienyllithium side chains ($M_n = 3000$) with the functionalized G0 substrate. Repetition of the functionalization and grafting cycles led to higher generations (G2-G4) of arborescent polybutadiene as represented in Figure 2.8. While the synthesis of dendrigraft star-comb polybutadienes of generations G0-G4 was reported, grafting yield data (66%) were only reported for the G1 polymer.

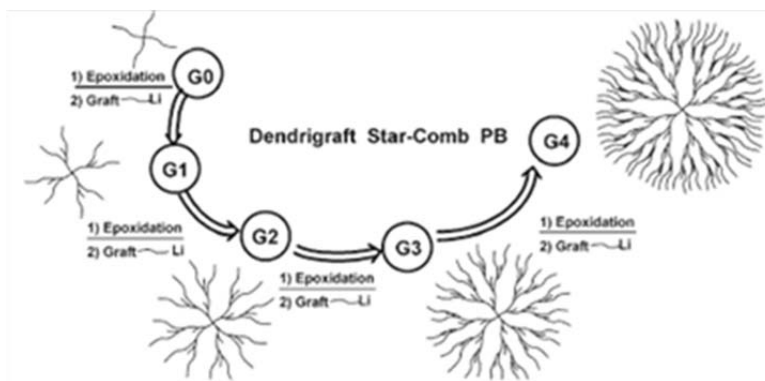


Figure 2.8. Synthetic scheme for dendrigraft star-comb polybutadiene. Adapted with permission from Reference 35. Copyright 2009 American Chemical Society.

2.10 “Click” Chemistry

The term “click” chemistry introduced by Sharpless and coworkers³⁸ refers to reactions that are broad in scope, proceed in high yield, have little side products, and use simple reaction conditions. The most popular “click” reaction that Sharpless identified is the copper (I) catalyzed 1,3-dipolar cycloaddition of azides and alkynes to afford 1,2,3-triazoles. The major advantage of this reaction is its functional group tolerance, which makes it ideal for obtaining many new materials that were hard or even impossible to achieve before. Azides and alkynes can be introduced easily into many molecules by utilizing well-known organic chemistry transformations, in addition to their relatively good stability under different conditions. The main focus of the current review is on the application of “click” chemistry in combination with several polymerization techniques for the synthesis of advanced macromolecular architectures. A number of examples are provided below that include the synthesis of block copolymers and star-shaped polymers.

2.10.1 Block Copolymers from “Click” Chemistry

The design of block copolymers with well-defined architectures is a very important research field.³⁹ Traditionally block copolymers with predetermined number-average molecular weights (M_n) and low polydispersity indices (PDI) were synthesized by two strategies: the sequential living polymerization of different monomers,^{40,41} and coupling reactions of polymers with preformed functional groups.^{42,43} AB diblock and ABC triblock copolymers have attracted much attention for their unique morphologies in comparison with their different homopolymer components, leading to potentially interesting properties.

Athanasios and Hadjichristidis⁴⁴ thus synthesized an α,ω -heterotelechelic block copolymer of polystyrene (PS) and polyisoprene (PI), α -acetylene- ω -azido-PS-*block*-PI, by (a) the sequential anionic polymerization of styrene and isoprene initiated with 5-triethylsilyl-4-pentynyllithium (TESPLi) to afford α -(TES-acetylene)- ω -lithium-PS-*block*-PI, (b) reaction of the living heterofunctionalized copolymer with an excess of 1,4-dibromobutane and sodium azide to give α -(TES-acetylene)- ω -azido-PS-*block*-PI, and (c) deprotection of the acetylene group to obtain α -acetylene- ω -azido-PS-*block*-PI. This α,ω -heterotelechelic block copolymer with “clickable” groups, in the presence of a Cu catalyst, led to a cyclic block copolymer in dilute solution whereas in concentrated solutions it gave multiblock copolymers. The step-growth reaction to obtain multiblock copolymers evolved very quickly (2 h), but the final product consisted of a mixture of polycondensates with various degrees of condensation. This result was expected due to the random nature of the step-growth reaction.

Yuan et al.⁴⁵ reported the synthesis of amphiphilic poly(L-lactide)-*block*-poly(2-(N,N-diethylamino)ethyl methacrylate)-*block*-poly(ethylene oxide) (DPLLA-*block*-PDEAEMA-*block*-

PEO) terpolymers by a combination of ring opening polymerization (ROP), atom transfer radical polymerization (ATRP), and “click” chemistry. DPLLA-OH was synthesized by ROP of L-lactide (LLA), and reacted with propargyl 3-carboxylic-propanoate to obtain alkynyl-DPLLA. PEO-*block*-PDEAEMA-Br was obtained by ATRP of DEAEMA, and then reacted with NaN₃ to obtain PEO-*block*-PDEAEMA-N₃. DPLLA-*block*-PDEAEMA-*block*-PEO was finally obtained by “click” coupling of the alkynyl-DPLLA and an excess of the PEO-*block*-PDEAEMA-N₃ component.

2.10.2 Star Copolymers from “Click” Chemistry

Star polymers are branched polymers that consist of multiple linear chains connected to a central core. Their multiarm structure, globular shape, and multiplicity of end groups impart unique properties on them in terms of crystallinity, mechanical and viscoelastic behaviors when compared with their linear analogues. There are three general strategies for the synthesis of star polymers, each of which exhibits particular advantages and disadvantages, namely the “core first”, “arms first”, and “grafting onto” approaches. The “core first” strategy calls for the polymerization of the arms from a polyfunctional core, and often leads to a non-uniform arm length because of potential differences in reactivity among the initiating sites. The “arm first” approach involves the polymerization of the arms followed by their coupling, usually by the addition of a cross-linking monomer. Although technically simple, this approach typically leads to materials with a variable number of arms and higher polydispersities. The third major path, the “grafting onto” approach, involves the coupling of preformed arms with core molecules via an efficient coupling reaction.

Altintas et al.⁴⁶ thus achieved the synthesis of ABCD 4-miktoarm star polymers with A = polystyrene (PS), B = poly(ϵ -caprolactone) (PCL), C = poly(methyl methacrylate) (PMMA) or poly(*tert*-butyl acrylate) (PtBA), and D = poly(ethylene glycol) (PEG) by “click” chemistry. Block copolymers obtained by different methods, namely PS-*block*-PCL-N₃ with an azide group, and PMMA-*block*-PEG-alkyne and PtBA-*block*-PEG-alkyne with alkyne functionalities, were combined in the presence of a copper catalyst to give the target 4-miktoarm star quarterpolymers as represented in Figure 2.9. The molar ratio of PMMA-*block*-PEG-alkyne to PS-*block*-PCL-N₃ was 1.3/1, and the efficiency of “click” reaction was found to be 88%. The miktoarm star polymers produced were contaminated with PS-*block*-PCL copolymer (10%) which was impossible to remove via precipitation, because of its similar solubility characteristics to the miktoarm star polymer. Yang et al.⁴⁷ also reported an ABCD 4-miktoarm star polymer based upon PS, PCL, PEG, and PMMA arms. In this case an ABC 3-miktoarm star composed of PS, PCL, and PMMA bearing an acetylene group was synthesized first, and then reacted with excess of PEO-N₃ to provide the 4-miktoarm star polymer with a coupling efficiency of 92%. The product had to be purified with an alkyne-functionalized resin to remove unreacted PEO-N₃.

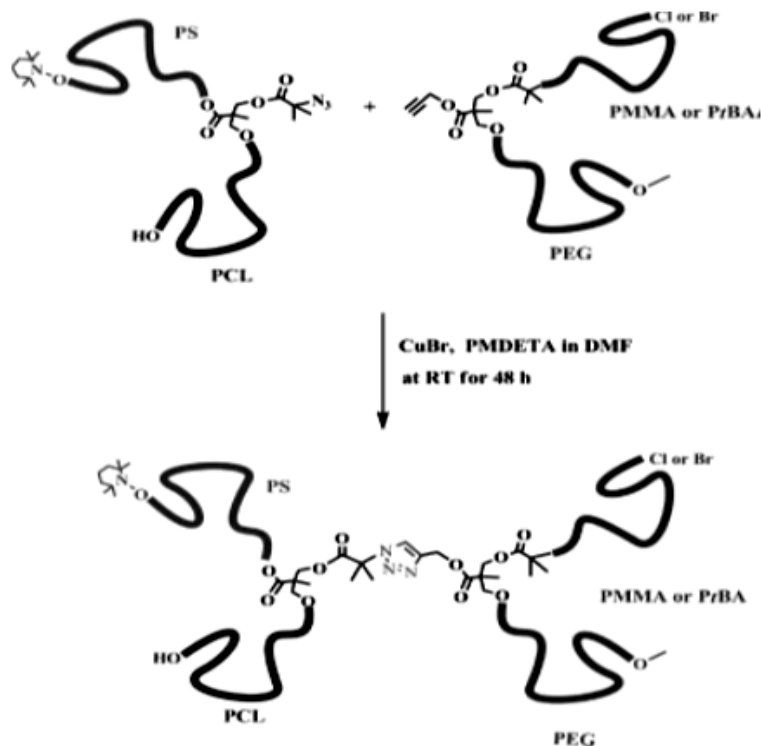


Figure 2.9. Preparation of PS-PCL-PMMA-PEG and PS-PCL-*Pt*BA-PEG 4-miktoarm star quarterpolymers via “click” reaction. Adapted with permission from Reference 46. Copyright 2008 John Wiley and Sons.

Altintas et al.⁴⁸ also reported the preparation of three-arm star homopolymers (A_3) based on the grafting onto technique, using a “click” strategy with well-defined azide-terminated PS, *Pt*BA, and PEG precursors and a trisalkyne-functional coupling agent, 1,1,1-tris[4-(2-propynyloxy)phenyl]-ethane. Star formation in all cases was monitored with SEC measurements, and it was observed that the reaction mixture contained mainly the A_3 star polymer, but also smaller amounts of A_2 block copolymer and A_1 homopolymer. Highly efficient “click” reactions were observed for PS₃, *Pt*BA₃, and PEG₃ star formation. The A_3 -type star yield was 87, 85, and 82% for PS, *Pt*BA, and PEG, respectively. The same group also reported hetero-arm star ABC

terpolymers⁴⁹ of PMMA-PS-*Pt*BA and PMMA-PS-PEG. In this case a PMMA-*block*-PS copolymer with an alkyne functionality at the junction point was prepared first and then “click” grafted with *Pt*BA-N₃ and PEG-N₃ to provide the ABC star terpolymers. Formation of the hetero-arm star terpolymer containing a *Pt*BA arm proceeded successfully, as confirmed by a peak shift to the high molecular weight region in the SEC curve, whereas a SEC trace for the PMMA-PS-PEG star polymer showed no shift. A molecular weight increase was nonetheless confirmed by NMR analysis to prove the formation of the terpolymer.

2.11 Conclusions

In this Chapter various synthetic methods developed for the preparation of dendrigraft (arborescent) homo- and copolymers over the past twenty years were presented. These techniques yield polymers differing in terms of composition, distribution and density of branching sites, ultimately leading to distinct molecular architectures and morphologies. Some of the interesting physical properties observed for arborescent polymers have been outlined; these open the door to a wide range of applications in areas including microencapsulation (solubilization and release of hydrophobic compounds), smart materials (temperature- and pressure-sensitive self-assembly), and catalysis (metallic nanoparticle preparation). The synthesis of various star and block copolymers by “click” chemistry coupling was also presented, which enables the convenient preparation of a wider range of materials with multiple applications in many fields. The main goal of this Thesis work was to further expand the scope of “click” chemistry techniques, by applying them to the synthesis of arborescent polymers with much higher branching functionalities than the star-branched systems described above.

Chapter 3

Synthesis of Arborescent Polystyrene by “Click” Grafting

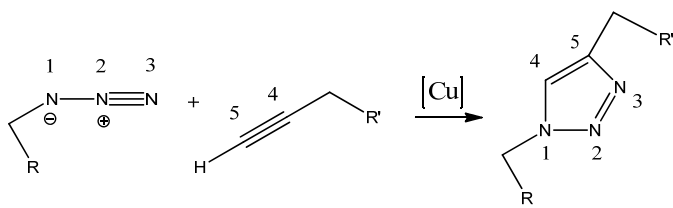
3.1 Outline

A novel method was developed for the preparation of arborescent polystyrene by “click” chemistry coupling. Acetylene functionalities were randomly introduced on linear polystyrene ($M_n = 5300$, $M_w/M_n = 1.05$) by acetylation and reaction with propargyl bromide in the presence of potassium hydroxide and 18-crown-6 in toluene. The anionic polymerization of styrene with 6-*tert*-butyldimethylsiloxyhexyllithium (TBDMS-O-Hexyl-Li) was used to synthesize polystyrene ($M_n = 5200$) with a protected hydroxyl chain end. Deprotection of the hydroxyl group, followed by conversion into tosyl and then azide functionalities, yielded the material serving as side chains. Coupling of the azide-terminated side chains with the acetylene-functionalized substrate in the presence of a Cu (I) catalyst proceeded in up to 94% yield. Repetition of the substrate functionalization and side chain coupling cycles led to well-defined ($M_w/M_n \leq 1.1$) arborescent polystyrene of generations G1 and G2 in 84 and 60% yield, respectively, with number average molecular weight and branching functionalities reaching 2.82×10^6 and 458, respectively, for the G2 polymer. Coupling of longer ($M_n = 45000$) side chains with acetylene-functionalized substrates was also examined. With a linear substrate ($M_n = 5800$), a G0 polymer with $M_n = 4.6 \times 10^5$ and $M_w/M_n \leq 1.1$ was obtained in 87% yield; coupling with a G0 ($M_n = 52,000$) acetylene-functionalized substrate yielded a G1 graft polymer ($M_n = 1.4 \times 10^6$, $M_w/M_n = 1.38$) in 28% yield. The complementary approach to synthesize arborescent polystyrene, using substrates randomly functionalized with azide groups and acetylene-terminated side chains, was also investigated but the yield of these reactions was lower.

3.2 Introduction

Dendritic polymers have attracted attention due to their compact structure and unusual properties making them potentially useful for many high technology applications. Consequently, significant efforts have been devoted to the synthesis of these materials over the past decades. Dendritic molecules can be subdivided into three main families: dendrimers, hyperbranched, and arborescent polymers.¹ All dendritic molecules are characterized by a multi-level branched architecture, but arborescent polymers are distinguished from dendrimers and hyperbranched polymers by their assembly from polymeric building blocks of uniform size rather than monomers, so that very high molecular weights are attained in few synthetic steps.

The development of living/controlled polymerization techniques has enabled the synthesis of a multitude of well-defined polymer structures. Well-known reactions in organic chemistry such as “click” coupling have also been adapted to polymer chemistry and yielded promising results to build novel structures by coupling preformed polymers.² This approach allows the combination of state-of-the-art living/controlled polymer chemistry techniques with the best coupling procedures known in organic chemistry. In this respect, the “click” chemistry concept introduced by Sharpless^{3,4} seems ideal to couple preformed polymer chains into more complex architectures. Sharpless and co-workers identified a number of reactions meeting the criteria of “click” chemistry, arguably the most powerful of which is the Cu (I)-catalyzed variant of the Huisgen 1,3-dipolar cycloaddition⁵ of azides and alkynes to afford 1,2,3-triazoles as shown in Scheme 3.1.



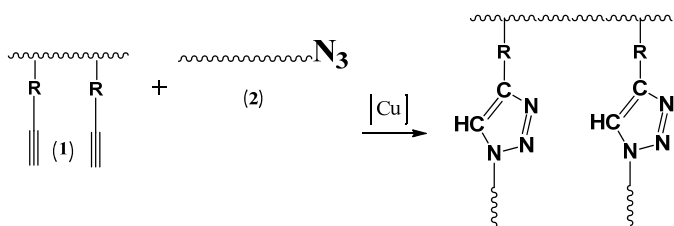
Scheme 3.1. “Click” coupling between a terminal azide and an alkyne to yield a 1,2,3-triazole.

This reaction owes its usefulness to the ease with which azides and alkynes can be introduced into molecules, and their relatively good stability under different conditions. Indeed, azides and alkynes are essentially inert under most physiological conditions including highly functionalized biological molecules, molecular oxygen, water, and many reaction conditions commonly encountered in organic synthesis.^{6,7} The application of “click” chemistry to polymer science is a quickly emerging field of research, since it typically allows the fast and simple creation of well-defined and complex polymeric structures in yields previously unattainable. Several polystyrene-containing block and star copolymers such as poly(vinylidene fluoride)-*b*-polystyrene,⁸ polystyrene-*b*-poly(γ -propargyl-L-glutamate-*g*-polyhedral oligomeric silsesquioxane),⁹ polystyrene-*b*-poly(ethylene oxide)-*b*-poly(*tert*-butyl acrylate),¹⁰ miktoarm stars of poly(ethylene oxide), polystyrene and poly(ϵ -caprolactone),¹¹ miktoarm star (polystyrene- poly(ethylene glycol)-poly(methyl methacrylate)),¹² three-arm stars (polystyrene, poly(*tert*-butyl acrylate), poly(ethylene glycol)),¹³ and 4-miktoarm stars (polystyrene, polycaprolactone, poly(methyl methacrylate), and poly(ethylene glycol))¹⁴ have been synthesized utilizing “click” chemistry. However to date there are no reports on the synthesis of arborescent polymers by “click” chemistry. In this Chapter the application of the azide-alkyne 1,3-dipolar cycloaddition reaction

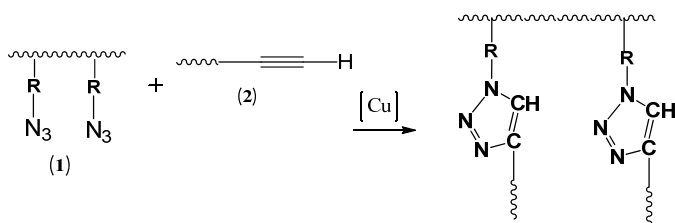
to the construction of well-defined arborescent polystyrene architectures will be demonstrated.

Two different strategies have been examined as shown in Scheme 3.2:

Strategy A:



Strategy B:



Scheme 3.2. Proposed strategies for the synthesis of arborescent polystyrene.

3.3 Experimental Section

Purification of the monomer and other reagents serving in the polymerization reactions used a high-vacuum line connected to a nitrogen (N₂) purification system and reusable glass ampoules. The ampoules were equipped with polytetrafluoroethylene (PTFE) stopcocks and ground glass joints for direct assembly onto the polymerization reactor.¹⁵

3.3.1 Solvent and Reagent Purification

Cyclohexane (Caledon, reagent grade) and toluene (Caledon, HPLC grade) were purified by refluxing with oligostyryllithium under dry N₂ atmosphere. Tetrahydrofuran (THF; Caledon, reagent grade) was purified by distillation from sodium-benzophenone ketyl under nitrogen. The solvents were introduced directly from the drying stills into the polymerization reactor and reaction setups through PTFE tubing.

Styrene (Aldrich, 99%) was purified by stirring with calcium hydride and distillation at reduced pressure. The purified monomer was stored under N₂ at -20 °C until a second purification step with phenylmagnesium chloride, as described in Section 3.3.2.1, immediately before polymerization. The initiator *sec*-butyllithium (*sec*-BuLi, Aldrich, 1.4 M solution in hexanes) was used as received; its exact concentration was determined by the method of Burchat et al.¹⁶ Anhydrous aluminum chloride (AlCl₃; Acros Organics, 98.5%), acetyl chloride (EMD, 98%), nitrobenzene (Alfa Aesar, 99%), potassium hydroxide (KOH; Caledon, reagent grade), 18-crown-6 ether (Sigma Aldrich, 99%), propargyl bromide (Aldrich, 80 wt% in toluene), lithium metal (Aldrich, wire 3.2 mm diameter, 98% in mineral oil), 6-chloro-1-hexanol (Aldrich, 96%), *tert*-butyldimethylsilyl chloride (Aldrich, 97% reagent grade), imidazole (Fluka, 99.5%), diethyl ether (Caledon, reagent grade), tetrabutylammonium fluoride (TBAF; Aldrich, 1 M solution in THF), dichloromethane (Caledon, HPLC grade), *p*-toluenesulfonyl chloride (TsCl; Alfa Aesar, 98%), pyridine (Caledon, reagent grade), *N,N*-dimethylformamide (Omnisolv, 99%), sodium azide (Sigma Aldrich, 99.5%), *N,N,N',N'',N'''*-pentamethyldiethylenetriamine (PMDETA; Aldrich, 99%), bipyridyl (Sigma Aldrich, 99.9%), copper (I) bromide (Aldrich, 99.999%), lithium aluminum hydride (LiAlH₄; Aldrich, 2 M solution in THF), thionyl chloride (SOCl₂, Aldrich), sodium hydride (NaH, Aldrich, 60% dispersion in mineral oil), 2,6-di-*tert*-butyl-4-

methylphenol (BHT, Aldrich, 99%), benzophenone (Sigma-Aldrich, reagent plus 99%), and sodium (Aldrich, $\geq 99\%$, stored under mineral oil) were used as received from the suppliers.

3.3.2 Backbone Synthesis and Functionalization (Strategy A)

3.3.2.1 Styrene Polymerization

The synthetic procedure used was as described by Li and Gauthier.¹⁷ Styrene (15 mL) was further purified with phenylmagnesium chloride solution (1.5 mL) immediately before polymerization by high-vacuum purification techniques, whereby the monomer was degassed with three freeze-pump-thaw cycles under vacuum before recondensation to an ampoule (10.1 g of styrene collected). A 2-L glass reactor was used to polymerize styrene; the reactor was first evacuated, flamed, and filled with nitrogen. Toluene (100 mL) was then introduced directly from the purification still and the reactor was cooled in an ice-water bath. Residual impurities were titrated by adding a few drops of styrene and enough *sec*-BuLi to obtain a persistent yellow-orange color, and the calculated amount of *sec*-BuLi solution (1.44 mL, 2.02 mmol, for a target $M_n = 5000$) was added, followed by the styrene monomer. The reaction mixture was warmed to room temperature (23 °C) after 15 min and stirred for 1 h before it was terminated with degassed methanol. The polymer was recovered by precipitation in 1 L of methanol, filtration, and drying under vacuum. The polymer, with a number-average molecular weight $M_n = 5300$ and a polydispersity index $M_w/M_n = 1.05$, was obtained in 92 % yield (9.3 g).

3.3.2.2 Acetylation of Polystyrene

The procedure used was described by Li and Gauthier.¹⁷ Polystyrene (2 g, 19 meq of styrene units) was dried under vacuum overnight in a 500 mL round-bottomed flask and dissolved in 40 mL of nitrobenzene. Anhydrous AlCl₃ (0.64 g, 4.8 mmol) was dissolved in 4 mL of nitrobenzene under nitrogen before adding acetyl chloride (0.41 mL, 5.2 mmol). This solution was stirred at room temperature for 30 min and added drop-wise to the polymer solution; the reaction was allowed to proceed for 45 min. Workup involved precipitation of the polymer in 400 mL of methanol acidified with 40 mL of concentrated (11 M) HCl as a first step. The polymer was recovered by filtration and further purified by two cycles of dissolution in THF (10 mL) and precipitation in 90 mL of methanol acidified with 10 mL of HCl. The polymer was then dissolved in chloroform (20 mL) and extracted twice with 20 mL portions of water. It was finally recovered by precipitation in 200 mL of methanol, suction filtration, and drying overnight under vacuum. The purified product (1.8 g, 82 % yield) had a substitution level of 24 % as determined by ¹H NMR spectroscopy. The procedure described above also served to obtain the acetylated branched polystyrene substrates used in the synthesis of the upper generation arborescent polymers.

3.3.2.3 Acetylenation of Polystyrene

The synthetic procedure used was adapted from a method reported for the alkylation of aryl methyl ketone under phase transfer catalysis conditions.^{18,19} Acetylated polystyrene (1 g, 2.3 meq of acetylated styrene units) was dried under vacuum overnight in a 250 mL round-bottomed flask and dissolved in 100 mL of toluene. 18-Crown-6 (61 mg) was added to the polymer solution,

followed by 0.64 g of powdered potassium hydroxide. The round-bottomed flask was capped with a rubber septum and purged with nitrogen. The solution was stirred for 1.5 h at room temperature (23 °C), cooled to 0 °C, and 1.3 mL of propargyl bromide was added drop-wise over 10 min. The reaction was then allowed to warm to room temperature and stirred for 12 h. The acetylenated polymer was first precipitated in 500 mL of methanol acidified with 5 mL of concentrated (11 M) HCl, recovered by suction filtration, and dried under vacuum for 1 h. The polymer was then dissolved in THF (25 mL) and filtered by suction to remove insoluble salts. The filtrate was concentrated to 5 mL and the polymer was recovered by precipitation in 50 mL of methanol, suction filtration, and drying under vacuum for 3 h. The purified product (0.82 g, 78 % yield) had a substitution level of 23 % as determined by ¹H NMR spectroscopy. The procedure used to obtain the acetylenated G0 and G1 polystyrene substrates was as described above except for extending the reaction time with potassium hydroxide to 2 and 3 h, respectively, before adding propargyl bromide.

3.3.3 Side Chain Synthesis and Functionalization (Strategy A)

3.3.3.1 Synthesis of 6-*tert*-Butyldimethylsiloxyhexyllithium

The procedure used for the synthesis of 6-*tert*-butyldimethylsiloxyhexyl chloride was similar to that reported by Williamson.²⁰ Cyclohexane (24 mL), 6-chloro-1-hexanol (3.4 mL), *tert*-butyldimethylsilyl chloride (3.76 g), and imidazole (1.7 g) were combined in a 100 mL round-bottomed flask which was sealed with a rubber septum and purged with nitrogen, and the mixture was stirred overnight at 35 °C. Workup involved suction filtration of the reaction

mixture, concentration of the filtrate, and distillation under vacuum to obtain the product in 76 % yield (2.6 mL).

A 500 mL three-neck round-bottomed flask was mounted on a high-vacuum line, with a rubber septum and a dry cyclohexane inlet on the two other openings. The flask was evacuated, flamed, and purged with nitrogen. The septum was removed, and diethyl ether (200 mL) and lithium metal (0.7 g, 97 mmol; 5 equiv with respect to 6-*tert*-butyldimethylsiloxyhexyl chloride) were added to the flask against nitrogen flow. The flask was sealed and cooled to -30 °C in a 2-propanol/water (3/1)-dry ice bath. 6-*tert*-Butyldimethylsiloxyhexyl chloride (2.6 mL, 19 mmol) was added drop-wise with a syringe over 30 min. The mixture was stirred at -30 °C for 4 h, after which time a turbid grey-colored dispersion was obtained. The temperature was increased to -10 °C with an ice-NaCl bath and the ether was removed under vacuum. Two 100 mL portions of dry cyclohexane were then added under nitrogen and evaporated before adding a last 25 mL portion of cyclohexane. The initiator was titrated according to the method of Burchat et al.¹⁶ to determine its exact concentration (0.73 M). The round-bottomed flask was purged with nitrogen and stored at 0 °C.

3.3.3.2 Styrene Polymerization with 6-*tert*-Butyldimethylsiloxyhexyllithium

Polystyrene side chains with $M_n \approx 5000$ were synthesized as reported in Section 3.3.2.1, starting from 17.4 g of purified styrene and 3.48 mmol of the initiator, for a target $M_n = 5000$. The polymer, with $M_n = 5200$ and $M_w/M_n = 1.09$, was obtained in 94 % yield (16.5 g).

3.3.3.3 Deprotection of the Hydroxyl Chain Ends

The deprotection procedure used was adapted from Dhara et al.²¹ The protected hydroxyl-terminated polystyrene (16 g) was dried under vacuum overnight in a 1-L round-bottomed flask and dissolved in 400 mL of THF, and 15.3 mL of TBAF solution (15.3 mmol, 5 equiv with respect to the protected hydroxyl groups) were added. The solution was refluxed overnight and the polymer (15.4 g, 96% yield) was recovered by precipitation in methanol. Complete cleavage of the protecting groups was confirmed by ¹H NMR analysis.

3.3.3.4 End Group Tosylation

The tosylation procedure adopted was similar to literature procedures.²²⁻²⁴ Tosyl chloride (5.49 g, 28.8 mmol; 10 equiv with respect to the hydroxyl groups) was loaded in a dry 500 mL round-bottomed flask and dissolved in dichloromethane (30 mL). The flask was sealed with a rubber septum, purged with nitrogen, and cooled to 0 °C. An equimolar amount of pyridine with respect to TsCl (2.32 mL, 28.8 mmol) was then added to the solution, which was stirred for 5 min. The hydroxyl-functionalized polystyrene (15 g), dried under vacuum overnight, was dissolved in 200 mL of dichloromethane and transferred to the TsCl/pyridine solution at 0 °C with a syringe. The mixture was allowed to warm to room temperature and stirred overnight. Workup involved precipitation in 1.5 L of methanol, two additional cycles of dissolution in 80 mL of THF and precipitation in 800 mL of methanol, filtration, and drying under vacuum. The tosylated polymer (14.6 g) was obtained in 97 % yield. Complete conversion to the tosylate functionality was confirmed by ¹H NMR spectroscopy.

3.3.3.5 End Group Azidation

The azidation procedure used was as reported by Fallais.²⁵ In a dry 500 mL round-bottomed flask, 14 g of dry tosylated polystyrene was dissolved in 200 mL of DMF. Sodium azide (1.75 g, 26.9 mmol, 10 equiv with respect to tosyl functionalities) was added to the polymer solution. **CAUTION:** Sodium azide is highly toxic and the reaction should only be carried out in a well-ventilated fume hood. The flask was purged with nitrogen and sealed, and the reaction was stirred overnight. Workup first involved the drop-wise addition of 4 mL of water and stirring for 1 h before precipitation in 1.5 L of methanol. The product was again dissolved in 80 mL of THF and precipitated in 800 mL of methanol, filtered, and dried under vacuum. The pure product (13.7 g) was obtained in 97 % yield. Complete conversion to the azide functionality was confirmed by ¹H NMR analysis.

3.3.3.6 Polystyrene Side Chains with $M_n \approx 50,000$

Polystyrene side chains with $M_n \approx 50,000$ were synthesized as reported in Section 3.3.2.1, starting from 10.5 g of purified styrene and 0.21 mmol of the initiator to target $M_n = 50,000$. The polymer, with $M_n = 45,000$ and $M_w/M_n = 1.05$, was obtained in 87 % yield (9.2 g).

The protecting groups were cleaved from the polymer as described in Section 3.3.3.3. Starting from 9.2 g of the protected polymer and 9.2 mmol of TBAF, the product was obtained in 97 % yield (9 g). Tosylation was achieved as reported in Section 3.3.3.4, starting from 9 g of polymer, and 17.28 mmol each of pyridine and tosyl chloride. The tosylation reaction was allowed to proceed for 48 h (rather than 24 h in the case of $M_n = 5200$ side chains). The product

was obtained in 96 % yield (8.7 g). Complete conversion to the tosylate functionality was confirmed by ^1H NMR spectroscopy.

Azidation was achieved as described in Section 3.3.3.5. Starting from 9 g of the tosylated polymer and 18 mmol of sodium azide, the product was obtained in 94 % yield (8.5 g). The azidation reaction was allowed to proceed for 48 h (rather than 24 h in the case of $M_n = 5200$ side chains). Complete conversion to the azide functionality was confirmed by ^1H NMR analysis.

3.3.4 Coupling of Azide-terminated Polystyrene with Acetylenated Polystyrene

In a dry 250 mL round-bottomed flask, 0.35 g of $M_n = 5800$ acetylenated linear polystyrene substrate (0.77 meq of acetylene groups) and 4 g of $M_n = 5200$ azide-functionalized polystyrene side chains (0.77 meq of azide groups) were dissolved in 80 mL of DMF. PMDETA (0.15 mL, 0.7 mmol) was added to the polymer solution, the flask was sealed with a rubber septum, and the solution was degassed by purging the solution with nitrogen through a needle for 30 min. After degassing, the rubber septum was removed and 0.1 g (0.7 mmol) of copper (I) bromide was added against nitrogen flow, the flask was sealed and degassed again with nitrogen for 15 min, and the reaction was left to stir at room temperature overnight. Workup first involved the addition of 30 mL of water and stirring for 15 min, followed by extraction of the polymer solution with 100 mL of chloroform. The chloroform layer was concentrated to 10 mL and the final product was obtained by precipitation twice in 100 mL of methanol and drying under vacuum for 3 h. The raw grafting product (4.1 g) was further purified by fractionation precipitation in a toluene/methanol mixture to remove unreacted side chains, yielding 3.1 g of pure comb-branched (G_0) arborescent polystyrene (75 % yield). Grafting of $M_n = 5200$ side

chains (0.97 g) onto an acetylenated G0 substrate (75 mg) yielded the G1 graft polymer in 58 % yield (0.61 g) under the same conditions; however grafting of the $M_n = 5200$ side chains (0.52 g) onto an acetylenated G1 substrate (50 mg) was performed at 45 °C in the presence of 5% BHT with respect to acetylene groups (32 % yield, 0.18 g). The fractionation procedure described above was used to purify all the branched polystyrene samples synthesized.

Azide-terminated polystyrene side chains with $M_n = 45,000$ were also coupled with a linear acetylenated polystyrene sample ($M_n = 5800$) as described above. Starting from 4.97 g of side chains and 0.05 g of substrate, the raw grafting product (4.8 g) was purified by fractionation precipitation in a toluene/methanol mixture to yield 3.2 g of pure comb branched polystyrene (66 % yield). The azide-terminated polystyrene side chains with $M_n = 45,000$ were also coupled with a G0 acetylenated polystyrene as described above. Starting from 2.6 g of side chains and 0.025 g of substrate, purification of the raw grafting product (2.5 g) by fractionation precipitation yielded 0.4 g of pure G1 arborescent polystyrene (16 % yield).

3.3.5 Backbone Synthesis and Functionalization (Strategy B)

3.3.5.1 Linear Polystyrene and Acetylation

The polymer used was the same as in Sections 3.3.2.1 and 3.3.2.2.

3.3.5.2 Reduction of Acetylated Polystyrene

The acetylated linear polystyrene sample ($M_n = 5700$, $M_w/M_n = 1.08$, 24 mole% acetylation) was reduced according to a procedure described by Zhu et al.²⁶ Acetylated polystyrene (1 g, 2.3 meq of acetylated styrene units) was dried overnight under vacuum in a 250 mL round-bottomed flask and dissolved in 100 mL of THF. The flask was purged with nitrogen, sealed with a rubber

septum, and cooled to 0 °C. LiAlH₄ (4.6 mL, 9.2 mmol; 4 molar equiv with respect to acetyl groups) was then added with a syringe to the polymer solution at 0 °C. The mixture was allowed to warm to room temperature and stirred for 4 h. The reaction was terminated by cooling to 0 °C and adding drop-wise 5 mL of a solution of methanol/HCl (90/10 v/v) under nitrogen. Workup first involved concentrating the solution to 5 mL, precipitation in 50 mL of methanol/H₂O (30/70 v/v), and recovery by suction filtration. The polymer was further purified by two cycles of dissolution in chloroform (10 mL) and extraction with 10 mL of water. The polymer was finally recovered by precipitation in 100 mL of methanol/H₂O (30/70 v/v), suction filtration, and drying under vacuum overnight. The purified product (0.85 g, 85 % yield) had a substitution level of 24 %, as determined by ¹H NMR analysis.

3.3.5.3 Chlorination of Hydroxylated Polystyrene

The hydroxylated polystyrene substrate was chlorinated by a procedure similar to that reported by Boehm.²⁷ The hydroxyl-functionalized polystyrene (0.8 g, 1.7 meq of hydroxyl groups) was dried overnight in a 250 mL round-bottomed flask and dissolved in 20 mL of THF. The flask was sealed with a rubber septum, purged with nitrogen, and cooled to 0 °C. Thionyl chloride (0.25 mL, 3.4 mmol; 2 molar equiv with respect to hydroxyl groups) was added with a syringe to the solution at 0 °C. The mixture was allowed to warm to room temperature and stirred for 2 h. Workup involved precipitation in 150 mL of methanol, suction filtration, and drying for 3 h under vacuum. The purified product (0.78 g, 95 % yield) had a substitution level of 24 %, as determined by ¹H NMR analysis.

3.3.5.4 Transformation from Chloride to Azide

Azidation was achieved as described in Section 3.3.3.5. Starting from 0.75 g of the chlorinated polymer and 17.3 mmol of sodium azide, the product was obtained in 92 % yield (0.69 g). Complete conversion to the azide functionality was confirmed by ^1H NMR analysis.

3.3.6 Side Chain Functionalization with Alkyne End Groups (Strategy B)

Polystyrene side chains with $M_n \approx 5000$ were synthesized as reported in Section 3.3.2.1, starting from 15.2 g of purified styrene and 3.04 mmol of the initiator for a target $M_n = 5000$. The polymer, with $M_n = 5100$ and $M_w/M_n = 1.08$, was obtained in 89 % yield (13.5 g). The protecting groups were cleaved from the polymer as described in Section 3.3.3.3. Starting from 13 g of the protected polymer and 12.7 mmol of TBAF, the product was obtained in 98 % yield (12.8 g).

The synthetic procedure used to transform the hydroxyl end groups into acetylene end groups was as described by Ergin et al.²⁸ Hydroxyl-functionalized polystyrene (12 g, 2.35 meq of hydroxyl groups), dried under vacuum overnight, was loaded in a dry 1 L round-bottomed flask and dissolved in 500 mL of THF. Sodium hydride (0.28 g, 11.75 mmol, 5 molar equiv with respect to hydroxyl groups) was added to the solution, the flask was sealed with a rubber septum, purged with nitrogen, and the reaction was stirred for 3 h before adding propargyl bromide (1.31 mL, 11.75 mmol) and stirring the reaction for 2 h longer. Workup involved removing the rubber septum followed by the slow addition of methanol to destroy any excess NaH, followed by concentration of the solution to 50 mL and precipitation in 500 mL of methanol; this was followed by two additional cycles of dissolution in 50 mL of THF and precipitation in 400 mL of

methanol, filtration, and drying under vacuum. The product was obtained in 94 % yield (4.7 g). Complete conversion to the acetylene functionality was confirmed by ^1H NMR spectroscopy.

3.3.7 Coupling of Acetylene End-functionalized Side Chains with the Azidated Substrate

Coupling of the acetylene end-functionalized side chains ($M_n = 5100$) with the linear azidated polystyrene substrate ($M_n = 5900$) was achieved as reported in Section 3.3.3. Starting from 2.35 g of side chains and 0.2 g of substrate, the raw grafting product (2.29 g) was purified by fractionation precipitation using a toluene/methanol mixture to remove unreacted side chains to yield 0.64 g of pure G0 polystyrene (28 % yield).

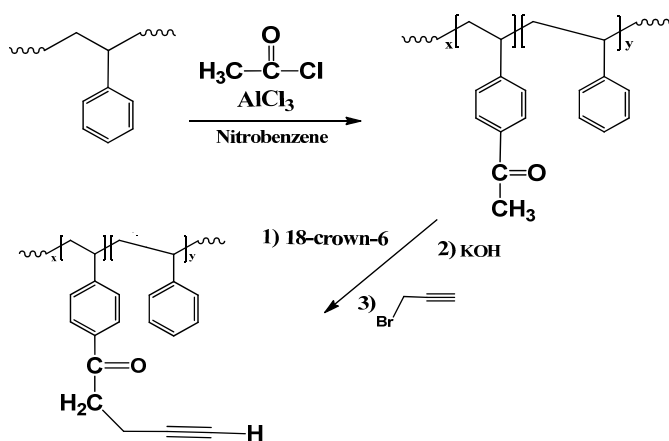
3.3.8 Polymer Characterization

Size exclusion chromatography (SEC) analysis was performed for the substrates and the side chains before and after the acetylation, acetylenation, reduction, chlorination, and azidation reactions, for the side chains, the raw grafting products, and the fractionated graft polymers. The system used consisted of a Viscotek GPCmax unit equipped with a VE 2001 GPC Solvent/sample Module, a Viscotek triple detector array equipped with refractive index, viscosity, and dual-angle light scattering detectors, an external Viscotek UV 2600 detector, and three PolyAnalytik organic mixed bed columns, PAS-103-L, PAS-104-L, and PAS-105-L, with dimensions of 8 mm (ID) \times 300 mm (L) and an overall polystyrene molecular weight range of 10^3 to 10^7 . The polymers were analyzed in THF at a flow rate of 1 mL/min. ^1H NMR analysis of

all the polymer samples was achieved in CDCl_3 on a Bruker Avance 300 MHz NMR instrument at a concentration of 40-50 mg/mL.

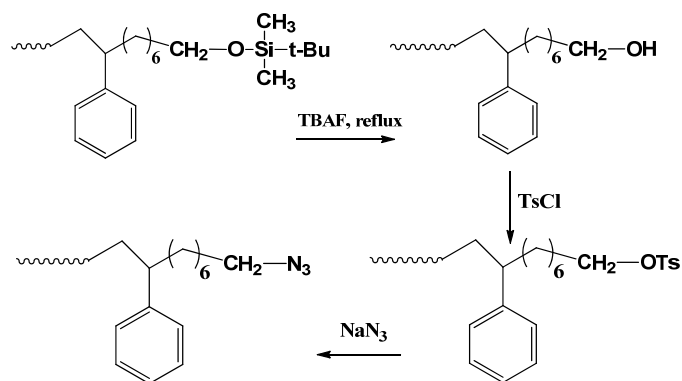
3.4 Results and Discussion

Two strategies were examined for the synthesis of arborescent polystyrene. The first strategy (A) involved the introduction of acetylene functionalities onto the substrate as described in Scheme 3.3, whereas azide groups were located at the end of the side chains, as described in Scheme 3.4. To this end styrene monomer was polymerized with *sec*-BuLi and acetylated (Scheme 3.3). The acetyl groups were then converted into alkyne functionalities by treatment with KOH in toluene, in the presence of 18-crown-6, and quenched with propargyl bromide.



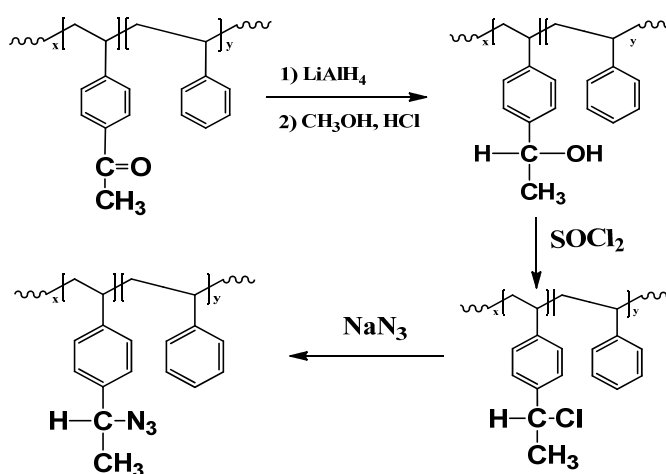
Scheme 3.3. Synthesis and acetylenation of polystyrene substrate.

The synthesis and functionalization of the side chains started with the polymerization of styrene initiated by TBDMS-O-Hexyl-Li, to provide polystyrene with a protected hydroxyl chain end (Scheme 3.4). Deprotection of the hydroxyl group, followed by conversion into tosyl and then azide functionalities, yielded the material serving as side chains.



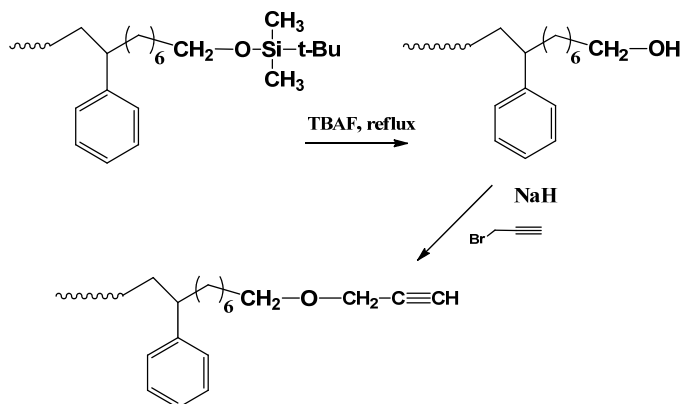
Scheme 3.4. Synthesis and azide-end functionalization of polystyrene side chains.

The alternate strategy (B) involved the introduction of azide functionalities onto the substrate as described in Scheme 3.5, whereas acetylene groups were introduced at the end of the side chains as described in Scheme 3.6. Polystyrene substrate synthesis and acetylation was achieved as described above for strategy A. These acetylated substrates were then reduced to hydroxylated polystyrene with LiAlH_4 , chlorinated with SOCl_2 , and then reacted with sodium azide to produce the azidated polystyrene substrates.



Scheme 3.5. Synthesis and azidation of polystyrene substrate.

The synthesis and functionalization of the side chain material was achieved by polymerization of styrene with TBDMS-O-Hexyl-Li, to provide polystyrene with a protected hydroxyl chain end. Deprotection of the hydroxyl group was followed by its conversion to an acetylene functionality with NaH and propargyl bromide.



Scheme 3.6. Synthesis and acetylene-end functionalization of polystyrene side chains.

3.4.1 Grafting Onto Acetylenated Substrates (Strategy A)

3.4.1.1 Linear Polystyrene and Acetylation

The linear polymer obtained in toluene had the expected molecular weight ($M_n = 5300$) and a narrow MWD ($M_w/M_n = 1.05$). Acetylation of this polymer yielded a substrate with a substitution level of 24 mol %, as determined by ^1H NMR spectroscopy. The acetylation level was controlled by nearly stoichiometric amounts of AlCl_3 and acetyl chloride.

The introduction of the acetyl group caused two new resonances in the ^1H NMR spectrum of polystyrene at 2.55 ppm (acyl protons) and 7.65 ppm (aromatic protons ortho to the acetyl group), as shown in Figure 3.1a. Variation in the acetylation level can provide control over the

branching density on the backbone. In the current investigation, the acetylation level was maintained at 20-30 mol % for all the generations. SEC analysis of the acetylated polymer, represented in Figure 3.2, yielded a polymer with a number-average molecular weight $M_n = 5700$ and $M_w/M_n = 1.08$. The SEC analysis results, including the low polydispersity indices obtained before and after acetylation, suggest that the acetylation reaction proceeded without cross-linking.

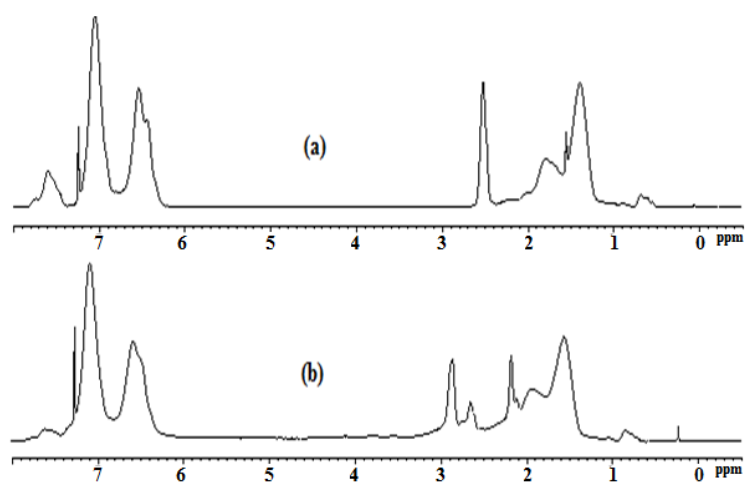


Figure 3.1. ^1H NMR spectra for (a) acetylated polystyrene and (b) acetylenated polystyrene.

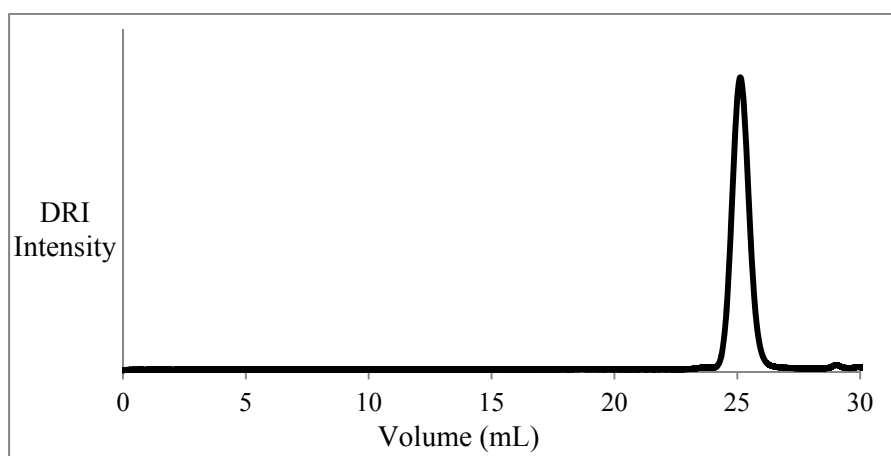


Figure 3.2. SEC trace for acetylated polystyrene ($M_n = 5700$, $M_w/M_n = 1.08$).

3.4.1.2 Acetylenation of Acetylated Polystyrene

Acetylenation of the acetylated polymer yielded a substrate with a substitution level of 23 mol %, as determined by ^1H NMR spectroscopy analysis. The acetylenation level attained was mainly determined by the acetylation level, since excess propargyl bromide was used in the reaction. The introduction of the acetylene functionality caused a new resonance at 2.8 ppm (methylene protons adjacent to the acetylene group), as shown in Figure 3.1b. The conversion from acetyl to acetylene functionalities was incomplete, as can be noticed from the ^1H NMR spectrum of Figure 3.1b where ca. 8 % of acetyl groups are still present. The 23 % acetylenation level achieved can be explained by the fact that not only monosubstitution but also di- and trisubstitution can occur on the acetyl groups, as determined for the alkynylation of aryl methyl ketones under phase-transfer catalysis conditions.^{18,19}

3.4.1.3 Synthesis of 6-*tert*-Butyldimethylsiloxyhexyl Chloride

The protection of 6-chloro-1-hexanol to yield 6-*tert*-butyldimethylsiloxyhexyl chloride was successful, as confirmed by ^1H NMR spectroscopy analysis. The introduction of the *tert*-butyldimethylsiloxy group onto 6-chloro-1-hexanol produces two new resonances at 0.8 ppm (*tert*-butyl protons) and 0 ppm (dimethylsiloxy protons) in the NMR spectrum as shown in Figure 3.3b, while the methylene protons adjacent to the oxygen and chlorine, causing resonances at 3.56 and 3.47 ppm, respectively, remain unchanged as shown in Figure 3.3a. Complete protection is supported by the consistency of peak integration for the *tert*-butyl and dimethylsiloxy protons after protection, as compared to the methylene protons adjacent to the oxygen and chlorine groups before protection.

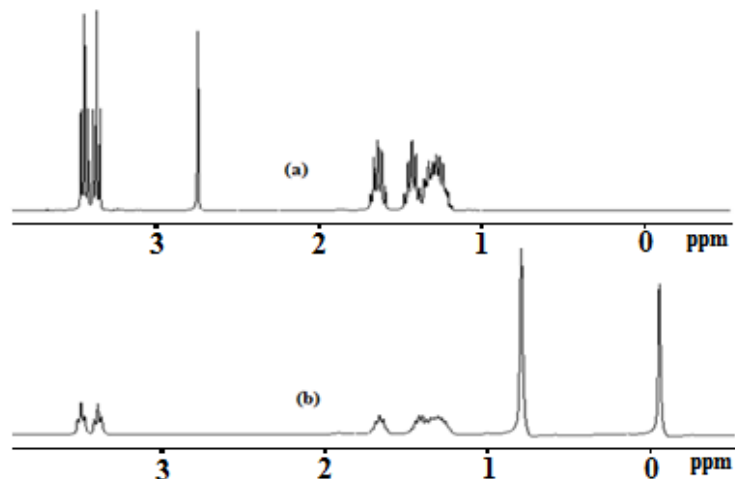


Figure 3.3. ^1H NMR spectra for (a) 6-chloro-1-hexanol and (b) 6-*tert*-butyldimethylsiloxyhexyl chloride.

3.4.1.4 Linear Polystyrene from 6-*tert*-Butyldimethylsiloxyhexyllithium (Target $M_n = 5000$)

The linear polymer synthesized in toluene had the expected molecular weight ($M_n = 5200$) and a narrow MWD ($M_w/M_n = 1.09$), as shown in Figure 3.4. A minor amount of tailing on the right (low molecular weight) side of the peak could be due to somewhat slow initiation in the polymerization reaction. The presence of the *tert*-butyldimethylsilyl group at the chain end causes two resonances at 0.8 ppm (*tert*-butyl protons) and 0 ppm (dimethylsiloxy protons) in the NMR spectrum, while the methylene protons adjacent to the oxygen cause a resonance at 3.56 ppm as shown in Figure 3.5. The absolute M_n of the sample was also estimated by ^1H NMR analysis, by comparing the integrated intensities for the methylene protons adjacent to the oxygen and the benzylic protons ($M_n = 5500$).

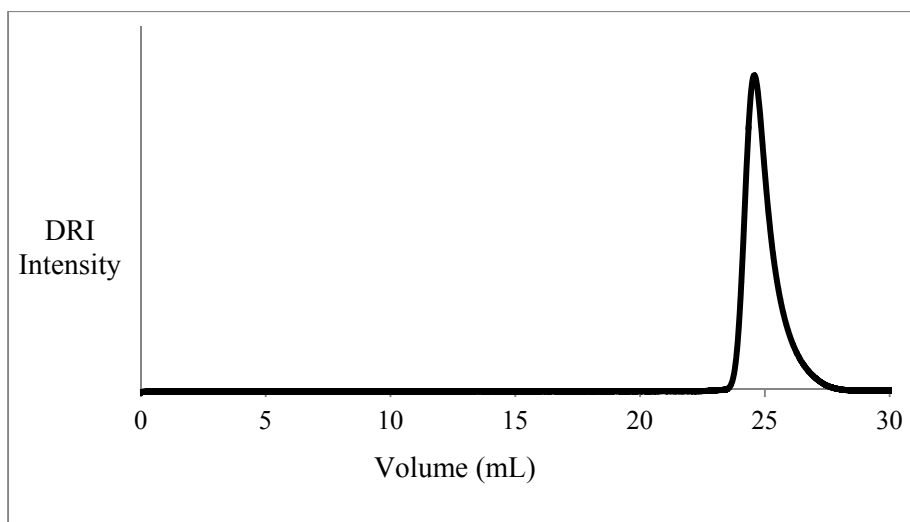


Figure 3.4. SEC trace for linear polystyrene with target $M_n = 5000$, synthesized using 6-*tert*-butyldimethylsiloxyhexyllithium (actual $M_n = 5200$, $M_w/M_n = 1.09$).

The use of a bifunctional initiator to synthesize the polystyrene side chains ensures that all the chains generated contain a protected hydroxyl group from the initiator fragment, to be subsequently transformed into an azide. This approach is advantageous over other techniques such as end-capping, since the presence of impurities in the capping reagent or side reactions may lead to termination of the living chains and thus contamination of the product with side chains not carrying the desired end group.

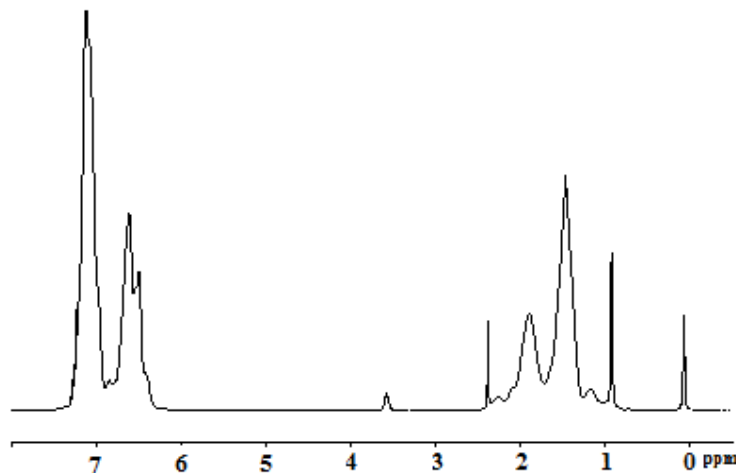


Figure 3.5. ^1H NMR spectrum for polystyrene with a silyl ether-protected chain end ($M_n = 5500$ from NMR analysis).

3.4.1.5 Deprotection of the *tert*-Butyldimethylsiloxy End Group and Conversion to an Azide

Successful deprotection of the *tert*-butyldimethylsiloxy group was confirmed by the complete disappearance of the two resonances at 0 and 0.8 ppm for the dimethylsiloxy and *tert*-butyl protons, respectively, as shown in Figure 3.6a. The methylene protons adjacent to the hydroxyl group still appeared at 3.56 ppm, and the integration of the peak was consistent before and after deprotection. The hydroxyl end group was successfully derivatized into a tosyl functionality, as confirmed by ^1H NMR analysis (Figure 3.6b): The resonance at 3.56 ppm for the methylene protons adjacent to the hydroxyl group shifted to 4.1 ppm. The tosyl to azide conversion could be likewise monitored through ^1H NMR analysis as shown in Figure 3.6c, since the methylene protons at 4.1 ppm shifted to 3.1 ppm when they became adjacent to the azide functionality. The SEC analysis results for the azide-terminated polystyrene are presented in Figure 3.7. The low

polydispersity index values obtained before (1.09) and after (1.09) the transformation of the chain end suggest that all these reactions proceeded without cross-linking or chain degradation. The absolute M_n of the azide-terminated sample was estimated by ^1H NMR analysis to be 5500. The integration of the peak for the methylene protons adjacent to the oxygen (3.56 ppm) in comparison with the benzylic protons (6.3-7.4 ppm) remained unchanged from the deprotection step to tosylation, and then azidation; this provides additional evidence for full conversion of the functional groups at the chain ends.

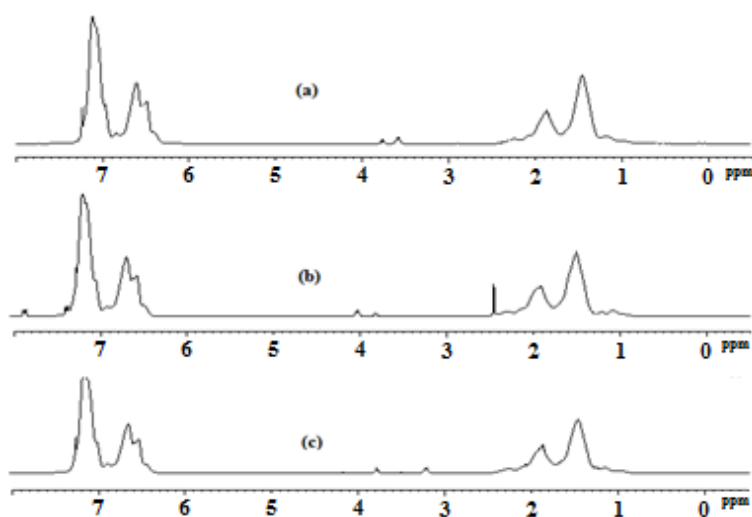


Figure 3.6. ^1H NMR spectra for (a) hydroxyl-, (b) tosyl-, and (c) azide-terminated polystyrene ($M_n = 5500$ from NMR analysis).

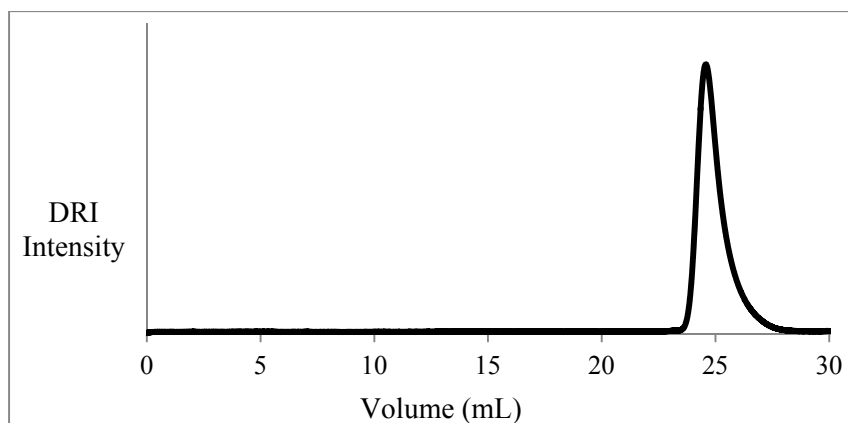


Figure 3.7. SEC trace for azide-terminated polystyrene ($M_n = 5200$, $M_w/M_n = 1.09$).

3.4.1.6 Linear Polystyrene from 6-*tert*-Butyldimethylsilyloxyhexyllithium (Target $M_n = 50,000$)

The linear polymer obtained in toluene had a molecular weight close to the expected value ($M_n = 45,000$) and a narrow MWD ($M_w/M_n = 1.05$), as shown in Figure 3.8. The narrower MWD obtained for this sample in comparison to the $M_n = 5200$ polymer is again consistent with slow initiation as discussed above, since the time required to grow longer chains increases relatively to the initiation step. The presence of the *tert*-butyldimethylsilyl group as a chain end causes two weak resonances at 0.8 ppm (*tert*-butyl protons) and 0 ppm (dimethylsiloxy protons) in the NMR spectrum, while the methylene protons adjacent to the oxygen cause a resonance at 3.56 ppm (Figure 3.9). The absolute $M_n = 43,000$ was also estimated from ^1H NMR analysis of the sample, but it is important to point out that the error on that value is necessarily larger since one of the peaks used in the calculation (methylene protons adjacent to the oxygen) is very small.

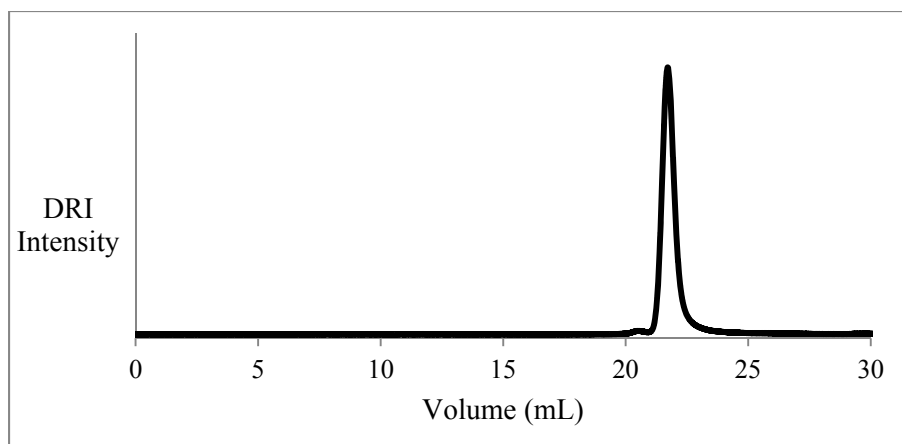


Figure 3.8. SEC trace for linear polystyrene with target $M_n = 50,000$, synthesized using 6-*tert*-butyldimethylsiloxyhexyllithium (actual $M_n = 45,000$, $M_w/M_n = 1.05$).

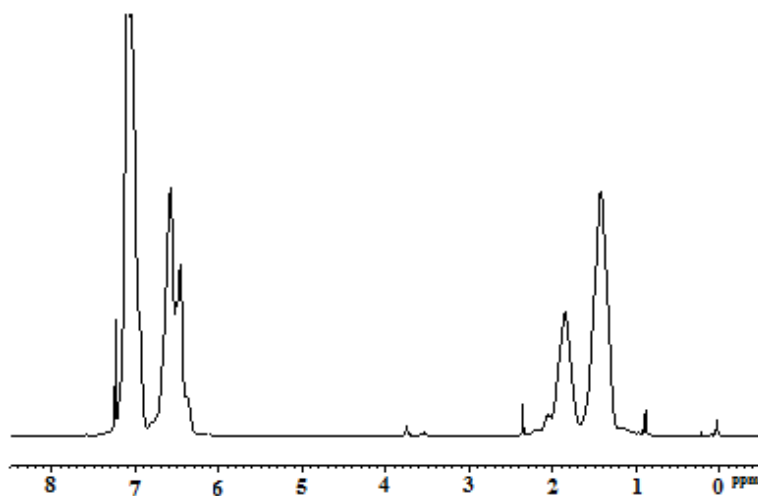


Figure 3.9. ^1H NMR spectrum for polystyrene with a silyl ether chain end ($M_n = 43,000$ from NMR analysis).

3.4.1.7 Deprotection of the *tert*-Butyldimethylsiloxy Group and Conversion to an Azide

Successful deprotection of the *tert*-butyldimethylsiloxy group was confirmed by the complete disappearance of the two resonances at 0 and 0.8 ppm for the dimethylsiloxy and *tert*-butyl protons, respectively. The methylene protons adjacent to the hydroxyl group still appear at 3.56 ppm and the integration of the peak is consistent before and after deprotection. The hydroxyl end group was derivatized into a tosyl functionality, as confirmed through ^1H NMR analysis (Figure 3.10b), where the resonance at 3.56 ppm for the methylene protons adjacent to the hydroxyl group shifted to 3.95 ppm, which is characteristic for methylene protons adjacent to a tosyl group. The tosyl to azide conversion was also monitored by ^1H NMR analysis as shown in Figure 3.10c, where the methylene protons at 3.95 ppm shifted to 3.2 ppm after the reaction. The SEC analysis results for the azide-terminated polystyrene are presented in Figure 3.11. The low polydispersity index values obtained before (1.05) and after (1.05) the transformation of the chain-end suggest all these reactions proceeded without cross-linking or chain degradation. An absolute $M_n = 43,000$ was estimated from ^1H NMR analysis of the azide-terminated sample. The integrated peak intensities in the ^1H NMR spectrum for the methylene protons adjacent to the oxygen (3.56 ppm) in comparison to the benzylic protons (6.3-7.4 ppm) remained unchanged from the deprotection step to tosylation and azidation, which is additional evidence for the full conversion of the functional groups at the chain ends.

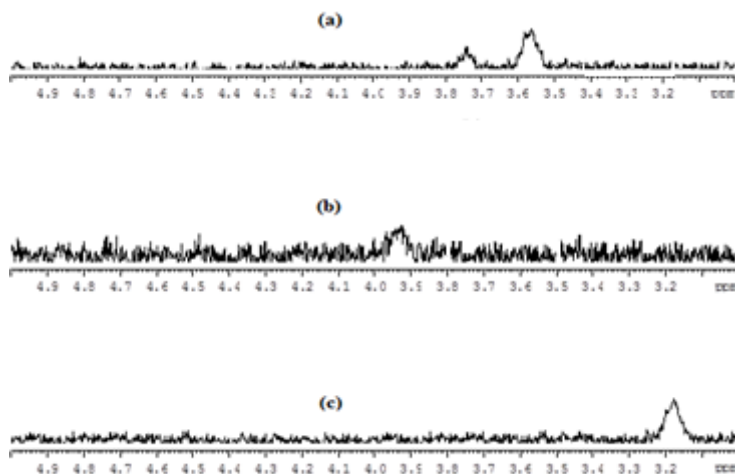


Figure 3.10. ^1H NMR spectra for (a) hydroxyl-, (b) tosyl-, and (c) azide-terminated polystyrene ($M_n = 43,000$ from NMR analysis).

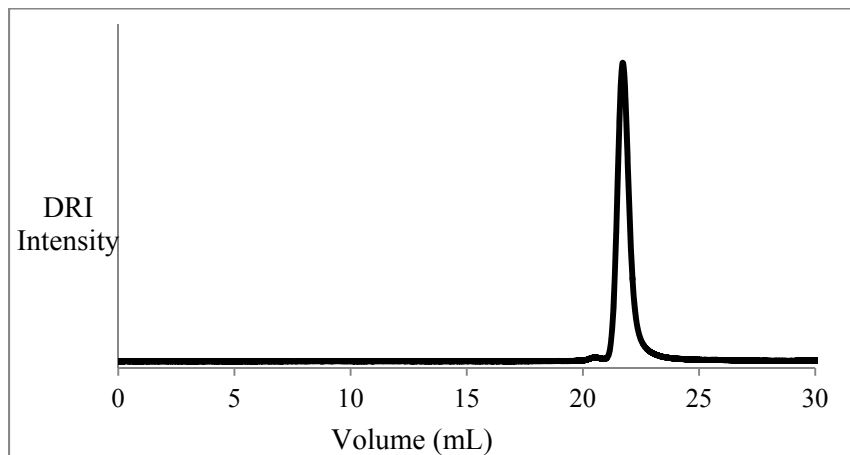


Figure 3.11. SEC trace for azide-terminated polystyrene ($M_n = 45,000$, $M_w/M_n = 1.05$).

3.4.1.8 Coupling of Azide-terminated Polystyrene ($M_n = 5200$) with Linear Acetylenated Polystyrene

The conditions were optimized for the “click” reaction of azide-terminated polystyrene ($M_n = 5200$) with linear acetylenated polystyrene to maximize the grafting yield, defined as the fraction

of side chains becoming attached to the substrate. The grafting yield can be approximated by SEC analysis using a differential refractometer index detector, from the peak areas for the graft polymer and the unreacted side chains, according to the following equation:

$$\text{Grafting yield} = \frac{\text{graft polymer peak area}}{\text{graft polymer} + \text{unreacted side chain areas}}$$

The variables investigated were the type of amine ligand used, solvent, temperature, and reaction time. All these reactions were performed with a 1:1 stoichiometric ratio of azide and acetylene functionalities. In each test reaction, $M_n = 5200$ azide-terminated polystyrene side chains were coupled with a randomly acetylenated $M_n = 5800$ linear polystyrene substrate.

To investigate the influence of these parameters on the grafting yield, the reactions were performed either in pure THF or in pure DMF, the reaction temperature was set to either 50 °C or 23 °C (room temperature), and the reaction time was varied from 1 to 4 days, whereas the ligands used were either PMDETA or 2,2'-bipyridyl. Table 3.1 summarize the results obtained for the coupling reactions performed at 50 °C with PMDETA as a ligand over 4 days, while varying the solvent type used.

Table 3.1. Grafting yield in DMF and THF at 50 °C using PMDETA as ligand.

Time (days)	Grafting yield (DMF)	Grafting yield (THF)
1	86%	82%
2	90%	86%
3	91%	89%
4	93%	89%

The results obtained for the coupling reactions performed at room temperature (23 °C) in the presence of PMDETA as ligand over 4 days, while varying the solvent as in the previous case, are provided in Table 3.2.

Table 3.2. Grafting yield in DMF and THF at room temperature, using PMDETA and bipyridyl as ligands.

Time (days)	Grafting yield (DMF/PMDETA)	Grafting yield (THF/PMDETA)	Grafting yield (DMF/bipyridyl)
1	87%	84%	55%
2	91%	87%	60%
3	91%	90%	60%
4	94%	90%	62%

It is clear that the reaction temperature does not have much influence on the grafting yield, but slightly higher yields were obtained when pure DMF was used as a solvent rather than THF. The SEC traces for the raw grafting products obtained after 4 days at room temperature in DMF and THF are compared in Figures 3.12a and 3.12b. The final grafting product (after 4 days) had $M_n = 52,000$ and $M_w/M_n = 1.09$ in DMF, while in THF $M_n = 49,000$ and $M_w/M_n = 1.09$ were obtained, which is consistent with a slightly higher grafting yield.

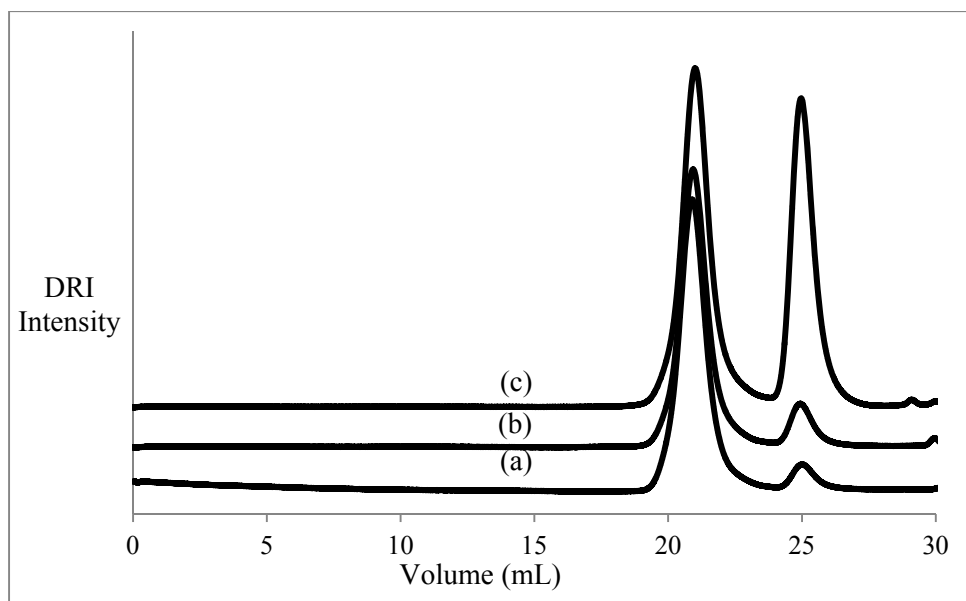


Figure 3.12. SEC traces for the reactions with (a) DMF/PMDETA, (b) THF/PMDETA, and (c) DMF/2,2'-bipyridyl at room temperature.

To investigate the influence of the ligand on the grafting yield, the coupling reaction was also performed in DMF at room temperature in the presence of 2,2'-bipyridyl. The selection of DMF to perform subsequent reactions was based on the fact that grafting proceeded in slightly higher yield in DMF than in THF, whereas since the temperature had no significant influence, the reactions were run at room temperature. Table 3.2 summarizes the grafting yields obtained over 4 days with 2,2'-bipyridyl. Grafting proceeded with only 55-62% yield, demonstrating that bipy was less efficient than PMDETA as a ligand. A SEC trace for the raw grafting product obtained after 4 days is provided in Figure 3.12c, and again confirms that grafting proceeded with a lower yield. The final grafting product obtained after 4 days had $M_n = 32,000$ and $M_w/M_n = 1.10$.

The results presented show that azide-terminated polystyrene side chains with $M_n = 5200$ can be grafted efficiently onto a randomly acetylenated linear polystyrene substrate ($M_n = 5800$) to

obtain a G0 arborescent (comb-branched) polystyrene. Systematic optimization of the reaction conditions made high grafting yields (up to 94%) possible.

3.4.1.9 Coupling of Azide-terminated Polystyrene ($M_n = 5200$) with G0 Acetylenated Polystyrene

Subsequent generations of arborescent polystyrene molecules (G1, G2) can be obtained through repetitions of the substrate functionalization and grafting reaction cycles. This was first attempted with short ($M_n = 5200$) side chains at every step of the grafting reaction. The conditions optimized for the grafting of azide-terminated polystyrene ($M_n = 5200$) onto linear acetylenated polystyrene ($M_n = 5800$) were first used to couple azide-terminated polystyrene ($M_n = 5200$) with an acetylenated G0 substrate to obtain G1 arborescent polystyrene. Grafting proceeded with 84 % yield under these conditions, as shown by the SEC trace obtained for the graft polymer after 4 days (Figure 3.13). The final grafting product had $M_n = 4.34 \times 10^5$ and $M_w/M_n = 1.12$.

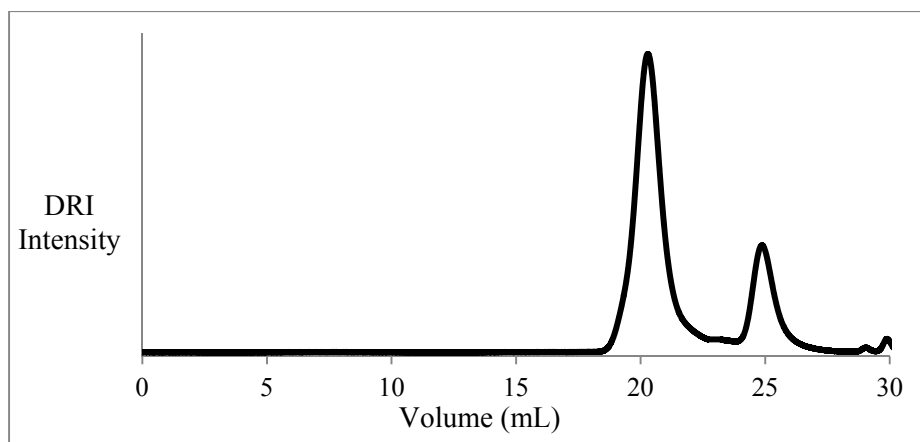


Figure 3.13. SEC trace for the grafting reaction of azide-terminated ($M_n = 5200$) side chains onto an acetylenated G0 substrate (the G1 polymer had $M_n = 4.34 \times 10^5$ and $M_w/M_n = 1.12$).

3.4.1.10 Coupling of Azide-terminated Polystyrene ($M_n = 5200$) with G1 Acetylenated Polystyrene

Grafting of azide-terminated polystyrene ($M_n = 5200$) onto an acetylenated G1 substrate was first attempted under the conditions used for the synthesis of the G0 and G1 polymers, but the reaction proceeded with a very poor yield and an asymmetrical peak was observed for the graft polymer, as seen in the SEC trace of Figure 3.14a. The reaction conditions were therefore reexamined for the synthesis of the G2 molecules. The conditions were first modified by running the reaction at 45 °C, and it was indeed observed that the grafting yield increased as compared to room temperature. This is presumably due to the more congested nature of the G1 substrate versus the linear and G0 molecules, and enhanced accessibility of the alkyne groups at higher temperatures. However the SEC peak for the graft polymer obtained under these conditions still looked asymmetrical (Figure 3.14b), with a shoulder on the left (high molecular weight) side of the peak suggesting the occurrence of a low level of cross-linking. Alkyne-alkyne coupling in the

presence of CuBr/PMDETA, known as Glaser coupling, has indeed been reported.²⁹ This type of reaction takes place in the presence of a copper source and is believed to involve a free radical mechanism. Consequently, the addition of 5% BHT to the grafting reaction as a free radical scavenger was investigated. Grafting proceeded with 60 % yield under these modified reaction conditions (Figure 3.14c), and the peak obtained for the graft polymer was symmetrical without signs of side reactions. The product obtained after 4 days had $M_n = 2.82 \times 10^6$ and $M_w/M_n = 1.10$.

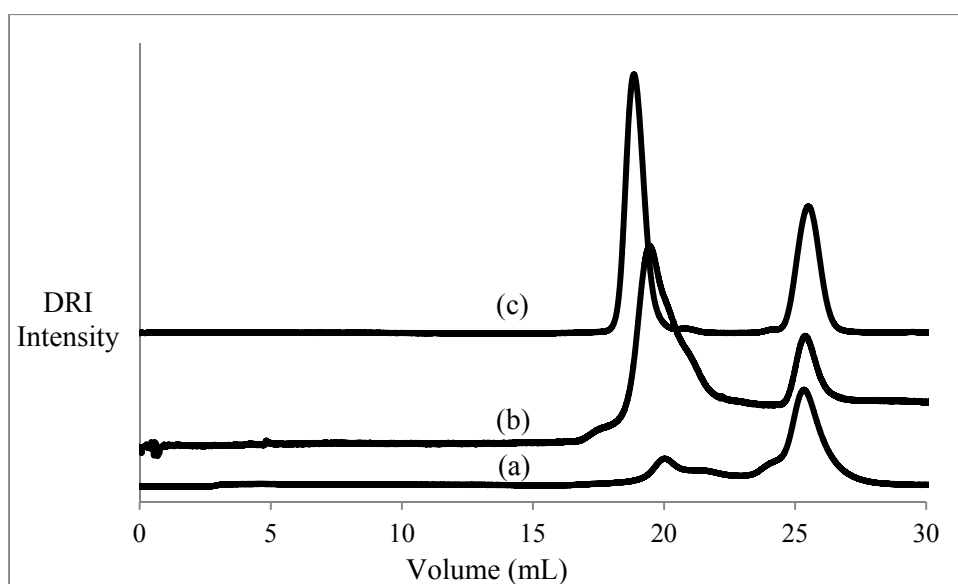


Figure 3.14. SEC traces for grafting azide-terminated ($M_n = 5200$) side chains onto an acetylenated G1 substrate at (a) 23 °C, (b) 45 °C, and (c) 45 °C with 5% BHT (the G2 polymer obtained in (c) had $M_n = 2.82 \times 10^6$ and $M_w/M_n = 1.10$).

3.4.1.11 Coupling of Azide-terminated Polystyrene ($M_n = 45,000$) with Linear Acetylenated Polystyrene

The optimal conditions determined for the reaction of azide-terminated $M_n = 5200$ polystyrene with linear acetylenated polystyrene were applied to grafting azide-terminated $M_n = 45,000$ polystyrene onto linear acetylenated polystyrene. This reaction was therefore performed in DMF at room temperature in the presence of PMDETA. Grafting proceeded with 87 % yield; the SEC trace for the raw grafting product obtained after 4 days is provided in Figure 3.15. The final grafting product had $M_n = 4.6 \times 10^5$ and $M_w/M_n = 1.10$. It can be noticed that the maximum grafting yield obtained after 4 days (87%) is slightly lower than for the analogous reaction with $M_n = 5200$ side chains (94%). This is attributed to the significantly larger size of the $M_n = 45,000$ side chains hindering the accessibility of the azide end groups to the alkyne functionalities on the substrate.

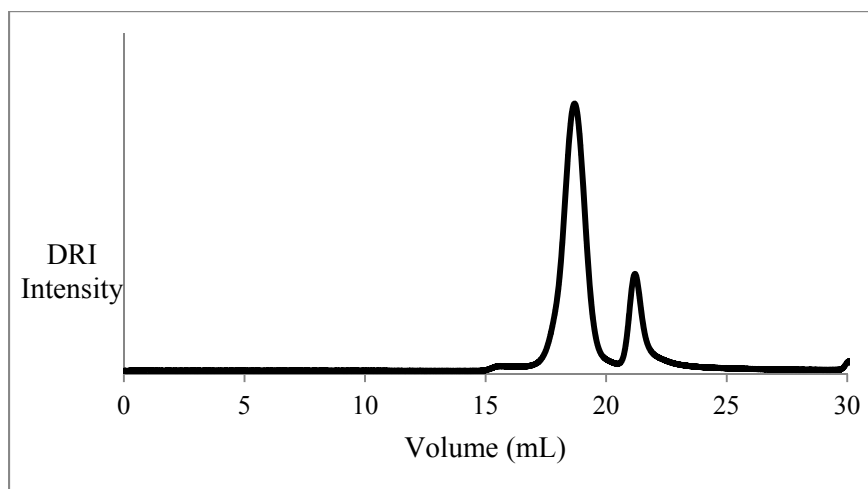


Figure 3.15. SEC trace for grafting azide-terminated ($M_n = 45,000$) side chains onto an acetylenated linear polystyrene substrate (the graft polymer obtained had $M_n = 4.6 \times 10^5$ and $M_w/M_n = 1.10$).

3.4.1.12 Coupling of Azide-terminated Polystyrene ($M_n = 45,000$) with G0 Acetylenated Polystyrene

The optimal conditions determined for grafting azide-terminated polystyrene ($M_n = 5200$) with linear acetylenated polystyrene ($M_n = 5800$), namely in DMF at room temperature with PMDETA, were used to graft $M_n = 45,000$ side chains onto a G0 substrate ($M_n = 52,000$, $M_w/M_n = 1.09$). Grafting proceeded with only 28 % yield, as determined from the SEC trace for the raw grafting product after 4 days (Figure 3.16). The graft polymer had $M_n = 1.4 \times 10^6$ and $M_w/M_n = 1.38$, but also marked peak asymmetry on the low molecular weight side. The significant drop in grafting yield is again explained by the difficulty for an azide chain end to access the alkyne coupling sites in a compact G0 substrate. The origin of the peak asymmetry is not completely clear, but it could be related to the occurrence of degradation of the graft polymer under the reaction conditions used.

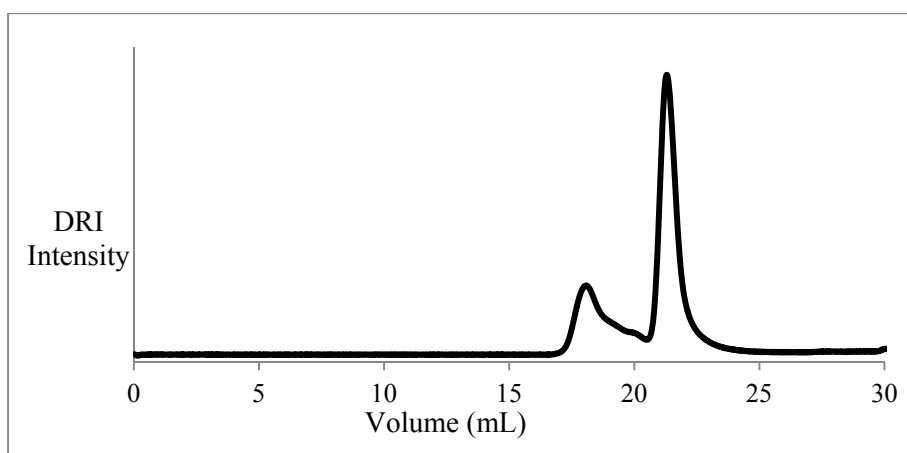


Figure 3.16. SEC trace for grafting $M_n = 45,000$ azide-terminated side chains onto a G0 acetylenated substrate (the graft polymer obtained had $M_n = 1.4 \times 10^6$ and $M_w/M_n = 1.38$).

3.4.1.13 Characterization of the Purified Arborescent Polymers

The polymers synthesized under the optimized conditions were purified by precipitation fractionation as described in Section 3.3.3 for characterization by SEC analysis. The results obtained for the series of samples obtained by grafting either $M_n = 5200$ or 45,000 side chains are summarized in Table 3.3. The corresponding SEC traces for the purified products are provided in Figure 3.17.

Table 3.3. Characteristics of arborescent polystyrene of different generations.

	Side chains		Graft polymer			
	M_n^a	M_w/M_n^a	yield (%) ^b	M_n^a	M_w/M_n^a	f_n
PS-PS5	5200	1.09	94	5.2×10^4	1.09	9
G0PS-PS5	5200	1.09	84	4.34×10^5	1.1	74
G1PS-PS5	5200	1.09	60	2.82×10^6	1.1	458
PS-PS45	45000	1.05	87	4.6×10^5	1.08	10
G0-PS45	45000	1.05	28	1.4×10^6	1.38	30

^a Absolute values determined by SEC-MALLS analysis.

^b Fraction of side chains becoming attached to the substrate.

It is clear that molecular weight and the branching functionality of the graft polymers increased rapidly with the generation number as well as the side chain molecular weight (Table 3.3). The number-average branching functionality of the polymers, defined as the number of chains added in the last grafting reaction, was calculated according to the equation

$$f_n = \frac{M_n(G) - M_n(G-1)}{M_n^{br}}$$

where $M_n(G)$, $M_n(G - 1)$, and M_n^{br} are the absolute number-average molecular weight of graft polymers of generation G, of the preceding generation and of the side chains, respectively. The sample nomenclature used in Table 3.3 identifies the generation number of the substrate as well as the molecular weight of the side chains grafted in the last reaction. For example, G0PS-PS5 refers to a G0 polystyrene substrate grafted with $M_n \approx 5000$ side chains. These results compare very well with previous reports on the synthesis of arborescent polystyrene by anionic grafting onto chloromethylated³⁰ and acetylated¹⁷ substrates. Grafting of living $M_n \approx 5000$ side chains onto chloromethylated and acetylated linear substrates proceeded in up to 95% yield, which is essentially identical to the 94% yield obtained by “click” coupling. Anionic grafting of living $M_n \approx 5000$ side chains onto G0 and G1 acetylated substrates proceeded in 89 and 84% yield, respectively, while 84 and 60% yield were obtained by “click” grafting onto the same substrates. However anionic grafting on the upper generation substrates was performed with up to 30% excess of coupling sites with respect to living chains, whereas “click” grafting was performed with a 1:1 stoichiometric ratio of azide and acetylene functionalities in all cases. Given the differences in experimental protocols used in both series of experiments, the usefulness of such a comparison may be limited; the “click” approach nevertheless appears to be a valid and efficient method to prepare arborescent polystyrene.

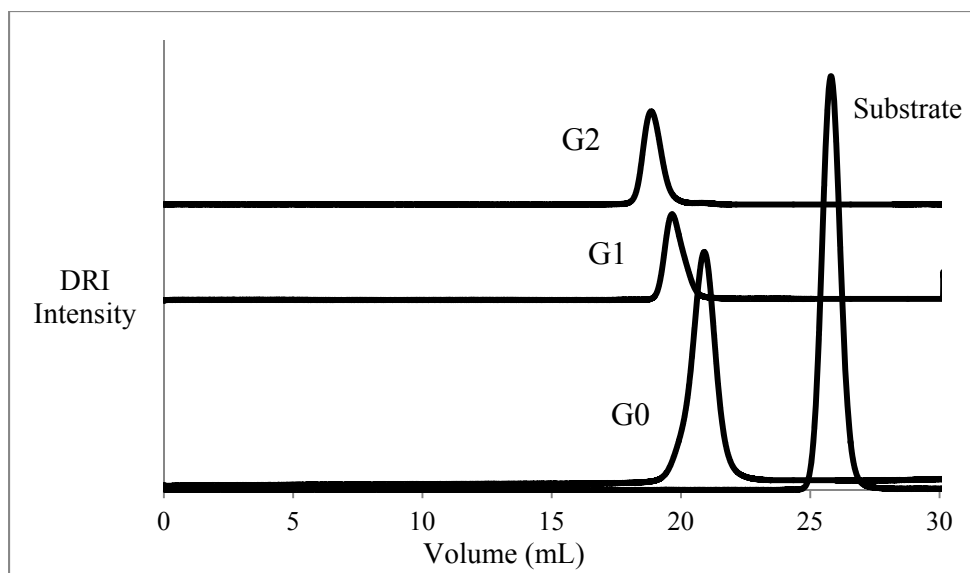


Figure 3.17. SEC traces for arborescent polystyrene of different generations with $M_n = 5200$ side chains.

3.4.2 Grafting Onto Azidated Substrates (Strategy B)

The investigation of this alternate synthetic path was an integral part of the reaction optimization process, to determine the best possible route to arborescent polystyrene by “click” chemistry. It is the reversed approach as compared to strategy A, whereby the side chains were functionalized with an acetylene end group and the substrates were randomly azidated.

3.4.2.1 Linear Polystyrene Acetylation, and Reduction

The linear acetylated polymer (substitution level of 24 mol %) used in this portion of the investigation was the same as in Section 3.4.1.1. The reduction of acetylated polystyrene with LiAlH_4 yielded a hydroxylated polymer with a substitution level of 24 mol % as determined by ^1H NMR spectroscopy analysis, which is consistent with a 100% conversion from the peak shifts

observed in the spectrum: The resonances at 2.55 and 7.65 ppm (associated with the presence of acetyl functionalities) disappeared, whereas a new resonance was observed at 4.8 ppm (proton adjacent to the hydroxyl group), as shown in Figure 3.18a. The integrated peak intensity for the methyl protons in the acetyl group at 2.55 ppm before reduction was also consistent with the integration of the peak for the proton adjacent to the hydroxyl group (4.8 ppm) after reduction, which supports full conversion from acetyl to hydroxyl functionalities.

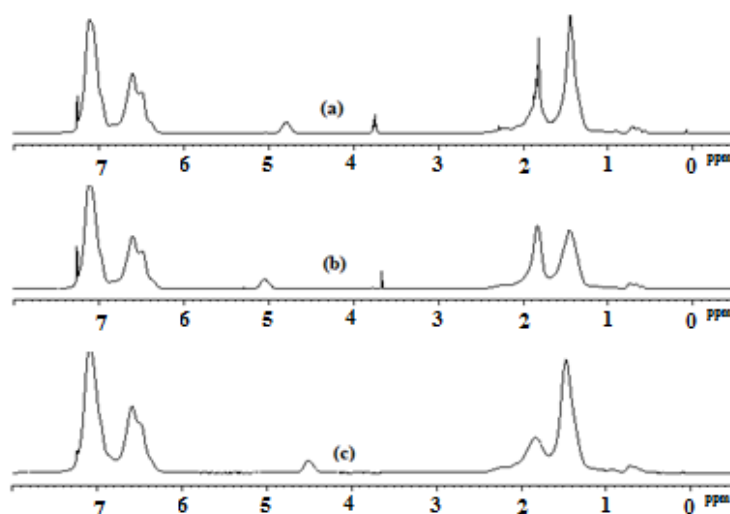


Figure 3.18. ^1H NMR spectra for (a) reduced, (b) chlorinated, and (c) azide-functionalized polystyrene.

3.4.2.2 Chlorination of Hydroxylated Polystyrene and Conversion to the Azide

Chlorination of the hydroxylated polystyrene yielded a substrate with likewise 24 mol % of 4-(2-chloroisopropyl)styrene units, as determined by ^1H NMR spectroscopy analysis. The resonance at 4.8 ppm, characteristic for the proton adjacent to hydroxyl group, disappeared and a

new resonance at 5.1 ppm appeared for the proton adjacent to chlorine (Figure 3.18b). Complete conversion of the hydroxyl to the chloroisopropyl functionality is also supported by the fact that the integration of the peak for the proton adjacent to the hydroxyl group at 4.8 ppm is the same as for the peak at 5.1 ppm. An azidation level of 24 mol % was likewise confirmed by ^1H NMR spectroscopy analysis. The introduction of the azide functionality caused a new resonance at 4.5 ppm (proton adjacent to the azide group), as shown in Figure 3.18c. Complete conversion of the chloride to the azide functionality is again supported by the consistent integration results for the peaks at 4.5 and 5.1 ppm.

3.4.2.3 Side Chain Functionalization with Alkyne End Groups

Polystyrene side chains were successfully synthesized and deprotected in the same manner as reported in Sections 3.4.1.4 and 3.4.1.5. The polymer obtained had $M_n = 5100$ and a narrow MWD ($M_w/M_n = 1.08$). The protecting groups were completely cleaved, as confirmed by ^1H NMR analysis.

The hydroxyl end group was derivatized into acetylene functionality by deprotonation with NaH, followed by treatment with propargyl bromide in THF. Complete conversion was confirmed by ^1H NMR analysis (Figure 3.19), whereby the resonance at 3.56 ppm for the methylene protons adjacent to the oxygen group remained unchanged while the methylene protons between the oxygen and the acetylene group appeared at 4.1 ppm. The integration result for the peak at 3.56 ppm before and after conversion remained. The SEC analysis results for the acetylene-terminated polystyrene are presented in Figure 3.20. The low polydispersity index values obtained before (1.08) and after (1.08) the transformation of the chain end suggest that these reactions proceed without cross-linking or chain degradation. An absolute $M_n = 5600$ was

estimated by ^1H NMR analysis of the samples, by comparing the integrated intensities for the methylene protons adjacent to the oxygen and the benzylic protons.

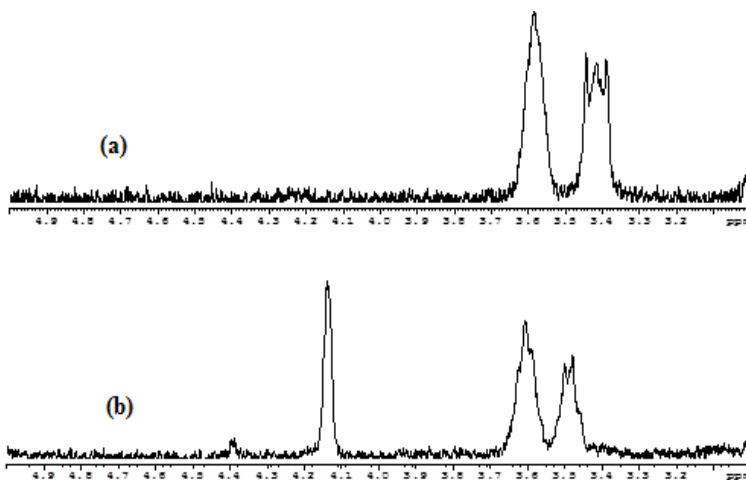


Figure 3.19. ^1H NMR spectra for (a) hydroxyl-, and (b) acetylene-terminated polystyrene.

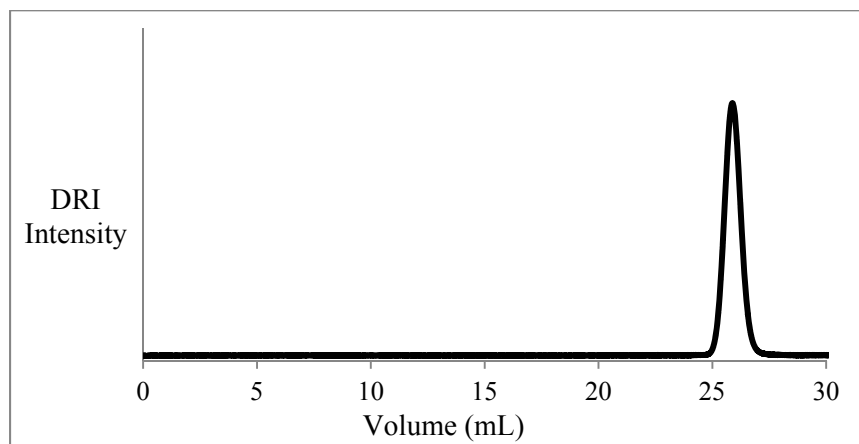


Figure 3.20. SEC trace for acetylene-terminated polystyrene ($M_n = 5100$, $M_w/M_n = 1.08$).

3.4.2.4 Coupling of Acetylene-terminated Polystyrene with Azidated Polystyrene

The optimal conditions determined for the reaction of $M_n = 5200$ azide-terminated polystyrene with linear acetylenated polystyrene were applied in grafting the $M_n = 5100$ acetylene-terminated polystyrene side chains onto linear azide polystyrene, using a 1:1 stoichiometric ratio of azide and acetylene functionalities as before. This reaction was therefore performed in DMF at room temperature in the presence of PMDETA. Grafting only proceeded with 36 % yield, as determined from the SEC trace obtained for the raw grafting product after 4 days (Figure 3.21). The final product had $M_n = 23,000$ and $M_w/M_n = 1.21$. The grafting yield achieved by this approach is significantly lower, and the PDI value is also higher than for the complementary reactions discussed earlier. The lower yield is attributed to the fact that “click” coupling takes place by activation of the alkyne groups through the formation of a π -complex with copper, followed by abstraction of the acetylenic proton by PMDETA to form a copper-acetylide which then adds to the azide group to form the triazole ring.⁷ Being located at the chain end, the copper-acetylide complex is bulkier than a free alkyne, which hinders its access to the azide coupling sites on the substrate. Increasing the reaction temperature to improve the grafting yield did not have any positive influence on the outcome of the reaction, in contrast to the effect observed for coupling azide-terminated side chains with an acetylenated G1 substrate. Consequently, the coupling of acetylene-terminated polystyrene side chains with azide-functionalized substrates was not explored further.

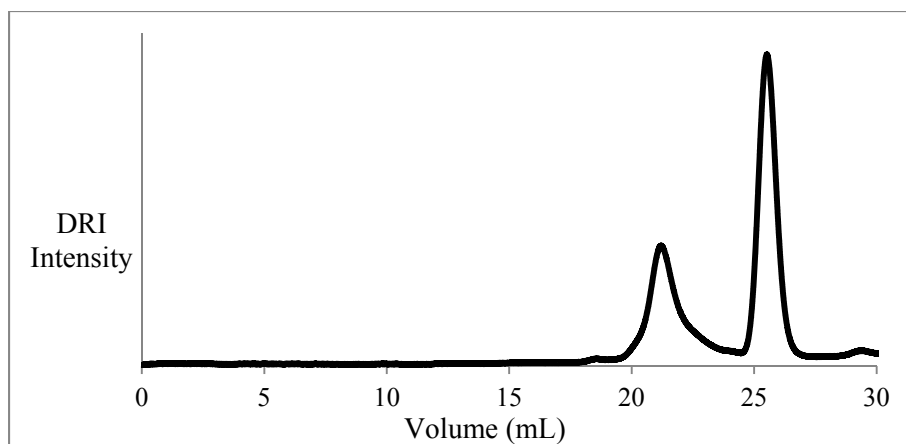


Figure 3.21. SEC trace for grafting acetylene-terminated ($M_n = 5100$) side chains onto an azide-functionalized linear polystyrene ($M_n = 5900$).

3.5 Conclusions

Different generations of arborescent polystyrene were synthesized based on “click” chemistry coupling. Two complementary approaches were investigated; however, the coupling reaction of azide-terminated side chains with randomly acetylenated substrate was found to provide far superior results as it led to higher grafting yields and low polydispersity indices. The initiator 6-*tert*-butyldimethylsiloxyhexyllithium allowed the synthesis of polystyrene side chains bearing a protected hydroxyl group at one end of every chain. Deprotection of the hydroxyl group, followed by successive conversions into tosyl and azide functionalities, yielded the material serving as side chains. The acetylene functionalities were randomly introduced on the grafting substrate by reacting acetylated polystyrene with propargyl bromide in the presence of potassium hydroxide and 18-crown-6 in toluene.

Coupling of the azide-terminated side chains ($M_n = 5200$) with the linear acetylene-functionalized substrate in the presence of a Cu (I) catalyst provided G0 polystyrene with a low

polydispersity index ($M_w/M_n = 1.09$) in high (94%) yield. Additional cycles of substrate functionalization and side chain coupling likewise led to arborescent polystyrene of generations G1 and G2 with low polydispersity indices in 84 and 60% yield, respectively. Grafting of azide-terminated side chains ($M_n = 45,000$) onto the same acetylenated linear and G0 substrates provided G0 and G1 polystyrene in 87 and 28% yield, with polydispersity indices of 1.09 and 1.38, respectively.

The complementary approach investigated to synthesize arborescent polystyrene, from substrates functionalized with azide groups ($M_n = 5900$) and acetylene-functionalized chain ends ($M_n = 5100$), only yielded a G0 polymer with $M_w/M_n = 1.21$ in 36% yield.

The results presented show that “click” chemistry coupling is very useful in the synthesis of arborescent polystyrene. It provides a new dimension to the preparation of these complex architectures, by avoiding tedious anionic grafting procedures at every step. The side chain material and the substrate can be stored and used at some later time without worrying about their stability. This approach should also be useful for the preparation of a wider range of arborescent copolymers, as anionic grafting was shown to be problematic when lower reactivity anions were involved in the coupling reaction.³¹

Chapter 4

Arborescent Polystyrene-*graft*-Poly(ethyl vinyl ether) Copolymers

4.1 Outline

A procedure was developed for the synthesis of graft copolymers with poly(ethyl vinyl ether) (PEVE) side chains, by cationic “grafting from” hydroxylated linear and dendritic (arborescent) polystyrene macroinitiators. The linear and branched hydroxylated substrates were synthesized by anionic polymerization and “click” grafting, acetylation, and either reduction with lithium aluminum hydride (to obtain secondary alcohol groups) or treatment with *n*-butyllithium (to obtain tertiary alcohol functionalities). The macroinitiators were activated with titanium tetrachloride in the presence of 2,6-di-*tert*-butylpyridine in dichloromethane, and ethyl vinyl ether was added to grow PEVE side chains with a target number-average molecular weight $M_n = 5000$ from the substrates. Grafting from both secondary and tertiary alcohol-functionalized substrates yielded graft copolymers free of contamination by PEVE homopolymer, but the secondary alcohol led to narrower molecular weight distributions as compared with the tertiary alcohol. The arborescent copolymers had M_n reaching up to 2.8×10^6 for G2 molecules derived from the G1 hydroxylated substrate. This demonstrates the application of arborescent polymers as cationic macroinitiators to synthesize novel branched materials.

4.2 Introduction

Graft copolymers are characterized by a number of variable molecular parameters such as their backbone and side chain composition, the degree of polymerization of both components, and the branching density. Graft copolymers with defined structures are obtained by three main strategies: (i) “grafting onto”, whereby a functional or living polymer with a reactive end group is coupled with reactive functionalities on another polymer; (ii) “grafting from”, involving a polymeric precursor with a predetermined number of reactive sites to initiate the polymerization

of a second monomer; and (iii) “grafting through”, relying upon the copolymerization of a preformed macromonomer with another monomer in a one-pot reaction.¹⁻³ For the “grafting from” methodology in particular, different polymerization techniques including anionic,⁴ controlled/“living” radical,⁵ coordination-insertion ring opening⁶ and cationic⁷ polymerization have been explored to grow the side chains. Designing copolymers by the grafting from technique is versatile yet challenging: Specific functional groups must be introduced on the macromolecular substrate that can be activated and yield active centers able to initiate the polymerization of another monomer and produce block or graft copolymers, depending on the location of the initiating site, viz. at the chain end or along the chain.

The discovery that tertiary and secondary alcohols in combination with Lewis acids are efficient cationic initiator systems^{8,9} enabled the synthesis of new graft and block copolymers such as polystyrene-*graft*-polyisobutylene, polyisobutylene-*graft*-polyindene, and polyisobutylene-*block*-polyindene.¹⁰ These syntheses involved the initiation of isobutylene or indene polymerization by polymeric alcohols (either randomly hydroxylated linear polystyrene or terminally hydroxylated linear polyisobutylene) in the presence of a Lewis acid, but the graft and block copolymers formed were contaminated with isobutylene or indene homopolymers in all cases, and the graft copolymers had side chains shorter than their target values; purification was therefore required to isolate the pure copolymers. Puskas et al.¹¹ also reported the synthesis of block copolymers comprised of a branched rubbery polyisobutylene substrate and glassy polystyrene blocks. The synthesis was accomplished using arborescent polyisobutylene macroinitiators bearing chloride groups at the chain ends in combination with titanium tetrachloride, followed by styrene monomer addition to grow polystyrene blocks from the polyisobutylene chain ends. The copolymers obtained were again contaminated with

homopolystyrene chains, and had broad molecular weight distributions ($M_w/M_n = 2.2-3.7$). The living cationic polymerization of vinyl ethers has been studied extensively¹² and many initiating systems were explored. Bennevault et al.¹³ thus examined the living cationic polymerization of chloroethyl vinyl ether using a dual component initiator (HI/trialkylaluminum) in combination with $ZnCl_2$. They also investigated the cationic polymerization of cyclohexyl vinyl ether initiated by α -halogeno ethers in the presence of a Lewis acid.¹⁴ The cationic polymerization of isobutyl vinyl ether using alcohols both as cationogens and as catalyst-modifying reagents was likewise examined.¹⁵ It was shown that the alcohol-initiated cationic polymerization of isobutyl vinyl ether with metal chloride Lewis acid catalysts proceeded in different manners, especially in terms of reaction rate and mechanism, depending on the combination of alcohol and acid used.

In this Chapter the preparation of novel copolymers of polystyrene-*graft*-poly(ethyl vinyl ether) by the grafting from methodology is demonstrated. The synthesis of such materials involved the preparation of hydroxylated polystyrene substrates as macroinitiators, and activation of the hydroxyl groups by a Lewis acid to initiate the cationic polymerization of ethyl vinyl ether. The substrates had either secondary or tertiary alcohol groups randomly distributed on linear or branched (arborescent) macromolecules prepared by “click” grafting as described in Chapter 3.

4.3 Experimental Section

4.3.1 Solvent and Reagent Purification

Toluene (Caledon, HPLC grade) was purified by refluxing with oligostyryllithium under dry N_2 atmosphere. Tetrahydrofuran (THF; Caledon, reagent grade) was purified by distillation from

sodium-benzophenone ketyl under nitrogen. The solvents were introduced directly from the stills into the polymerization reactor and the reaction setups through PTFE tubing.

Styrene (Aldrich, 99%) was purified by stirring with calcium hydride (CaH_2 , Sigma Aldrich, lumps, +4 mesh, reagent grade, 95%) overnight and distillation at reduced pressure. The purified monomer was stored under N_2 at $-20\text{ }^\circ\text{C}$ until a second purification step with phenylmagnesium chloride, as described in Section 4.3.2.1, immediately before polymerization. Dichloromethane (DCM, Sigma Aldrich, Chromasolv for HPLC, $\geq 99.8\%$) and ethyl vinyl ether (EVE, Aldrich, containing 0.1% KOH as stabilizer, 99%) were purified by stirring and distillation over CaH_2 , and were stored under N_2 at $5\text{ }^\circ\text{C}$ until further use. The initiator *sec*-butyllithium (*sec*-BuLi, Aldrich, 1.4 M solution in hexanes) was used as received; its exact concentration was determined by the method of Burchat et al.¹⁶ *n*-Butyllithium (*n*-BuLi, Aldrich, 2 M solution in hexanes), anhydrous aluminum chloride (AlCl_3 ; Acros Organics, 98.5%), acetyl chloride (EMD, 98%), phenylmagnesium chloride (Aldrich, 2.0 M solution in THF), nitrobenzene (Alfa Aesar, 99%), lithium aluminum hydride (LiAlH_4 ; Aldrich, 2 M solution in THF), benzophenone (Sigma Aldrich reagent plus; 99%), sodium (Aldrich, $\geq 99\%$, stored under mineral oil), hydrochloric acid (HCl, Fisherbrand ACS reagent, 11 M), sodium hydroxide (NaOH, Sigma Aldrich ACS reagent, $\geq 97\%$, pellets), 2,6-di-*tert*-butylpyridine (2,6-DTBP, Aldrich, $\geq 97\%$), and titanium tetrachloride (TiCl_4 , Sigma Aldrich ReagentPlus, 99.9% trace metals basis) were used as received from the suppliers.

4.3.2 Synthesis of Hydroxylated Substrates

4.3.2.1 Styrene Polymerization

The synthetic procedure used was as described by Li and Gauthier.¹⁷ Styrene (10 mL) was further purified with 10% phenylmagnesium chloride solution (1 mL) using high-vacuum purification techniques immediately before polymerization, whereby the monomer was degassed with three freeze-thaw cycles under vacuum before recondensation to an ampule (8.5 g of styrene collected). A 1-L glass reactor was used to polymerize styrene; the reactor was first evacuated, flamed, and then purged with nitrogen. Toluene (100 mL) was introduced directly from the purification still and the temperature was brought to 0 °C. Residual impurities were titrated by adding a few drops of styrene and enough *sec*-BuLi to obtain a persistent yellow-orange color. Then the calculated amount of *sec*-BuLi solution (1.21 mL, 1.7 mmol, for a target $M_n = 5000$) was added, followed by the styrene monomer. The solution was warmed to room temperature (23 °C) after 15 min and stirred for 1 h. The reaction was terminated with degassed methanol and the polymer was recovered by precipitation in 1 L of methanol, filtration, and drying under vacuum. The polymer was obtained in 95 % yield (8.1 g), with a number-average molecular weight $M_n = 5400$ and a polydispersity index $M_w/M_n = 1.06$.

4.3.2.2 Acetylation of Polystyrene

The acetylation procedure used was as described by Li and Gauthier.¹⁷ Polystyrene (4 g, 38 meq of styrene units) was dried under vacuum in a 500 mL round-bottomed flask, and dissolved in 80 mL of nitrobenzene. Anhydrous AlCl_3 (1.28 g, 9.6 mmol) was dissolved in 8 mL of nitrobenzene under nitrogen before adding acetyl chloride (0.82 mL, 11.5 mmol). This solution

was stirred at room temperature for 30 min before adding it drop-wise to the polymer solution, and the reaction was allowed to proceed for 45 min. Workup of the products first involved precipitation of the acetylated polymer in 600 mL of methanol acidified with 60 mL of concentrated (11 M) HCl as a first step. The polymer was recovered by filtration and further purified by two cycles of dissolution in THF (20 mL) and precipitation in 200 mL of methanol acidified with 20 mL of HCl (11 M). The polymer was then dissolved in chloroform (40 mL) and extracted twice with 40 mL of water. The polymer was finally recovered by precipitation in 300 mL of methanol, filtered by suction, and dried overnight under vacuum. The purified product (3.6 g, 86 % yield) had a substitution level of 21 % as determined by ^1H NMR spectroscopy.

4.3.2.3 Secondary Alcohol Groups from Acetylated Polystyrene

The reduction procedure used was similar to that reported by Zhu et al.¹⁸ Acetylated polystyrene (1.00 g, 1.85 meq of acetyl styrene units) was dried overnight under vacuum in a 250 mL round-bottomed flask and dissolved in 100 mL of THF. The flask was sealed with a rubber septum, purged with nitrogen, and cooled to 0 °C. LiAlH_4 (3.7 mL, 7.43 mmol; 4 molar equiv with respect to acetyl groups) was then added to the polymer solution at 0 °C with a syringe. The mixture was warmed to room temperature over 30 min and stirred for 4 h. The reaction was terminated by cooling to 0 °C and the drop-wise addition of 5 mL (90/10 v/v) of methanol/HCl under nitrogen. Workup of the product first involved concentrating the solution to 5 mL, precipitation in 50 mL (30/70 v/v) of methanol/ H_2O , and suction filtration. The polymer was further purified by two cycles of dissolution in chloroform (10 mL) and extraction with 10 mL of water. The polymer was finally recovered by precipitation in 100 mL of methanol/ H_2O (30/70 v/v), suction filtration, and drying overnight under vacuum. The purified product (0.86 g, 86 %

yield) had a substitution level of 21 mol % secondary alcohol as determined by ^1H NMR spectroscopy.

4.3.2.4 Tertiary Alcohol Groups from Acetylated Polystyrene

Acetylated polystyrene (1.00 g, 1.85 meq of acetylstyrene units) was dried overnight under vacuum in a 250 mL round-bottomed flask and dissolved in 100 mL of THF. The flask was sealed with a rubber septum, purged with nitrogen, and cooled to $-78\text{ }^\circ\text{C}$ in a 2-propanol/dry ice bath. *n*-BuLi (1.8 mL, 3.7 mmol; 2 molar equiv with respect to the acetyl groups) was added to the polymer solution at $-78\text{ }^\circ\text{C}$ with a syringe. The mixture was warmed to room temperature over 30 min and stirred for 1 h. The reaction was terminated by cooling to $0\text{ }^\circ\text{C}$ and the drop-wise addition of 5 mL (90/10 v/v) of methanol/HCl under nitrogen. Workup of the product first involved concentrating the solution to 10 mL, precipitation in 100 mL of methanol/ H_2O (90/10 v/v), suction filtration, and drying overnight under vacuum. The purified product (0.91 g, 78 % yield) had a substitution level of 18 mol % tertiary alcohol groups, as determined by ^1H NMR spectroscopy.

4.3.2.5 Functionalization of G0 Polystyrene

The acetylation of a G0 polymer ($M_n = 52,000$, $M_w/M_n = 1.09$, $f_n = 9$, side chain $M_n = 5200$) was achieved as reported in Section 4.3.2.2. The G0 (comb-branched) polystyrene substrate was synthesized by the procedure provided in Chapter 3. Starting from 1.00 g of G0 polymer, 0.32 g of AlCl_3 , and 0.2 mL of acetyl chloride, the polymer obtained in 82 % yield (0.91 g) had a substitution level of 28 mol % as determined by ^1H NMR analysis.

Reduction of the acetylated G0 polymer was achieved as described in Section 4.3.2.3 using 0.40 g of acetylated polymer and 2.15 mL of LiAlH₄ solution; the polymer obtained (0.36 g, 90% yield) had a substitution level of 28 mol % as determined by ¹H NMR analysis.

The introduction of tertiary alcohol groups on the acetylated G0 polymer was done as described in Section 4.3.2.4, starting from 0.35 g of acetylated polymer and 1.34 mL *n*-BuLi. The polymer obtained (0.33 g, 85% yield) had a substitution level of 19% as determined by ¹H NMR analysis.

4.3.2.6 Functionalization of G1 Polystyrene

Acetylation of the G1 polymer ($M_n = 4.34 \times 10^5$, $M_w/M_n = 1.10$, $f_n = 74$, side chain $M_n = 5200$) was done as reported in Section 4.3.2.2. The G1 polystyrene substrate used was synthesized according to the procedure provided in Chapter 3. Starting from 0.60 g of G1 polymer, 0.19 g of AlCl₃, and 0.12 mL of acetyl chloride, the polymer obtained (0.53 g, 82% yield) had a substitution level of 24 mol % as determined by ¹H NMR analysis.

Reduction of the acetylated G1 polymer was achieved as described in Section 4.3.2.3, starting from 0.20 g of acetylated polymer and 0.93 mL LiAlH₄. The polymer obtained (0.18 g, 90% yield) had a substitution level of 24 mol % as determined by ¹H NMR analysis.

The introduction of tertiary alcohol groups on the acetylated G1 polymer was done as described in Section 4.3.2.4, starting from 0.20 g of acetylated polymer and 0.65 mL of *n*-BuLi. The polymer obtained (0.19 g, 86% yield) had a substitution level of 15 mol % as determined by ¹H NMR analysis.

4.3.3 Grafting of Poly(ethyl vinyl ether) from Hydroxylated Substrates

4.3.3.1 Grafting from Linear Polystyrene

Hydroxylated linear polystyrene (0.10 g, 0.20 meq of secondary alcohol groups) was dried overnight under vacuum in a 100 mL round-bottomed flask. The flask was then sealed with a rubber septum, purged with nitrogen, and the sample was dissolved in 5 ml of dry DCM introduced with a syringe.

A 250 mL three-neck round-bottomed flask was connected to a high-vacuum line, and a rubber septum and a glass stopcock were installed on the two other openings. The flask was evacuated, flamed, and filled with nitrogen. The polymer solution, DCM (100 mL), and 2,6-DTBP (0.09 mL, 0.4 mmol; 2 molar equiv with respect to hydroxyl groups) were introduced into the flask with a syringe through the rubber septum and the temperature was brought to -20 °C in a methanol/water mixture and dry ice. TiCl_4 (0.11 mL, 1.0 mmol, 5 molar equiv with respect to hydroxyl groups) was added with a syringe to the mixture, resulting instantly in a dark orange color. The mixture was left stirring for 10 min and the temperature was decreased to -40 °C with a 2-propanol/water mixture and dry ice before adding EVE (1.34 mL, 14.0 mmol, for a target side chain $M_n = 5000$) with a syringe. The color changed instantly to dark green after adding the EVE; the mixture was stirred further for 30 min at -40 °C before the reaction was terminated with 0.5 ml of chilled methanol/NaOH solution. Workup of the product first involved filtration through filter paper to remove initiator decomposition residues, extraction with 100 mL of 0.1 M sodium hydroxide solution, and two extractions with 100 mL of water. The polymer solution was concentrated to 10 mL and the final product was recovered by precipitation in 100 mL (30/70

v/v) of methanol/H₂O, and drying for 4 h under vacuum. The purified product (0.89 g) was dissolved in 10 mL of THF and stored at 5 °C.

Grafting of PEVE from the linear substrate functionalized with tertiary hydroxyl groups was done as described above, using the polymer described in Section 4.3.2.4. The hydroxylated linear polystyrene (0.10 g, 0.17 meq of tertiary alcohol groups), 2,6-DTBP (0.08 mL, 0.35 mmol; 2 molar equiv with respect to hydroxyl groups), TiCl₄ (0.095 mL, 0.86 mmol, 5 molar equiv with respect to hydroxyl groups), and EVE (1.15 mL, 12 mmol, for a target side chain $M_n = 5000$) were used. The purified product (0.81 g) was dissolved in THF and stored at 5 °C.

4.3.3.2 Grafting from G0 Polystyrene

Grafting of PEVE from the G0 substrate functionalized with secondary hydroxyl groups was achieved as described in Section 4.3.3.1, using the G0 sample of Section 4.3.2.5 (0.1 g, 0.27 meq of secondary alcohol groups), 2,6-DTBP (0.12 mL, 0.54 mmol; 2 molar equiv with respect to hydroxyl groups), TiCl₄ (0.15 mL, 1.35 mmol, 5 molar equiv with respect to hydroxyl groups), and EVE (1.78 mL, 18.6 mmol, for a target side chain $M_n = 5000$). The purified product (1.21 g) was dissolved in THF and stored at 5 °C.

Grafting of PEVE from the G0 substrate functionalized with tertiary alcohol groups was as described in Section 4.3.3.1, using the G0 polymer of Section 4.3.2.5 (0.10 g, 0.18 meq of tertiary alcohol groups), 2,6-DTBP (0.08 mL, 0.36 mmol; 2 molar equiv with respect to hydroxyl groups), TiCl₄ (0.1 mL, 0.9 mmol, 5 molar equiv with respect to hydroxyl groups), and EVE (1.21 mL, 12.6 mmol, for a target side chain $M_n = 5000$). The purified product (0.82 g) was dissolved in THF and stored at 5 °C.

4.3.3.3 Grafting from G1 Polystyrene

Grafting of PEVE from the G1 substrate with secondary alcohol functionalities was done as described in Section 4.3.3.1, using the G1 substrate of Section 4.3.2.6 (0.10 g, 0.23 meq of secondary alcohol groups), 2,6-DTBP (0.1 mL, 0.46 mmol; 2 molar equiv with respect to hydroxyl groups), TiCl_4 (0.13 mL, 1.15 mmol, 5 molar equiv with respect to hydroxyl groups), and EVE (1.5 mL, 16 mmol, for a target side chain $M_n = 5000$). The purified product (1.06 g) was dissolved in THF and stored at 5 °C.

Grafting of PEVE from tertiary alcohol functionalities was achieved as described in Section 4.3.3.1, using the G1 polymer of Section 4.3.2.6 (0.10 g, 0.14 meq of tertiary alcohol groups), 2,6-DTBP (0.06 mL, 0.28 mmol; 2 molar equiv with respect to hydroxyl groups), TiCl_4 (0.08 mL, 0.7 mmol, 5 molar equiv with respect to hydroxyl groups), and EVE (0.95 mL, 10 mmol, for a target side chain $M_n = 5000$). The purified product (0.66 g) was dissolved in THF and stored at 5 °C.

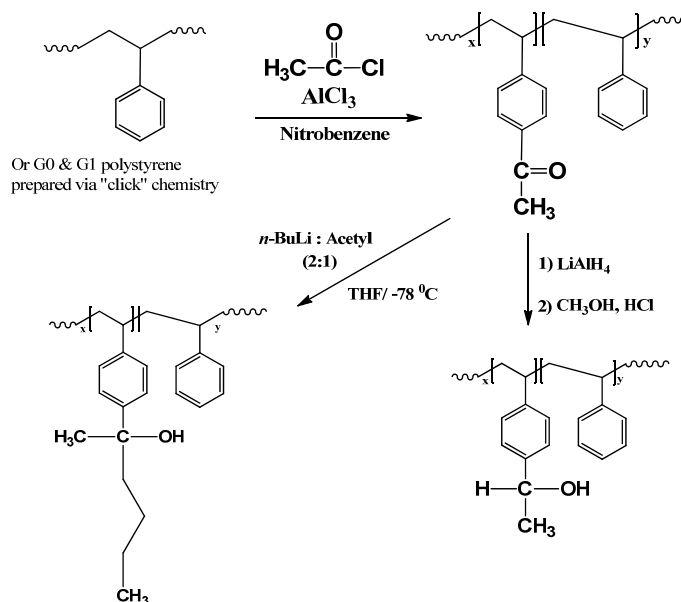
4.3.4 Polymer Characterization

Size exclusion chromatography (SEC) analysis was performed for the substrates before and after acetylation, reduction, after treatment with *n*-BuLi, and for the graft copolymers. The system used consisted of a Viscotek GPC max unit equipped with a VE 2001 GPC Solvent/sample Module, a Viscotek triple detector array equipped with a refractive index, viscosity, and dual-angle light scattering detectors, an external Viscotek UV 2600 detector, and three PolyAnalytik organic mixed bed columns, PAS-103-L, PAS-104-L, and PAS-105-L, with dimensions of 8 mm (ID) \times 300 mm (L) each, and an overall polystyrene molecular weight range

of 10^3 to 10^7 . The polymers were analyzed in THF at a flow rate of 1 mL/min. ^1H NMR analysis of all the polymer samples was achieved in CDCl_3 on a Bruker Avance 300 MHz NMR instrument at a concentration of 40-50 mg/mL.

4.4 Results and Discussion

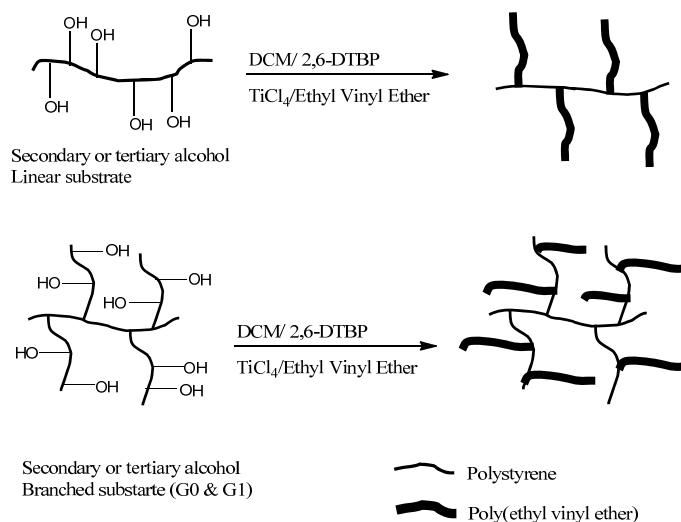
The introduction of secondary and tertiary hydroxyl functionalities onto polystyrene substrates was achieved as described in Scheme 4.1. The acetylation reaction was followed by reduction with lithium aluminum hydride to obtain secondary alcohol groups, whereas treatment of the acetylated substrates with *n*-BuLi led to tertiary alcohol functionalities.



Scheme 4.1. Synthesis of polystyrene substrates with secondary or tertiary alcohol functionalities.

Grafting of PEVE chains from the hydroxylated substrates was achieved as described in Scheme 4.2. The polymers with secondary or tertiary alcohol groups (either linear or branched)

were activated with titanium tetrachloride in the presence of 2,6-DTBP (as a proton trap) in dichloromethane, and ethyl vinyl ether was added to grow the PEVE chains from the initiating sites.



Scheme 4.2. Grafting of poly(ethyl vinyl ether) chains from hydroxylated polystyrene.

4.4.1 Synthesis of Hydroxylated Substrates

4.4.1.1 Linear Polystyrene and Acetylation

The linear polymer synthesized in toluene had the expected number-average molecular weight ($M_n = 5400$) and a narrow MWD (polydispersity $M_w/M_n = 1.06$). Acetylation of this polymer yielded a substrate with a substitution level of 21 mol %, as determined by ¹H NMR spectroscopy. The acetylation level was controlled by nearly stoichiometric amounts of AlCl₃ and acetyl chloride as described previously.

The introduction of the acetyl group caused two new resonances at 2.55 ppm (acetyl protons) and 7.65 ppm (aromatic protons ortho to the acetyl group) in the ^1H NMR spectrum (Figure 4.1a).

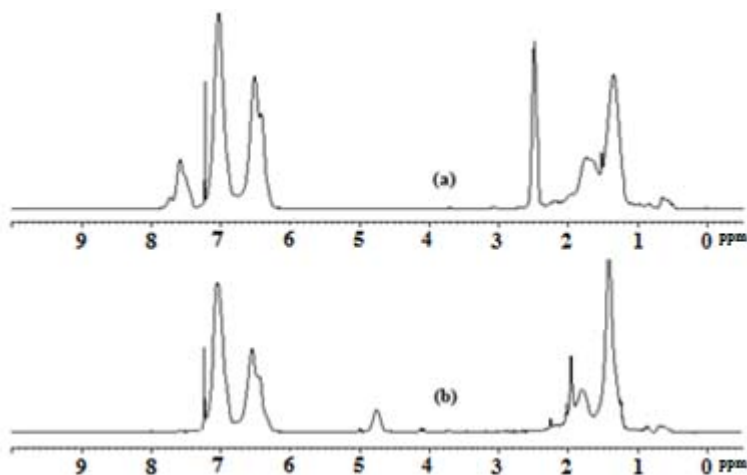


Figure 4.1. ^1H NMR spectra for (a) acetylated polystyrene and (b) secondary alcohol-functionalized linear polystyrene.

4.4.1.2 Secondary Alcohol-functionalized Linear Polystyrene

Reduction of the acetylated polymer yielded a substrate with 21 % of the styrene units containing a secondary alcohol group, as determined by ^1H NMR spectroscopy analysis. The resonances at 2.55 and 7.65 ppm related to the presence of the acetyl functionalities disappeared, whereas a new resonance appeared at 4.8 ppm (proton adjacent to the hydroxyl group) as shown in Figure 4.1b. The SEC analysis of the hydroxylated polymer, represented in Figure 4.2, yielded a number-average molecular weight $M_n = 5600$ and a polydispersity index $M_w/M_n = 1.08$. The SEC analysis results, in addition to the low polydispersity index values obtained before and after acetylation and reduction, suggest that these reactions proceeded without cross-linking or chain degradation. The integration of the peak intensity for the methyl protons in the acetyl group at

2.55 ppm before reduction is also consistent with the peak intensity for the proton adjacent to the hydroxyl group at 4.8 ppm after reduction, which further confirms full conversion from the acetyl to the hydroxyl functionality.

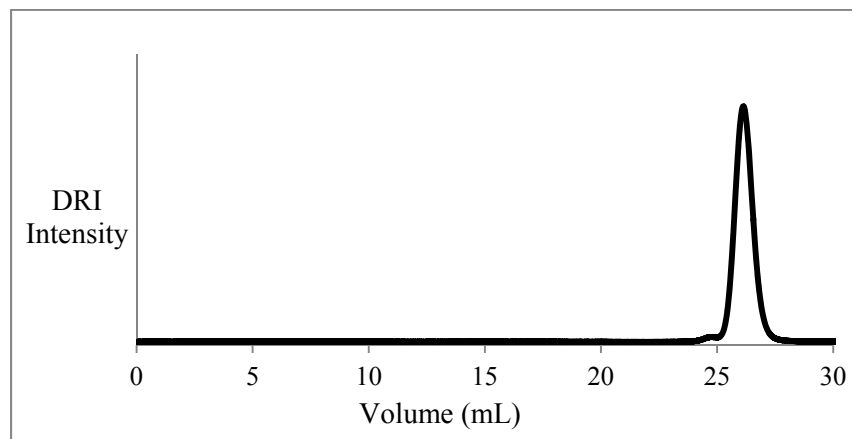


Figure 4.2. SEC trace for linear hydroxyl-functionalized polystyrene with secondary alcohol groups ($M_n = 5600$, $M_w/M_n = 1.08$).

4.4.1.3 Tertiary Alcohol-functionalized Linear Polystyrene

Treatment of the acetylated polymer with *n*-BuLi yielded a substrate with 18 % of the styrene units bearing a tertiary hydroxyl group, as determined by ^1H NMR spectroscopy analysis. The intensity of the resonances at 2.55 and 7.65 ppm, related to the presence of acetyl functionalities, strongly decreased since most of them reacted, whereas the introduction of the hydroxyl functionality caused a new resonance at 0.8 ppm (methyl protons in the butyl group) as shown in Figure 4.3. Integration of the peak for the acyl protons (2.55 ppm) for comparison with the peak for the aromatic protons (7.6-7.9 ppm) showed that 3% of acetyl groups were left unreacted. Integration of the peak for the methyl protons in the butyl group (0.8 ppm) yielded 18% functionalization with tertiary alcohol groups, which is again consistent with the original 21%

substitution level before *n*-BuLi addition. SEC analysis of the hydroxylated polymer, represented in Figure 4.4, yielded $M_n = 5700$ and $M_w/M_n = 1.05$. The low PDI values measured before and after hydroxylation suggest that these reactions proceeded without cross-linking or degradation.

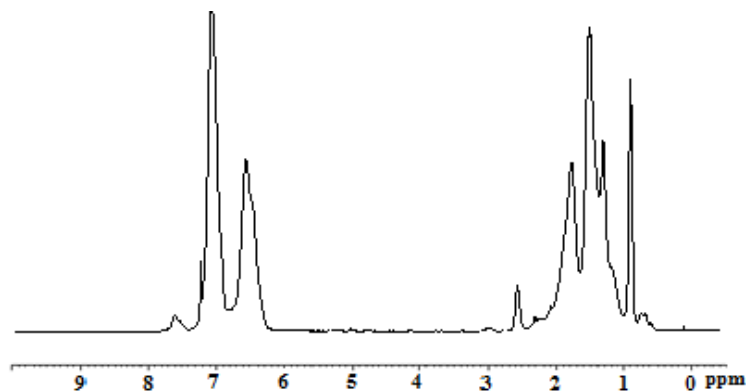


Figure 4.3. ¹H NMR spectrum for tertiary alcohol-functionalized polystyrene.

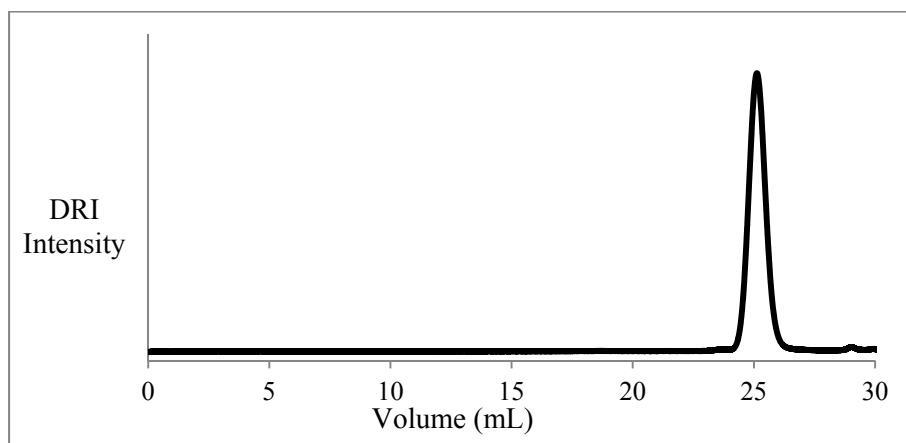


Figure 4.4. SEC trace for tertiary alcohol-functionalized polystyrene ($M_n = 5700$, $M_w/M_n = 1.05$).

4.4.1.4 Functionalization of G0 and G1 Polystyrene

The introduction of acetyl groups onto the G0 substrate (synthesized by “click” grafting as described in Chapter 3) and their subsequent conversion to secondary or tertiary alcohol functionalities led to NMR spectrum features similar to the ones described above for the linear polymers. The G0 acetylated substrate, with a substitution level of 28 mol %, $M_n = 5.8 \times 10^4$, and $M_w/M_n = 1.14$, yielded 28 mol % of styrene units with secondary alcohol groups upon reduction with LiAlH_4 ($M_n = 5.8 \times 10^4$ and $M_w/M_n = 1.18$), while 9 % of acetyl groups and 19% of tertiary alcohol group functionalization were obtained after *n*-BuLi addition ($M_n = 6.1 \times 10^4$ and $M_w/M_n = 1.15$)

The functionalization of the G1 polystyrene substrate (prepared by “click” grafting as described in Chapter 3) yielded an acetylation level of 24 mol %, with $M_n = 4.6 \times 10^5$ and $M_w/M_n = 1.10$. Reduction of that polymer yielded a substrate with 24 mol % of secondary alcohol groups ($M_n = 4.6 \times 10^5$ and $M_w/M_n = 1.15$), while treatment with *n*-BuLi led to 9% of unreacted acetyl groups and 15% of tertiary alcohol functionalities ($M_n = 4.8 \times 10^5$ and $M_w/M_n = 1.13$)

4.4.2 Grafting of Poly(ethyl vinyl ether) from Hydroxylated Substrates

4.4.2.1 Grafting of Poly(ethyl vinyl ether) from Linear Polystyrene

Polystyrene-*graft*-poly(ethyl vinyl ether) (PS-*graft*-PEVE) was successfully synthesized by grafting PEVE from the secondary and tertiary alcohol-functionalized linear polystyrene macroinitiators. Grafting was carried out in DCM at $-40\text{ }^\circ\text{C}$ in the presence of 2,6-DTBP; TiCl_4 was added to the hydroxylated substrate at $-20\text{ }^\circ\text{C}$ to activate the hydroxyl groups before adding

EVE. A color change to red-orange was observed immediately after the addition of TiCl_4 , which is an indication of the activation of the hydroxyl groups. After the addition of EVE a dark green color was observed, due to the propagation of the PEVE chains. The reaction was carried out in the presence of 2,6-DTBP, a sterically hindered pyridine containing two *tert*-butyl substituents, which has long been recognized as a ‘non-nucleophilic’ base useful in cationic polymerization. It is unreactive towards Lewis acids^{19,20} and carbocations,²¹ and useful to thwart chain transfer²² and to prevent protic initiation²³ in such polymerizations. DCM was the solvent of choice among others suitable for cationic polymerization because the hydroxylated substrates were soluble in DCM even at $-20\text{ }^\circ\text{C}$, thus allowing the activation of the hydroxyl groups at that temperature. A sample was removed from all the grafting reactions for SEC analysis, to confirm that no linear homopolymers was formed along with the graft copolymer.

Grafting of PEVE from secondary hydroxylated substrates was very successful in terms of grafting efficiency and MWD of the copolymer obtained, as seen from the SEC trace in Figure 4.5. The comb-branched PS-*graft*-PEVE obtained had $M_n = 5.6 \times 10^4$ and $M_w/M_n = 1.16$, without any evidence of contamination by homo PEVE, in contrast to previous reports,^{10,11} so that no further purification was required to isolate the graft copolymers. The number-average molecular weight obtained for the graft copolymer is 5.6×10^4 , which compares well with the theoretical M_n for full monomer conversion ($M_n = 6.0 \times 10^4$). If 100% initiation efficiency is assumed, the branching functionality f_n would be equal to the number of initiating sites on the substrate; and hence the corresponding number-average molecular weight per side chain (M_n^{br}) can be calculated from the equation

$$M_n^{\text{br}} = \frac{M_n(G) - M_n(G - 1)}{f_n}$$

where $M_n(G)$ and $M_n(G - 1)$, are the absolute number-average molecular weight of graft polymers of generation G and of the substrate, respectively. The M_n^{br} per side chain calculated for the graft copolymer derived from the linear secondary alcohol-functionalized substrate on that basis was 4600.

Grafting of PEVE from the substrate functionalized with tertiary alcohol groups also proceeded successfully and again without the formation of any homo PEVE, as seen from the SEC trace in Figure 4.6. The theoretical M_n for the graft polymer (for full monomer conversion) was 5.2×10^4 but the comb-branched PS-*graft*-PEVE obtained had $M_n = 4.3 \times 10^4$, $M_w/M_n = 1.44$, and the corresponding M_n^{br} per side chain is 4000. It can be noticed that the MWD of the graft copolymer obtained from the tertiary alcohol-functionalized substrate is significantly broader than for the one derived from secondary alcohol groups. This result is in good agreement with analogous reactions using secondary and tertiary alcohols to initiate the cationic polymerization of certain vinyl ether monomers such as isobutyl, chlorohexyl, and *tert*-butyl vinyl ether, where the polymers generated from secondary alcohols had narrower MWD than those obtained from tertiary alcohols.²⁴ This was attributed to the more “uncontrolled” character of the tertiary alcohol reactions. The tertiary alcohol-functionalized polystyrene substrates used in our investigation had a limited solubility in DCM at -20 °C: They precipitated from the reaction mixture when the temperature dropped to about -25 to -30 °C. It is therefore suggested that, given the poor solubility of these macroinitiators even at -20 °C, the higher PDI values obtained for the tertiary alcohol macroinitiator may be due to aggregation of the substrate polymer under the conditions used in the current study.

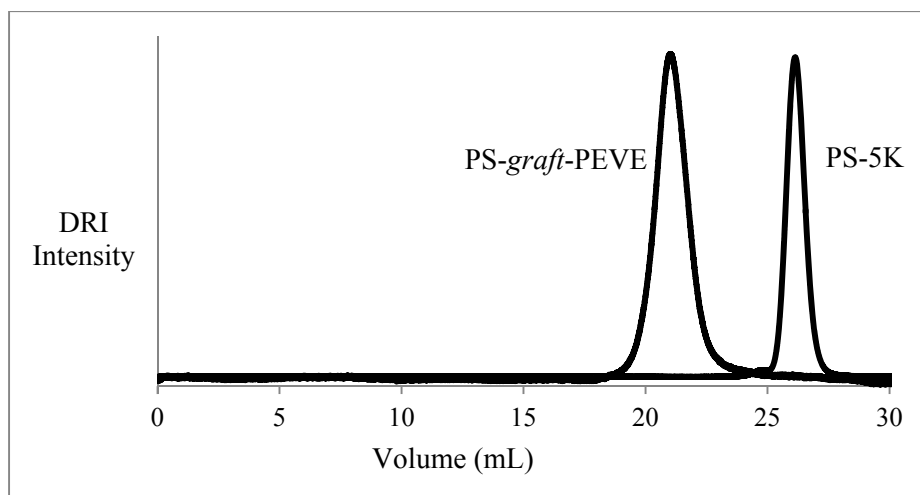


Figure 4.5. SEC traces for grafting poly(ethyl vinyl ether) chains from linear polystyrene with secondary alcohol sites ($M_n = 56,000$, $M_w/M_n = 1.16$).

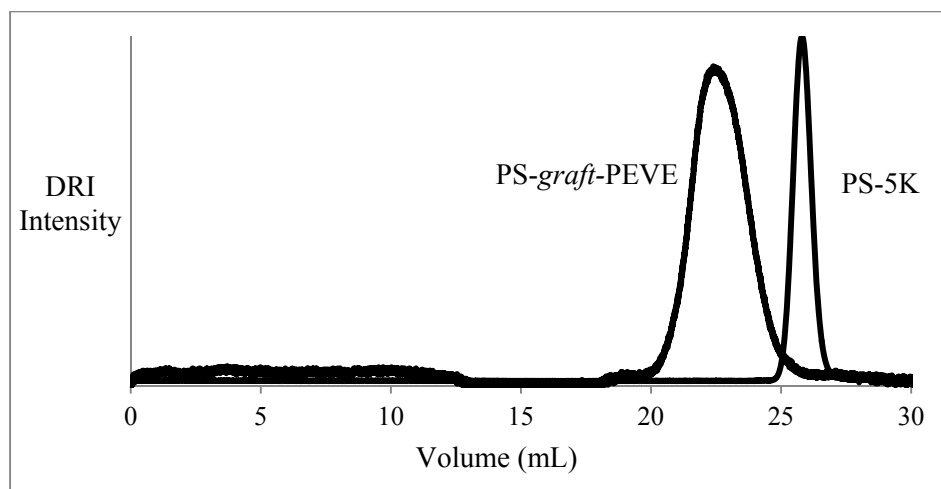


Figure 4.6. SEC traces for grafting poly(ethyl vinyl ether) chains from linear polystyrene with tertiary alcohol sites ($M_n = 43,000$, $M_w/M_n = 1.44$).

4.4.2.2 Grafting of Poly(ethyl vinyl ether) from G0 Polystyrene

Grafting of PEVE from G0 substrates with secondary or tertiary alcohol functionalities was performed under the same conditions described for the linear substrates. Grafting from the secondary hydroxylated G0 substrate was successful without the formation of homo PEVE (Figure 4.7). The theoretical M_n for the graft polymer (for full monomer conversion) was 6.02×10^5 but the G1 PS-*graft*-PEVE obtained had $M_n = 3.2 \times 10^5$, $M_w/M_n = 1.45$, and the corresponding M_n^{br} per side chain is 1900. Grafting of PEVE from the G0 tertiary alcohol-functionalized substrate was likewise successful (Figure 4.8). The theoretical M_n for the graft polymer (for full monomer conversion) was 4.75×10^5 but the G1 PS-*graft*-PEVE obtained had $M_n = 2.6 \times 10^5$, $M_w/M_n = 1.58$, and the corresponding M_n^{br} per side chain is 2100. It can be noticed again that the MWD of the graft copolymer derived from the tertiary alcohol-functionalized G0 substrate was slightly broader than for the secondary alcohol, similarly to the linear systems. However the PDI values for both G1 copolymers are higher than for the analogous G0 (comb- branched) copolymers, derived from the linear substrates. The G0 substrates are more congested than their linear analogues and thus, upon activation by TiCl_4 , some of the hydroxyl groups on the G0 polymer may not be activated initially and/or the solubility of the substrate may be reduced. After the addition of EVE and chain growth starts the remainder of the hydroxyl groups may become activated by the excess of TiCl_4 present and chain growth may take place from these initiating sites, but side chains with different lengths may be produced under these conditions and lead to higher PDI values for the copolymers.

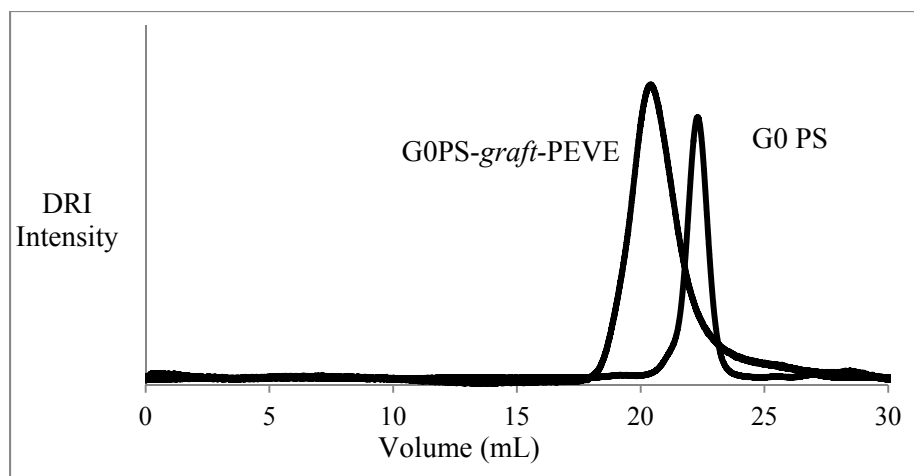


Figure 4.7. SEC traces for grafting poly(ethyl vinyl ether) chains from secondary alcohol-functionalized G0 polystyrene ($M_n = 3.2 \times 10^5$, $M_w/M_n = 1.45$).

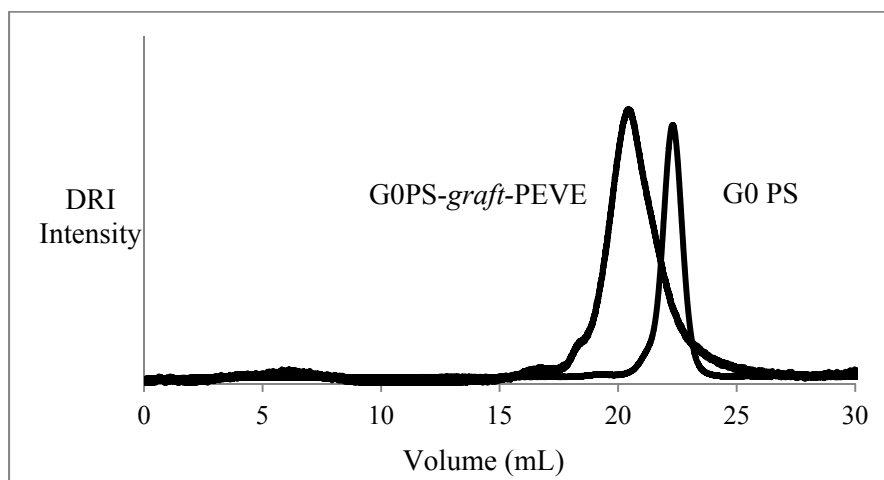


Figure 4.8. SEC traces for grafting poly(ethyl vinyl ether) chains from tertiary alcohol-functionalized G0 polystyrene ($M_n = 2.6 \times 10^5$, $M_w/M_n = 1.58$).

4.4.2.3 Grafting of Poly(ethyl vinyl ether) from G1 Polystyrene

Grafting of PEVE from the G1 hydroxylated substrates was performed under the same conditions used for the linear substrates and proceeded successfully without the formation of

homo PEVE chains. This is seen from the SEC traces in Figures 4.9 and 4.10 for the grafting substrates with secondary and tertiary alcohol functionalities, respectively. The corresponding G2 copolymers (G1PS-*graft*-PEVE) had $M_n = 2.8 \times 10^6$ and $M_w/M_n = 1.49$ (secondary alcohol) and $M_n = 1.6 \times 10^6$ and $M_w/M_n = 2.1$ (tertiary alcohol). The theoretical M_n for the graft polymer (for full monomer conversion) was 5.4×10^6 (secondary alcohol) and 3.6×10^6 (tertiary alcohol) but the G2 PS-*graft*-PEVE obtained had $M_n = 2.8 \times 10^6$ and $M_w/M_n = 1.49$ (secondary alcohol) and $M_n = 1.6 \times 10^6$ and $M_w/M_n = 2.1$ (tertiary alcohol); whereas the corresponding M_n^{br} per side chain is 2300 (secondary alcohol) and 1800 (tertiary alcohol). As noticed for the linear and G0 substrates, the tertiary alcohol led to a broader MWD for the G2 graft copolymer. The PDI values for the G2 copolymers are also higher than for the G1 and G0 systems, presumably for the same accessibility and/or solubility arguments discussed above for the G1 copolymers.

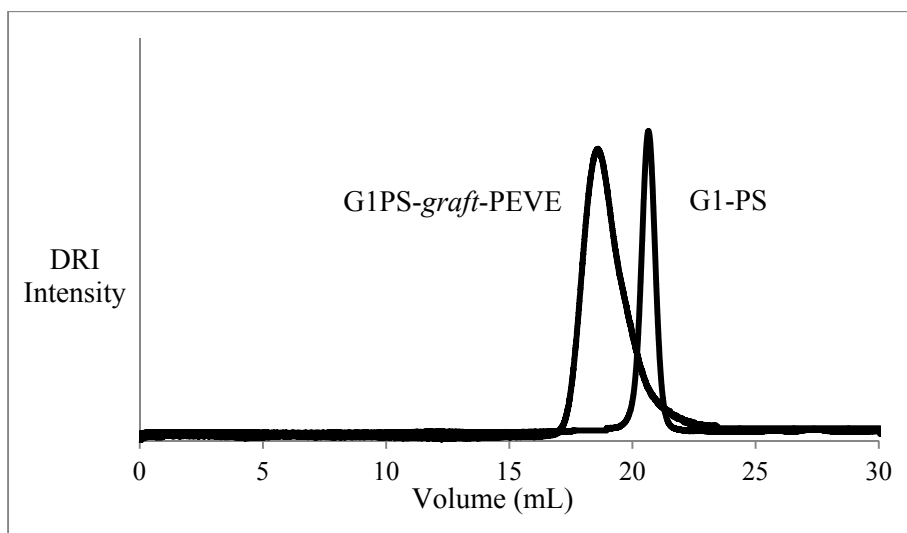


Figure 4.9. SEC traces for grafting poly(ethyl vinyl ether) chains from secondary alcohol-functionalized G1 polystyrene ($M_n = 2.8 \times 10^6$, $M_w/M_n = 1.49$).

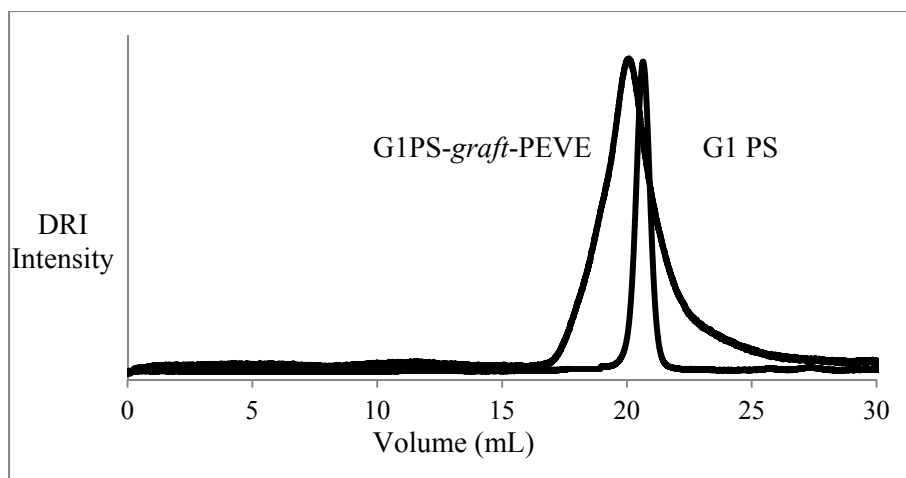


Figure 4.10. SEC traces for grafting poly(ethyl vinyl ether) chains from tertiary alcohol-functionalized G1 polystyrene ($M_n = 1.6 \times 10^6$, $M_w/M_n = 2.10$).

The characteristics of the graft copolymers obtained from the secondary and tertiary alcohol-functionalized substrates are summarized in Table 4.1. It is clear that the graft copolymers derived from the tertiary alcohol have broader MWD than those obtained from the secondary alcohol. Additionally, the experimental M_n^{br} for the copolymers became significantly smaller than the target values ($M_n = 5000$) as the size (generation number) of the grafting substrate increased. This is presumably the result of incomplete monomer conversion; unfortunately this parameter was not monitored during experimental work.

Table 4.1. Characteristics of arborescent graft PEVE copolymers.

	<u>Secondary Alcohol</u>			<u>Tertiary Alcohol</u>		
	M_n^a	M_w/M_n^a	$M_n^{br\ b}$	M_n^a	M_w/M_n^a	$M_n^{br\ b}$
PS-PEVE	5.6×10^4	1.16	4.6×10^3	4.3×10^4	1.44	4.0×10^3
G0PS-PEVE	3.2×10^5	1.45	1.9×10^3	2.6×10^5	1.58	2.1×10^3
G1PS-PEVE	2.8×10^6	1.49	2.3×10^3	1.6×10^6	2.10	1.8×10^3

^a Absolute values for the graft copolymers determined by SEC-MALLS analysis.

^b Calculated values for the side chains, when assuming 100% initiator efficiency.

4.5 Conclusions

Linear and branched (arborescent G0 and G1) polystyrene substrates were synthesized by anionic polymerization and “click” grafting. Acetylation of these substrates followed by reduction produced secondary alcohol groups, whereas their treatment with *n*-butyllithium led to tertiary alcohol-functionalized polystyrene. The hydroxylated substrates were activated with TiCl₄ in the presence of 2,6-di-*tert*-butylpyridine in dichloromethane, and ethyl vinyl ether was added to graft PEVE chains from the hydroxylated substrates. Grafting of PEVE from the linear and branched secondary and tertiary alcohol-functionalized substrates was successful and produced G0-G2 graft copolymers with molecular weights increasing with the generation number ($M_n = 5.6 \times 10^4$, 3.2×10^5 , and 2.8×10^6 for G0, G1, and G2 copolymers obtained from the secondary alcohol-functionalized substrates, respectively). The MWD of the graft copolymers derived from the tertiary alcohol was broader than from the secondary alcohol, as it was also observed for secondary and tertiary alcohol small molecule initiators in the cationic polymerization of isobutyl, cyclohexyl, and *tert*-butyl vinyl monomers. The MWD of the graft copolymers also broadened with the generation number ($M_w/M_n = 1.16$, 1.45, and 1.49 for the

G0, G1, and G2 copolymers derived from secondary alcohol-functionalized substrates, respectively), presumably due to limited hydroxyl group activation in the initiation step as a result of the congested structure of the branched substrates and/or limited solubility. None of the graft copolymers synthesized were contaminated with homo PEVE chains, in contrast to previous investigations using alcohols or alkyl halides with Lewis acids to obtain graft or block copolymers. The hydroxylated polystyrene macroinitiators, in combination with cationic polymerization, thus seem to provide a promising new path to the synthesis of novel arborescent materials with a wider range of properties.

Chapter 5

Synthesis of Arborescent Polybutadiene by “Click” Grafting

5.1 Outline

A novel strategy combining the anionic polymerization and “click” grafting techniques was developed for the synthesis of arborescent polybutadiene. Azide functionalities were randomly introduced on the grafting substrate by a reaction sequence of epoxidation, reduction, tosylation, and azidation. The anionic polymerization of butadiene initiated with 6-*tert*-butyldimethylsiloxyhexyllithium (TBDMS-O-Hexyl-Li) served to synthesize polybutadiene with a protected hydroxyl chain end. Deprotection of the hydroxyl group, followed by treatment with sodium hydride and propargyl bromide, yielded the material serving as side chains. Coupling of the acetylene-terminated side chains ($M_n = 5200$) with a linear azide-functionalized substrate ($M_n = 5200$) in the presence of a Cu (I) catalyst proceeded in up to 76 % yield under optimized conditions. Repetition of cycles of substrate functionalization and side chain coupling led to arborescent polybutadiene of generations G1 and G2 in 59 and 40% yield, respectively, with $M_n = 3.4 \times 10^6$ and a branching functionality $f_n = 530$ reached for the G2 polymer. The complementary approach to synthesize arborescent polybutadiene by “click” chemistry, using substrates randomly functionalized with acetylene groups and azide-terminated polybutadiene side chains, was also examined. Coupling of the azide-terminated side chains ($M_n = 5200$) with an acetylene-functionalized substrate ($M_n = 5300$) proceeded in 86 % yield, but the G0 substrate functionalized with alkyne groups was very unstable and cross-linked too rapidly to be used in grafting reactions.

5.2 Introduction

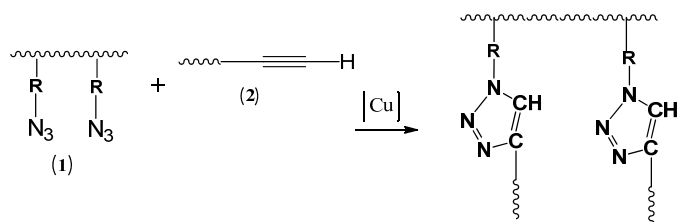
Arborescent polymers have attracted attention because of their controllable architecture, but also due to their peculiar rheological properties¹⁻³ potentially interesting for applications as

rheological modifiers for other polymers.⁴ Since these dendritic macromolecules are constructed from polymeric building blocks of uniform size rather than monomers, very high molecular weights are attained in few synthetic steps. Living anionic polymerization techniques have enabled the synthesis of a wide range of well-defined dendritic polymers.⁵ The adaptation of well-known reactions from organic chemistry to polymer science has also yielded promising results to obtain novel structures by coupling preformed polymers.² The combination of state-of-the-art living/controlled polymerization techniques with “click” chemistry coupling, as introduced by Sharpless,^{6,7} may thus be useful to couple preformed polymer chains into more complex constructs.

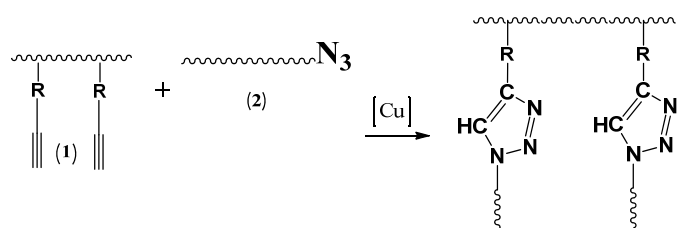
One of the most widely investigated reactions within the “click” chemistry concept is the azide-alkyne Huisgen cycloaddition catalyzed by Cu (I).⁸ Azide and alkyne functionalities are easily introduced into molecules, and their relatively good stability under different conditions has favored the emergence of this field in polymer science, as it allows the fast and simple creation of well-defined, complex polymeric structures that were previously unattainable. There have been few attempts to modify polybutadiene by “click” chemistry, most of which involved thiolene “click”, such as in the synthesis of amphiphilic poly(ethylene oxide)-*block*-poly(butadiene-*graft*-liquid crystal) copolymers,⁹ and in the modification of 1,2-polybutadiene using UV light or sunlight.¹⁰ Kukut et al.¹¹ developed self-curable benzoxazine-functionalized polybutadiene by azide-alkyne “click” chemistry, whereas Guo et al.¹² studied the surface modification of nanoporous 1,2-polybutadiene by azide-alkyne “click” chemistry. However to date there are no reports on the synthesis of arborescent polymers by “click” chemistry. In this report, the application of the azide-alkyne 1,3-dipolar cycloaddition to the preparation of well-defined polybutadiene architectures is discussed. Two different strategies were explored to this end, as

described in Scheme 5.1, whereby one type of reactive group was randomly distributed on the substrate, while the side chains contained the complementary functionality type. The merits of each approach will be considered.

Strategy A:



Strategy B:



Scheme 5.1. Proposed strategies for the synthesis of arborescent polybutadiene.

5.3 Experimental Section

Purification of the monomer and other reagents serving in the polymerization reactions was achieved in reusable glass ampules on a high-vacuum line connected to a nitrogen (N_2) purification system. The ampules were equipped with polytetrafluoroethylene (PTFE) stopcocks and ground glass joints for direct assembly onto the polymerization reactor.¹³

5.3.1 Solvent and Reagent Purification

Tetrahydrofuran (THF; Caledon, reagent grade) was purified by distillation from sodium-benzophenone ketyl under nitrogen. Cyclohexane (Caledon, reagent grade) and toluene (Caledon, HPLC grade) were purified by refluxing with oligostyryllithium under dry N₂ atmosphere. The solvents were introduced directly from the stills into the polymerization reactor and reaction setups through PTFE tubing.

Butadiene (Praxair, 99 %) was purified with *n*-butyllithium as described in Section 5.3.2.1. The initiator *sec*-butyllithium (*sec*-BuLi, Aldrich, 1.4 M solution in hexanes) was used as received; its exact concentration was determined by the method of Burchat et al.¹⁴ Propargyl bromide (Aldrich, 80 wt% in toluene), tetrabutylammonium fluoride (TBAF; Aldrich, 1 M solution in THF), dichloromethane (Caledon, HPLC grade), *p*-toluenesulfonyl chloride (TsCl; Alfa Aesar, 98%), pyridine (Caledon, reagent grade), N,N-dimethylformamide (Omnisolv, 99%), sodium azide (Sigma Aldrich, 99.5%), *N,N,N',N'',N''*-pentamethyldiethylenetriamine (PMDETA; Aldrich, 99%), 2,2'-bipyridyl (Sigma Aldrich, 99.9%), copper (I) bromide (Aldrich, 99.999%), lithium aluminum hydride (LiAlH₄; Aldrich, 2 M solution in THF), benzophenone (Sigma Aldrich, reagent plus; 99%), sodium (Aldrich, ≥99%, stored under mineral oil), *n*-butyllithium (*n*-BuLi, Aldrich, 2M in hexane), 3-chloroperbenzoic acid (Aldrich, 77%), sodium hydroxide (Caledon), and sodium hydride (NaH, Aldrich, 60% dispersion in mineral oil) were all used as received from the suppliers.

5.3.2 Backbone Synthesis and Functionalization (Strategy A)

5.3.2.1 Butadiene Polymerization

The polymerization procedure used was described by Yuan and Gauthier.¹⁵ Butadiene (9.6 g, 0.17 mol; 15 mL) was stirred with *n*-butyllithium (1.5 mL) in a high-vacuum manifold for 30 min at -30 °C, condensed into a calibrated ampule, and diluted with 15 mL of dry toluene. The ampule was stored at -20 °C until further use. A 2-L glass reactor served to polymerize butadiene; it was first evacuated and flamed, then purged with nitrogen. Toluene (150 mL) was introduced directly from the still and the temperature was brought to 0 °C. Residual impurities were titrated by adding a few drops of a 0.1 M solution of 2,2'-bipyridyl in toluene and enough *sec*-BuLi to obtain a persistent red-orange color. Then the calculated amount of *sec*-BuLi solution (1.37 mL, 1.92 mmol, for a target $M_n = 5000$) was added, followed by the butadiene monomer. The reaction mixture was warmed to room temperature (23 °C) after 15 min and stirred for 3 h. The reaction was terminated with degassed methanol and the polymer was recovered by precipitation in 1.2 L of methanol, and dried under vacuum. The reaction yielded 9.1 g (95 % yield) of polybutadiene with a microstructure consisting of 87% 1,4-units and 13% 1,2-units, with a number-average molecular weight $M_n = 5100$ and a polydispersity index $M_w/M_n = 1.04$.

5.3.2.2 Epoxidation of Polybutadiene

The epoxidation procedure used was adapted from Moingeon et al.¹⁶ Polybutadiene (2 g, 32 meq of 1,4-butadiene units) was dissolved in dichloromethane (100 mL) in a 250 mL round-bottomed flask. The solution was cooled to 0°C before adding 3-chloroperbenzoic acid (1.68 g,

9.7 mmol), capping the flask with a rubber septum, and purging with nitrogen. The reaction was stirred for 4 h at 0 °C and then worked up by extraction with 100 mL of a 0.1 M NaOH solution, and twice with 100 mL of water. The dichloromethane phase was concentrated to 10 mL and the polymer was recovered by precipitation in 100 mL of methanol, and dried overnight under vacuum. The purified product (1.78 g, 84 % yield) had a substitution level of 26 mol %, as determined by ¹H NMR spectroscopy.

5.3.2.3 Reduction of Epoxidized Polybutadiene

The reduction procedure used was similar to that reported by Zhu et al.¹⁷ Epoxidized polybutadiene (1.5 g, 6.28 meq of epoxidized butadiene units) was dried overnight under vacuum in a 250 mL round-bottomed flask and dissolved in 150 mL of THF. The flask was sealed with a rubber septum, purged with nitrogen, and cooled to 0 °C. LiAlH₄ solution (12.5 mL, 25.1 mmol; 4 molar equiv with respect to the epoxide groups) was added to the polymer solution at 0 °C with a syringe. The mixture was allowed to warm to room temperature over 30 min and stirred for 4 h. The reaction was terminated by cooling to 0 °C and drop-wise addition of 8 mL (90/10 v/v) of methanol/HCl under nitrogen before concentrating the solution to 10 mL and precipitation of the polymer in 100 mL (30/70 v/v) of methanol/H₂O. The polymer was further purified by two cycles of dissolution in chloroform (20 mL) and extraction with 20 mL of water. The polymer was finally recovered by precipitation in 100 mL (30/70 v/v) of methanol/H₂O, and dried overnight under vacuum. The purified product (1.28 g, 85 % yield) had a substitution level of 26 mol % of hydroxyl groups as determined by ¹H NMR spectroscopy.

5.3.2.4 Tosylation of Hydroxylated Polybutadiene

The tosylation method used was adapted from literature procedures.¹⁸⁻²⁰ Hydroxyl-functionalized polybutadiene (1 g, 4.18 meq of hydroxyl groups) was dried under vacuum overnight and dissolved in 20 mL of dichloromethane. Tosyl chloride (7.96 g, 41.8 mmol; 10 equiv with respect to the hydroxyl groups) was loaded in a dry 500 mL round-bottomed flask and dissolved in 100 mL of dichloromethane. The flask was sealed with a rubber septum, purged with nitrogen, and cooled to 0 °C. An equimolar amount of pyridine with respect to tosyl chloride (3.37 mL, 41.8 mmol) was added to the solution and stirred for 5 min. The polymer solution was then transferred to the TsCl/pyridine solution at 0 °C with a syringe, and the mixture was allowed to warm to room temperature over 30 min and stirred overnight. Workup of the products involved concentrating the polymer solution to 20 mL and precipitation in 200 mL of methanol, two additional cycles of dissolution in 10 mL of THF and precipitation in 100 mL of methanol, and drying under vacuum. The polybutadiene randomly functionalized with tosyl group was obtained in 68 % yield (0.93 g). Complete conversion to the tosylate functionality was confirmed by ¹H NMR spectroscopy.

5.3.2.5 Transformation from Tosyl to Azide

The azidation procedure used was reported by Fallais et al.²¹ In a dry 50 mL round-bottomed flask, 0.75 g of tosylated polybutadiene (3.14 meq of tosyl groups) was dissolved in 40 mL of THF and 5 mL of DMF. Sodium azide (1 g, 15.7 mmol, 5 equiv with respect to tosyl functionalities) was added to the polymer solution. The flask was sealed, purged with nitrogen, and the reaction was stirred overnight. Workup first involved the drop-wise addition of 3 mL of

water, and stirring for 1 h before concentrating the solution to 20 mL and precipitation in 200 mL of methanol. The polymer was again dissolved in 10 mL of THF and precipitated in 100 mL of methanol. The polybutadiene randomly functionalized with azide groups was obtained in 96 % yield (0.62 g). Complete conversion to the azide functionality was confirmed by ^1H NMR spectroscopy.

5.3.3 Side Chain Synthesis and Functionalization (Strategy A)

5.3.3.1 Butadiene Polymerization Using 6-*tert*-Butyldimethylsiloxyhexyllithium

Polybutadiene side chains with a target $M_n = 5000$ were synthesized as reported in Section 5.3.2.1, but starting from 19.84 g of purified butadiene and 3.96 mmol of the initiator (TBDMS-O-Hexyl-Li, prepared as described in Chapter 3, Section 3.3.3.1). The polymer, with $M_n = 5200$ and $M_w/M_n = 1.09$, was obtained in 96 % yield (19.1 g).

5.3.3.2 Deprotection of Hydroxyl Chain End

The deprotection procedure used was adapted from Dhara et al.²² The protected hydroxyl-terminated polybutadiene (19 g) was dried under vacuum overnight in a 1-L round-bottomed flask, dissolved in 400 mL of THF, and 17.9 mL of TBAF solution (17.9 mmol, 5 equiv with respect to the protected hydroxyl groups) were added to the polymer solution. The reaction was refluxed overnight and the polymer was recovered by precipitation in methanol. The deprotected product was obtained in 98% yield (18.7 g). Complete cleavage of the protecting groups was confirmed by ^1H NMR analysis.

5.3.3.3 Transformation from Hydroxyl to Acetylene

The synthetic procedure used to transform the hydroxyl end groups into acetylene functionalities was similar to that described by Ergin et al.²³ Hydroxyl-functionalized polybutadiene (18 g, 3.46 meq of hydroxyl groups), dried under vacuum overnight, was loaded in a dry 1-L round-bottomed flask and dissolved in 600 mL of THF. Sodium hydride (0.41 g, 17.3 mmol, 5 equiv with respect to hydroxyl groups) was added to the solution, the flask was sealed with a rubber septum, purged with nitrogen, and the reaction was stirred for 3 h before adding propargyl bromide (1.97 mL, 17.3 mmol) and stirring for 2 h longer. Workup involved the slow addition of methanol to destroy excess NaH, concentration of the solution to 50 mL, and precipitation in 500 mL of methanol; this was followed by two additional cycles of dissolution in 50 mL of THF and precipitation in 400 mL of methanol, and drying under vacuum. The product (17.6 g) was obtained in 97 % yield. Complete conversion to the acetylene functionality was confirmed by ¹H NMR spectroscopy.

5.3.4 Grafting of Acetylene-terminated Polybutadiene onto Azidated Polybutadiene

In a dry 250-mL round-bottomed flask 0.1 g of azidated polybutadiene (0.41 meq of azide groups) and 2.17 g of acetylene-terminated polybutadiene side chains (0.41 meq of acetylene groups) were dissolved in 40 mL of toluene and 10 mL of DMF. PMDETA (0.42 mL, 2.05 mmol) and BHT (45 mg, 5 mol % with respect to alkyne groups) were added to the polymer solution, the flask was sealed with a rubber septum, and the solution was degassed by purging with nitrogen through a needle for 30 min. Copper (I) bromide (0.29 g, 2.05 mmol) was added to

the reaction and the flask was sealed, purged with nitrogen, and left to stir at 50 °C overnight. Workup of the products involved cooling to room temperature, the addition of 20 mL of water and stirring for 15 min, removal of the toluene on a rotary evaporator, and extraction of the polymer solution with 20 mL of chloroform. The final product was obtained by precipitation in 300 mL of methanol, another cycle of dissolution in 20 mL of THF and precipitation in 200 mL of methanol, and drying under vacuum. The raw grafting product (2.13 g) was further purified by precipitation fractionation in a hexane/2-propanol mixture to remove the side chain contaminant and obtain the pure comb branched polybutadiene in 57 % yield (1.21 g). The fractionation procedure described above was used to purify all the branched polybutadiene samples synthesized.

5.3.5 Backbone Synthesis and Functionalization with Acetylene Groups (Strategy B)

The butadiene polymerization, polybutadiene epoxidation, and reduction procedures used were as described in Sections 5.3.2.1, 5.3.2.2, and 5.3.2.3 respectively. The synthetic procedure used to transform the hydroxyl groups into acetylene functionalities was as described in Section 5.3.3.3, starting from 1 g of hydroxylated polybutadiene, 0.5 g of NaH, and 2.34 mL of propargyl bromide. The polymer obtained (0.86 g, 77 % yield) had a substitution level of 26 mol % acetylene groups as confirmed by ¹H NMR analysis.

5.3.6 Side Chain Functionalization with Azide End Groups (Strategy B)

The procedures for butadiene polymerization and the deprotection of the chain ends were as described in Sections 5.3.3.1 and 5.3.3.2, respectively. Tosylation of the hydroxyl groups of polybutadiene was achieved as described in Section 5.3.2.4, starting from 18.5 g of hydroxyl-functionalized polymer, 6.65 g of TsCl, and 2.81 mL of pyridine. The polymer (18.2 g) was obtained in 98% yield; complete conversion to the tosylate functionality was confirmed by ¹H NMR analysis.

The transformation from tosyl to azide ends was achieved as described in Section 5.3.2.5, starting from 18 g of polymer and 2.2 g of sodium azide. The polybutadiene with an azide chain end was obtained in 97 % yield (17.6 g), and complete conversion was confirmed by ¹H NMR analysis.

5.3.7 Grafting of Azide-terminated Polybutadiene on Acetylenated Polybutadiene

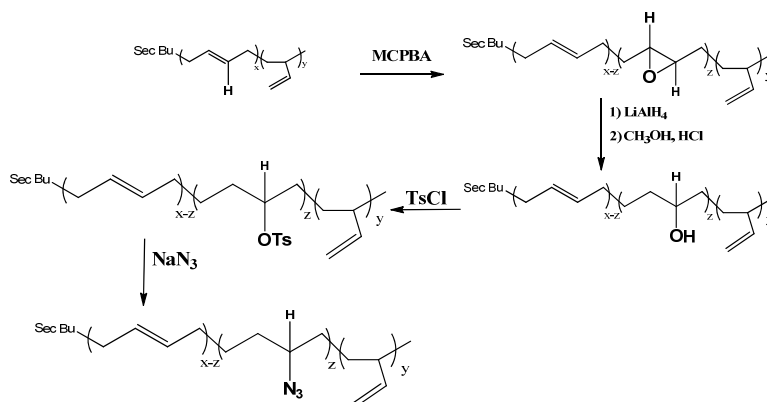
Grafting of the azide-terminated side chains onto the acetylene substrates was achieved as described in Section 5.3.4, starting from 0.1 g of acetylenated polymer, 2.17 g of azide-terminated side chains, 0.42 mL PMDETA, and 0.29 g of copper (I) bromide. The raw grafting product obtained (2.2 g) was further purified by fractionation precipitation to produce pure G0 polymer in 65% yield (1.43 g).

5.3.8 Polymer Characterization

Size exclusion chromatography (SEC) analysis was performed for the substrates before and after epoxidation, reduction, tosylation, azidation, and acetylation. It was likewise performed for the side chains after each transformation step, for the raw grafting products, and the fractionated graft polymer samples. The system used consisted of a Viscotek GPCmax unit equipped with a VE 2001 GPC Solvent/Sample Module, a Viscotek Triple Detector Array equipped with refractive index, viscosity, and dual-angle light scattering detectors, an external Viscotek UV 2600 detector, and three PolyAnalytik organic mixed bed columns, PAS-103-L, PAS-104-L, and PAS-105-L, with dimensions of 8 mm (ID) × 300 mm (L) each, and an overall polystyrene molecular weight range of 10^3 to 10^7 . The polymers were analyzed in THF at a flow rate of 1 mL/min. ^1H NMR analysis of all the polymer samples was achieved in CDCl_3 on a Bruker Avance 300 MHz NMR instrument at a concentration of 40-50 mg/mL.

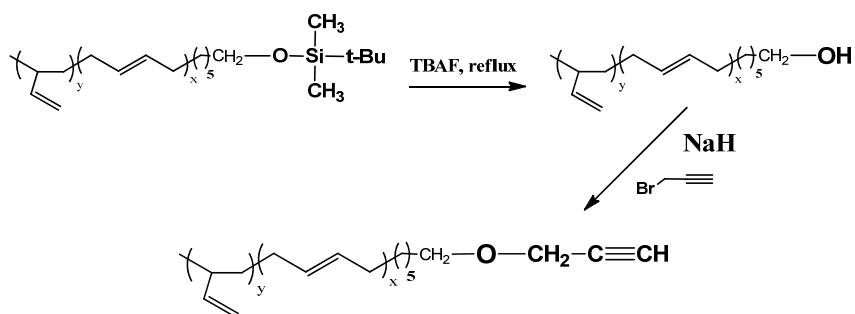
5.4 Results and Discussion

Two strategies were examined for the synthesis of arborescent polybutadiene. The first approach (A) involved the random introduction of azide functionalities on the substrate (Scheme 5.2), whereas acetylene groups were introduced at one end of the material serving as side chains (Scheme 5.3). The butadiene monomer was reacted with *sec*-BuLi to produce a linear polymer, followed by epoxidation to introduce epoxide functionalities which, upon reduction with LiAlH_4 , provided hydroxyl functionalities. The hydroxylated polymer was then converted into the tosylated derivative, which was displaced with sodium azide to obtain the azide-functionalized polybutadiene substrate.



Scheme 5.2. Synthesis of azidated polybutadiene substrate.

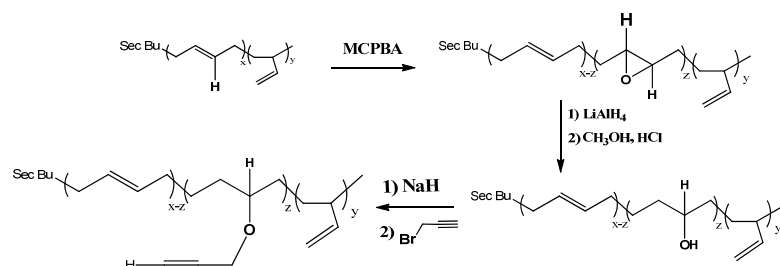
The synthesis of the side chain material started with the polymerization of butadiene initiated with TBDMS-O-Hexyl-Li, to provide chains with a protected hydroxyl chain end. Deprotection of the hydroxyl group, followed by reaction with NaH and propargyl bromide, yielded the desired acetylene end group.



Scheme 5.3. Synthesis of alkyne-terminated polybutadiene side chains.

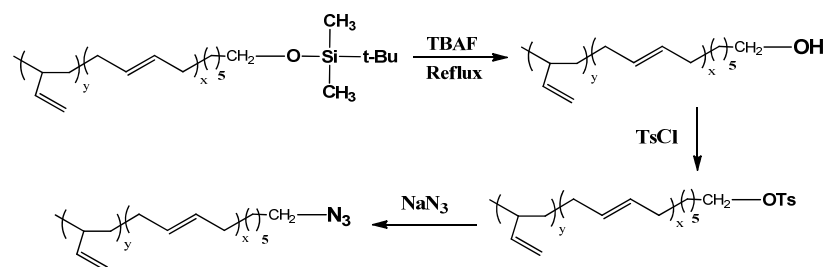
The alternate strategy (B) examined involved the random introduction of alkyne functionalities on the substrate (Scheme 5.4), whereas azide groups were introduced at the end of the side chain material (Scheme 5.5). The polymerization, epoxidation, and reduction reactions to produce randomly hydroxylated substrates were carried out in a manner similar to the first

strategy. The introduction of the alkyne functionalities was achieved by treatment of the hydroxylated substrates with NaH and propargyl bromide, to give propargyl ether substituents.



Scheme 5.4. Synthesis of alkyne-terminated polybutadiene substrate.

The synthesis of side chains with azide ends was likewise achieved by the polymerization of butadiene with TBDMS-O-Hexyl-Li, deprotection of the hydroxyl group, tosylation, and treatment with sodium azide.



Scheme 5.5. Synthesis of azide-terminated polybutadiene side chains.

5.4.1 Grafting onto Azidated Substrates (Strategy A)

5.4.1.1 Random Hydroxylation of Linear Polybutadiene

The linear polymer synthesized in toluene had the expected molecular weight ($M_n = 5100$) and a narrow MWD ($M_w/M_n = 1.04$), as seen in the SEC trace of Figure 5.1. ^1H NMR analysis

indicated that the chains had a microstructure with 87 % of 1,4-units and 13% of 1,2-units, with the protons on the 1,4-units causing a resonance at 5.3-5.6 ppm, whereas the 1,2-units led to a resonance at 4.9-5 ppm (Figure 5.2a). Such a microstructure is consistent with the fact that more non-polar solvents lead to a higher 1,4-units content in the anionic polymerization of butadiene.²⁴ Epoxidation of this polymer yielded a substitution level of 26 mol %, as determined by ¹H NMR spectroscopy. The introduction of the epoxide group caused two new resonances at 2.65 and 2.95 ppm (protons on the epoxide ring), as seen in Figure 5.2b. The epoxidation level is easily controlled by the amount of 3-chloroperbenzoic acid added in the epoxidation reaction. Variation in the epoxidation level could provide control over the branching density of the polymer, albeit it was maintained at 20-30 mol % for all the generations in the current investigation.

Reduction of the epoxidized polymer with an excess of LiAlH₄ yielded a substrate randomly functionalized with hydroxyl groups and a substitution level of 26 mol %, as determined by ¹H NMR spectroscopy analysis. The resonances at 2.65 and 2.95 ppm due to the epoxide functionality completely disappeared, whereas the introduction of the hydroxyl functionality caused a new resonance at 3.56 ppm (proton adjacent to the hydroxyl group), as seen in Figure 5.2c. Quantitative conversion of the epoxide functionalities to hydroxyl groups was therefore achieved under the reaction conditions used.

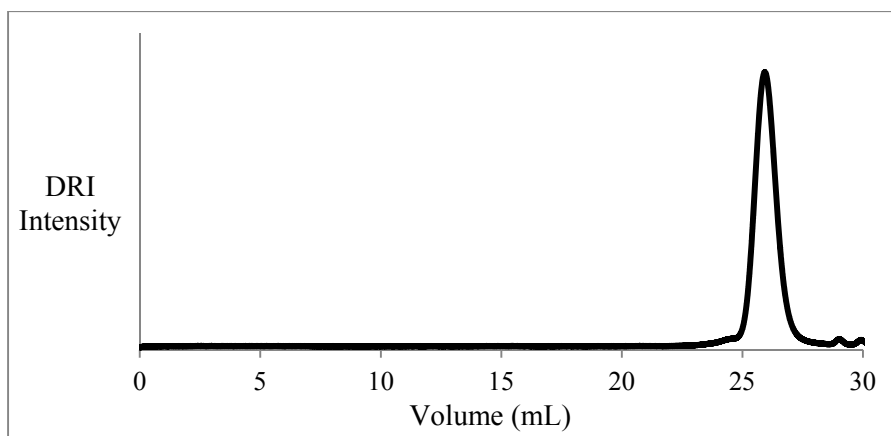


Figure 5.1. SEC trace for linear polybutadiene ($M_n = 5100$, $M_w/M_n = 1.04$).

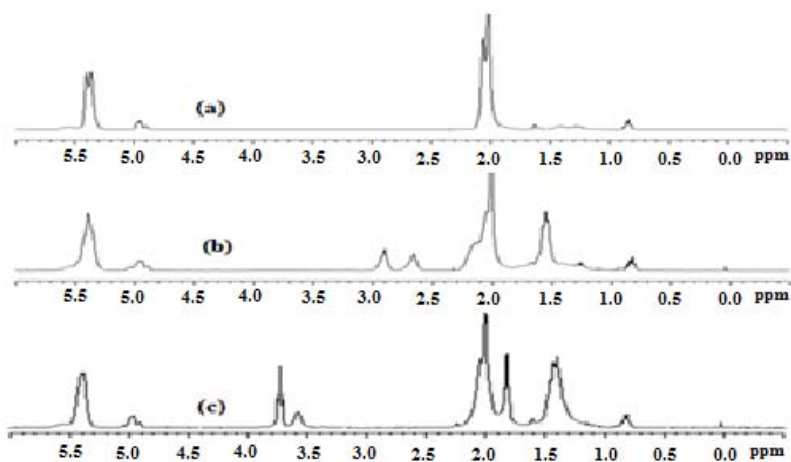


Figure 5.2. ^1H NMR spectra for (a) polybutadiene, (b) epoxidized polybutadiene, and (c) hydroxylated polybutadiene.

5.4.1.2 Tosylation of Hydroxylated Polybutadiene and Conversion to Azide

Tosylation yielded a substrate with 26 % of tosylated polybutadiene units, corresponding to full conversion to the tosylate as determined by ^1H NMR spectroscopy analysis. The resonance

at 3.56 ppm (characteristic for the proton adjacent to the hydroxyl group) disappeared, while a new resonance at 4.56 ppm for the proton adjacent to the tosyl group appeared (Figure 5.3a).

Azidation of the tosylated polymer yielded a substrate with a substitution level of likewise 26 mol %, i.e. complete conversion of the tosylate, as determined by ^1H NMR spectroscopy analysis. The resonance at 4.56 ppm completely disappeared, whereas a new resonance at 3.2 ppm (proton adjacent to the azide group) appeared (Figure 5.3b). SEC analysis of the azide-functionalized polymer, depicted in Figure 5.4, yielded $M_n = 5600$ and $M_w/M_n = 1.07$. The low polydispersity index value obtained after azidation suggests that the functionalization steps proceeded without cross-linking.

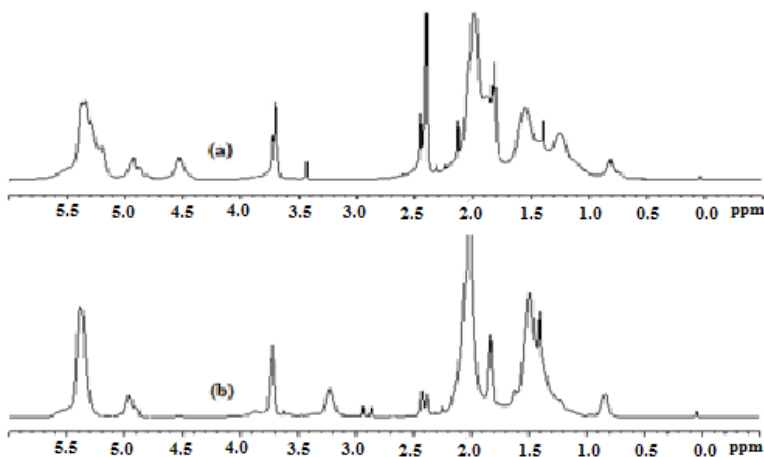


Figure 5.3. ^1H NMR spectra for (a) tosylated polybutadiene, and (b) azide-functionalized polybutadiene.

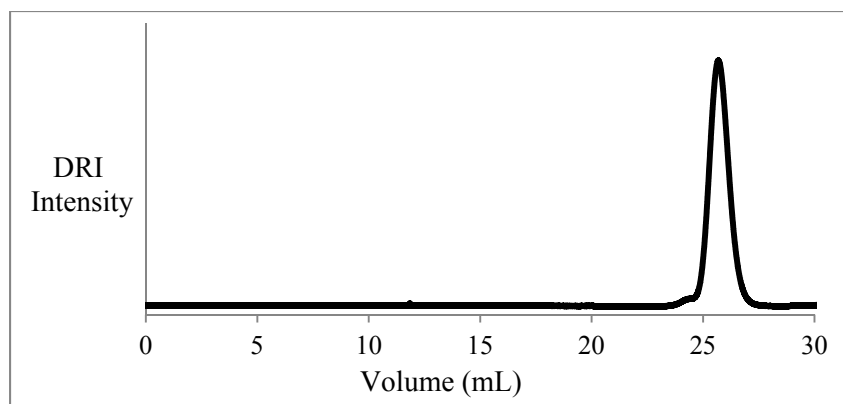


Figure 5.4. SEC trace for azidated polybutadiene ($M_n = 5600$, $M_w/M_n = 1.07$).

5.4.1.3 Linear Polybutadiene from 6-*tert*-Butyldimethylsiloxyhexyllithium

The linear polymer obtained in toluene had $M_n = 5200$ and a narrow MWD ($M_w/M_n = 1.09$), as seen in the SEC trace of Figure 5.5. The *tert*-butyldimethylsiloxy chain end caused two resonances at 0.8 ppm (*tert*-butyl protons) and 0 ppm (dimethylsiloxy protons) in the NMR spectrum, while the methylene protons adjacent to the oxygen caused a resonance at 3.6 ppm (Figure 5.6a). The polymer obtained had a microstructure with 81 % of 1,4-units and 19 % of 1,2-units.

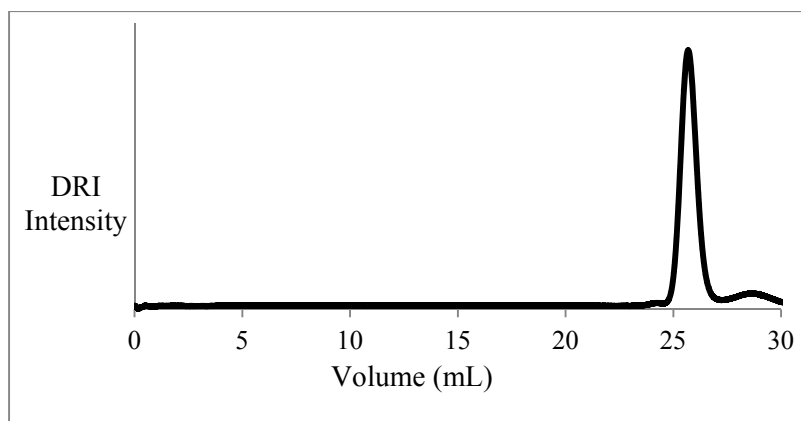


Figure 5.5. SEC trace for linear polybutadiene synthesized with 6-*tert*-butyldimethylsiloxyhexyllithium ($M_n = 5200$, $M_w/M_n = 1.09$).

The use of a bifunctional initiator to synthesize the polybutadiene side chains ensured that all the chains contained a protected hydroxyl group that could be subsequently transformed into an acetylene functionality. This approach is advantageous over other strategies such as capping the living chains with an electrophile, since protic impurities in the capping reagent or side reactions could terminate the macroanions and lead to contamination of the product with unreactive chains.

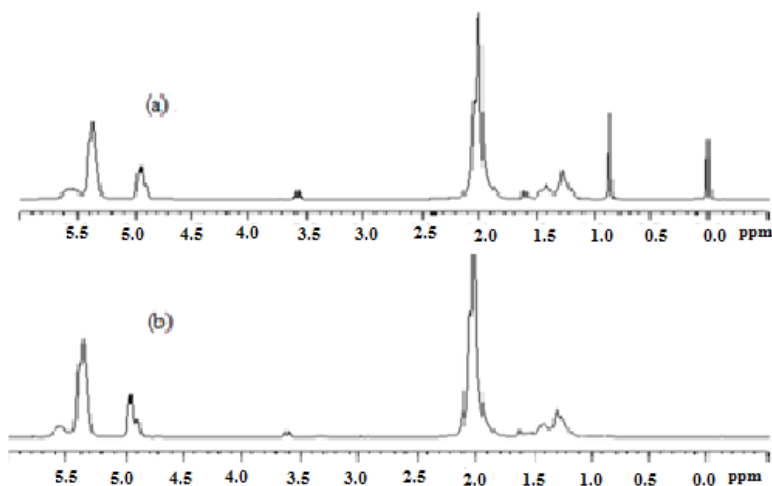


Figure 5.6. ^1H NMR spectra for polybutadiene with (a) a silyl ether end group, and (b) a hydroxyl end group ($M_n = 5200$).

5.4.1.4 Deprotection of the *tert*-Butyldimethylsiloxy Group and Conversion to an Acetylene

Complete deprotection of the *tert*-butyldimethylsiloxy group was confirmed by the disappearance of the two clearly visible resonances at 0 and 0.8 ppm for the dimethylsiloxy and *tert*-butylsiloxy protons, respectively, as seen in Figure 5.6b. The methylene protons adjacent to the hydroxyl group remained at 3.6 ppm, and the relative area of that peak was constant before and after deprotection. The hydroxyl end group was successfully derivatized into an acetylene functionality, as confirmed through ^1H NMR analysis (Figure 5.7), since the resonance for the methylene protons adjacent to the hydroxyl group still appeared at 3.6 ppm whereas the propargyl group gave rise to a new resonance at 4.1 ppm for the methylene protons. Integration of this peak yielded the same intensity as for the methylene protons at 3.6 ppm, which confirmed full conversion of the hydroxyl group to acetylene functionalities.

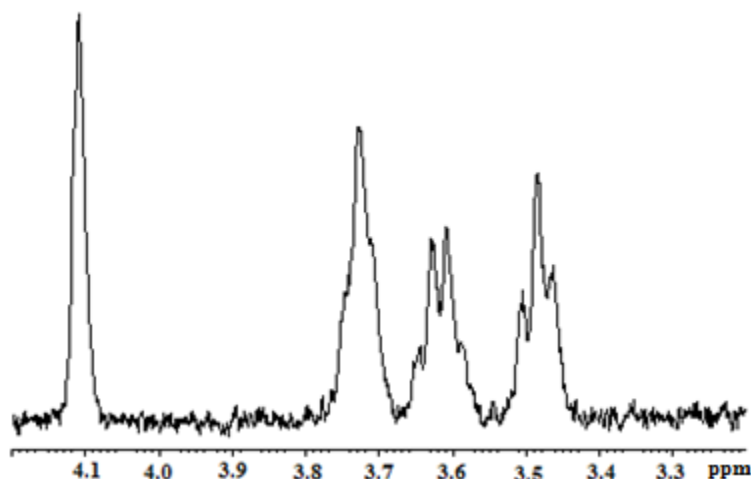


Figure 5.7. ^1H NMR spectrum for acetylene-terminated polybutadiene ($M_n = 5200$).

5.4.1.5 Coupling of Acetylene-terminated Polybutadiene with Randomly Azidated Polybutadiene

The conditions for the grafting reaction were optimized to obtain graft polymers with a low polydispersity index in high yield. The grafting yield, defined as the fraction of side chains becoming attached to the substrate, can be approximated by SEC analysis using a differential refractometer detector, from the peak areas for the graft polymer and the unreacted side chains according to the equation:

$$\text{Grafting yield} = \frac{\text{graft polymer peak area}}{\text{graft polymer} + \text{unreacted side chain peak areas}}$$

The variables investigated in optimizing the reaction were the type of amine ligand and solvent used, the reaction temperature, and the reaction time. In all the reactions a 1:1 stoichiometric ratio of azide to acetylene functionalities was used. In each test reaction, $M_n =$

5200 acetylene-terminated polybutadiene side chains were coupled with an azidated linear polybutadiene substrate having $M_n = 5600$.

To investigate the influence of the solvent on the grafting yield, the reactions were performed either in pure toluene, toluene/DMF (80/20), or THF/DMF (80/20) mixtures. The reaction temperature was set to either 50 °C (in the presence of 5% of BHT with respect to the alkyne/azide groups), or room temperature (23 °C). The ligands used were either PMDETA or 2,2'-bipyridyl, and the reaction time was initially set to 24 h. The results obtained for the coupling reactions performed at 23 °C with PMDETA or bipyridyl as ligand, while varying the solvent, are summarized in Table 5.1.

Table 5.1. Grafting yield in DMF, THF, and toluene using PMDETA or bipyridyl as ligands.

Ligand	Toluene	Toluene/DMF	THF/DMF
PMDETA	23	43	29
Bipyridyl	19	31	22

It is clear from the grafting yields provided in Table 5.1 that PMDETA is more efficient as a ligand in comparison with 2,2'-bipyridyl, regardless of the solvent composition used. It is also noticeable that the toluene/DMF (80/20) mixture led to higher yields; this is attributed to the better solubility of both the polymer (in toluene) and the catalyst (in DMF) in that solvent composition, whereas in the other solvent compositions investigated the solubility of either the polymer or the catalyst was limited. The SEC traces for the raw grafting products obtained at room temperature in the different solvent systems with PMDETA are compared in Figure 5.8. The final products had number-average molecular weights $M_n = 24,000$ in toluene, $M_n = 32,000$

in THF/DMF, and $M_n = 45,000$ in toluene/DMF, which is consistent with the grafting yield variations observed.

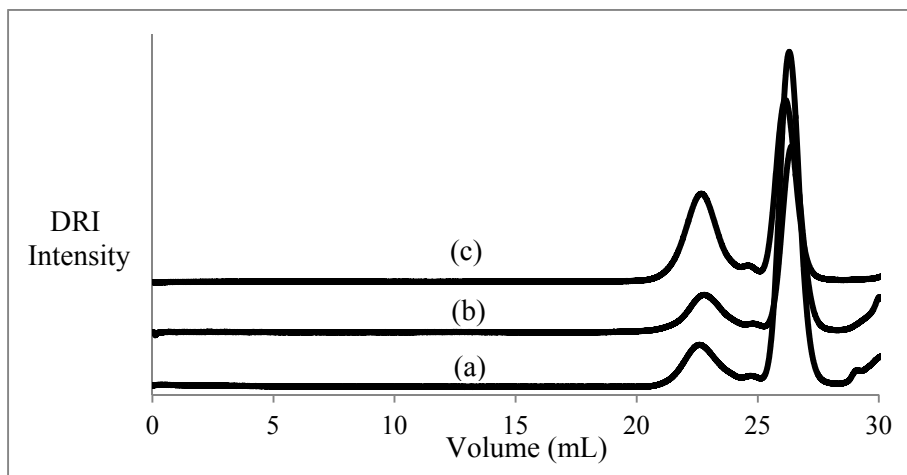


Figure 5.8. SEC traces for the reactions in (a) toluene, (b) THF/DMF, and (c) toluene/DMF at 23 °C, using PMDETA as ligand.

The next step in optimizing the grafting reaction involved varying the temperature with the toluene/DMF (80/20) solvent system and PMDETA as ligand, consequently the reaction was repeated at 50 °C for 24 h, but 5% of BHT with respect to the alkyne/azide groups was also added as a radical scavenger when the reaction was performed at 50 °C since polybutadiene is sensitive to cross-linking, particularly due to the presence of the 1,2-butadiene units.²⁵ The SEC traces for the raw grafting products obtained at 23 and 50 °C are compared in Figure 5.9. The grafting yield attained at 50 °C (76 %) is significantly higher than for the analogous reaction at room temperature (43 %). This significant increase can be explained by the fact that “click” coupling requires activation of the alkyne group through the formation of a π -complex with copper,²⁶ followed by abstraction of the acetylenic proton by PMDETA to form a copper-

acetylide which then adds to the azide group to form the triazole ring. Since the copper-acetylide complex located at a chain end is bulkier than a small molecule alkyne, its accessibility to azide groups on the substrate is less hindered when the reaction is carried out at 50 °C as chain mobility is increased. The graft polymer obtained at 50 °C had $M_n = 84,000$ (as compared to $M_n = 45,000$ attained at room temperature), and $M_w/M_n = 1.12$.

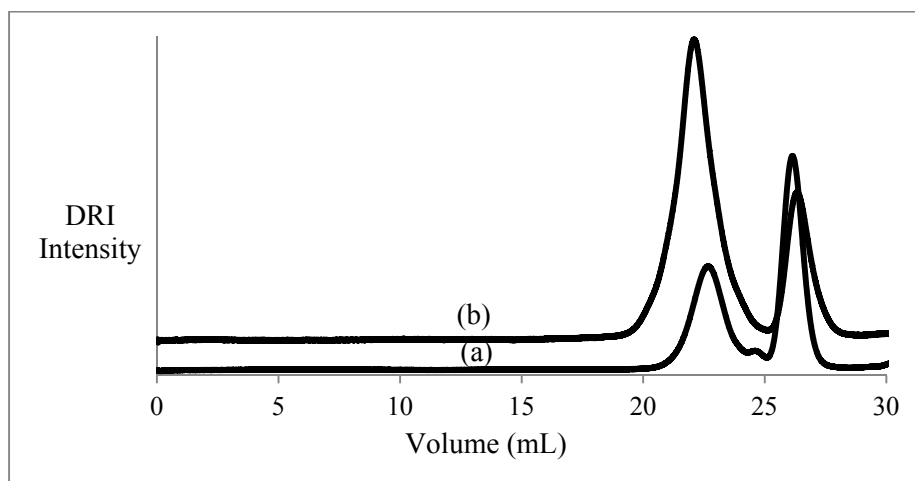


Figure 5.9. SEC trace for the reactions in toluene/DMF using PMDETA as ligand at (a) room temperature and (b) 50 °C.

All the above-mentioned reactions were performed for a period of 24 h; therefore the next step was to allow the reaction to proceed for 48 h at 50 °C, in toluene/DMF with 5% of BHT, and to monitor the grafting yield. The reaction did proceed with a slightly higher yield (83%) under these conditions, as seen in Figure 5.10, however as it can be noticed from the SEC curve that side reactions started to occur for the graft polymer. Consequently, it was deemed preferable to allow the reaction to proceed for only 24 h in spite of the slightly lower grafting yield attained. After systematic optimization of the reaction conditions for acetylene-terminated polybutadiene

side chains with $M_n = 5200$ and an azidated linear polybutadiene substrate ($M_n = 5600$) to obtain a G0 arborescent (comb-branched) polybutadiene, a grafting yield of 76 % was therefore attained.

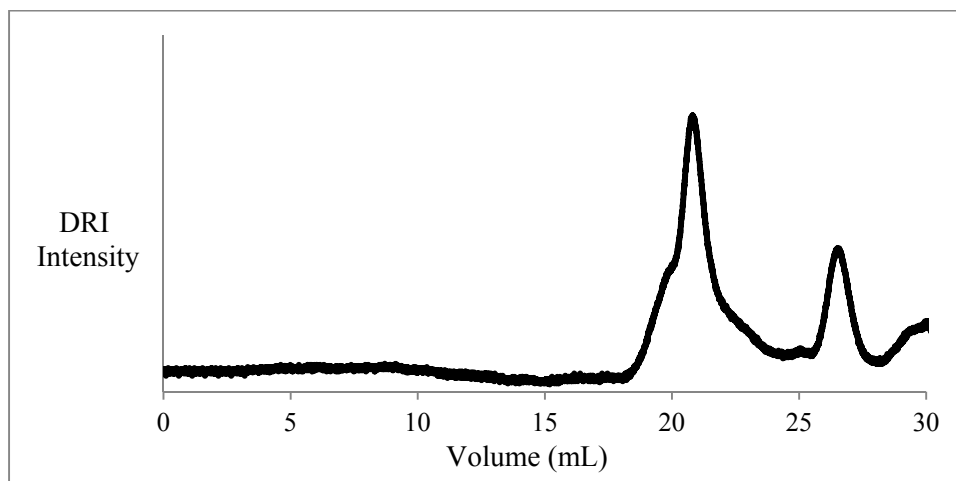


Figure 5.10. SEC trace for grafting in toluene/DMF with PMDETA at 50 °C for 48 h.

5.4.1.6 Coupling of Acetylene-terminated Polybutadiene with G0 and G1 Azidated Polybutadiene

Cycles of substrate functionalization and side chain grafting were repeated to obtain the subsequent generations (G1, G2) of arborescent polymers under the conditions determined to be optimal for the synthesis of the G0 polymer (24 h at 50 °C with PMDETA and 5% of BHT, in toluene/DMF mixtures). This was achieved using $M_n = 5200$ side chains at every step. Grafting of the side chains onto the G0 azidated polybutadiene proceeded in 59 % yield under these conditions, as shown by the SEC trace for the raw grafting product in Figure 5.11. The final product had $M_n = 6.2 \times 10^5$ and $M_w/M_n = 1.14$.

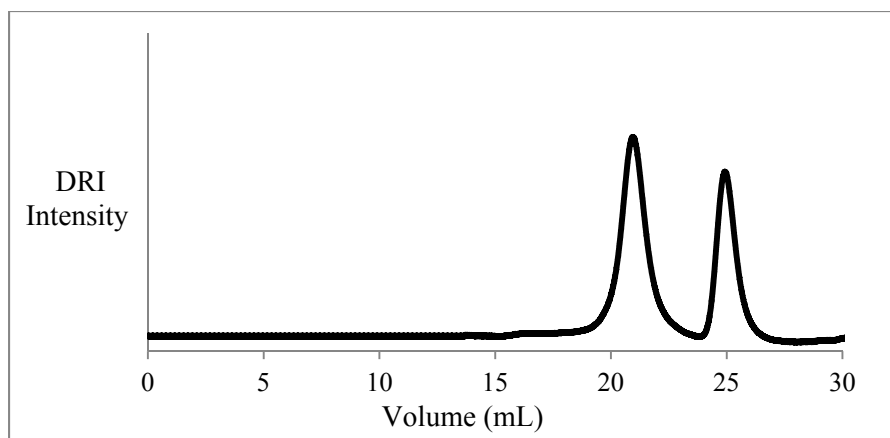


Figure 5.11. SEC trace for grafting acetylene-terminated side chains ($M_n = 5200$) onto an azidated G0 substrate. The G1 polymer obtained had $M_n = 6.2 \times 10^5$, $M_w/M_n = 1.14$.

Grafting of the side chains onto the G1 azidated polybutadiene substrate to obtain the G2 polymer proceeded in 40 % yield, as shown by the SEC trace for the raw grafting product in Figure 5.12. The polymer had $M_n = 3.4 \times 10^6$ and $M_w/M_n = 1.12$. It can be noticed that the grafting yield decreased as the generation number increased; this is attributed to the structure of the azidated substrates becoming increasingly congested from the linear to the G0 and G1 polymers, which decreases the accessibility of the azide coupling sites to the acetylene ends of the side chains.

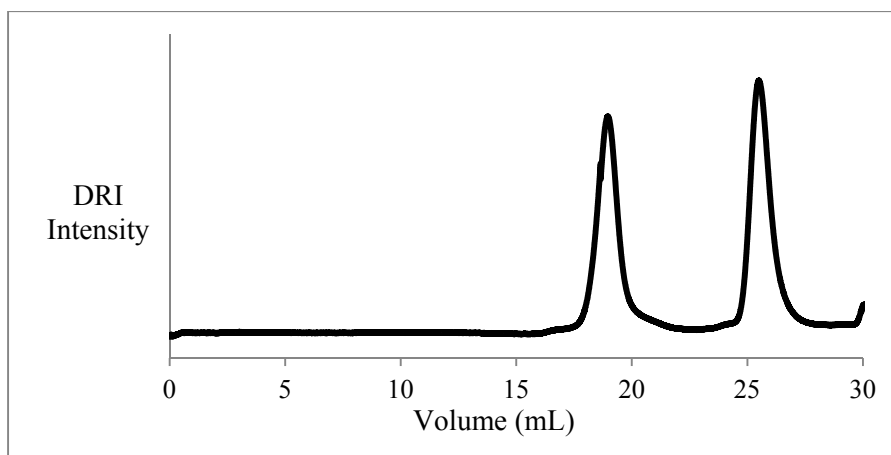


Figure 5.12. SEC trace for grafting acetylene-terminated side chains ($M_n = 5200$) onto an azidated G1 substrate. The G2 polymer obtained had $M_n = 3.4 \times 10^6$, $M_w/M_n = 1.12$.

5.4.1.7 Characterization of the Purified Arborescent Polymers

The polymers synthesized under the optimized conditions were purified by precipitation fractionation as described in Section 5.3.4 for characterization by SEC analysis. The results obtained when grafting side chains with $M_n = 5200$ at every step are summarized in Table 5.2. The sample nomenclature used in Table 5.2 identifies the generation number of the substrate as well as the molecular weight of the side chains grafted in the last reaction. For example, G0PBD-PBD5 refers to a G0 polybutadiene substrate grafted with $M_n \approx 5000$ side chains.

Table 5.2. Characteristics of arborescent polybutadiene molecules of successive generations. The side chains had $M_n = 5200$ and $M_w/M_n = 1.09$ in all cases.

	Graft polymer			
	yield (%) ^b	M_n^a	M_w/M_n^a	f_n
PBD-PBD5	76	8.4×10^4	1.12	15
G0PBD-PBD5	59	6.2×10^5	1.14	103
G1PBD-PBD5	40	3.4×10^6	1.12	534

^a Absolute values determined from SEC-MALLS analysis.

^b Fraction of side chains becoming attached to the substrate.

The number-average branching functionality of the polymers, defined as the number of chains added in the last grafting reaction, was calculated according to the equation

$$f_n = \frac{M_n(G) - M_n(G - 1)}{M_n^{br}}$$

where $M_n(G)$, $M_n(G - 1)$, and M_n^{br} are the absolute number-average molecular weight of graft polymers of generation G, of the preceding generation and of the side chains, respectively. It is clear that the molecular weight and the branching functionality of the graft polymers increased roughly geometrically over successive generations; however the grafting yield decreased (Table 5.2). These results are comparable with those reported in Chapter 6 for the synthesis of arborescent polybutadiene by anionic grafting onto chlorosilane-functionalized substrates, thus demonstrating that the “click” grafting approach is an equally efficient method to synthesize arborescent polybutadiene. A major advantage of “click” grafting over anionic grafting is that the experimental procedure is less tedious and time-consuming, since the functionalized substrates and the side chains can be prepared, stored, and utilized in grafting reactions at a later time. As will be seen in Chapter 6, the synthesis of every generation of arborescent polybutadiene by

anionic grafting requires the chemical modification of the substrate immediately before the reaction, since the chlorosilane intermediates are unstable, as well as the anionic synthesis of (equally unstable) living side chains with careful exclusion of any protic impurities that would terminate the chains and affect the outcome of the reaction dramatically.

5.4.2 Grafting onto Acetylenated Substrates (Strategy B)

5.4.2.1 Random Acetylenation of Polybutadiene

Acetylenation of the hydroxylated linear polymer (synthesized as described in Section 5.4.1.1) yielded a substrate with a substitution level of 26 mol %, as determined by ^1H NMR spectroscopy analysis. The acetylenation level was determined by the epoxidation and hydroxylation levels, since excess propargyl bromide and NaH were used in the reaction. The introduction of the acetylene functionality caused new resonances at 2.4 ppm (acetylenic proton) and 4.1 (methylene protons adjacent to the acetylene group), as shown in Figure 5.13. The integrated intensity of the peak at 4.1 ppm after acetylenation was consistent with the integrated intensity of the peak at 3.56 ppm (for the methylene protons adjacent to the hydroxyl group) before and after acetylenation, which confirms full conversion from hydroxyl to acetylene functionalities. SEC analysis of the acetylene-functionalized polymer, represented in Figure 5.14, yielded $M_n = 5500$ and $M_w/M_n = 1.08$. The low polydispersity index value obtained after acetylenation suggests that the functionalization steps proceeded without cross-linking.

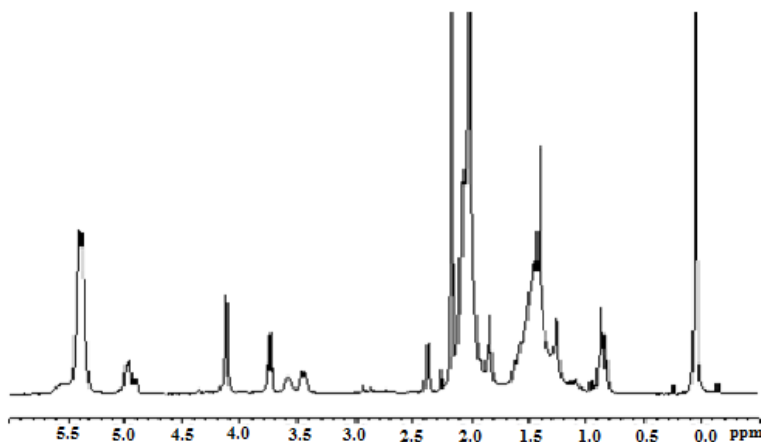


Figure 5.13. ^1H NMR spectrum for linear acetylenated polybutadiene ($M_n = 5500$).

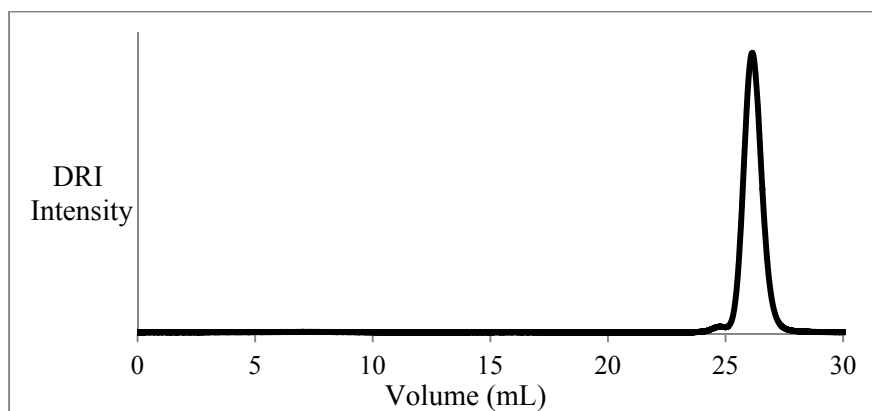


Figure 5.14. SEC trace for randomly acetylene-functionalized polybutadiene ($M_n = 5500$, $M_w/M_n = 1.08$).

5.4.2.2 Conversion of the Hydroxyl Chain End to an Azide

The hydroxyl-terminated side chains described in Section 5.4.1.4 were successfully derivatized into a tosylate, as confirmed by ^1H NMR analysis (Figure 5.15b). The resonance at 3.56 ppm for the methylene protons adjacent to the hydroxyl group shifted to 4.1 ppm upon conversion, which is characteristic for methylene protons adjacent to a tosyl group. The

integration of the peak at 3.56 ppm (before tosylation) yielded a result consistent with the integration of the peak at 4.1 ppm (after tosylation). The conversion to an azide was likewise monitored by ^1H NMR analysis, as shown in Figure 5.15c, where the methylene protons at 4.1 ppm shifted to 3.2 ppm when they became adjacent to the azide functionality. Integration of the peaks for the methylene protons adjacent to the functional groups of interest was again consistent before and after azidation.

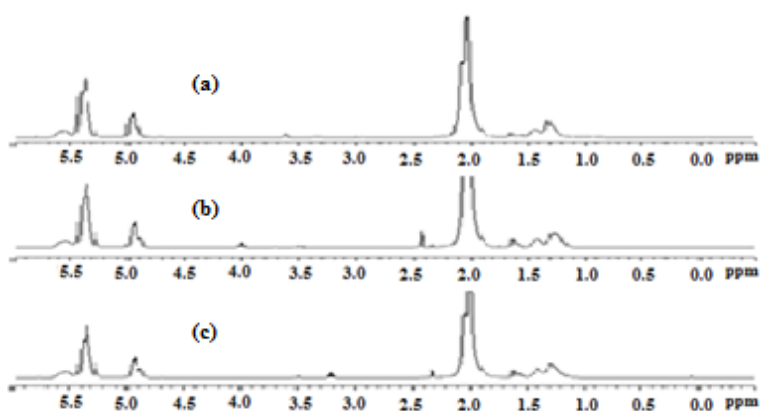


Figure 5.15. ^1H NMR spectra for (a) hydroxyl-, (b) tosyl-, and (c) azide-terminated polybutadiene with $M_n = 5200$.

5.4.2.3 Coupling of Azide-terminated Polybutadiene ($M_n = 5200$) with Linear Acetylene Polybutadiene

The optimal conditions determined for coupling acetylene-terminated polybutadiene with linear azidated polybutadiene were applied in the reaction of the azide-terminated polybutadiene with linear acetylenated polybutadiene, again using a 1:1 stoichiometric ratio of azide and acetylene functionalities. This reaction was therefore performed at 50 °C for 24 h, in the

presence of 5% BHT, using a toluene/DMF mixture and PMDETA as ligand. Grafting proceeded with 86 % yield, as determined from the SEC trace for the raw grafting product (Figure 5.16); the graft polymer obtained had $M_n = 92,000$ and $M_w/M_n = 1.21$. The grafting yield achieved by this approach (86 %) was higher than for the complementary reaction discussed earlier (76 %), which is consistent with the results obtained when comparing the two strategies for the synthesis of arborescent polystyrene by “click” coupling in Chapter 3. The higher grafting yield attained is likewise attributed to easier access of the azide-terminated side chains to the activated alkyne groups on the substrate, the diffusion of a bulky Cu-activated alkyne chain end to an azide group on the substrate (in Strategy A) being more difficult. It can also be noticed that the polydispersity of the graft polymer (1.21) is significantly higher than for the previous approach (1.12). This may be due to the occurrence of alkyne-alkyne coupling, known as Glaser coupling,²⁷ taking place intermolecularly for the substrate. This is supported by the presence of a shoulder on the left side of the graft polymer peak in Figure 5.16, which likely corresponds to dimerization of the substrate.

The alkyne-functionalized G0 polymer was found to be very unstable, cross-linking rapidly and becoming insoluble within a few minutes after it was isolated. Consequently, Strategy B is clearly unsuitable for the preparation of arborescent polybutadiene of higher generations.

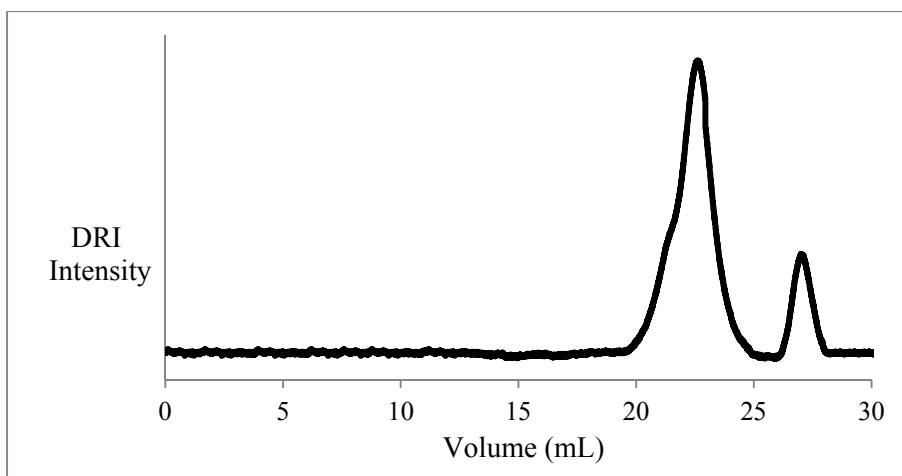


Figure 5.16. SEC trace for grafting azide-terminated ($M_n = 5200$) side chains onto a linear acetylenated substrate ($M_n = 5500$). The G0 polymer had $M_n = 9.2 \times 10^3$, $M_w/M_n = 1.21$.

5.5 Conclusions

The synthesis of successive generations of arborescent polybutadiene was achieved by “click” grafting. Two complementary approaches were investigated, but the reaction of acetylene-terminated side chains with randomly azidated substrates was determined to be the only practical approach to achieve this. The polymerization of butadiene initiated with 6-*tert*-butyldimethylsiloxyhexyllithium provided polybutadiene side chains bearing a protected hydroxyl group at one end of every chain. Deprotection of this group, followed by its conversion to an acetylene functionality, yielded the material serving as side chains in the grafting reactions. Azide functionalities were randomly introduced on the grafting substrates by a sequence of epoxidation, reduction, tosylation, and azidation reactions.

Coupling of acetylene-terminated side chains ($M_n = 5200$) with a linear azide-functionalized substrate in the presence of a Cu (I)-PMDETA catalyst system provided G0 polybutadiene with a low polydispersity index ($M_w/M_n = 1.12$) in up to 76% yield. Repetition cycles of substrate

functionalization and side chain coupling led to arborescent polybutadiene of generations G1 and G2 in 59% and 40 % yield, respectively.

The complementary approach for the synthesis of arborescent polybutadiene by “click” grafting, using $M_n = 5200$ azide-terminated side chains and a linear substrate randomly functionalized with acetylene groups yielded a G0 polymer in 86% yield, with $M_w/M_n = 1.21$. Unfortunately this approach had to be abandoned due to instability of the G0 acetylenated polymer.

The results presented demonstrate the successful synthesis of arborescent polybutadiene by “click” coupling. This provides a new dimension in the synthesis of complex polymer architectures, by avoiding the use of tedious anionic polymerization and grafting procedures for every grafting cycle (generation). In this new method, the side chain material and substrates can be functionalized with suitable groups and safely stored, to be used at some later time worrying about their stability.

Chapter 6

Synthesis of Arborescent Polybutadiene by Anionic Grafting

6.1 Outline

Arborescent polymers were synthesized by reaction cycles consisting in hydrosilylation of the vinyl groups of polybutadiene with chlorodimethylsilane, and coupling with living polybutadienyllithium chains. A polybutadiene substrate ($M_n = 5500$, $M_w/M_n = 1.08$, 56% of 1,2-units) was hydrosilylated with chlorodimethylsilane and coupled with high 1,2-microstructure content polybutadienyllithium chains ($M_n = 5800$, $M_w/M_n = 1.08$). The comb-branched (G0) substrate was again hydrosilylated with chlorodimethylsilane and reacted with high (92-93 %) 1,4-microstructure content polybutadienyllithium chains to generate G1 arborescent polymers. A series of G1 arborescent polymers was synthesized with side chains having $M_n \approx 5$, 30, 50, or 80,000. The G0 polybutadiene substrate was further hydrosilylated and grafted with high 1,2-microstructure content polybutadienyllithium chains ($M_n = 5700$, $M_w/M_n = 1.06$) to generate a G1 substrate, that was also grafted with high 1,4-microstructure content side chains having $M_n \approx 5$, 30, 50, or 80,000 to produce a series of G2 arborescent polybutadiene samples. Size exclusion chromatography analysis of the polymers confirmed that a narrow molecular weight distribution was maintained ($M_w/M_n \leq 1.1$) for most graft polymers, which had branching functionalities reaching 2100 and $M_n = 6.5 \times 10^7$ for the G2 polymers.

6.2 Introduction

Dendritic polymers can be subdivided into three main families, namely dendrimers, hyperbranched polymers, and arborescent polymers.¹ All these molecules are characterized by a multi-level branched architecture, but arborescent polymers are distinguished from dendrimers and hyperbranched polymers by their assembly from polymeric building blocks of uniform size

rather than monomers, so that very high molecular weights are attained in much fewer synthetic steps.

Arborescent polymers are of interest among others because of their controllable architectures, peculiar rheological properties,²⁻⁴ and potential application as modifiers for other polymers.⁵⁻⁷ The physical properties of these materials can be tuned through variations in parameters such as their side chain molecular weight, composition, and branching functionality. The synthesis of arborescent polymers relies on a generation-based scheme to obtain dendritic (multi-level) graft polymer architectures.⁸ A linear polymer is first modified to introduce coupling sites serving in a grafting reaction for linear chains. The comb-branched (G0) polymer thus obtained is subjected to additional cycles of functionalization and grafting reactions to yield higher generation (G1, G2...) arborescent polymers, with a branching functionality and molecular weight increasing geometrically over successive generations.

Different methods have been developed for the synthesis of star-branched and arborescent polybutadiene, mainly utilizing chlorosilane-functionalized or epoxidized substrates and anionic coupling. The reaction of living polybutadienyllithium chains with small molecule chlorosilane linkers has been known to be a very successful method for the synthesis of star-branched polybutadiene for a long time.⁹ Roovers et al.¹⁰ produced high branching functionality polybutadiene stars, containing up to 128 arms, starting from polyfunctional chlorosilane coupling agents derived from carbosilane dendrimers. A dendrimer containing 64 vinyl end groups was thus derivatized via hydrosilylation with methyldichlorosilane to obtain a coupling agent with 128 chlorosilane groups, which upon reaction with polybutadienyllithium ultimately yielding a 128-arm star. The reaction was allowed to proceed for 8 weeks, using a 200% excess

of living ends with respect to chlorosilane groups, to ensure the formation of the well-defined 128-arm star structure.

Munam and Gauthier¹¹ rather focused on the synthesis of hybrid polymers with high branching functionalities by combining the carbosilane dendrimer substrates, first grafted with short chain segments and hydrosilylated, with anionic grafting techniques.

Hempenius et al.¹² produced arborescent polybutadiene from $M_n \approx 10^4$ side chains, by anionic polymerization in *n*-hexane (to obtain a microstructure with 6% of 1,2-units), exhaustive hydrosilylation with chlorodimethylsilane, and grafting with a 20% excess of $M_n \approx 10^4$ polybutadienyllithium. Additional cycles of functionalization and grafting led to arborescent polybutadiene of generations up to G2. Zhang et al.¹³ also used living anionic polymerization techniques, but in combination with epoxidized substrates to synthesize arborescent polymers (identified as star-comb polymers), in a generation-based approach, but unfortunately grafting yields were not reported. Recently Alturk¹⁴ reported on the optimization of that synthetic route, with very promising grafting yields.

In this Chapter, a strategy combining substrate functionalization with chlorosilane coupling sites and anionic grafting is presented for the synthesis of high branching functionality arborescent polybutadiene. The strategy employed differs from previous investigations in two major ways: The side chains grafted have high molecular weights (M_n reaching up to 80,000), and uses substrates with a high ($\approx 55\%$) 1,2-microstructure content to maximize the branching functionality of the molecules.

6.3 Experimental Section

Purification of the monomer and other reagents serving in the polymerization reactions used a high-vacuum line connected to a nitrogen (N₂) purification system and reusable glass ampoules. The ampoules were equipped with polytetrafluoroethylene (PTFE) stopcocks and ground glass joints for direct assembly onto the polymerization reactor.¹⁵

6.3.1 Solvent and Reagent Purification

Tetrahydrofuran (THF; Caledon, reagent grade) was purified by distillation from sodium-benzophenone ketyl under N₂. Cyclohexane (Caledon, reagent grade) and toluene (Caledon, HPLC grade) were purified by refluxing and distillation from oligostyryllithium under N₂ atmosphere. The solvents were introduced directly from the stills into the polymerization reactor and reaction setups through PTFE tubing.

Butadiene (Praxair, 99%) was purified by stirring with *n*-butyllithium (1 mL for 10 mL of monomer) for 30 min at -30 °C and condensation to an ampoule under vacuum. The monomer was diluted by condensing an equal volume of dry THF or cyclohexane under vacuum, and the ampoule was stored at -20 °C until used. The initiator *sec*-butyllithium (*sec*-BuLi, Aldrich, 1.4 M solution in hexanes) was used as received; its exact concentration was determined by the method of Burchat et al.¹⁶ Styrene (Aldrich, 99%) was purified by stirring with CaH₂ and distillation at reduced pressure before it was stored under N₂ at 5 °C. Benzophenone (Sigma Aldrich, reagent plus; 99%), sodium (Aldrich, ≥ 99%, under mineral oil), *n*-butyllithium (*n*-BuLi, Aldrich, 2 M in hexane), chlorodimethylsilane (Sigma Aldrich, 98%), 2,2'-bipyridyl (Sigma Aldrich, Reagent

Plus, $\geq 99\%$), and platinum(0)-1,3-divinyl-1,1,3,3-tetramethyldisiloxane complex solution (Aldrich, in xylene, Pt $\sim 2\%$) were all used as received from the suppliers.

6.3.2 Synthesis of High 1,2-Microstructure Content G0 polybutadiene

6.3.2.1 Butadiene Polymerization

The polymerization procedure used was as described by Yuan and Gauthier.¹⁷ Butadiene (7.0 g, 0.13 mol; 11 mL) was stirred with *n*-butyllithium (1.1 mL) in a high-vacuum manifold for 30 min at $-30\text{ }^{\circ}\text{C}$, condensed into a calibrated ampule, and diluted with 15 mL of THF. The ampule was stored at $-20\text{ }^{\circ}\text{C}$ until further use. A 2-L glass reactor was used to polymerize butadiene; the reactor was first evacuated, flamed, and then filled with nitrogen. THF (100 mL) was introduced directly from the still and the temperature was brought to $0\text{ }^{\circ}\text{C}$. Residual impurities were titrated by adding a few drops of a 0.1 M 2,2'-bipyridyl solution in toluene, and enough *sec*-BuLi was added to obtain a persistent red-orange color. The calculated amount of *sec*-BuLi solution (1 mL, 1.4 mmol) for a target $M_n = 5000$ was then added, followed by butadiene. The reaction mixture was warmed to room temperature after 15 min and stirred for 2 h. The reaction was terminated with degassed methanol and the polymer solution was concentrated to 20 mL. The polymer was recovered by precipitation in 200 mL of methanol, decantation, and drying under vacuum. The reaction yielded 6.2 g of polybutadiene (88% yield) with a microstructure consisting of 44% 1,4-units and 56% 1,2-units, with $M_n = 5500$ and $M_w/M_n = 1.05$.

6.3.2.2 Hydrosilylation of Linear Polybutadiene

The modification method was adapted from the hydrosilylation procedure reported by Hempenius et al.¹² Polybutadiene (0.69 g, 7.1 mmol of 1,2-units) was dissolved in 20 mL of toluene and dried with three azeotropic distillation cycles on a high-vacuum line. The polymer was then dissolved in 20 mL of toluene, and the ampule was filled with nitrogen and cooled to 0°C. Chlorodimethylsilane (0.39 mL, 3.57 mmol, 50% target functionalization of 1,2-units) and platinum catalyst (0.07 mL, 5 mol % with respect to chlorodimethylsilane) were added to the ampule through the stopcock opening against nitrogen flow. The ampule was then sealed, disconnected from the manifold, and the reaction was allowed to proceed for 24 h. After 20 min a light-yellow color, indicative of the start of hydrosilylation, was observed. After 24 h the ampule was reconnected to the manifold to remove a sample for ¹H NMR analysis through the stopcock opening with a syringe and needle.

6.3.2.3 Grafting of High 1,2-Microstructure Content Polybutadienyllithium onto Linear Hydrosilylated Polybutadiene

Polybutadienyllithium side chains were prepared from butadiene (9.6 g, 0.17 mol; 15 mL) and *sec*-BuLi solution (1.37 mL, 1.92 mmol, for a target $M_n = 5000$) as described in Section 6.3.2.1. The reaction mixture was warmed to room temperature (23 °C) after 15 min and stirred for 1 h. A sample of the polymer solution was removed from the reactor and terminated with degassed methanol, to determine the molecular weight of the side chains. The solution of linear hydrosilylated polybutadiene was then added drop-wise and the mixture was left stirring overnight. The reaction was terminated with degassed methanol after that time and the polymer

solution was concentrated to 25 mL. The polymer was recovered by precipitation in 250 mL of methanol, and purified by a second precipitation from THF. The raw grafting product (9.9 g) was further purified by fractionation precipitation in a hexane/2-propanol mixture, to remove unreacted side chains and yield 3.2 g of pure comb-branched polybutadiene (32% overall yield). The comb-branched polybutadiene had a microstructure with 45% of 1,4-units and 55% of 1,2-units, $M_n = 1.04 \times 10^5$, and $M_w/M_n = 1.06$.

6.3.3 Synthesis of High 1,4-Microstructure Content G1 Polybutadiene

6.3.3.1 Hydrosilylation of High 1,2-Microstructure Content G0 Polybutadiene

Different amounts of the G0 polymer (0.5 g, 0.14 g, 88 mg, and 55 mg) were hydrosilylated with chlorodimethylsilane (0.28, 0.08, 0.05, and 0.031 mL) and platinum catalyst (0.056 mL, 0.016 mL, 10 μ L, and 6.2 μ L) as described in Section 6.3.2.2 to obtain the substrates for grafting $M_n \approx 5, 30, 50,$ and $80,000$ side chains, respectively.

6.3.3.2 Grafting of $M_n \approx 5, 30, 50,$ and $80,000$ High 1,4-Microstructure Content Polybutadienyllithium onto Hydrosilylated G0 Polybutadiene

Grafting of $M_n \approx 5000$ (high 1,4-microstructure content) polybutadienyllithium onto the hydrosilylated G0 polymer was achieved as described in Section 6.3.2.3, but the polymerization of butadiene (12.8 g) with *sec*-BuLi (1.82 mL) was carried out in cyclohexane rather than THF, the polymerization time was 5 h, and the hydrosilylated G0 polymer (0.5 g) described in Section 6.3.3.1 was used.

Grafting of $M_n \approx 30, 50, \text{ and } 80,000$ (high 1,4-microstructure content) polybutadienyllithium onto G0 chlorosilane-functionalized polybutadiene was achieved by a slightly modified procedure. Butadiene (22.4 g, 0.41 mol; 35mL) was stirred with *n*-butyllithium (3.5 mL) in a high-vacuum manifold for 30 min at $-30\text{ }^\circ\text{C}$, condensed to a calibrated ampule. The ampule, maintained in a $-20\text{ }^\circ\text{C}$ bath, was reconnected to a high-vacuum manifold along with a 2-L ampule with a stirring bar. The monomer was condensed from the ampule and further purified by a second cycle of stirring with *n*-butyllithium (3.5 mL), condensed to the 2-L ampule, and diluted with 350 mL of cyclohexane. The manifold and ampule were then filled with nitrogen, the temperature was brought to $0\text{ }^\circ\text{C}$, and the calculated amount of *sec*-BuLi solution (0.53 mL, 0.74 mmol for a target $M_n = 30,000$; 0.32 mL, 0.45 mmol for a target $M_n = 50,000$; and 0.20 mL, 0.28 mmol for a target $M_n = 80,000$; 1 equiv with respect to chlorosilane groups on the substrate) was added through the stopcock opening against nitrogen flow. The ampule was sealed, disconnected from the manifold, and the reaction was stirred overnight. The ampule containing the hydrosilylated G0 polymer (0.14 g for grafting $M_n = 30,000$ side chains, 88 mg for $M_n = 50,000$ side chains, and 55 mg for $M_n = 80,000$ side chains), prepared as described in Section 6.3.3.1, and the polymerization ampule were connected to a high-vacuum manifold which was evacuated, flamed under high-vacuum, and purged with nitrogen. A sample from the polymerization ampule was removed to determine the molecular weight of the side chains, then the hydrosilylated substrate was transferred to the polymerization ampule by syringe under nitrogen. The ampule was sealed and the reaction was left stirring for 48 h for $M_n \approx 30,000$ side chains, and 96 h for $M_n \approx 50$ and 80,000 side chains.

The reactions were terminated with degassed methanol and the polymer solution was concentrated to 100 mL in all cases. The polymers were recovered by precipitation twice in 1 L

of methanol. The raw grafting products were further purified by fractionation precipitation from hexane/2-propanol mixtures as described in Section 6.3.2.3, to remove unreacted side chains and yield the pure G1 polymers with a microstructure composition of 94% 1,4-units and 6% 1,2-units.

6.3.4 Synthesis of High 1,2-Microstructure Content G1 Polybutadiene

The G0 polybutadiene substrate (0.57g) obtained as described in Section 6.3.2.3 ($M_n = 1.04 \times 10^5$, $M_w/M_n = 1.06$, 55% 1,2-units), chlorodimethylsilane (0.32 mL), and platinum catalyst (0.064 ml) were used to synthesize the substrate.

Grafting of $M_n \approx 5000$ (high 1,2-microstructure content) polybutadienyllithium onto the hydrosilylated G0 polybutadiene substrate (0.57 g) was achieved as described in Section 6.3.2.3. The side chains were prepared from butadiene (14.7 g) and *sec*-BuLi (2.1 mL) as described in Section 6.3.2.1. The polymer obtained had a microstructure with 56% of 1,2-units, $M_n = 2.1 \times 10^6$ and $M_w/M_n = 1.09$.

6.3.5 Synthesis of High 1,4-Microstructure Content G2 Polybutadiene

6.3.5.1 Hydrosilylation of High 1,2-Microstructure Content G1 Polybutadiene

The method employed was as described in Section 6.3.2.2, using the G1 polymer ($M_n = 2.1 \times 10^6$, $M_w/M_n = 1.09$, 56% of 1,2-units) of Section 6.3.4. Different amounts of G1 polymer (0.55 g, 0.12 g, 80 mg, and 55 mg), chlorodimethylsilane (0.32, 0.07, 0.05, and 0.032 mL), and

platinum catalyst (0.06 mL, 14 μ l, 9.2 μ l, and 6.3 μ l) were used to obtain the substrates used for grafting $M_n \approx 5, 30, 50,$ and 80,000 side chains, respectively.

6.3.5.2 Grafting of $M_n \approx 5, 30, 50,$ and 80,000 High 1,4-Microstructure Content

Polybutadienyllithium onto Hydrosilylated G1 Polybutadiene

This procedure was performed as described in Section 6.3.3.2, using the hydrosilylated G1 polymer of Section 6.3.5.1. Butadiene (14.1 g), *sec*-BuLi (2.0 mL), and the hydrosilylated G1 polymer (0.55 g) were used to graft the $M_n \approx 5000$ side chains; the grafting reaction was allowed to proceed for 48 h. Butadiene (19.2 g), *sec*-BuLi (0.46 mL), and the hydrosilylated G1 polymer (0.12 g) were used to graft the $M_n \approx 30,000$ side chains; the grafting reaction was left for 72 h. Butadiene (20.48 g), *sec*-BuLi (0.29 mL), and the hydrosilylated G1 polymer (80 mg) were used to graft the $M_n \approx 50,000$ side chains; the grafting reaction was left for 120 h. Butadiene (22.4 g), *sec*-BuLi (0.2 mL), and the hydrosilylated G1 polymer (55 mg) were used to graft the $M_n \approx 80,000$ side chains; the grafting reaction was left for 120 h. Preparative SEC served to purify the graft polymer samples, which were then characterized on an analytical SEC instrument for molecular weight analysis.

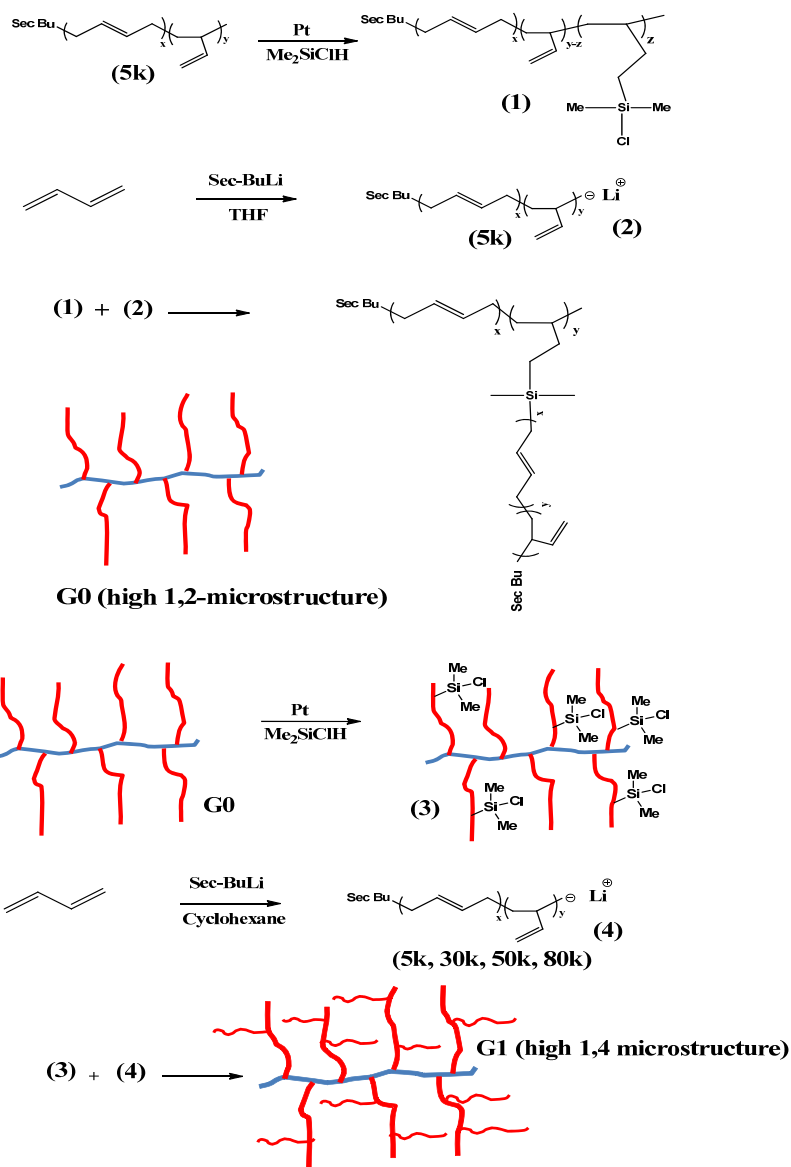
6.3.6 Polymer Characterization

Size exclusion chromatography (SEC) analysis was performed for the substrates, the side chains, the raw grafting products, and the fractionated graft polymers. The system used consisted of a Viscotek GPCmax unit equipped with a VE 2001 GPC Solvent/sample Module, a Viscotek triple detector array with a refractive index, viscosity, and dual-angle light scattering detectors,

an external Viscotek UV 2600 detector, and three PolyAnalytik organic mixed bed columns, PAS-103-L, PAS-104-L, and PAS-105-L, with dimensions of 8 mm (ID) \times 300 mm (L) each and an overall polystyrene molecular weight range of 10^3 to 10^7 . The polymers were analyzed in THF at a flow rate of 1 mL/min. ^1H NMR analysis of all the polymer samples was achieved in CDCl_3 on a Bruker Avance 300 MHz NMR instrument at a concentration of 40 mg/mL. Preparative SEC was carried out on a system consisting of a Waters M45 HPLC pump, a Waters R401 differential refractometer detector, and a Jordi Gel DVB preparative SEC column in THF as the mobile phase. The crude polymer was injected as a 20 mg/mL solution at a flow rate of 3.0 mL/min.

6.4 Results and Discussion

The synthesis of arborescent polybutadiene structures incorporating side chains with a high 1,4-microstructure content in the last grafting cycle and different molecular weights was achieved as described in Scheme 6.1, taking the synthesis of a G1 sample as an example. The grafting substrates were obtained by first polymerizing butadiene in THF, to produce linear polybutadiene with a high 1,2-microstructure content. The linear polymer was functionalized with chlorosilane groups by hydrosilylation with chlorodimethylsilane, and then grafted with $M_n \approx 5000$ side chains synthesized in THF to obtain a G0 polymer with a high 1,2-microstructure content in the backbone and the side chains. The G0 polymer was further functionalized with chlorosilane groups and grafted with side chains having a high 1,4-microstructure content (synthesized in cyclohexane) and either $M_n \approx 5, 30, 50,$ or $80,000$ to obtain a series of analogous G1 polymers.



Scheme 6.1. Synthesis of G1 polybutadiene by grafting onto hydrosilylated substrates.

The synthesis of a series of G2 polybutadiene samples with different side chain molecular weights, likewise with a high 1,4-microstructure content in the last grafting cycle, was achieved as described in Scheme 6.1, but rather starting from a G1 substrate with a high 1,2-microstructure content. This polymer was obtained through an additional grafting cycle with $M_n \approx 5000$ side chains synthesized in THF for the chlorosilane-functionalized G0 substrate in

Scheme 6.1. The hydrosilylated G1 polymer was then coupled with side chains having a high 1,4-microstructure content (synthesized in cyclohexane) and $M_n \approx 5, 30, 50, \text{ or } 80,000$ to obtain the G2 polymers.

6.4.1 Synthesis of High 1,2-Microstructure Content G0 polybutadiene

6.4.1.1 Butadiene Polymerization and Hydrosilylation

The linear polymer obtained in toluene had the expected molecular weight ($M_n = 5500$) and a narrow MWD ($M_w/M_n = 1.05$), as seen from the SEC trace in Figure 6.1. ^1H NMR analysis (Figure 6.2a) yielded a microstructure with 56% of 1,2-units, causing a resonance at 4.9-5 ppm, whereas the protons on the 1,4-units resonated at 5.3-5.6 ppm. The vinyl groups of the 1,2-units were converted to coupling sites by hydrosilylation with chlorodimethylsilane. This led to a new resonance at 0.4 ppm (methyl protons of the chlorosilyl group), as shown in Figure 6.2b. Analysis using the 1,2-unit and the dimethylchlorosilyl signals yielded a hydrosilylation level corresponding to 49% of the 1,2-units (27 % of the butadiene units overall), and it is clear that the intensity of the peak at 4.9-5 ppm in Figure 6.2a decreased significantly after this reaction. Integration of the peak intensity for the protons in the residual 1,2-units for comparison with the protons in the 1,4-units before hydrosilylation was also consistent with 49% hydrosilylation. Variation of the hydrosilylation level can potentially provide control over the branching density on the backbone, but it was maintained at 45-50 % of the 1,2-units for every generation in the current investigation.

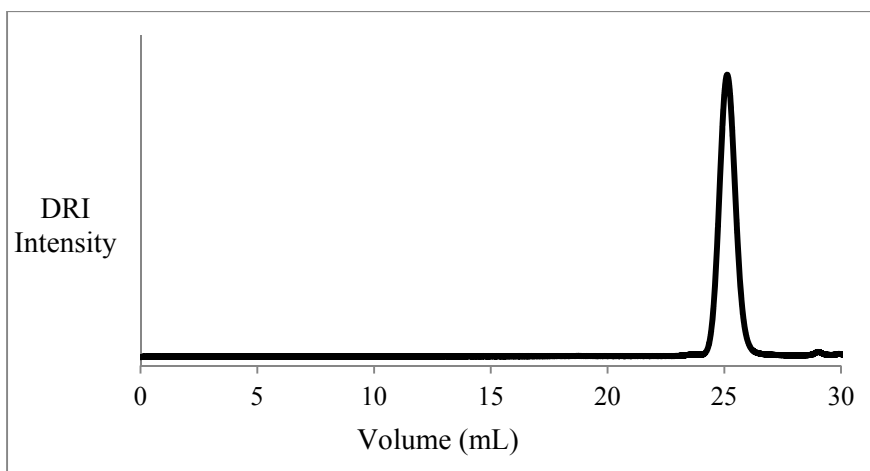


Figure 6.1. SEC trace for linear polybutadiene ($M_n = 5500$, $M_w/M_n = 1.05$).

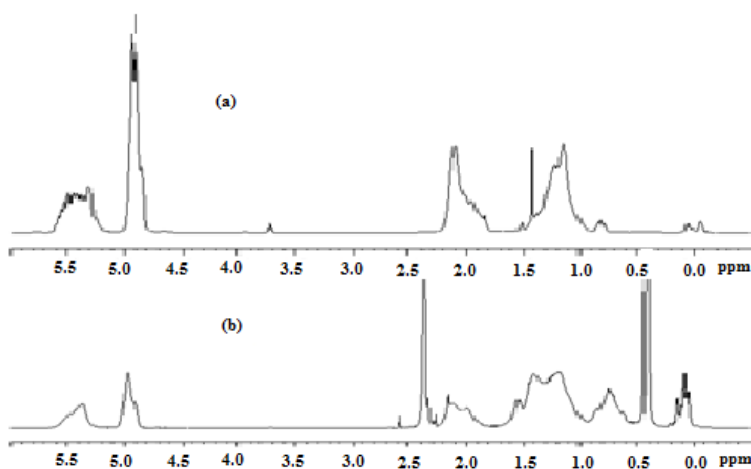


Figure 6.2. ¹H NMR spectra for (a) linear polybutadiene and (b) hydrosilylated polybutadiene.

6.4.1.2 Grafting of High 1,2-Microstructure Content $M_n \approx 5000$ Polybutadienyllithium onto Linear Hydrosilylated Polybutadiene

Grafting of high 1,2-microstructure content polybutadienyllithium (55% 1,2-units, $M_n = 5800$, $M_w/M_n = 1.08$) onto the linear hydrosilylated polybutadiene substrate of Section 6.4.1.1 was achieved with a 1:1 stoichiometric ratio of chlorosilane groups to living ends in THF. The

reaction was allowed to proceed overnight, after which time the light yellow color faded completely and a sample was withdrawn for SEC analysis. The reaction was left running for 24 h longer and another sample was withdrawn for SEC analysis; it produced the same grafting yield as the sample withdrawn after 24 h, confirming that the grafting reaction was already completed after 24 h. The grafting yield (defined as the fraction of living chains becoming attached to the substrate) reached 43%, as determined from the SEC trace for the raw grafting product in Figure 6.3. The grafting yield was approximated, by SEC analysis with a differential refractometer detector, from the peak areas for the graft polymer and the unreacted side chains according to the equation:

$$\text{Grafting yield} = \frac{\text{graft polymer peak area}}{\text{graft polymer} + \text{unreacted side chain areas}}$$

The raw product was further purified by precipitation fractionation from a hexane/2-propanol mixture to yield the pure G0 polymer (Figure 6.4), having $M_n = 1.04 \times 10^5$ and $M_w/M_n = 1.06$.

The grafting yield attained in 24 h is in agreement with the fact that anionic grafting in polar solvents proceeds at a fast rate,¹⁸ partly due to increased reactivity of the macroanions in polar solvents such as THF that solvate the lithium counterion more efficiently.^{19,20} Unfortunately the living chains are also subject to termination in the presence of THF; which explains the relatively low grafting yield attained. Another effect of THF is its influence on the microstructure of polybutadiene chains: A high 1,2-microstructure content is obtained in THF, as desired for the G0 polymer; the sample had 55% of 1,2-units and 45% of 1,4-units. The small peak on the left of the side chains in the SEC trace of Figure 6.3 corresponds to dimerization of the living chains. This could be due to contamination of the reaction by O₂ or CO₂ during the grafting process, possibly during sample removal to monitor the progress of the reaction. Dimer formation was observed for all the grafting reactions reported herein.

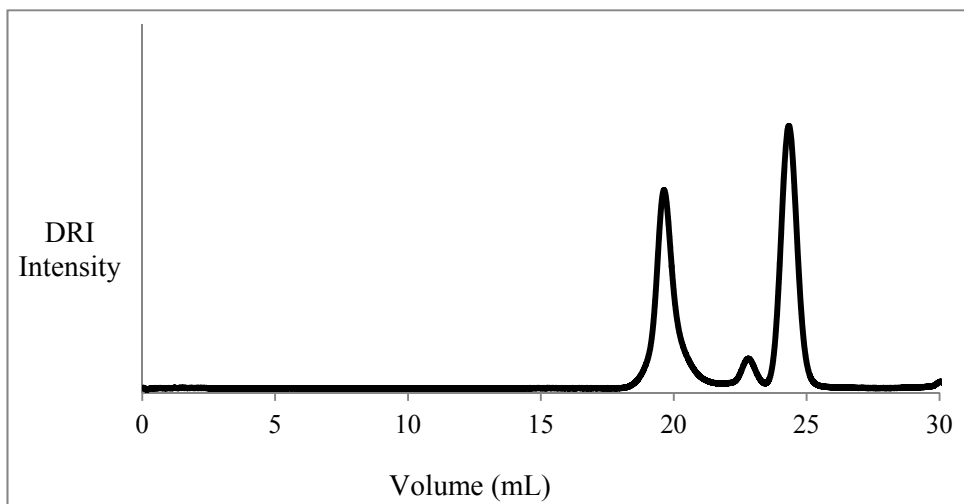


Figure 6.3. SEC trace for grafting $M_n = 5800$ high 1,2-microstructure content polybutadienyllithium onto linear hydrosilylated polybutadiene.

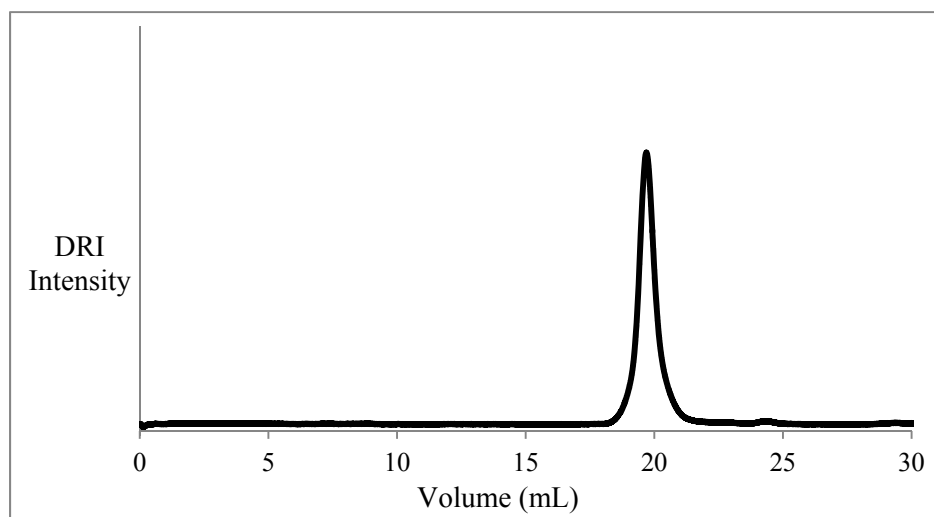


Figure 6.4. SEC trace for purified G0 polybutadiene with a high 1,2-microstructure content ($M_n = 1.04 \times 10^5$, $M_w/M_n = 1.06$).

6.4.2 Synthesis of High 1,4-Microstructure Content G1 Polybutadiene with $M_n \approx 5, 30, 50,$ and $80,000$ Side Chains

Grafting of polybutadienyllithium side chains with a high 1,4-microstructure content (92-93% 1,4-units) onto a hydrosilylated G0 substrate (51 % of the 1,2-units) was achieved using a 1:1 stoichiometric ratio of chlorosilane groups and living chain ends in cyclohexane. The polymerization and grafting reactions were allowed to proceed for a longer time period than when grafting $M_n \approx 5000$ side chains in THF, particularly when grafting longer side chains ($M_n \approx 30, 50,$ and $80,000$). This is partly because (as discussed above) solvent polarity plays an important role in the grafting reactions. The different microstructure (high 1,4-content) of the polybutadiene side chains may also have played a role in the reaction, given the different reactivity of the living chains and their longer contour length. Furthermore, high molecular weight polybutadienyllithium chains ($M_n \approx 30, 50,$ and $80,000$) require a longer polymerization time because of the slow rate of propagation in non-polar solvents such as cyclohexane, combined with the very low concentration of propagating centers. In all cases, the reactions were terminated on the basis of the SEC analysis results obtained: Samples were withdrawn every 24 h, and the reactions were terminated when the grafting yield remained constant over the subsequent 24 h time interval. Grafting of side chains with $M_n = 5600$ and $M_w/M_n = 1.07$ onto a hydrosilylated G0 substrate proceeded with 57% yield in 24 h, as determined from the SEC trace of Figure 6.5. The final product had $M_n = 3.94 \times 10^6$ and $M_w/M_n = 1.03$.

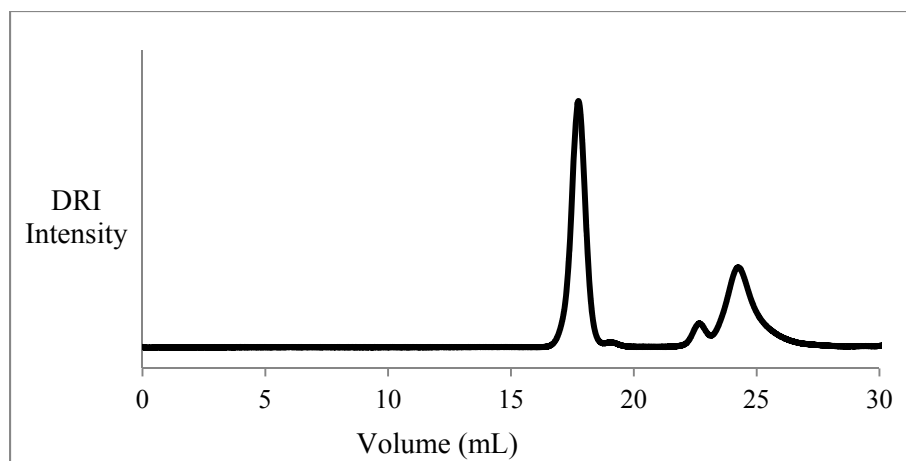


Figure 6.5. SEC trace for grafting high 1,4-microstructure content $M_n = 5600$ polybutadienyllithium onto a hydrosilylated G0 substrate. The graft polymer had $M_n = 3.94 \times 10^6$ and $M_w/M_n = 1.03$.

Grafting of side chains with $M_n = 31,000$ and $M_w/M_n = 1.07$ onto the hydrosilylated G0 substrate was performed for 48 h and proceeded with 22% yield (Figure 6.6); the final product had $M_n = 5.79 \times 10^6$ and $M_w/M_n = 1.07$. Grafting of side chains with $M_n = 51,000$ and $M_w/M_n = 1.04$, as well as $M_n = 78,000$ and $M_w/M_n = 1.06$ onto the hydrosilylated G0 substrate, likewise performed in cyclohexane, required 96 h for completion. The reactions proceeded with 17 and 10% yield when grafting side chains with M_n of 51,000 and 78,000, respectively. The purified products had $M_n = 7.63 \times 10^6$, $M_w/M_n = 1.10$ for the $M_n = 51,000$ side chains (Figure 6.7), and $M_n = 10.1 \times 10^6$, $M_w/M_n = 1.09$ for the G1 polymer with $M_n = 78,000$ side chains (Figure 6.8).

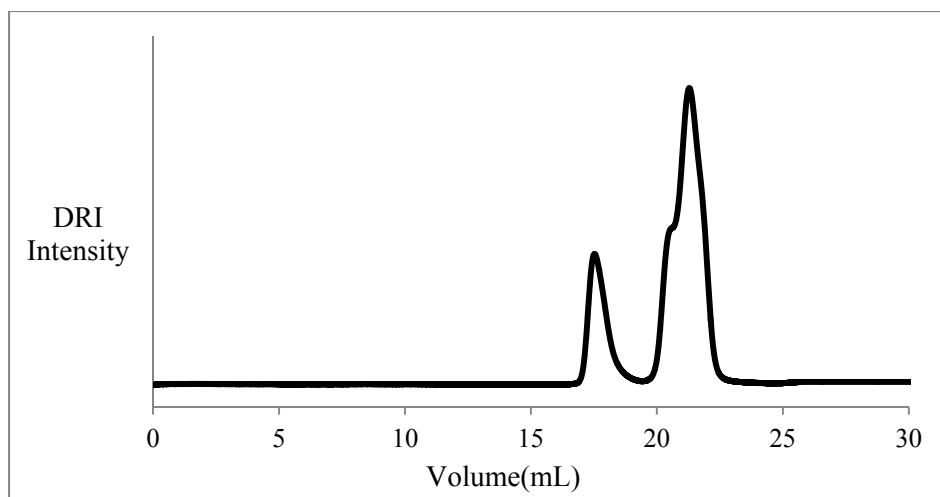


Figure 6.6. SEC trace for grafting high 1,4-microstructure content $M_n = 31,000$ polybutadienyllithium onto a hydrosilylated G0 substrate. The graft polymer had $M_n = 5.79 \times 10^6$ and $M_w/M_n = 1.07$.

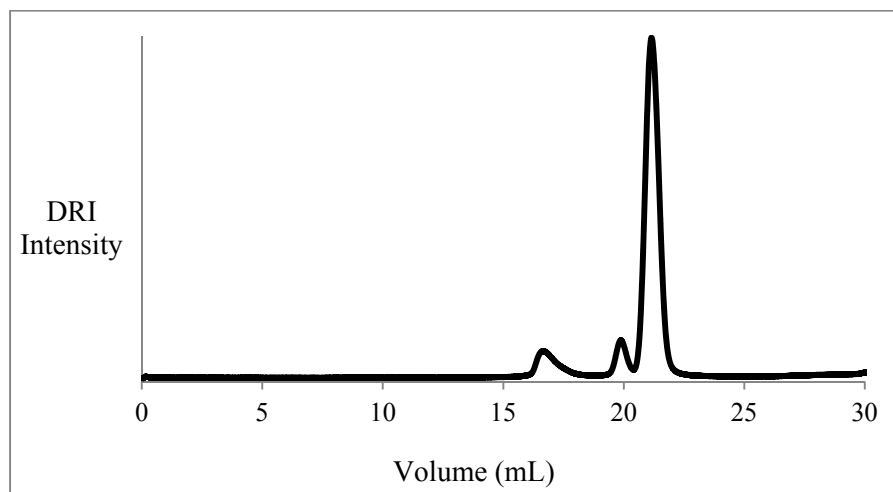


Figure 6.7. SEC trace for grafting high 1,4-microstructure content $M_n = 51,000$ polybutadienyllithium onto a hydrosilylated G0 substrate. The graft polymer had $M_n = 7.63 \times 10^6$ and $M_w/M_n = 1.10$.

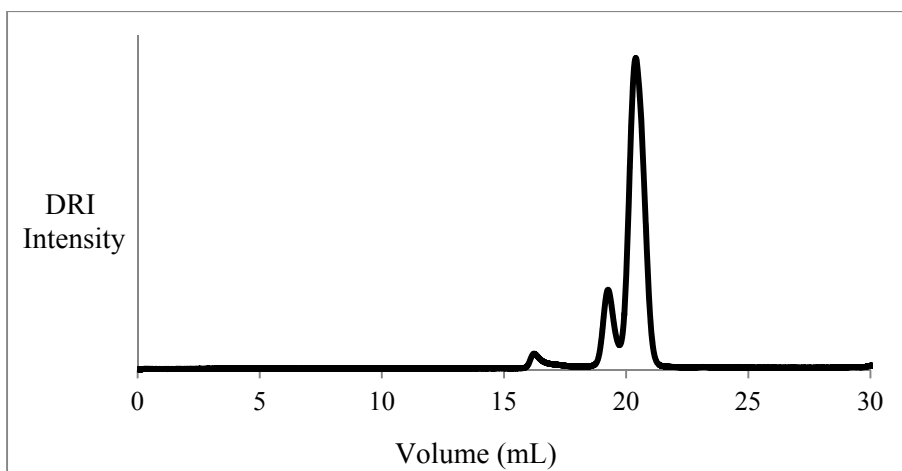


Figure 6.8. SEC trace for grafting high 1,4-microstructure content $M_n = 78,000$ polybutadienyllithium onto a hydrosilylated G0 substrate. The graft polymer had $M_n = 10.1 \times 10^6$ and $M_w/M_n = 1.09$.

The SEC analysis results for the series of G1 polymers synthesized with the different side chain molecular weights are summarized in Table 6.1. The data clearly show that as the side chain molecular weight increases, the overall molecular weight of the graft polymers increases whereas the grafting yield and the branching functionality both decrease. The number-average branching functionality of the polymers, defined as the number of chains added in the last grafting reaction, was calculated according to the equation

$$f_n = \frac{M_n(G) - M_n(G - 1)}{M_n^{br}}$$

where $M_n(G)$, $M_n(G - 1)$, and M_n^{br} are the absolute number-average molecular weight of graft polymers of generation G, of the preceding generation, and of the side chains, respectively.

The decrease in grafting yield and branching functionality of the graft polymers can be explained on several grounds. The congested structure of the hydrosilylated G0 substrate sterically hinders the access of the living ends to the coupling sites, especially for high molecular weight side chains ($M_n = 51$ and $78,000$). Decreased reactivity of the macroanions in non-polar solvents such as cyclohexane, and termination of the living ends by residual chlorodimethylsilane in the hydrosilylation reaction product may also have contributed to the decreases in grafting yield observed.

Table 6.1. Characteristics of the G1 arborescent polybutadiene samples.

	Side chains		Graft polymer			
	M_n^a	M_w/M_n^a	Yield (%) ^b	M_n^a	M_w/M_n^a	f_n
G1-5K	5600	1.07	57	3.94×10^6	1.03	685
G1-30K	31×10^3	1.07	22	5.79×10^6	1.07	183
G1-50K	51×10^3	1.04	17	7.63×10^6	1.10	147
G1-80K	78×10^3	1.06	10	10.1×10^6	1.09	128

^a Absolute values from SEC-MALLS analysis.

^b Fraction of side chains generated becoming attached to the substrate.

6.4.3 Synthesis of High 1,2-Microstructure Content G1 Polybutadiene

Grafting of high 1,2-microstructure content polybutadienyllithium side chains (56 % 1,2-units, $M_n = 5700$, $M_w/M_n = 1.06$) onto the G0 polybutadiene substrate ($M_n = 1.04 \times 10^5$)

hydrosilylated on 50 % of the 1,2-units, using a 1:1 stoichiometric ratio of chlorosilane groups to living chain ends, was also performed in THF to obtain mainly 1,2-units; the grafting reaction was allowed to proceed overnight. The reaction proceeded in 41% yield, as determined from the SEC trace for the raw grafting product (Figure 6.9). The polymer was purified by precipitation fractionation from a hexane/2-propanol mixture (Figure 6.10) and had $M_n = 2.1 \times 10^6$, $M_w/M_n = 1.09$. Grafting in THF produced a G1 polymer with 56% of 1,2-microstructure content, allowing the introduction of a large number of chlorosilane groups after hydrosilylation, to serve as substrate for the synthesis of G2 polybutadienes by grafting side chains with a high 1,4-microstructure content.

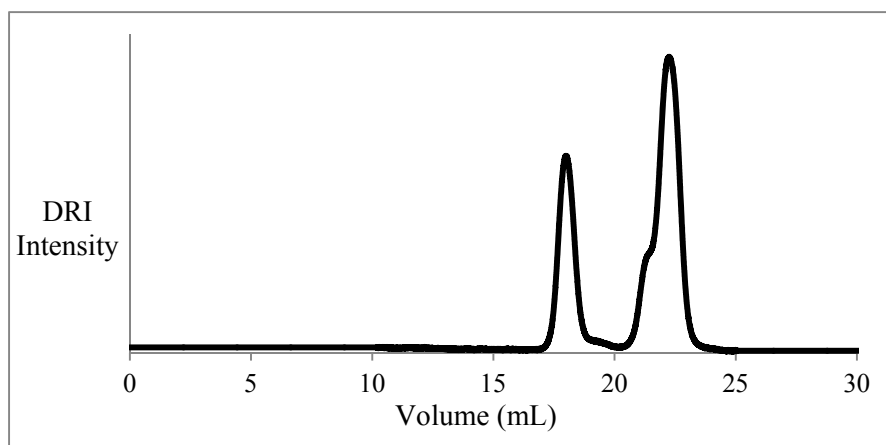


Figure 6.9. SEC trace for grafting $M_n = 5700$ high 1,2-microstructure content polybutadienyllithium onto hydrosilylated G0 polybutadiene.

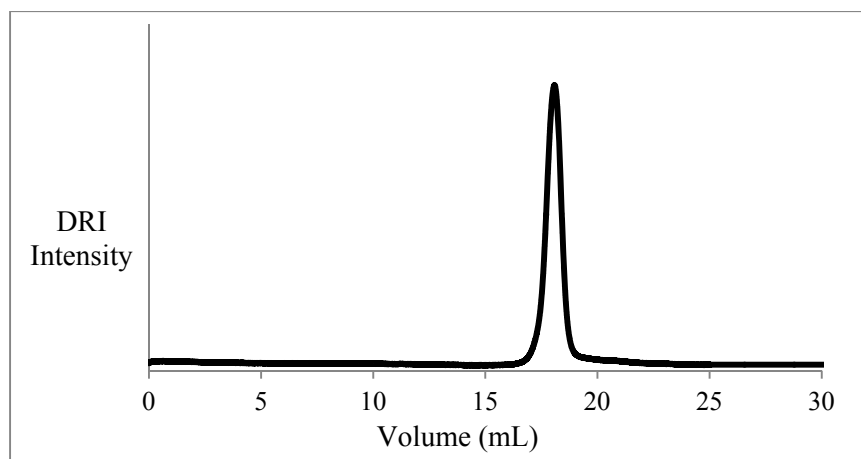


Figure 6.10. SEC trace for purified G1 graft polybutadiene with a high 1,2-microstructure content ($M_n = 2.1 \times 10^6$, $M_w/M_n = 1.09$).

6.4.4 Synthesis of High 1,4-Microstructure Content G2 Polybutadiene with $M_n \approx 5, 30, 50,$ and $80,000$ Side Chains

Grafting of polybutadienyllithium side chains with a high (92-93%) 1,4-microstructure content onto a G1 substrate hydrosilylated on 50 % of the 1,2-units, obtained as described in Section 6.4.3, was carried out with a 1:1 stoichiometric ratio of chlorosilane groups to living chain ends in cyclohexane. These grafting reactions were performed for even longer time periods in comparison to the G1 polymers of Section 6.4.2. As discussed earlier, grafting in non-polar solvents such as cyclohexane is slow, and even synthesizing high molecular weight side chains ($M_n = 50$ and $80,000$) can be challenging due to the low concentration of propagating centers in the reactions, and thus their increased sensitivity to termination by impurities. Grafting of short side chains ($M_n = 5400$, $M_w/M_n = 1.09$) proceeded with 13% yield after 48 h, as determined from the SEC trace of Figure 6.11a, while the purified product had $M_n = 1.26 \times 10^7$ and $M_w/M_n = 1.08$.

Grafting longer side chains ($M_n = 29000$, $M_w/M_n = 1.07$) required 72 h and proceeded with 11% yield; the purified product had $M_n = 4.53 \times 10^7$ and $M_w/M_n = 1.08$ (Figure 6.11b). Grafting of even longer side chains ($M_n = 51,000$, $M_w/M_n = 1.08$; and $M_n = 79,000$, $M_w/M_n = 1.09$) proceeded in 7 and 4% yield, respectively. The purified G2 products had $M_n = 6.51 \times 10^7$, $M_w/M_n = 1.09$ and $M_n = 5.03 \times 10^7$, $M_w/M_n = 1.28$, respectively (Figure 6.12). Isolation of the pure graft polymers used for the analytical SEC work was achieved with a preparative SEC column.

The SEC analysis results obtained for the G2 polymers with $M_n \approx 5, 30, 50,$ and $80,000$ side chains are summarized in Table 6.2. It is clear that the trends observed are again similar to the analogous series of G1 polymers (Table 6.1). The overall molecular weight of the graft polymers increased with the molecular weight of the side chains, whereas the grafting yield and the branching functionality decreased. The decrease in grafting yield and branching functionality of the graft polymers is attributed to the same reasons discussed in Section 6.4.2. The yield obtained when grafting polybutadiene ($M_n \approx 5000$) side chains onto G0 substrates anionically (57%) and by “click” coupling (59%) is comparable. However “click” grafting onto G1 substrates proceeded in 40% yield, whereas the anionic grafting yield was 13%. The origin of this significant difference was discussed earlier, namely the decreased reactivity of the macroanions in non-polar solvents (cyclohexane) and termination of the living ends by residual chlorodimethylsilane from the hydrosilylation reaction.

Table 6.2. Characteristics of G2 arborescent polybutadiene samples.

	Side chains		Graft polymer			
	M_n^a	M_w/M_n^a	Yield (%) ^b	M_n^a	M_w/M_n^a	f_n
G2-5K	5400	1.09	13	1.26×10^7	1.08	2111
G2-30K	29×10^3	1.07	11	4.53×10^7	1.08	1610
G2-50K	51×10^3	1.08	7	6.51×10^7	1.09	1347
G2-80K	79×10^3	1.09	4	5.03×10^7	1.28	717

^a Absolute values from SEC-MALLS analysis.

^b Fraction of side chains generated becoming attached to the substrate.

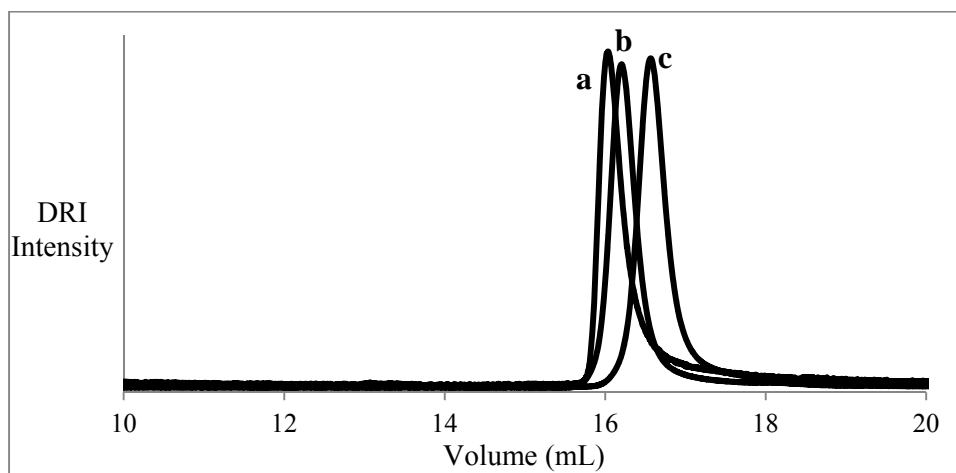


Figure 6.11. SEC traces for grafting (a) $M_n = 51,000$ (b) $M_n = 29,000$ and (c) $M_n = 5400$ high 1,4-microstructure content polybutadienyllithium onto the G1 hydrosilylated substrate.

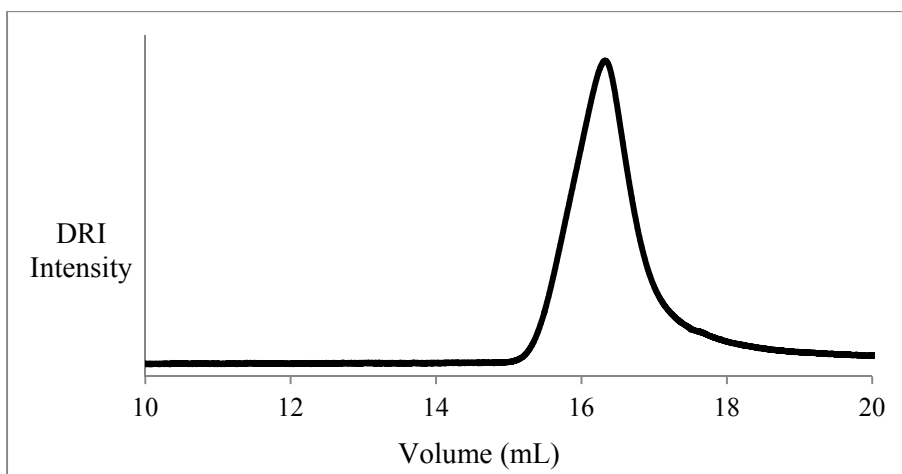


Figure 6.12. SEC trace for grafting $M_n = 79,000$ high 1,4-microstructure content polybutadienyllithium onto the G1 hydrosilylated substrate.

6.5 Conclusions

Arborescent polybutadienes of generations G1 and G2, with side chains of different molecular weights, were synthesized by anionic coupling of living polybutadienyllithium chains with chlorosilane-functionalized substrates. First a comb-branched (G0) substrate with $M_n \approx 5000$ side chains was synthesized in THF, to obtain a microstructure with 55% of 1,2-units which were converted into coupling sites by hydrosilylation with chlorodimethylsilane. The hydrosilylated G0 polymer was grafted with a series of high 1,4-microstructure content side chains having $M_n \approx 5, 30, 50,$ and $80,000$ to produce a series of G1 graft polymers with molecular weight reaching up to 1.01×10^7 . The hydrosilylated G0 substrate was also grafted with $M_n \approx 5000$ side chains in THF, to produce a G1 polymer with 56% of 1,2-units to be converted into coupling sites. Grafting of the hydrosilylated G1 polymer with $M_n \approx 5, 30, 50,$ and $80,000$

side chains produced G2 arborescent polymers with molecular weights reaching 6.5×10^7 , albeit the grafting yields were low (4-13%).

The results presented show that hydrosilylation and anionic grafting can be successfully applied to the synthesis of arborescent polybutadiene of different generations, even for side chains with a high molecular weight. The solvent used in the polymerization provides control on the microstructure of the branched macromolecules, while the molecular weight of the side chains determines the overall dimensions of the molecules. This will allow the investigation of the physical properties of these materials over a wide concentration range.²¹⁻²³

Chapter 7

Concluding Remarks and Suggestions for Future Work

7.1 Original Contributions to Knowledge

The research described in this Thesis focused mainly on the synthesis of arborescent polystyrene and polybutadiene by “click” chemistry coupling, and the investigation of hydroxylated polystyrene substrates (serving as intermediates in the synthesis of arborescent polystyrene by “click” grafting) as macroinitiators for the synthesis of arborescent poly(ethyl vinyl ether) copolymers. The synthesis of arborescent polybutadiene was also carried out by anionic grafting, mainly for the purpose of comparing the grafting yields achieved by “click” and anionic grafting and to provide samples for rheological measurements.

The synthesis of arborescent polymers has thus far mainly relied upon anionic grafting,¹ but these synthetic procedures are very time-consuming and experimentally demanding. Consequently, the implementation of a different coupling technique based upon copper-catalyzed azide-alkyne “click” coupling² was explored to prepare arborescent polymers. The synthesis of arborescent polymers by “click” coupling was demonstrated for the first time, using successive grafting reactions of substrates randomly functionalized with either azide or acetylene coupling sites, and side chains containing the complementary type of chemical functionality.

For styrene-based arborescent systems, grafting was most conveniently achieved for azide-terminated side chains and randomly acetylenated substrates. Graft polymers up to generation G2 were obtained with number-average molecular weights and branching functionalities reaching up to 2.82×10^6 and 458, respectively. The results obtained compared favorably with previous achievements for the synthesis of arborescent polystyrene by anionic grafting,³ thus establishing the “click” coupling approach as an efficient alternative to the synthesis of arborescent polystyrene.

Samples of linear and branched polystyrene (obtained by “click” grafting) were also functionalized with secondary and tertiary hydroxyl groups, to be tested as macroinitiators for the cationic polymerization of ethyl vinyl ether. Grafting proceeded successfully from the linear and branched, secondary and tertiary alcohol-functionalized substrates, but the secondary alcohol systems provided narrower molecular weight distributions for the graft polymers than the tertiary alcohol initiator system. Both the secondary and tertiary alcohol initiator systems produced graft copolymers without linear contaminant, which represents a clear advantage over previously tested systems^{4,5} marred by the production of homopolymer.

The synthesis of arborescent polybutadiene was also achieved by “click” coupling, likewise by a route never explored before. In this case the preferred approach involved acetylene groups at the end of the side chains, and azide groups randomly introduced on the substrates. Grafting of acetylene-terminated side chains onto the azidated substrates proceeded successfully up to generation G2. The polymers obtained had molecular weights and branching functionalities reaching 3.4×10^6 and 530, respectively.

For comparison purposes, the synthesis of G1 and G2 arborescent polybutadiene molecules was achieved by anionic grafting onto chlorosilane-functionalized substrates. Polybutadienyllithium side chains with a high (92-93 %) 1,4-microstructure content and molecular weights $M_n \approx 5, 30, 50, \text{ or } 80,000$ were reacted with G0 and G1 substrates hydrosilylated with dimethylchlorosilane. Anionic grafting of living chains onto chlorosilane-functionalized substrates has been reported before,⁶ but it was limited to side chains having $M_n \approx 10,000$ and low substrate functionalization levels. The side chains explored in the current investigation encompassed a much wider range of molecular weights, which was very challenging when performing the polymerization and grafting in a non-polar solvent like

cyclohexane. The rheological properties of these types of materials are currently being investigated through a collaboration with another institution.⁷⁻⁹

7.2 Suggestions for Future Work

The work presented in this Thesis is the first investigation into the synthesis of arborescent polystyrene and polybutadiene by “click” coupling. The purpose of this effort was to establish “click” coupling as a new technique to prepare arborescent polymers. The investigation of linear and branched hydroxylated polystyrene as macroinitiators for the cationic polymerization of ethyl vinyl ether was also performed, to study the reactivity of these systems and to demonstrate their potential usefulness to produce arborescent polymers by cationic *grafting from* methodologies.

7.2.1 Synthesis of G3 and G4 Polystyrene by “Click” Coupling

The synthesis of arborescent polystyrene by “click” coupling was reported for the first time, and grafting was achieved up to generation G2. Since the synthesis of arborescent polystyrene of generations up to G4 has been achieved before,³ it would be interesting to explore the “click” synthesis of the G3 and G4 materials when using the reaction conditions optimized for the G2 polymers. The functionalization of the G2 and G3 substrates with acetylene groups may take a longer time. Since these structures are more congested, the accessibility of the acetyl groups to KOH and 18-crown-6 may be more limited. The grafting reactions to obtain the G3 and G4

polymers should also take a longer time, and temperatures above 45 °C may be worthwhile investigating to increase the grafting yield.

7.2.2 Synthesis of G3 and G4 Arborescent Polybutadiene by “Click”

Coupling and Optimization of the Alternate “Click” Coupling

Method

The synthesis of arborescent polybutadiene up to generation G2 was achieved by “click” coupling of acetylene-terminated side chains onto azidated substrates. Similarly to polystyrene, G3 and G4 polymers could be obtained by utilizing the conditions optimized for the G2 polymers. It is worth noting that the synthesis of G3 and G4 polybutadiene by anionic grafting has thus far failed, so it would be of great interest if these generations could be obtained by “click” coupling. The functionalization of a G2 substrate with azide groups might be tedious as it becomes more sensitive to cross-linking during the functionalization steps, but certain reaction parameters could be modified to minimize this problem, for example by working under more dilute conditions, and by storing the functionalized materials in solution at low temperature. The alternative route to obtain branched polybutadiene was successful up to the G0 level, however that polymer was unstable when functionalized with acetylene groups. This is presumably related to the high degree of unsaturation of polybutadiene, the addition of acetylene groups making it even more unstable and prone to cross linking. Consequently, further optimization of the functionalization of the G0 polymer with acetylene groups would be essential for the success of this approach. The functionalization level investigated in this Thesis was between 20-30 mol %; decreasing the degree of functionalization to 15 mole % may improve the stability of these materials and allow further grafting.

7.2.3 Synthesis of Arborescent Polystyrene and Polybutadiene

Copolymers by “Click” Coupling

One aspect of great interest is the development of paths to the synthesis of both existing and novel arborescent copolymer structures. The “click” grafting technique developed could be applied to the synthesis of several polystyrene-containing copolymer systems that were difficult to obtain by anionic grafting,^{10,11} such as polystyrene-*graft*-poly(2-vinyl pyridine) and polystyrene-*graft*-poly(ethylene oxide) for example. In addition to that, several copolymers containing polystyrene or polybutadiene could be obtained by utilizing a combination of “click” coupling and other polymerization techniques such as ring-opening (ROP) or atom transfer radical polymerization (ATRP), that are applicable to different types of monomers.^{12,13} For example, ATRP provides polymers with a halogen chain end that can be easily converted into azide in a single step,¹⁴ whereas ROP can provide chain ends with functional groups that can be converted into either an azide or an alkyne.¹⁵ These different combinations of “click” coupling with other polymerization techniques may therefore allow the design of many copolymer systems of interest in higher yield and less time.

7.2.4 Application of the Cationic Macroinitiators to Other Monomers and to Sequential Monomer Addition

The utilization of the linear and arborescent polystyrene substrates functionalized with secondary and tertiary alcohol moieties as macroinitiators for the cationic polymerization of ethyl vinyl ether was highly successful, branched copolymers being exclusively produced. The

investigation of these macroinitiators with other monomers such as styrene, substituted oxazolines, or cyclic ethers would allow the synthesis of interesting new arborescent copolymer structures hitherto unattainable. Even in the case of the polystyrene systems, this *grafting from* approach could facilitate the synthesis of arborescent polystyrene structures with longer side chains, which have only been obtained in low yield by “click” grafting. Sequential monomer addition could also be interesting to produce more complex branched polymer architectures, albeit this may also be more problematic. End capping of the living ends with 1,1-diphenylethylene has been shown to attenuate the reactivity of the living ends,¹⁶ and this approach could be helpful to enhance the living character of the arborescent cationic macroinitiator systems as well.

References

Chapter 1

- (1) Gauthier, M.; Möller, M. *Macromolecules* **1991**, *24*, 4548-4553.
- (2) Teertstra, S.; Gauthier, M. *Prog. Polym. Sci.* **2004**, *29*, 277-327.
- (3) Hempenius, M. A.; Michelberger, W.; Möller, M. *Macromolecules* **1997**, *30*, 5602-5605.
- (4) Yuan, Z.; Gauthier, M. *Macromolecules* **2005**, *38*, 4124-4132.
- (5) Kee, A.; Gauthier, M. *Macromolecules* **1999**, *32*, 6478-6484.
- (6) Gauthier, M.; Li, J.; Dockendorff, J. *Macromolecules* **2003**, *36*, 2642-2648.
- (7) Kolb, H.C.; Finn, M.G.; Sharpless, K.B. *Angew. Chem., Int. Ed.* **2001**, *40*, 2004-2021.
- (8) Franc, G.; Kakkar, A. *Chem. Soc. Rev.* **2010**, *39*, 1536-1544.

Chapter 2

- (1) Roovers, J. In *Encyclopedia of Polymer Science and Engineering*, 2nd ed., Vol. 2; Kroschwitz J. I. Ed.; Wiley: New York, 1985; p 478.
- (2) Rempp, P.; Franta, E.; Herz, J.-E. *Adv. Polym. Sci.* **1988**, *86*, 145-173.
- (3) *Dendrimers and other Dendritic Polymers*; Fréchet, J. M. J.; Tomalia, D. A. Eds.; Wiley: New York, 2001.
- (4) Tomalia, D. A.; Hedstrand, D. M.; Ferritto, M. S. *Macromolecules* **1991**, *24*, 1435-1438.
- (5) Gauthier, M.; Möller, M. *Macromolecules* **1991**, *24*, 4548-4553.
- (6) Gauthier, M. In *Tailored Polymers and Applications*, Yagci, Y.; Mishra, M. K.; Nuyken, O.; Ito, K.; Wnek, G. Eds., VSP: Utrecht, 2000, p 43.
- (7) Kee, R. A.; Gauthier, M.; Tomalia, D. A. In Reference 3, Chapter 9.
- (8) Teertstra, S. J.; Gauthier, M. *Prog. Polym. Sci.* **2004**, *29*, 277-327.
- (9) Gauthier, M.; Tichagwa, L.; Downey, J. S.; Gao, S. *Macromolecules* **1996**, *29*, 519-527.
- (10) Li, J.; Gauthier, M. *Macromolecules* **2001**, *34*, 8918-8924.
- (11) Munam, A.; Gauthier, M. *J. Polym. Sci., Part A: Polym. Chem.* **2008**, *46*, 5742-5751.
- (12) Moingeon, F.; Wu, Y.; Cadena-Sanchez, L. E.; Gauthier, M. *J. Polym. Sci., Part A: Polym. Chem.* **2012**, *50*, 1819-1826.
- (13) Yuan, Z.; Gauthier, M. *Macromolecules* **2006**, *39*, 2063-2071.
- (14) Il Yun, S.; Lai, K.-C.; Briber, R. M.; Teertstra, S. J.; Gauthier, M.; Bauer, B. J. *Macromolecules* **2008**, *41*, 175-183.
- (15) Choi, S.; Briber, R. M.; Bauer, B. J.; Liu, D.-W.; Gauthier, M. *Macromolecules* **2000**, *33*, 6495-6501.

- (16) Striolo, A.; Prausnitz, J. M.; Bertucco, A.; Kee, R. A.; Gauthier, M. *Polymer* **2001**, *42*, 2579-2584.
- (17) Lieu, J. G.; Prausnitz, J. M.; Gauthier, M. *Polymer* **2000**, *41*, 219-224.
- (18) Gauthier, M.; Chung, J.; Choi, L.; Nguyen, T. T. *J. Phys. Chem., Part B.* **1998**, *102*, 3138-3142.
- (19) Kee, R. A.; Gauthier, M. *Macromolecules* **2002**, *35*, 6526-6532.
- (20) Gauthier, M.; Li, J.; Dockendorff, J. *Macromolecules* **2003**, *36*, 2642-2648.
- (21) Yuan, Z.; Gauthier, M. *Macromol. Chem. Phys.* **2007**, *208*, 1615-1624.
- (22) Il Yun, S.; Briber, R. M.; Kee, R. A.; Gauthier, M. *Polymer* **2003**, *44*, 6579-6587.
- (23) Il Yun, S.; Briber, R. M.; Kee, R. A.; Gauthier, M. *Polymer* **2006**, *47*, 2750-2759.
- (24) Briber, R. M.; Bauer, B. J.; Hammouda, B.; Tomalia, D. *Abstr. Pap. Am. Chem. Soc.* **1992**, *204*, 225.
- (25) Njikang, G.; Gauthier, M.; Li, J. *Polymer* **2008**, *49*, 1276-1284.
- (26) Njikang, G. N.; Gauthier, M.; Li, J. *Polymer* **2008**, *49*, 5474-5481.
- (27) Il Yun, S.; Gadd, G. E.; Lo, V.; Gauthier, M.; Munam, A. *Macromolecules* **2008**, *41*, 7166-7172.
- (28) Dockendorff, J.; Gauthier, M.; Mourran, A.; Möller, M. *Macromolecules* **2008**, *41*, 6621-6623
- (29) Li, J.; Teertstra, S. J.; Gauthier, M.; Xu, H.; Sheiko, S. S. *Macromolecules* **2004**, *37*, 795-802.
- (30) Teertstra, S. J.; Gauthier, M. *Macromolecules* **2007**, *40*, 1657-1666.
- (31) Gauthier, M.; Lin, W. Y.; Teertstra, S. J.; Tzoganakis, C. *Polymer* **2010**, *51*, 3123-3129.
- (32) Kee, R. A.; Gauthier, M. *J. Polym. Sci., Part A: Polym. Chem.* **2008**, *46*, 2335-2346.

- (33) Njikang, G. N.; Cao, L.; Gauthier, M. *Macromol. Chem. Phys.* **2008**, *209*, 907-918.
- (34) Njikang, G. N.; Cao, L.; Gauthier, M. *Langmuir* **2008**, *24*, 12919-12927.
- (35) Yuan, Z.; Gauthier, M. *Macromolecules* **2005**, *38*, 4124-4132.
- (36) Hempenius, A. M.; Michelberger, W.; Möller, M. *Macromolecules* **1997**, *30*, 5602-5605.
- (37) Zhang, H.; Li, Y.; Zhang C.; Li, Z.; Li, X.; Wang, Y. *Macromolecules* **2009**, *42*, 5073-5079.
- (38) Kolb, H. C.; Finn, M. G.; Sharpless, K. B. *Angew. Chem., Int. Ed.* **2001**, *40*, 2004-2021.
- (39) Hirao, A.; Hayashi, M.; Loykulnant, S.; Sugiyama, K.; Ryu, S. W.; Haraguchi, N.; Matsuo, A.; Higashihara, T. *Prog. Polym. Sci.* **2005**, *30*, 111-182.
- (40) Wang, G.; Huang, J. *Macromol. Rapid Commun.* **2007**, *28*, 298-304.
- (41) Huang, J.; Li, Z.; Xu, X.; Ren, Y.; Huang, J. *J. Polym. Sci., Part A: Polym. Chem.* **2006**, *44*, 3684-3691.
- (42) Bellas, V.; Rehahn, M. *Macromol. Rapid Commun.* **2007**, *28*, 1415-1421.
- (43) Huang, L.; Hu, J.; Lang, L.; Wang, X.; Zhang, P.; Jing, X.; Wang, X.; Chen, X.; Lelkes, P. I.; MacDiarmid, A. G.; Wei, Y. *Biomaterials* **2007**, *28*, 1741-1751.
- (44) Athanasios, T.; Hadjichristidis, N. *Macromolecules* **2011**, *44*, 1969-1976.
- (45) Weizhong, Y.; Jinchun, Z.; Jingren, W.; Cong, Z.; Jie, R. *Eur. Polym. J.* **2011**, *47*, 949-958.
- (46) Altintas, O.; Hizal, G.; Tunca, U. *J. Polym. Sci., Part A: Polym. Chem.* **2008**, *46*, 1218-1228.
- (47) Yang, L.; Zhou, H.; Shi, G.; Wang, Y.; Pan, C. *J. Polym. Sci., Part A: Polym. Chem.* **2008**, *46*, 6641-6653.
- (48) Altintas, O.; Yankul, B.; Hizal, G.; Tunca, U. *J. Polym. Sci., Part A: Polym. Chem.* **2006**, *44*, 6458-6465.

(49) Altintas, O.; Hizal, G.; Tunca, U. *J. Polym. Sci., Part A: Polym. Chem.* **2006**, *44*, 5699-5707.

Chapter 3

- (1) Aridi, T.; Gauthier, M. In *Complex Macromolecular Architectures: Synthesis, Characterization, and Self-Assembly*. Hadjichristidis, N., Hirao, A., Tezuka, Y., Prez, F. D., editors. John Wiley & Sons, 2011; Chapter 6.
- (2) Hawker, C. J.; Wooley, K. L. *Science* **2005**, *309*, 1200-1205.
- (3) Kolb, H. C.; Finn, M. G.; Sharpless, K. B. *Angew. Chem., Int. Ed.* **2001**, *40*, 2004-2021.
- (4) Kolb, H. C.; Sharpless, K. B. *Drug Discovery Today* **2003**, *8*, 1128-1137.
- (5) Huisgen, R.; In *1,3-Dipolar Cycloadditional Chemistry*, Padwa, A., editor. Wiley: New York, 1984.
- (6) (a) Saxon, E.; Bertozzi, C. R. *Science* **2000**, *287*, 2007-2010. (b) Kiick, K. L.; Saxon, E.; Tirrel, D. A.; Bertozzi, C. R. *Proc. Natl. Acad. Sci USA.* **2002**, *99*, 19-24.
- (7) Rostovtsev, V.; Green, L. G.; Fokin, V. V.; Sharpless, K. B. *Angew. Chem., Int. Ed.* **2002**, *41*, 2596-2599.
- (8) Vukicevic, R.; Schwadtke, U.; Schmucker, S.; Schafer, P.; Kuckling, D.; Beuermann, S. *Polym. Chem.* **2012**, *3*, 409-414.
- (9) Lin, Y.; Kuo, S. *Polym. Chem.* **2012**, *3*, 882-891.
- (10) Jing, R.; Wang, G.; Zhang, Y.; Huang, J. *Macromolecules* **2011**, *44*, 805-810.
- (11) Deng, G.; Ma, D.; Xu, Z. *Eur. Polym. J.* **2007**, *43*, 1179-1187.
- (12) Durmaz, H.; Dag, A.; Tunca, U.; Hizal, G. *J. Polym. Sci., Part A: Polym. Chem.* **2012**, *50*, 2406-2414.
- (13) Altintas, O.; Yankul, B.; Hizal, G.; Tunca, U. *J. Polym. Sci., Part A: Polym. Chem.* **2006**, *44*, 6458-6465.

- (14) Altintas, O.; Yankul, B.; Hizal, G.; Tunca, U. *J. Polym. Sci., Part A: Polym. Chem.* **2008**, *46*, 1218-1228.
- (15) Gauthier, M.; Tichagwa, L.; Downey, J. S.; Gao, S. *Macromolecules* **1996**, *29*, 519-527.
- (16) Burchat, A. F.; Chong, J. M.; Nielsen, N. *J. Organomet. Chem.* **1997**, *542*, 281-283.
- (17) Li, J.; Gauthier, M. *Macromolecules* **2001**, *34*, 8918-8924.
- (18) Zakharkin, L. I.; Churilova, I. M.; Nesmeyanov, A. N. Translated from *Izvestiya Akademii Nauk SSSR, S. Khimicheskaya*, **1991**, *4*, 963-965.
- (19) Abele, E.; Abele, R.; Popelis, Y.; Mazheika, I.; Iukevics, E. *Chem. Heterocycl. Compd.* **1999**, *35*, 436-438.
- (20) David, T.H. *PhD. Thesis*, Virginia Polytechnic Institute: Virginia, 2003.
- (21) Dhara, M. G.; Baskaran, D.; Sivaram, S. *J. Polym. Sci., Part A: Polym. Chem.* **2008**, *46*, 2132-2144.
- (22) Moberg, C.; Rakos, L. *Reactive Polymers* **1992**, *16*, 171-179.
- (23) Wagner, J. M.; McElhinny, C. J.; Lewin, A. H.; Carroll, F. I. *Tetrahedron: Asymmetry.* **2003**, *14*, 2119-2125.
- (24) Dahlin, N.; Bøgevig, A.; Adolfsson, H. *Adv. Synth. Catal.* **2004**, *346*, 1101-1105.
- (25) Fallais, I.; Devaux, J.; Jérôme, R. *J. Polym. Sci., Part A: Polym. Chem.* **2000**, *38*, 1618-1629.
- (26) Zhu, L.; Liu, L.; Jiang, M. *Macromol. Rapid Commun.* **1996**, *17*, 37-42.
- (27) Boehm, R. L. *J. Org. Chem.* **1958**, *23*, 1716-1720.
- (28) Ergin, M.; Kiskan, B.; Gacal, B.; Yagci, Y. *Macromolecules* **2007**, *40*, 4724-4727.
- (29) Wang, G.; Hu, B.; and Huang, J. *Macromolecules* **2010**, *43*, 6939-6942.
- (30) Gauthier, M.; Möller, M. *Macromolecules* **1991**, *24*, 4548-4553.

(31) Gauthier, M.; Li, J.; Dockendorff, J. *Macromolecules* **2003**, *36*, 2642-2648.

Chapter 4

- (1) Gao, H.; Matyjaszewski, K. *Macromolecules* **2008**, *41*, 1118-1125.
- (2) Gao, H.; Matyjaszewski, K. *Macromolecules* **2007**, *40*, 399-401.
- (3) Teertstra, S.J.; Gauthier, M. *Prog. Polym. Sci.* **2004**, *29*, 277-327.
- (4) Dekker, M. *Anionic Polymerization: Principles and Practical Applications*, Hsieh, H. L.; Quirk, R. P. editors, 1996; p 369.
- (5) Beorner, H. G.; Matyjaszewski, K. *Macromol. Symp.* **2002**, *177*, 1-15.
- (6) Mecerreyes, D.; Jérôme, R.; Dubois, P. *Adv. Polym. Sci.* **1999**, *147*, 1-59.
- (7) Charleux, B.; Faust, R. *Adv. Polym. Sci.* **1999**, *142*, 1-69.
- (8) Nguyen, H. A.; Kennedy, J. P. *Polym. Bull.* **1981**, *6*, 55-60.
- (9) Nguyen, H. A.; Kennedy, J. P. *Polym. Bull.* **1981**, *6*, 61-65.
- (10) Nguyen, H. A.; Kennedy, J. P. *Polym Bull.* **1983**, *10*, 74-81.
- (11) Puskas, J. E.; Kwon, Y.; Antony, P.; Bhowmick, A. K. *J. Polym. Sci., Part A: Polym. Chem.* **2005**, *43*, 1811-1826.
- (12) Miyamoto, M.; Sawamoto, M.; Higashimura, T. *Macromolecules* **1984**, *17*, 265-268.
- (13) Bennevault, V.; Peruch, F.; Deffieux, A. *Macromol. Chem. Phys.* **1996**, *197*, 2603-2613.
- (14) Cramail, H.; Deffieux, A. *Macromol. Chem. Phys.* **1994**, *195*, 217-227.
- (15) Kanazawa, A.; Kanaoka, S.; Aoshima, S. *J. Polym. Sci., Part A: Polym. Chem.* **2010**, *48*, 2509-2516.
- (16) Burchat, A. F.; Chong, J. M.; Nielsen, N. *J. Organomet. Chem.* **1997**, *542*, 281-283.
- (17) Li, J.; Gauthier, M. *Macromolecules* **2001**, *34*, 8918-8924.
- (18) Zhu, L.; Liu, L.; Jiang, M. *Macromol. Rapid Commun.* **1996**, *17*, 37-42.

- (19) (a) Brown, H. C.; Kanner, B. *J. Am. Chem. Soc.* **1953**, *75*, 3865. (b) Brown, H. C.; Kanner, B. *J. Am. Chem. Soc.* **1966**, *88*, 986-992.
- (20) (a) Anderson, A. G.; Stang, P. J. *J. Org. Chem.* **1976**, *41*, 3034-3036. (b) Forbus, T.R. Jr.; Martin, J. C. *J. Org. Chem.* **1979**, *44*, 313-314.
- (21) Kennedy, J.P., Marechal, E. *Carbocationic Polymerization*, Wiley-Interscience: New York, 1982.
- (22) Guhaniyogi, S.C.; Kennedy, J. *Polym. Bull.* **1981**, *4*, 267-274.
- (23) Moulis, J. M.; Collomb, M.; Gandini, A.; Cheradame, H. *Polym. Bull.* **1980**, *3*, 197-202.
- (24) Nakatani, K.; Ouchi, M.; Sawamoto, M. *J. Polym. Sci., Part A: Polym. Chem.* **2009**, *47*, 4194-4201.

Chapter 5

- (1) Roovers, J. *Macromolecules* **1991**, *24*, 5895-5896.
- (2) Roovers, J.; Toporowski, P. M. *Macromolecules* **1987**, *20*, 2300-2306.
- (3) Masuda, T.; Ohta, Y.; Onogi, S. *Macromolecules* **1986**, *19*, 2524-2532.
- (4) (a) Khadir, A.; Gauthier, M. *Polym. Mater. Sci. Eng.* **1997**, *77*, 174-175. (b) Schmaljohann, D.; Pötschke, P.; Hässler, R.; Voit, B. I.; Froehling, P. E.; Mostert, B.; Loontjens, J. A. *Macromolecules* **1999**, *32*, 6333-6339. (c) Nunez, C. M.; Chiou, B. S.; Andraday, A. L.; Khan, S. A. *Macromolecules* **2000**, *33*, 1720-1726.
- (5) Teertstra, S. J.; Gauthier, M. *Prog. Polym. Sci.* **2004**, *29*, 277-327.
- (6) Kolb, H.C.; Finn, M.G.; Sharpless, K.B. *Angew. Chem., Int. Ed.* **2001**, *40*, 2004-2021.
- (7) Kolb, H.C.; Sharpless, K.B. *Drug Discovery Today* **2003**, *8*, 1128-1137.
- (8) Huisgen, R. *In 1,3-Dipolar Cycloadditional Chemistry*, Padwa, A. editor, Wiley: New York, 1984.
- (9) Yang, H.; Zhu, C.H.; Di Cicco, A.; Lévy, D.; Albouy, P.A.; Li, M.H.; Keller, P. *Macromolecules* **2010**, *43*, 10442-10451.
- (10) Brummelhuis, N.T.; Diehl, C.; Schlaad, H. *Macromolecules* **2008**, *41*, 9946-9947.
- (11) Kukut, M.; Kiskan, B.; Yagci, Y. *Designed Monomers and Polymers* **2009**, *12*, 167-176.
- (12) Guo, F.; Jankova, K.; Schulte, L.; Vigild, M.E.; Ndoni, S. *Langmuir* **2010**, *26*, 2008-2013.
- (13) Gauthier, M.; Tichagwa, L.; Downey, J.S.; Gao, S. *Macromolecules* **1996**, *29*, 519-527.
- (14) Burchat, A. F.; Chong, J. M.; Nielsen, N. *J. Organomet. Chem.* **1997**, *542*, 281-283.
- (15) Yuan, Z.; Gauthier, M. *Macromolecules* **2005**, *38*, 4124-4132.
- (16) Moingeon, F.; Wu, Y. R.; Sanchez-Cadena, L.; Gauthier, M. *J. Polym. Sci., Part A: Polym. Chem.* **2012**, *50*, 1819-1826.

- (17) Zhu, L.; Liu, L.; Jiang, M. *Macromol. Rapid Commun.* **1996**, *17*, 37-42.
- (18) Mobergm, C.; Tkos, I.I. *Reactive Polymers* **1992**, *16*, 171-179.
- (19) Wagner, J.M.; McElhinny, C.J.; Lewin, A.H.; Carroll, F.I. *Tetrahedron: Asymmetry* **2003**, *14*, 2119-2125.
- (20) Dahlin, N.; Bogevig, A.; Adolfsson, H. *Adv. Synth. Catal.* **2004**, *346*, 1101-1105.
- (21) Fallais, I.; Devaux, J.; Jérôme, R. *J. Polym. Sci., Part A: Polym. Chem.* **2000**, *38*, 1618-1629.
- (22) Dhara, M.G.; Baskaran, D.; Sivaram, S. *J. Polym. Sci., Part A: Polym. Chem.* **2008**, *46*, 2132-2144.
- (23) Ergin, M.; Kiskan, B.; Gacal, B.; Yagci, Y. *Macromolecules* **2007**, *40*, 4724-4727.
- (24) Odian, G. *Principles of polymerization*, 3rd ed., Wiley: New York, 1991; p 629.
- (25) Rossiello, L.; Buttafava, A.; Martinotto, L.; Peruzzotti, F.; Ghisoni, G. M.; Faucitano, A. *Res. Chem. Intermed.* **2002**, *28*, 89-100.
- (26) Rostovtsev, V.; Green, L. G.; Fokin, V. V.; Sharpless, K. B. *Angew. Chem., Int. Ed.* **2002**, *41*, 2596-2599.
- (27) Wang, G.; Hu, B.; Huang, J. *Macromolecules* **2010**, *43*, 6939-6942.

Chapter 6

- (1) Aridi, T.; Gauthier, M. In *Complex Macromolecular Architectures: Synthesis, Characterization, and Self-Assembly*. Hadjichristidis, N.; Hirao, A.; Tezuka, Y.; Du Prez, F., eds. Wiley (Asia), 2011; Chapter 6.
- (2) Roovers, J. *Macromolecules* **1991**, *24*, 5895-5896.
- (3) Roovers, J.; Toporowski, P. M. *Macromolecules* **1987**, *20*, 2300-2306.
- (4) Masuda, T.; Ohta, Y.; Onogi, S. *Macromolecules* **1986**, *19*, 2524-2532.
- (5) Khadir, A.; Gauthier, M. *Polym. Mater. Sci. Eng.* **1997**, *77*, 174-175.
- (6) Schmaljohann, D.; Pötschke, P.; Hässler, R.; Voit, B. I.; Froehling, P. E.; Mostert, B.; Loontjens, J. A. *Macromolecules* **1999**, *32*, 6333-6339.
- (7) Nunez, C. M.; Chiou, B.S.; Andrady, A. L.; Khan, S. A. *Macromolecules* **2000**, *33*, 1720-1726.
- (8) Teertstra, S. J.; Gauthier, M. *Prog. Polym. Sci.* **2004**, *29*, 277-327.
- (9) (a) Rempp, P.; Franta, E.; Herz, J. E. *Adv. Polym. Sci.* **1988**, *86*, 145-173. (b) Hsieh, H. L., Quirk, R. P. In *Anionic Polymerization: Principles and Practical Applications*, Dekker: New York, 1996; Chapter 13.
- (10) Roovers, J.; Zhou, L.; Toporowski, M. P.; Zwan, M.; Iatrou, H.; Hadjichristidis, N. *Macromolecules* **1993**, *26*, 4324-4331.
- (11) Munam, A.; Gauthier, M. *Macromolecules* **2010**, *43*, 3672-3681.
- (12) Hempenius, A. M.; Michelberger, W.; Möller, M. *Macromolecules* **1997**, *30*, 5602-5605.
- (13) Zhang, H.; Li, Y.; Zhang, C.; Li, Z.; Li, X.; Wang, Y. *Macromolecules* **2009**, *42*, 14-16.
- (14) Alturk, A. *M. Sc. Thesis*, University of Waterloo: Waterloo, 2012.
- (15) Gauthier, M.; Tichagwa, L.; Downey, J. S.; Gao, S. *Macromolecules* **1996**, *29*, 519-527.

- (16) Burchat, A. F.; Chong, J. M.; Nielsen, N. *J. Organomet. Chem.* **1997**, *542*, 281-283.
- (17) Yuan, Z.; Gauthier, M. *Macromolecules* **2005**, *38*, 4124-4132.
- (18) Smid, J. *J. Polym. Sci., Part A: Polym. Chem.* **2002**, *40*, 2101-2107.
- (19) Bywater, S.; Firat, Y.; Black, P. E. *J. Polym. Sci., Polym. Chem. Ed.* **1984**, *22*, 669-672.
- (20) Bhattacharyya, D. N.; Smid, J.; Szwarc, M. *J. Phys. Chem.* **1965**, *69*, 624-627.
- (21) Erwin, B.M.; Cloitre, M.; Gauthier, M.; Vlassopoulos, D. *Soft Matter*. **2010**, *6*, 2825-2833.
- (22) Erwin, B.M.; Cloitre, M.; Gauthier, M.; Vlassopoulos, D. *Phys. Rev. E.* **2011**, *83*, 061402-061407.
- (23) Truzzolillo, D.; Vlassopoulos, D.; Gauthier, M. *Macromolecules* **2011**, *44*, 5043-5052.

Chapter 7

- (1) Gauthier, M.; Möller, M. *Macromolecules* **1991**, *24*, 4548-4553.
- (2) Kolb, H. C.; Finn, M. G.; Sharpless, K. B. *Angew. Chem. Int. Ed.* **2001**, *40*, 2004-2021.
- (3) Li, J.; Gauthier, M. *Macromolecules* **2001**, *34*, 8918-8924.
- (4) Nguyen, H. A.; Kennedy, J. R. *Polym. Bull.* **1983**, *10*, 74-81.
- (5) Puskas, J. E.; Kwon, Y.; Antony, P.; Bhowmick, A. K. *J. Polym. Sci., Part A: Polym. Chem.* **2005**, *43*, 1811-1826.
- (6) Hempenius, A. M.; Michelberger, W.; Möller, M. *Macromolecules* **1997**, *30*, 5602-5605.
- (7) Erwin, B.M.; Cloitre, M.; Gauthier, M.; Vlassopoulos, D. *Soft Matter* **2010**, *6*, 2825-2833.
- (8) Erwin, B.M.; Cloitre, M.; Gauthier, M.; Vlassopoulos, D. *Phys. Rev. E.* **2011**, *83*, 061402-061407.
- (9) Truzzolillo, D.; Vlassopoulos, D.; Gauthier, M. *Macromolecules* **2011**, *44*, 5043-5052.
- (10) Kee, R. A.; Gauthier, M. *Macromolecules* **2002**, *35*, 6526-6532.
- (11) Gauthier, M.; Li, J.; Dockendorff, J. *Macromolecules* **2003**, *36*, 2642-2648.
- (12) Khanna, K.; Varshney, S.; Kakkar, A.K. *Polym. Chem.* **2010**, *1*, 1171-1185.
- (13) Khanna, K.; Varshney, S.; Kakkar, A.K. *Macromolecules* **2010**, *43*, 5688-5698.
- (14) Reinicke, S.; Schmalz, H. *Colloid Polym. Sci.* **2011**, *289*, 497-512.
- (15) Zhang, Y.; Li, C.; Liu, S. *J. Polym. Sci., Part A: Polym. Chem.* **2009**, *47*, 3066-3077.
- (16) Fodor, Z.; Faust, R. *Pure Appl. Chem.* **1994**, *A31*, 1985-2000.